frontiers | Research Topics

Adult diffuse glioma microenvironment: Insight into cancer ecology

Edited by
Aleksi Sedo, Ahmed Idbaih and Bozena Kaminska

Published in
Frontiers in Oncology

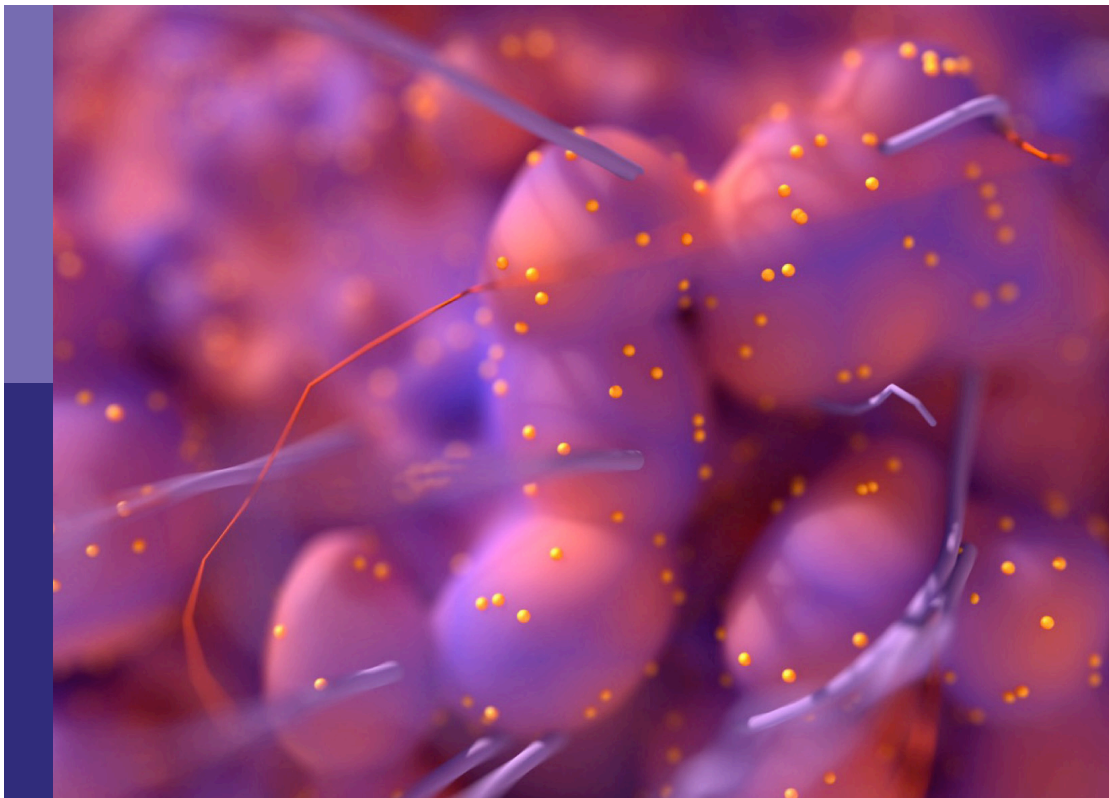

ISSN 1664-8714
ISBN 978-2-83251-912-7
DOI 10.3389/978-2-83251-912-7

About Frontiers

Frontiers is more than just an open access publisher of scholarly articles: it is a pioneering approach to the world of academia, radically improving the way scholarly research is managed. The grand vision of Frontiers is a world where all people have an equal opportunity to seek, share and generate knowledge. Frontiers provides immediate and permanent online open access to all its publications, but this alone is not enough to realize our grand goals.

Frontiers journal series

The Frontiers journal series is a multi-tier and interdisciplinary set of open-access, online journals, promising a paradigm shift from the current review, selection and dissemination processes in academic publishing. All Frontiers journals are driven by researchers for researchers; therefore, they constitute a service to the scholarly community. At the same time, the *Frontiers journal series* operates on a revolutionary invention, the tiered publishing system, initially addressing specific communities of scholars, and gradually climbing up to broader public understanding, thus serving the interests of the lay society, too.

Dedication to quality

Each Frontiers article is a landmark of the highest quality, thanks to genuinely collaborative interactions between authors and review editors, who include some of the world's best academicians. Research must be certified by peers before entering a stream of knowledge that may eventually reach the public - and shape society; therefore, Frontiers only applies the most rigorous and unbiased reviews. Frontiers revolutionizes research publishing by freely delivering the most outstanding research, evaluated with no bias from both the academic and social point of view. By applying the most advanced information technologies, Frontiers is catapulting scholarly publishing into a new generation.

What are Frontiers Research Topics?

Frontiers Research Topics are very popular trademarks of the *Frontiers journals series*: they are collections of at least ten articles, all centered on a particular subject. With their unique mix of varied contributions from Original Research to Review Articles, Frontiers Research Topics unify the most influential researchers, the latest key findings and historical advances in a hot research area.

Find out more on how to host your own Frontiers Research Topic or contribute to one as an author by contacting the Frontiers editorial office: frontiersin.org/about/contact

Adult diffuse glioma microenvironment: Insight into cancer ecology

Topic editors

Aleksi Sedo — Charles University, Czechia

Ahmed Idbaih — Sorbonne Universités, France

Bozena Kaminska — Nencki Institute of Experimental Biology, Polish Academy of Sciences, Poland

Citation

Sedo, A., Idbaih, A., Kaminska, B., eds. (2023). *Adult diffuse glioma microenvironment: Insight into cancer ecology*. Lausanne: Frontiers Media SA. doi: 10.3389/978-2-83251-912-7

Table of contents

frontiers in Oncology

ORIGINAL RESEARCH
published: 15 July 2021
doi: 10.3389/fonc.2021.702983

METTL3 Promotes the Resistance of Glioma to Temozolomide *via* Increasing MGMT and ANPG in a m^{6}A Dependent Manner

Jia Shi[1,2†], Gang Chen[3†], Xuchen Dong[1], Haoran Li[1], Suwen Li[1], Shan Cheng[1], Yongdong Li[1], Liping Wang[1], Jiaqi Yuan[1], Zhiyuan Qian[1] and Jun Dong[1]*

[1] Department of Neurosurgery, The Second Affiliated Hospital of Soochow University, Suzhou, China, [2] Department of Neurosurgery, The Third Affiliated Hospital of Soochow University, Changzhou, China, [3] Department of Neurosurgery, Zhuhai People's Hospital, Zhuhai Hospital Affiliated With Jinan University, Zhuhai, China

Acquired chemoresistance is a major limiting factor in the clinical treatment of glioblastoma (GBM). However, the mechanism by which GBM acquires therapeutic resistance remains unclear. Here, we aimed to investigate whether METTL3-mediated N6-methyladenosine (m^{6}A) modification contributes to the temozolomide (TMZ) resistance in GBM. We demonstrated that METTL3 METTL3-mediated m^{6}A modification were significantly elevated in TMZ-resistant GBM cells. Functionally, METTL3 overexpression impaired the TMZ-sensitivity of GBM cells. In contrast, METTL3 silencing or DAA-mediated total methylation inhibition improved the sensitivity of TMZ-resistant GBM cells to TMZ *in vitro* and *in vivo*. Furthermore, we found that two critical DNA repair genes (MGMT and APNG) were m^{6}A-modified by METTL3, whereas inhibited by METTL3 silencing or DAA-mediated total methylation inhibition, which is crucial for METTL3-improved TMZ resistance in GBM cells. Collectively, METTL3 acts as a critical promoter of TMZ resistance in glioma and extends the current understanding of m^{6}A related signaling, thereby providing new insights into the field of glioma treatment.

Keywords: glioblastoma, temozolomide, resistance, N6-methyladenosine (m 6 A), METTL3

OPEN ACCESS

Edited by:
Aleksi Sedo,
Charles University, Czechia

Reviewed by:
Dan Qi,
Baylor Scott and White Health, United States
Tomas Buchler,
Charles University, Czechia

****Correspondence:***
Jun Dong
dongjun@suda.edu.cn

†These authors have contributed equally to this work

Specialty section:
This article was submitted to Neuro-Oncology and Neurosurgical Oncology, a section of the journal Frontiers in Oncology

Received: *30 April 2021*
Accepted: *05 July 2021*
Published: *15 July 2021*

Citation:
Shi J, Chen G, Dong X, Li H, Li S, Cheng S, Li Y, Wang L, Yuan J, Qian Z and Dong J (2021) METTL3 Promotes the Resistance of Glioma to Temozolomide via Increasing MGMT and ANPG in a m^{6}A Dependent Manner. Front. Oncol. 11:702983. doi: 10.3389/fonc.2021.702983

INTRODUCTION

Owing to the introduction of temozolomide (TMZ), an alkylation agent, and the use of radiotherapy in combination with TMZ adjuvant therapy, the median survival of patients with glioblastoma multiforme (GBM) was increased from 12.1 months to 14.6 months (1–5). However, the overall clinical efficacy of this regimen remains disappointing, mainly because of inherent or induced resistance to TMZ treatment (6–11). Mostly, TMZ-resistant cell lines highly expressed O^6-methylguanine-DNA methyltransferase (MGMT) and alkylpurine–DNA–N-glycosylase (ANPG) (12, 13). TMZ methylated 12 kinds of DNA bases at different sites, of which, O^6-meG was considered the most toxic lesion (14). MGMT repairs O^6-meG through a suicidal response, thereby becoming resistant to TMZ. On the other hand, ANPG repairs the cytotoxic lesions N^3-methyladenine and N^7-methylguanine and contributes to TMZ resistance (12). Therefore, the clinical treatment of this deadly tumor urgently requires a more comprehensive understanding of its progression, mechanisms of resistance, and new therapeutic targets.

In the eukaryotic cells, N6-methyladenosine (m^6A) is the predominant modification of mRNA and long non-coding RNAs (15). m^6A is a dynamic and reversible RNA modification in mammalian cells that occurs after transcription by the m^6A methyltransferase complex, which contains the enzyme subunit methyltransferase-like 3 protein (METTL3) and its co-cofactors methyltransferase-like 14 protein (METTL14) and WT1-associated protein (WTAP) (16). With the deepening understanding of RNA methylation, a number of regulatory factors involved in the regulation of mammalian m^6A have been identified (17).

The m^6A modification of the methyltransferase-imprinted RNA prioritizes the recognition and delivery of the reader protein and is cleared by RNA demethylase (18). Therefore, three types of regulators dynamically controlling m^6A are defined as writers, readers, and erasers (19). Under the control of these three regulatory factors, m^6A methylation epigenetic regulation of a large number of gene expression plays multiple roles in the regulation of biological processes (20). The acquisition of m^6A reduces the stability of transcription and mediates the attenuation of target mRNA, suggesting that m^6A modification is a negative regulator of mRNA translation. Instead, m^6A deficiency increases the abundance and longevity of transcripts, as well as the overall expression of the protein. m^6A can also change the structure of RNA, promote the binding of protein regulators, affect mRNA maturation, and regulate gene expression.

It has been reported that m^6A modification plays a variety of regulatory roles in tumor initiation, progression, and radiation resistance (21, 22). In addition, a growing body of evidences suggests that genetic alterations and dysregulation of m^6A RNA methylation regulators are closely associated with the malignant progression of a variety of cancers (23). In recent years, increasing evidences have shown that METTL3 plays an important role in cancer as an m^6A methyltransferase, both as an oncogene and as a tumor suppressor gene. In most cases, METTL3 has been reported as an oncogene that promotes the occurrence and progression of a variety of cancers, including hematopoietic malignancies and solid tumors, by depositing m^6A modifications on key transcripts (24, 25).

However, the clinicopathological effects of METTL3-mediated RNA m^6A modification and the related mechanisms of TMZ resistance in glioma have not been elucidated. In this study, we demonstrated that METTL3 acts as a critical promoter of TMZ resistance in glioma. Based on these findings, we provide new insights into the METTL3-mediated modification of m^6A. We also explored the molecular mechanisms underlying TMZ resistance of glioma by identifying downstream target genes and signals. Therefore, our work extends the current understanding of m^6A-related signaling and provides new insights into the field of glioma research.

MATERIALS AND METHOD

Cell Lines and Cell Culture

Human glioblastoma-derived U87-MG and U251 cell lines were obtained from the American Type Culture Collection (ATCC, Manassas, VA, USA). All cell lines were cultured in DMEM (Gibco, Grand Island, NY, USA) supplemented with 10% FBS (Gibco) and 1% PS (Invitrogen, Carlsbad, CA, USA), and maintained at 37°C and 5% CO_2 in a humidified atmosphere. TMZ-resistant cell lines were generated by exposure of U87-MG and U251 cells with 200 μM TMZ for over 6 months. The derived resistant cell lines were designated as U87-MG-TMZ resistant and U251-TMZ resistant, respectively. The cell survival ratio and half maximal inhibitory concentration (IC_{50}) of TMZ for U87-MG and U251 was evaluated using the CCK-8 assay (**Supplementary Figure 1**).

Real-Time Quantitative PCR (qRT-PCR)

RNA extraction and real-time fluorescent quantitative PCR (qRT-PCR) were performed as previously described. The relative gene expression of mRNA was calculated by $2^{-\Delta\Delta CT}$ method. GAPDH was used as an endogenous control to normalize the data.

Plasmid Transfection

Stable overexpression of METTL3 was achieved by constructing a lentiviral vector (Biospec Technology, Shanghai). In addition, we synthesized shRNA-targeting genes. Transfection of the expression plasmid in glioma cells was performed using Lipofectamine 3000 kit (Invitrogen, Carlsbad, CA, USA) according to the manufacturer's instructions.

Western Blot

The cells were directly lysed in 1× SDS-PAGE loading buffer. Protein bands were detected sequentially with primary and HRP-bound secondary antibodies, visualized using a Chemiluminescence Detection Kit (Servicebio, Wuhan, China), and detected with an imaging system (Bio-Rad, USA). Antibodies against METTL3 (AB195352, 1:2000) were obtained from Abcam. GAPDH (60004, 1:5000) antibodies were purchased from Proteintech.

Total RNA m^6A Quantification

The total level of m^6A in the treated glioma cells was determined using the EpiQuik^{TM} m^6A RNA Methylation Quantitative Kit (Epigentek, USA). Briefly, 200 ng of RNA was added to each well, followed by a mixture of capture and detection antibodies. After several weeks of incubation, the m^6A content was quantified at 450 nm and calculated according to the standard curve.

Dot Blot

The mRNA samples were dissolved in a 3-fold volume of RNA incubation buffer, denatured at 65°C for 5 min, and loaded onto an Amersham Hybond-N+membrane (GE Healthcare, USA) mounted on a Bio-Dot device (Bio-Rad, USA). After blocking the membrane with 5% skimmed milk, the specific m^6A antibody (1:1000, Abcam) was incubated overnight at 4°C. Mouse immunoglobulin G (IgG) was incubated with HRP-conjugated immunoglobulin G (IgG) for 1 h, and imaging was performed using an imaging system (Bio-Rad, USA).

Methylated RNA Immunoprecipitation (Me-RIP)

Total RNA or poly(A)+mRNA was isolated using the above methods. The purified mRNAs and magnetic bead-antibody

complexes were then added to IP buffers and incubated overnight at 4°C, followed by elution with eluent and purification. MGMT and ANPG in RNA were extracted using RT-qPCR.

Cell Viability Assay

Cell viability was measured after treatment with different concentrations of TMZ (Selleck Chemicals, Houston, TX, USA). After 4 h of normal culture, 10 μL CCK-8 reagent (Dojindo) was added and absorbance at 450 nm was detected using an ultra-multifunctional microplate analyzer (Tecan, Durham, NC, USA). Using GraphPad Prism 9.0 (GraphPad Software, San Diego, CA, USA), the "log (inhibitor) *vs* normalized slope of response variable" method was used to calculate the 50% inhibition concentration (IC_{50}) of TMZ.

Colony Formation Experiments

Glioma cells were seeded in a 6-well culture plate containing 500 cells per well for 14 d. The colonies were washed with PBS and fixed with 4% paraformaldehyde. Photographs were taken using a microscope (Olympus, Ishikawa, Japan).

Subcutaneous Glioma Xenograft Model

All experiments involving mice were conducted in accordance with the ethical standards of the animal care and use committee of the third hospital affiliated to Soochow University and the NIH guidelines for the care and use of laboratory animals. To establish the xenograft model of glioma in mice, 1×10^7 human U87-MG-TMZ cells (sh-Con, sh-METTL3, or normal U87-MG-TMZ) were subcutaneously inoculated into the right posterior limb of BALB/c nude mice (6-week-old, female) in 80 μL PBS. Tumor volume was measured with calipers every 5 d. After approximately 30 d, all mice were euthanized, and the tumor masses were removed, weighed, and embedded for further pathological study.

Statistical Analyses

SPSS 21.0 statistical software (IBM Corp. Armonk, NY) was used for statistical analyses, and statistical significance was set at $P<0.05$. Data are expressed as mean ± standard deviation. Multiple sets of data were evaluated using one-way analysis of variance (ANOVA), and multiple comparisons were performed using Tukey's post-hoc test. Time-based multiple comparisons were tested by repeated analysis of variance and the Bonferroni post facto test.

RESULTS

METTL3 Mediated m^6A Is Elevated in the TMZ-Resistant GBM Cells

Previously, elevated METTL3 levels have been associated with malignant characteristics of cancer cells (21), but its role in TMZ resistance in GBM has not been fully understood. Here, upon comparing the METTL3 levels between the TMZ-sensitive cells and the resistant cells, we found that the mRNA level of METTL3 was significantly higher (about 4.78-fold in U87-MG-TMZ and 4.48-fold in U251-TMZ) in the TMZ-resistant group than in the sensitive group (**Figure 1A**), which was further confirmed by western blot analysis (**Figure 1B**). We then examined m^6A levels in the total RNAs from TMZ-sensitive cells and resistant cells using the colorimetric m^6A quantification strategy, revealing significantly increased m^6A levels in TMZ-resistant cells (**Figure 1C**) compared with TMZ-sensitive cells (approximately 4.16-fold in U87-MG-TMZ and 5.92-fold in U251-TMZ), confirmed by dot blot analysis (**Figure 1D**). These results suggest that METTL3 mediated m^6A may contribute to TMZ-resistant GBM cells.

METTL3 Contributes to the TMZ Resistance in GBM Cells

To further study the functional role of METTL3 in the regulation of TMZ resistance, we established METTL3-stable overexpression and knockdown U87-MG-TMZ and U251-TMZ cell lines. The efficiency of overexpression and knockdown on the mRNA and protein levels of METTL3 was verified by qRT-PCR (**Figure 2A**) and western blot (**Figure 2B**), respectively. Consistently, the m^6A levels were significantly increased in METTL3 overexpressed U87-MG-TMZ and U251-TMZ cells, whereas decreased in METTL3 knockdown U87-MG-TMZ and U251-TMZ cells (**Figure 2C**). Compared with parental control, METTL3 knockdown GBM cells had a significantly lower ability to form colonies (**Figure 2D**), while TMZ-Resistant cells overexpressing METTL3 had no effect (**Figure 2D**). More importantly, METTL3 level was positively correlated with TMZ sensitivity. When METTL3 was knocked down, the IC_{50} value decreased from approximately 268.9 μM to 95.6 μM in U87-MG-TMZ cells and 296.0 μM to 110.6 μM in U251-TMZ, whereas the IC_{50} value remained unchanged in METTL3 overexpressing cells (**Figure 2E**). These results suggest that METTL3 silencing caused TMZ-resistant cells more sensitive to TMZ.

METTL3 Contributes to the TMZ Resistance *via* m^6A Modification

To further study the functional role of METTL3-mediated m^6A modification in the regulation of TMZ resistance, we inhibited methylation with a methylation inhibitor, 3-deazaadenosine (DAA, 100 μM). Consistent with our hypothesis, treating U87-MG/U251-TMZ cells with DAA led to a remarkable reduction in total m^6A level (**Figure 3A**), which was verified by dot blot (**Figure 3B**). Moreover, compared with the parental control, DAA-treated GBM cells had a significantly lower ability to form colonies (**Figure 3C**). Furthermore, the IC_{50} value decreased from approximately 275.4 μM to 98.6 μM in U87-MG-TMZ cells and 288.2 μM to 108.3 μM in U251-TMZ (**Figure 3D**). The major repair enzymes, O6-methylguanine–DNA methyltransferase (MGMT) and alkylpurine–DNA–N-glycosylase (APNG), repairs the most cytotoxic lesions generated by TMZ. To analyze the underlying mechanism of METTL3-mediated m^6A modification in the regulation of TMZ resistance, we screened a series of TMZ-resistant genes (ANPG, CBX5, MGMT, MSH2, MSH6, MLH1,

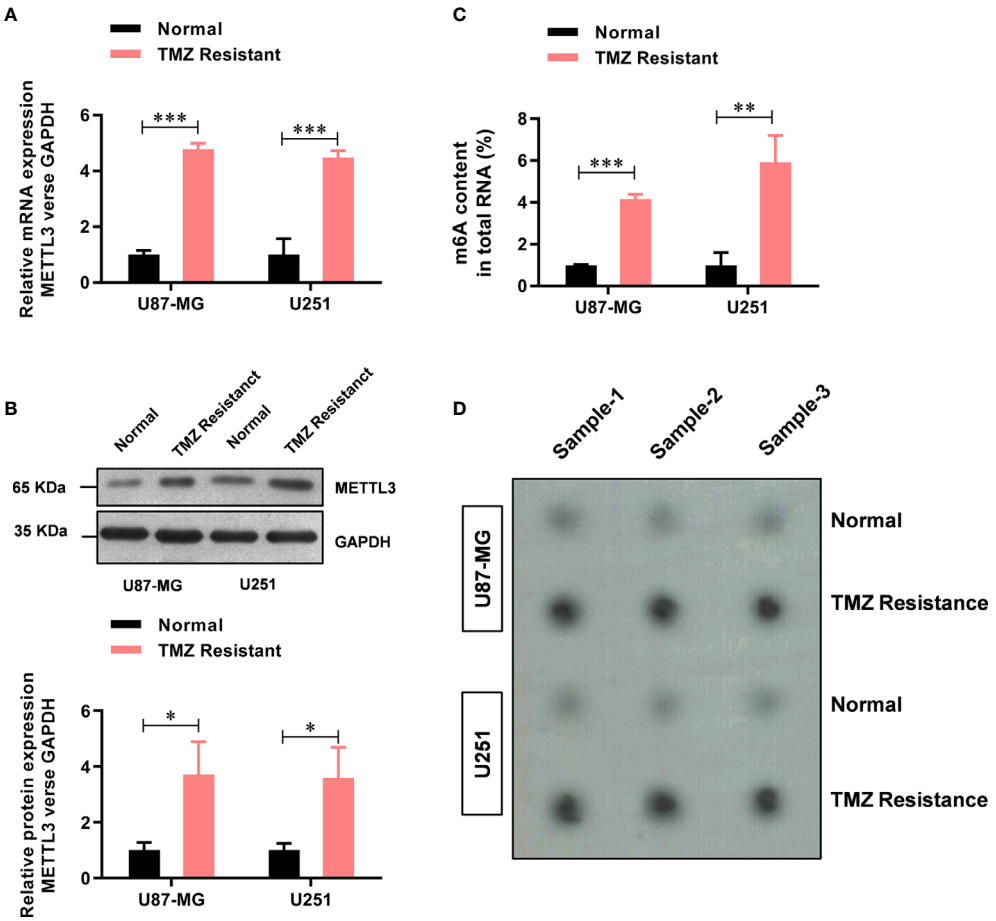

FIGURE 1 | METTL3-mediated m^{6}A is elevated in the TMZ-resistant GBM cells. **(A)** The mRNA level of METTL3 in TMZ sensitive and resistant U87-MG/U251 cells was analyzed by real-time PCR. **(B)** The protein level of METTL3 in TMZ sensitive and resistant U87-MG/U251 cells was analyzed by western blot. **(C)** The colorimetric m^{6}A quantification assay was used to examine the total m^{6}A levels in the TMZ sensitive cells and the resistant U87-MG/U251 cells. **(D)** The dot blot was used to confirm the total m^{6}A levels in the TMZ sensitive cells and the resistant U87-MG/U251 cells. *P < 0.05, **P < 0.01, and ***P< 0.001 *versus* normal U87-MG/U251 cells.

MPG, XRCC3, and XPC), revealing that METTL3 overexpression significantly increased the MGMT and ANPG expression in GBM cells (**Figure 4A**).

Furthermore, the m^{6}A methylation level (**Figure 4B**) of MGMT and ANPG were significantly increased in TMZ-resistant GBM cells. Notably, the m^{6}A methylation level (**Figure 4C**) of MGMT and ANPG was significantly increased by METTL3 overexpression, which decreased by METTL3 knockdown or DAA treatment (**Figure 4D**). Collectively, these results demonstrate that METTL3 contributes to TMZ resistance *via* m^{6}A modification.

METTL3-Mediated m^{6}A Modification Contributes to the TMZ Resistance *In Vivo*

To investigate whether METTL3-mediated m^{6}A modification was TMZ-resistant *in vivo*, we subcutaneously injected shMETTL3 or shNC-expressing U87-MG-TMZ cells into BALB/c NOD mice. After confirmation of GBM implantation, mice were treated with TMZ (66 mg/kg/d, 5 d per week, for 3 cycles). The tumor volume (**Figures 5A, B**) and weight (**Figure 5C**) of mice injected with shMETTL3 were significantly lower than those of xenografts expressing shNC. In contrast, mice treated with DAA (50 mg/kg/d, 5 d per week, for 3 cycles) and TMZ also resulted in a smaller tumor volume (**Figures 5A, B**) and weight (**Figure 5C**) than the blank group. IHC staining was performed to verify the expression of cleaved caspase-3. TMZ-treated xenografts with shMETTL3 expressing or DAA treatment had significantly increased level of cleaved caspase-3 compared with shNC or blank xenografts (**Figure 5D**). Taken together, these results demonstrate that METTL3-mediated m^{6}A modification contributes to TMZ resistance *in vivo*.

DISCUSSION

GBM is one of the most aggressive types of cancer, for which no effective way of treatment is available (1). Despite advances in the development of chemotherapeutic agents, including targeted

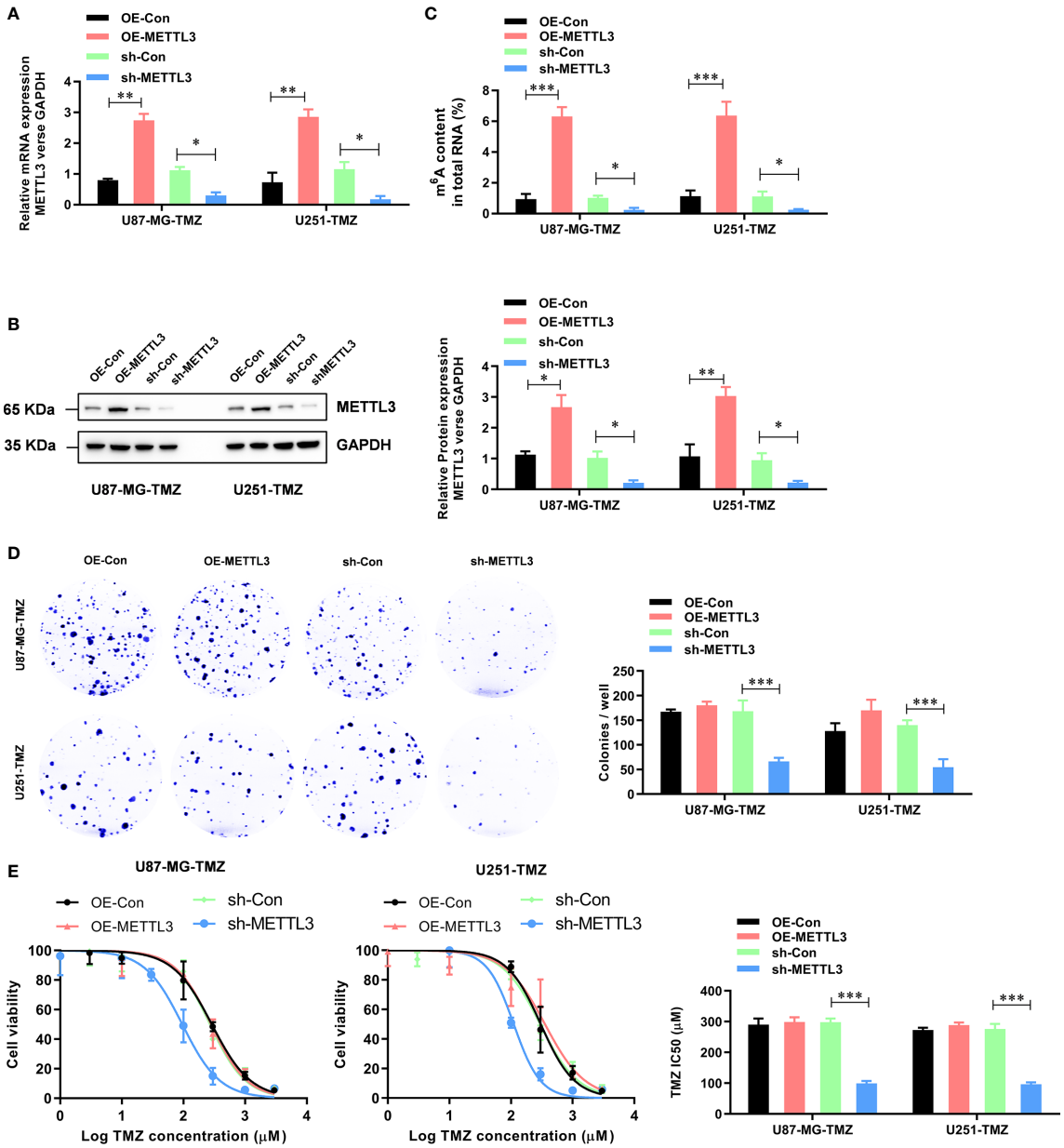

FIGURE 2 | METTL3 contributes to the TMZ resistance in GBM cells. **(A)** The efficiency of overexpression and knockdown on the mRNA levels of METTL3 were analyzed by qRT-PCR. **(B)** The efficiency of overexpression and knockdown on the protein levels of METTL3 were analyzed by western blot. **(C)** The effect of METTL3 overexpression and knockdown on the total m^{6}A RNA level was analyzed by the colorimetric m^{6}A quantification assay. **(D)** The effect of METTL3 overexpression and knockdown on the cell proliferation was analyzed by the colony formation assay. **(E)** The effect of METTL3 overexpression and knockdown on the sensitivity to TMZ was analyzed by CCK-8 assay. *$P < 0.05$, **$P < 0.01$, and ***$P < 0.001$ *versus* indicated control U87-MG/U251 cells.

therapies, the overall survival after diagnosis is usually less than two years (26, 27). Recent experimental and clinical studies have shown that epigenetic regulation of GBM also plays an important role in promoting tumorigenesis and the development of drug resistance (2, 28, 29). m^{6}A RNA methylation is an important RNA modification that has been shown to play an important role in the genesis and development of glioblastoma (30). In this study, we investigated the potential role of m^{6}A methylation modification in the regulation of TMZ resistance and the feasibility of using the M^{6}A inhibitor DAA as a therapeutic candidate.

In this study, we first analyzed the level of m^{6}A RNA methylation in TMZ-sensitive and TMZ-resistant GBM cells and critical role of a major m^{6}A methyltransferase METTL3 in TMZ resistance. METTL3 is an effective therapeutic target for various cancers, including pancreatic cancer (31), melanoma (32), colorectal cancer (33), and lung adenocarcinoma (16).

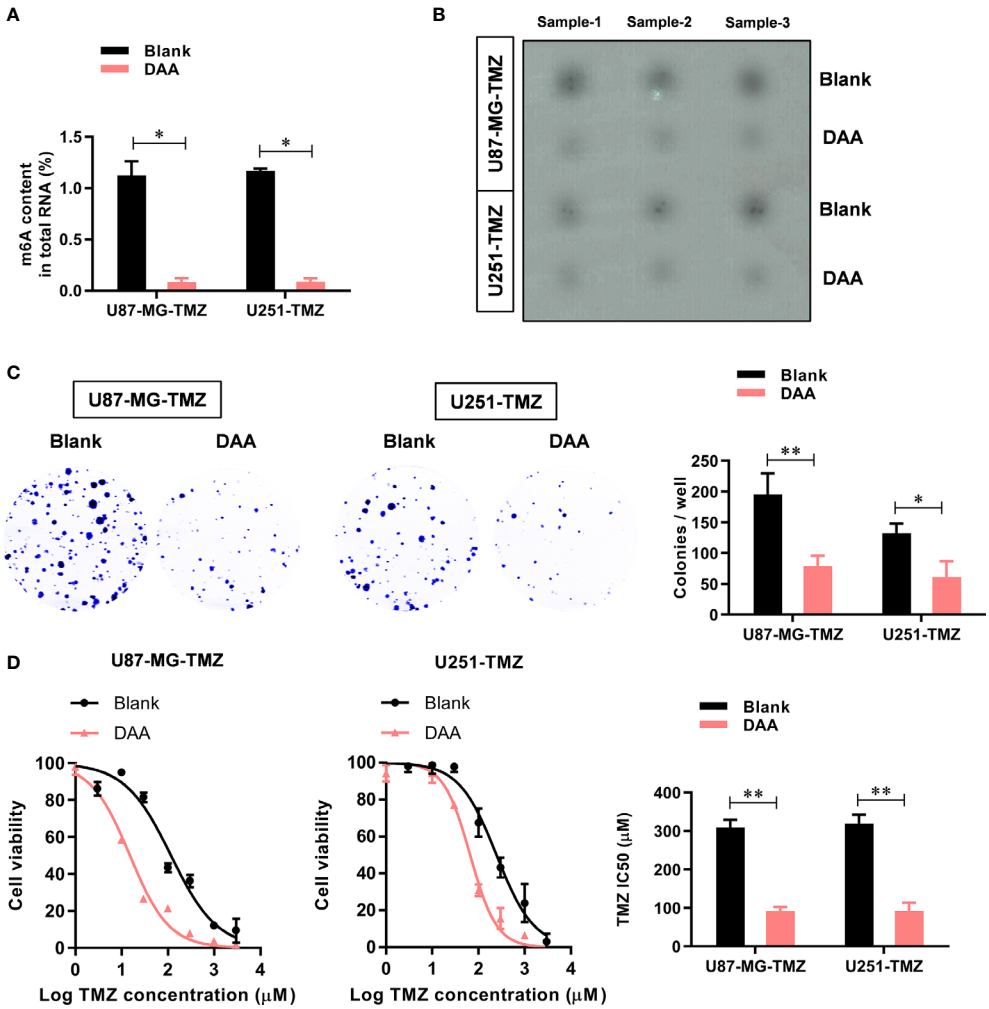

FIGURE 3 | METTL3-mediated m^{6}A modification contributes to the TMZ resistance. **(A)** The colorimetric m^{6}A quantification assay was used to examine the total m^{6}A levels in the control or DAA-treated U87-MG/U251-TMZ cells. **(B)** The dot blot was used to confirm the total m^{6}A levels in the control or DAA-treated U87-MG/U251-TMZ cells. **(C)** The effect of DAA treatment on the cell proliferation was analyzed by the colony formation assay. **(D)** The effect of DAA treatment on the sensitivity to TMZ was analyzed by CCK-8 assay. *$P < 0.05$ and **$P < 0.01$ *versus* blank U87-MG/U251 cells.

METTL3 is overexpressed in hepatic cancer cells (HCC), and is associated with poor prognosis (34). METTL3 is highly expressed in ovarian cancer, significantly correlating with ovarian cancer grade, PT status, PN/PM status, and FIGO staging (35). These studies suggest that METTL3 is a potential oncogene. METTL3 enhances the m^{6}A methylation by improving the stability of SOX2 in GBM, thereby promoting the stemness of glioma stem cells (GSCs) (25). Controversially, another team found that downregulation of METTL3 significantly promoted GSC self-renewal and tumorigenesis (36). In addition, ALKBH5 reduces m^{6}A modification in GSCs and plays an important role in tumorigenesis in the progression of GBM by regulating FOXM1 expression (37). These findings highlight the importance of modifying m^{6}A methylation in GBM progression. However, its role in TMZ resistance in GBM remains unclear. We found no significant difference in the METTL3 expression between normal and GBM tissues, and no association was observed between its expression level and the prognosis in GBM patients (GEPIA, data not shown). However, its expression is significantly elevated in TMZ-resistant GBM cells, compared to its parent TMZ-sensitive cells. Moreover, we verified the critical role of METTL3-mediated m^{6}A modification in TMZ resistance in GBM cells. Both METTL3 silencing or total methylation inhibition with DAA increased the sensitivity of GBM cells to TMZ *in vitro* and *in vivo*. Meanwhile, we discovered that METTL3 overexpression dramatically increased the m^{6}A methylation of MGMT and APNG, but did not affect the level of METTL14 (**Supplementary Figure 2**). However, METTL3 overexpression showed no effect on the colony formation of TMZ-resistant GBM cells, suggesting that a highly expressed and super-functional role of METTL3 in TMZ-resistant GBM cells, thus further overexpression of

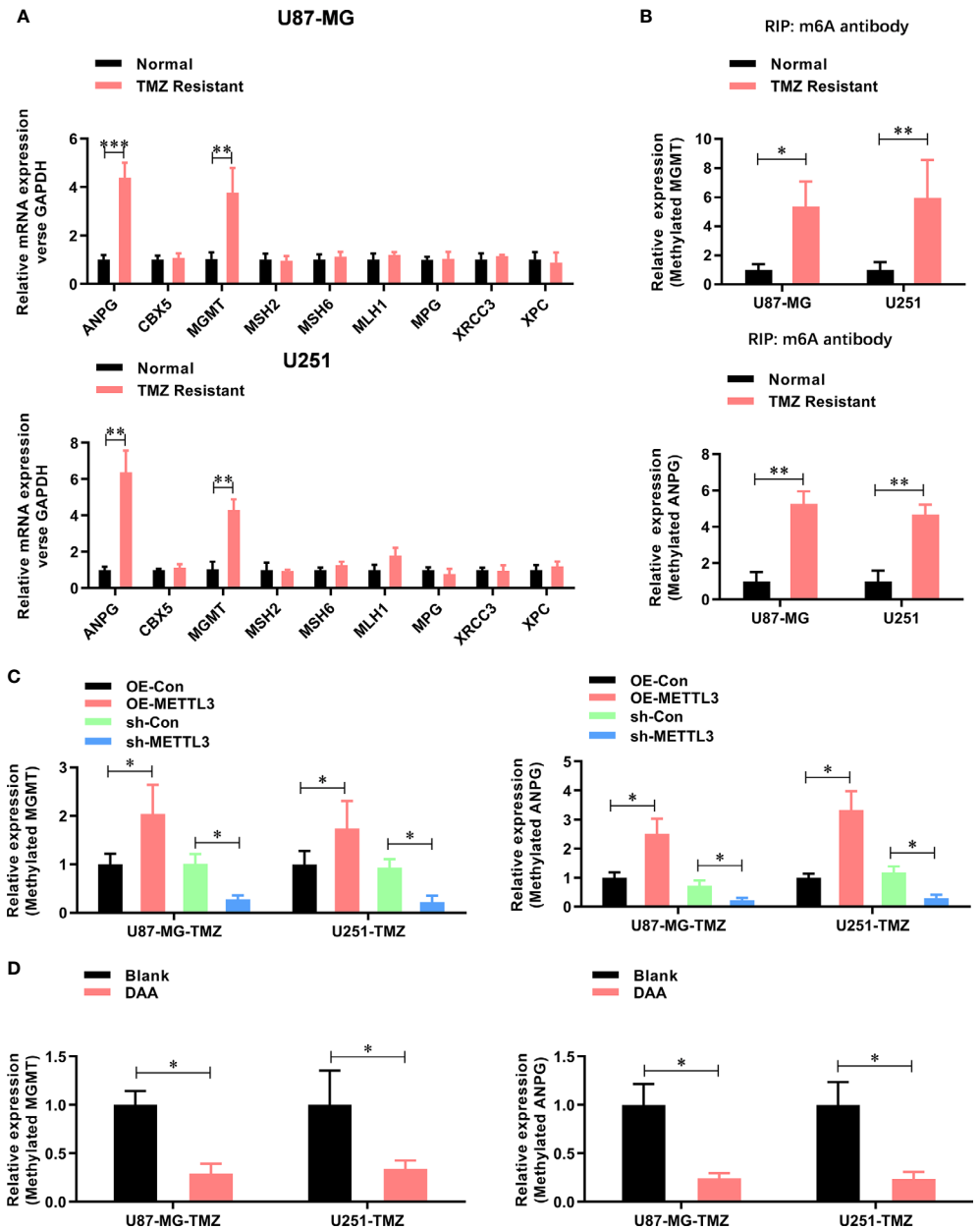

FIGURE 4 | METTL3 contributes to the TMZ resistance *via* m^{6}A modification of MGMT and ANPG mRNAs. **(A)** The expression mRNA level of TMZ resistant genes (ANPG, CBX5, MGMT, MSH2, MSH6, MLH1, MPG, XRCC3, and XPC) in normal and TMZ-resistant U87-MG/U251 cells were analyzed by real-time PCR. **(B)** The m^{6}A-methylated level of MGMT and ANPG in normal and TMZ resistant U87-MG/U251 cells were analyzed by Me-RIP-real-time PCR. **(C)** The effect of METTL3 overexpression and knockdown on the m^{6}A methylated level of MGMT and ANPG were analyzed by Me-RIP-real-time PCR. **(D)** The effect of DAA treatment on the m^{6}A-methylated level of MGMT and ANPG were analyzed by Me-RIP-real-time PCR. *$P < 0.05$ and **$P < 0.01$ *versus* indicated control U87-MG/U251 cells.

METTLE3 increased the total m^{6}A methylated mRNAs, but did not enhance the cell proliferation ability of TMZ-resistant GBM cells.

Considering the molecular mechanism underlying the resistance of glioma cells to TMZ, a DNA alkylation agent, is currently the only chemotherapeutic drug having some efficacy against GBM, accompanied by surgery and radiation therapy (28). In *in vitro* and animal models, TMZ resistance can be mediated by MGMT, a DNA repair protein that removes the methyl group produced by TMZ from the O6 site of guanine, which represents the most cytotoxic damage (13, 38). GBM patients with methylated MGMT promoter had an increased overall survival compared with radiotherapy alone, and responded better in combination with TMZ and radiotherapy (14). However, 50%

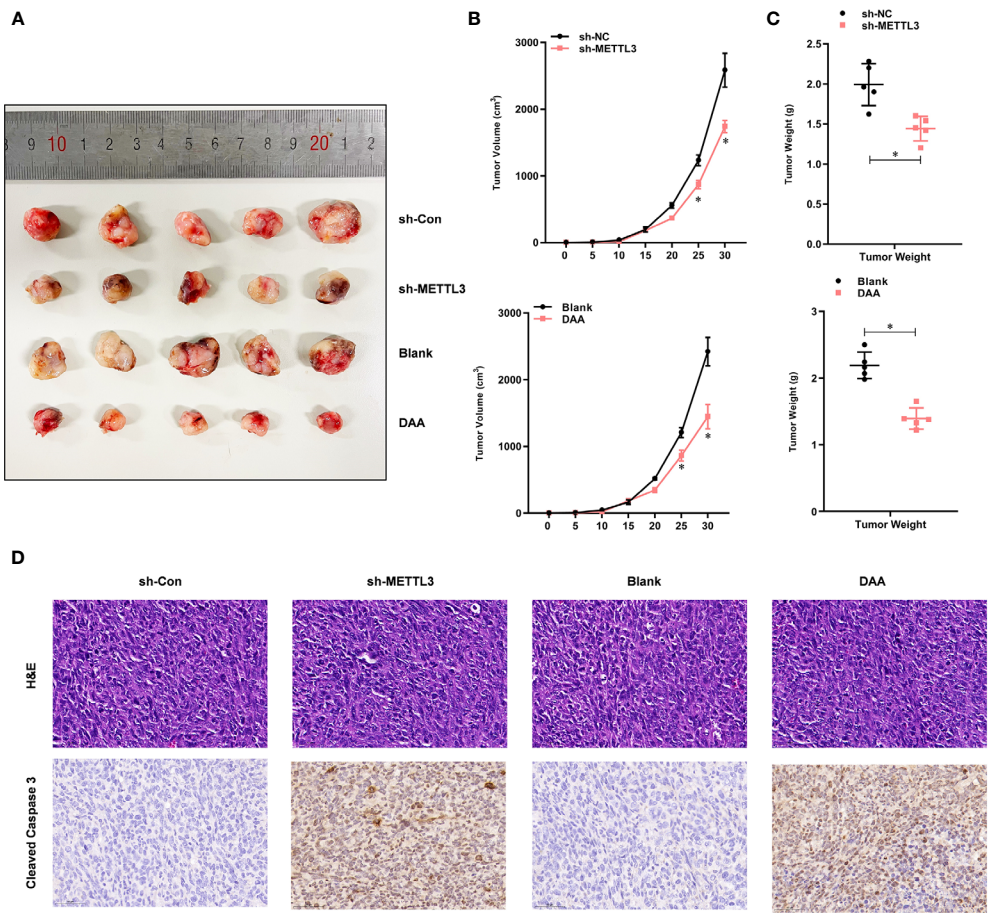

FIGURE 5 | METTL3-mediated m^{6}A modification contributes to the TMZ resistance in *vivo*. **(A)** Representative images of four groups of U87-MG-TMZ cells (shNC, shMETTL3, blank, and DAA)-derived subcutaneous tumors in the presence of TMZ. **(B)** Growth curve of tumor xenografts originated from four groups of U87-MG-TMZ cells (shNC, shMETTL3, blank, and DAA) in the presence of TMZ, **(C)** Weight of tumor xenografts originated from four groups of U87-MG-TMZ cells (shNC, shMETTL3, blank, and DAA) in the absence of TMZ. **(D)** IHC analysis of cleaved caspase-3 in tumor xenografts originated from four groups of U87-MG-TMZ cells (shNC, shMETTL3, blank, and DAA) in the presence of TMZ. *$P < 0.05$ *versus* indicated control U87-MG/U251 cells.

of GBM patients with MGMT methylation promoters do not survive for 2 years, and therefore receive only moderate benefits from TMZ treatment, suggesting additional resistance factors. Similarly, GBM patients with unmethylated MGMT also showed some response to TMZ, strongly suggesting that MGMT promoter methylation was not the only predictor of response to TMZ (39). In this study, we demonstrated that the expression of MGMT mRNA is also regulated by METTL3-mediated m^{6}A modification, which contributes to TMZ resistance. Moreover, our investigation into other DNA repair modulating systems, including GATA4-mediated TMZ sensitivity (40), showed increased levels of APNG in METTL3 over-expressed GBM cells. The m^{6}A or total mRNA levels of MGMT and APNG were elevated by METTL3 overexpression, whereas decreased by METTL3-silencing or DAA treatment. In summary, we have demonstrated that METTL3 promotes the TMZ resistance of glioma cells by increasing MGMT and ANPG in an m^{6}A-dependent manner.

DATA AVAILABILITY STATEMENT

The original contributions presented in the study are included in the article/**Supplementary Material**. Further inquiries can be directed to the corresponding author.

ETHICS STATEMENT

The animal study was reviewed and approved by The Ethics Committee of The Second Affiliated Hospital of Soochow University.

AUTHOR CONTRIBUTIONS

JS and GC were major contributors to the molecular experiments and manuscript writing. XD and HL performed statistical

analyses of the experimental data. SL and SC cultured the cells. YL and LW performed animal experiments. JY and ZQ reviewed the manuscript. JD designed and supervised the experiments. All authors contributed to the article and approved the submitted version.

FUNDING

1. The Natural Science Foundation of Jiangsu Province (grant no. BK20201172). 2. Clinical Special Disease Diagnosis and Treatment Technology in Suzhou (grant no. LCZX201807). 3. Key project of the Jiangsu Health Commission (ZDB2020016). 4. Young Talent Development Plan of Changzhou Health Commission (grant no. 2020-233-CZQM2020013).

SUPPLEMENTARY MATERIAL

The Supplementary Material for this article can be found online at: https://www.frontiersin.org/articles/10.3389/fonc.2021.702983/full#supplementary-material

Supplementary Figure 1 | Generation of TMZ-resistant U87-MG and U251 cell lines. TMZ-resistant cell lines were generated by exposure of U87-MG and U251 cells to 200 μM of TMZ for over 6 months. The derived resistant cell lines were designated as U87-MG-TMZ resistant and U251-TMZ resistant, respectively. The cell survival ratio and half maximal inhibitory concentration (IC_{50}) of TMZ for U87-MG and U251 was evaluated by CCK-8 assay.

Supplementary Figure 2 | METTL3 overexpression or knockdown did not affect the level of METTL14 in the TMZ-resistance GBM cells. **(A)** The mRNA level of METTL14 in the METTL3 overexpression or knockdown TMZ-resistance GBM cells were analyzed by qRT-PCR. **(B)** The protein level of METTL14 in the METTL3 overexpression or knockdown TMZ-resistance GBM cells were analyzed by western blot.

REFERENCES

1. Sung H, Ferlay J, Siegel RL, Laversanne M, Soerjomataram I, Jemal A, et al. Global Cancer Statistics 2020: GLOBOCAN Estimates of Incidence and Mortality Worldwide for 36 Cancers in 185 Countries. *CA Cancer J Clin* (2021) 71(3):209–49. doi: 10.3322/caac.21660
2. Phillips RE, Soshnev AA, Allis CD. Epigenomic Reprogramming as a Driver of Malignant Glioma. *Cancer Cell* (2020) 38(5):647–60. doi: 10.1016/j.ccell.2020.08.008
3. Sidaway P. Low-Grade Glioma Subtypes Revealed. *Nat Rev Clin Oncol* (2020) 17(6):335. doi: 10.1038/s41571-020-0380-4
4. Tan AC, Ashley DM, Lopez GY, Malinzak M, Friedman HS, Khasraw M. Management of Glioblastoma: State of the Art and Future Directions. *CA Cancer J Clin* (2020) 70(4):299–312. doi: 10.3322/caac.21613
5. Tuleasca C, Knisely J, Leroy HA, Hottinger AF, Peciu-Florianu I, Levivier M, et al. Glioma Patient-Reported Outcome Assessment in Clinical Care. *Lancet Oncol* (2020) 21(5):e230. doi: 10.1016/S1470-2045(20)30141-8
6. Chen X, Zhang M, Gan H, Wang H, Lee JH, Fang D, et al. A Novel Enhancer Regulates MGMT Expression and Promotes Temozolomide Resistance in Glioblastoma. *Nat Commun* (2018) 9(1):2949. doi: 10.1038/s41467-018-05373-4
7. Guo G, Gong K, Puliyappadamba VT, Panchani N, Pan E, Mukherjee B, et al. Efficacy of EGFR Plus TNF Inhibition in a Preclinical Model of Temozolomide-Resistant Glioblastoma. *Neuro Oncol* (2019) 21(12):1529–39. doi: 10.1093/neuonc/noz127
8. Lu C, Wei Y, Wang X, Zhang Z, Yin J, Li W, et al. DNA-Methylation-Mediated Activating of lncRNA SNHG12 Promotes Temozolomide Resistance in Glioblastoma. *Mol Cancer* (2020) 19(1):28. doi: 10.1186/s12943-020-1137-5
9. Meng X, Zhao Y, Han B, Zha C, Zhang Y, Li Z, et al. Dual Functionalized Brain-Targeting Nanoinhibitors Restrain Temozolomide-Resistant Glioma *via* Attenuating EGFR and MET Signaling Pathways. *Nat Commun* (2020) 11(1):594. doi: 10.1038/s41467-019-14036-x
10. Wu L, Bernal GM, Cahill KE, Pytel P, Fitzpatrick CA, Mashek H, et al. BCL3 Expression Promotes Resistance to Alkylating Chemotherapy in Gliomas. *Sci Transl Med* (2018) 10(448):eaar2238. doi: 10.1126/scitranslmed.aar2238
11. Yi GZ, Huang G, Guo M, Zhang X, Wang H, Deng S, et al. Acquired Temozolomide Resistance in MGMT-Deficient Glioblastoma Cells Is Associated With Regulation of DNA Repair by DHC2. *Brain* (2019) 142(8):2352–66. doi: 10.1093/brain/awz202
12. Agnihotri S, Gajadhar AS, Ternamian C, Gorlia T, Diefes KL, Mischel PS, et al. Alkylpurine-DNA-N-Glycosylase Confers Resistance to Temozolomide in Xenograft Models of Glioblastoma Multiforme and Is Associated With Poor Survival in Patients. *J Clin Invest* (2012) 122(1):253–66. doi: 10.1172/JCI59334
13. Bell EH, Zhang P, Fisher BJ, Macdonald DR, McElroy JP, Lesser GJ, et al. Association of MGMT Promoter Methylation Status With Survival Outcomes in Patients With High-Risk Glioma Treated With Radiotherapy and Temozolomide: An Analysis From the NRG Oncology/RTOG 0424 Trial. *JAMA Oncol* (2018) 4(10):1405–9. doi: 10.1001/jamaoncol.2018.1977
14. Lee SY. Temozolomide Resistance in Glioblastoma Multiforme. *Genes Dis* (2016) 3(3):198–210. doi: 10.1016/j.gendis.2016.04.007
15. Frye M, Harada BT, Behm M, He C. RNA Modifications Modulate Gene Expression During Development. *Science* (2018) 361(6409):1346–9. doi: 10.1126/science.aau1646
16. Lin S, Choe J, Du P, Triboulet R, Gregory RI. The M(6)A Methyltransferase METTL3 Promotes Translation in Human Cancer Cells. *Mol Cell* (2016) 62(3):335–45. doi: 10.1016/j.molcel.2016.03.021
17. Dominissini D, Moshitch-Moshkovitz S, Schwartz S, Salmon-Divon M, Ungar L, Osenberg S, et al. Topology of the Human and Mouse M6a RNA Methylomes Revealed by M6a-Seq. *Nature* (2012) 485(7397):201–6. doi: 10.1038/nature11112
18. Akichika S, Hirano S, Shichino Y, Suzuki T, Nishimasu H, Ishitani R, et al. Cap-Specific Terminal N (6)-Methylation of RNA by an RNA Polymerase II-Associated Methyltransferase. *Science* (2019) 363(6423):eaav0080. doi: 10.1126/science.aav0080
19. Wang H, Hu X, Huang M, Liu J, Gu Y, Ma L, et al. Mettl3-Mediated mRNA M(6)A Methylation Promotes Dendritic Cell Activation. *Nat Commun* (2019) 10(1):1898. doi: 10.1038/s41467-019-09903-6
20. Winkler R, Gillis E, Lasman L, Safra M, Geula S, Soyris C, et al. M(6)A Modification Controls the Innate Immune Response to Infection by Targeting Type I Interferons. *Nat Immunol* (2019) 20(2):173–82. doi: 10.1038/s41590-018-0275-z
21. Liu J, Harada BT, He C. Regulation of Gene Expression by N(6)-Methyladenosine in Cancer. *Trends Cell Biol* (2019) 29(6):487–99. doi: 10.1016/j.tcb.2019.02.008
22. Pan Y, Ma P, Liu Y, Li W, Shu Y. Multiple Functions of M(6)A RNA Methylation in Cancer. *J Hematol Oncol* (2018) 11(1):48. doi: 10.1186/s13045-018-0590-8
23. Wang S, Chai P, Jia R, Jia R. Novel Insights on M(6)A RNA Methylation in Tumorigenesis: A Double-Edged Sword. *Mol Cancer* (2018) 17(1):101. doi: 10.1186/s12943-018-0847-4
24. Visvanathan A, Patil V, Abdulla S, Hoheisel JD, Somasundaram K. N(6)-Methyladenosine Landscape of Glioma Stem-Like Cells: METTL3 Is Essential for the Expression of Actively Transcribed Genes and Sustenance of the Oncogenic Signaling. *Genes (Basel)* (2019) 10(2):141. doi: 10.3390/genes10020141
25. Visvanathan A, Patil V, Arora A, Hegde AS, Arivazhagan A, Santosh V, et al. Essential Role of METTL3-Mediated M(6)A Modification in Glioma Stem-Like Cells Maintenance and Radioresistance. *Oncogene* (2018) 37(4):522–33. doi: 10.1038/onc.2017.351
26. Cheng X, Geng F, Pan M, Wu X, Zhong Y, Wang C, et al. Targeting DGAT1 Ameliorates Glioblastoma by Increasing Fat Catabolism and Oxidative Stress. *Cell Metab* (2020) 32(2):229–42.e8. doi: 10.1016/j.cmet.2020.06.002
27. Gao X, Li S, Ding F, Liu X, Wu Y, Li J, et al. A Virus-Mimicking Nucleic Acid Nanogel Reprograms Microglia and Macrophages for Glioblastoma Therapy. *Adv Mater* (2021) 33(9):e2002116. doi: 10.1002/adma.202006116
28. Kamson DO, Grossman SA. The Role of Temozolomide in Patients With Newly Diagnosed Wild-Type IDH, Unmethylated MGMTp Glioblastoma During the COVID-19 Pandemic. *JAMA Oncol* (2021) 7(5):675–6. doi: 10.1001/jamaoncol.2020.6732

29. Luo X, Weiss WA. Utility of Human-Derived Models for Glioblastoma. *Cancer Discov* (2020) 10(7):907–9. doi: 10.1158/2159-8290.CD-20-0493
30. Dixit D, Prager BC, Gimple RC, Poh HX, Wang Y, Wu Q, et al. The RNA M6a Reader YTHDF2 Maintains Oncogene Expression and Is a Targetable Dependency in Glioblastoma Stem Cells. *Cancer Discov* (2021) 11(2):480–99. doi: 10.1158/2159-8290.CD-20-0331
31. Zhang J, Bai R, Li M, Ye H, Wu C, Wang C, et al. Excessive miR-25-3p Maturation *via* N(6)-Methyladenosine Stimulated by Cigarette Smoke Promotes Pancreatic Cancer Progression. *Nat Commun* (2019) 10(1):1858. doi: 10.1038/s41467-019-09712-x
32. Wang L, Hui H, Agrawal K, Kang Y, Li N, Tang R, et al. M(6) A RNA Methyltransferases METTL3/14 Regulate Immune Responses to Anti-PD-1 Therapy. *EMBO J* (2020) 39(20):e104514. doi: 10.15252/embj.2020104514
33. Li T, Hu PS, Zuo Z, Lin JF, Li X, Wu QN, et al. METTL3 Facilitates Tumor Progression *via* an M(6)A-IGF2BP2-Dependent Mechanism in Colorectal Carcinoma. *Mol Cancer* (2019) 18(1):112. doi: 10.1186/s12943-019-1038-7
34. Zuo X, Chen Z, Gao W, Zhang Y, Wang J, Wang J, et al. M6A-Mediated Upregulation of LINC00958 Increases Lipogenesis and Acts as a Nanotherapeutic Target in Hepatocellular Carcinoma. *J Hematol Oncol* (2020) 13(1):5. doi: 10.1186/s13045-019-0839-x
35. Liang S, Guan H, Lin X, Li N, Geng F, Li J. METTL3 Serves an Oncogenic Role in Human Ovarian Cancer Cells Partially *via* the AKT Signaling Pathway. *Oncol Lett* (2020) 19(4):3197–204. doi: 10.3892/ol.2020.11425
36. Cui Q, Shi H, Ye P, Li L, Qu Q, Sun G, et al. M(6)A RNA Methylation Regulates the Self-Renewal and Tumorigenesis of Glioblastoma Stem Cells. *Cell Rep* (2017) 18(11):2622–34. doi: 10.1016/j.celrep.2017.02.059
37. Zhang S, Zhao BS, Zhou A, Lin K, Zheng S, Lu Z, et al. M(6)A Demethylase ALKBH5 Maintains Tumorigenicity of Glioblastoma Stem-Like Cells by Sustaining FOXM1 Expression and Cell Proliferation Program. *Cancer Cell* (2017) 31(4):591–606.e6. doi: 10.1016/j.ccell.2017.02.013
38. Lamba N, Chukwueke UN, Smith TR, Ligon KL, Aizer A, Reardon DA, et al. Socioeconomic Disparities Associated With MGMT Promoter Methylation Testing for Patients With Glioblastoma. *JAMA Oncol* (2020) 6(12):1972–4. doi: 10.1001/jamaoncol.2020.4937
39. Killock D. Lomustine-Temozolomide Combination Efficacious in Newly Diagnosed Glioblastoma. *Nat Rev Clin Oncol* (2019) 16(5):273. doi: 10.1038/s41571-019-0192-6
40. Fosmark S, Hellwege S, Dahlrot RH, Jensen KL, Derand H, Lohse J, et al. APNG as a Prognostic Marker in Patients With Glioblastoma. *PloS One* (2017) 12(6):e0178693. doi: 10.1371/journal.pone.0178693

Conflict of Interest: The authors declare that the research was conducted in the absence of any commercial or financial relationships that could be construed as a potential conflict of interest.

frontiers in Oncology

ORIGINAL RESEARCH
published: 09 August 2021
doi: 10.3389/fonc.2021.710695

Single-Cell Transcriptomics of Glioblastoma Reveals a Unique Tumor Microenvironment and Potential Immunotherapeutic Target Against Tumor-Associated Macrophage

Xiaoteng Cui[1], Qixue Wang[1], Junhu Zhou[1], Yunfei Wang[1], Can Xu[2], Fei Tong[1], Hongjun Wang[3] and Chunsheng Kang[1]**

[1] Lab of Neuro-oncology, Tianjin Neurological Institute, Key Laboratory of Post-Neuroinjury Neuro-repair and Regeneration in Central Nervous System, Department of Neurosurgery, Tianjin Medical University General Hospital, Tianjin, China, [2] Department of Neurosurgery, Affiliated Hospital of Hebei University, Baoding, China, [3] Department of Neurosurgery, The Second Affiliated Hospital of Harbin Medical University, Harbin, China

OPEN ACCESS

Edited by:
Aleksi Sedo,
Charles University, Czechia

Reviewed by:
Zuzana Saidak,
University Hospital Center (CHU) of Amiens, France
Jason M. Miska,
Northwestern University, United States

***Correspondence:**
Chunsheng Kang
kang97061@tmu.edu.cn
Hongjun Wang
wanghongjun8000@sina.com

Specialty section:
This article was submitted to Neuro-Oncology and Neurosurgical Oncology, a section of the journal Frontiers in Oncology

Received: 17 May 2021
Accepted: 09 July 2021
Published: 09 August 2021

Citation:
Cui X, Wang Q, Zhou J, Wang Y, Xu C, Tong F, Wang H and Kang C (2021) Single-Cell Transcriptomics of Glioblastoma Reveals a Unique Tumor Microenvironment and Potential Immunotherapeutic Target Against Tumor-Associated Macrophage. Front. Oncol. 11:710695. doi: 10.3389/fonc.2021.710695

Background: The main immune cells in GBM are tumor-associated macrophages (TAMs). Thus far, the studies investigating the activation status of TAM in GBM are mainly limited to bulk RNA analyses of individual tumor biopsies. The activation states and transcriptional signatures of TAMs in GBM remain poorly characterized.

Methods: We comprehensively analyzed single-cell RNA-sequencing data, covering a total of 16,201 cells, to clarify the relative proportions of the immune cells infiltrating GBMs. The origin and TAM states in GBM were characterized using the expression profiles of differential marker genes. The vital transcription factors were examined by SCENIC analysis. By comparing the variable gene expression patterns in different clusters and cell types, we identified components and characteristics of TAMs unique to each GBM subtype. Meanwhile, we interrogated the correlation between SPI1 expression and macrophage infiltration in the TCGA-GBM dataset.

Results: The expression patterns of TMEM119 and MHC-II can be utilized to distinguish the origin and activation states of TAMs. In TCGA-Mixed tumors, almost all TAMs were bone marrow-derived macrophages. The TAMs in TCGA-proneural tumors were characterized by primed microglia. A different composition was observed in TCGA-classical tumors, which were infiltrated by repressed microglia. Our results further identified SPI1 as a crucial regulon and potential immunotherapeutic target important for TAM maturation and polarization in GBM.

Conclusions: We describe the immune landscape of human GBM at a single-cell level and define a novel categorization scheme for TAMs in GBM. The immunotherapy against

SPI1 would reprogram the immune environment of GBM and enhance the treatment effect of conventional chemotherapy drugs.

Keywords: immune landscape, glioblastoma, single-cell RNA sequencing, macrophage polarization, SPI1

INTRODUCTION

Glioblastoma (GBM), which comprises grade IV gliomas, is a notoriously malignant brain tumor with high inter- and intratumoral heterogeneity (1, 2). Based on integrated genomic analysis from both bulk RNA sequencing and single-cell RNA sequencing (scRNA-seq) of GBM tumors, four distinct molecular subtypes have been described. These subtypes (referred to as classical, neural, proneural, and mesenchymal) were defined based on unique characteristics regarding DNA copy number variations, somatic mutations, and transcriptional profiles (3–6). The subtypes have also been identified in different regions of the same tumor, suggesting that the original tumor included a combination of various cells with distinct transcriptomic features (7, 8). Genetic mutations, epigenetic alterations, and differing tumor microenvironments alter the cellular character of GBM and drive its heterogeneity, and are among the primary reasons for the dismal prognosis and inevitable therapeutic resistance of this cancer (9, 10). The standard treatment for GBM is extensive surgery resection, followed by adjuvant radiotherapy and chemotherapy with temozolomide. However, the clinical efficacy of this regimen is still limited, and the median survival of GBM patients is less than 1½ years (1, 11, 12). Recently, various immunotherapies directed towards different targets, especially the programmed cell death protein 1 (PD-1)/PD-1 ligand (PD-L1) pathway, have been revealed as favorable strategies to treat several tumor types, such as melanoma and non-small-cell lung cancer (13, 14). However, contrary to expectations, the treatment of GBM with a PD-1 inhibitor did not yield a satisfactory response (15, 16). As the nature of the immune cells involved in GBM correspond with treatment efficacy, it is critical to illustrate the GBM immune environment by clarifying the orientation and state of tumor-infiltrated immune cells and characterizing their transcriptomic features.

The tumor microenvironment contains complex cellular components, including non-neoplastic cells such as myeloid cells and lymphocytes (17, 18). In GBM, the majority of immune cells are tumor-associated macrophages (TAMs), which comprise 30–40% of the cell mass, whereas T cells account for less than 0.23% of the total cell count (19, 20). TAMs in GBM consist of two different cell populations: resident microglia, which arise during brain development (21), and bone marrow–derived macrophages that infiltrate the tumor *via* blood vessels (22). However, the activation states and transcriptional features of immune cells in GBM remain unclear.

scRNA-seq has been widely used to comprehensively characterize gene expression at the level of individual cells, and it has been employed to analyze intratumoral heterogeneity in glioma (23). In the present study, we analyzed data from scRNA-seq that was performed using tissue from nine glioblastomas, covering 16,201 cells in total. These data were integrated to depict the immune landscape of glioblastoma at the single-cell level. Primed and repressed TAM states were defined based on the expression profiles of key genes. By comparing variable gene expression and regulons in different clusters and cell types, we not only identified components and characteristics unique to each GBM subtype but also discovered a potential immunotherapeutic target for GBM, Spleen Focus Forming Virus Proviral Integration Oncogene (*SPI1*), which is expressed in TAM and essential for macrophage maturation and polarization, and correlated with tumor grades and poor prognosis.

MATERIALS AND METHODS

Acquisition of scRNA-Seq Datasets

Normalized expression matrices processed as Transcripts Per Kilobase of exon model per Million mapped reads (TPM) from scRNA-seq performed using a 10 × genomics platform were downloaded from the Gene Expression Omnibus (GEO) (https://www.ncbi.nlm.nih.gov/geo/) database. The sequencing analyses were conducted on samples from nine fresh GBM tumors from adult patients in Massachusetts General Hospital (MGH) (GSE131928) (4). A total of 16,201 cells were acquired. A seurat file was created by importing the expression matrix data into the version 3.6.2 R studio program and saving the data in RDS format.

Dimensionality Reduction and Unsupervised Clustering

The data were normalized using the global-scaling method "LogNormalize" and preprocessing the data by linear conversion. To detect the most variable genes used for dimensionality reduction, we employed the "FindVariableFeatures" function in R studio. Next, we utilized PCA to reduce the dimensional linearity based on the variable genes. JackStraw plots and Elbow plots were used to decide the number of dimensionalities. Finally, graph-based unsupervised clustering was conducted and visualized using a non linear t-SNE plot, with a resolution of 0.4, defined by the functions of "FindNeighbors" and "FindClusters". All the operations were processed by using the seurat R package in R studio.

Identification of Cell Types and Marker Genes in Different Clusters

To identify the cell types, we first analyzed the Spearman correlation coefficient between the transcriptomes of each cell across all nine tumors in our dataset and each cell type-specific gene expression profile in the HPCA reference set using SingleR package. Then, the expression levels of distinct cell type-specific marker genes based on the CellMarker databases (24) were utilized to further confirm the

cell types. Markers for macrophage were *C1QA*, *C1QB*, *C1QC*, *TYROBP*, and *CD68*. For T lymphocyte, the markers were *CD3G*, *GZMH*, *IL2RB*, *PRF1*, and *ICOS*. *TMEM119* was employed to distinguish the microglia from TAM clusters. The relatively positive expressions of *MHC-II molecules* in TAMs were considered as distinct features of primed state. The cell type information was visualized by t-SNE plot in R studio.

The marker genes of distinct clusters were identified using the "FindAllMarkers" function of the seurat package and visualized as a heat map, violin plots, and feature plots using the ggplot2 package in R studio. The positive percentage of the cells where the gene is defined as the marker is at least 25%.

Identification of Gene Regulatory Network and Specific Transcription Factors

The gene regulatory network and specific transcription factors were identified by employing the Single Cell Regulatory Network Inference and Clustering (SCENIC) tool (25) using default parameters. The SCENIC analysis was run as described on the cells that passed the filtering using the 20,000 motifs database for RcisTarget and GRNboost R packages. The regulated genes and AUCell score of each transcription factor were calculated to estimate the specificity to each cell type. The AUCell scores were visualized by t-SNE plot and heat map. The top three regulons in each cell type were acquired by calculating the RSS. The relationships among transcription factors were shown in heat map by connection specificity index (CSI).

KEGG Pathway Analysis

DAVID (https://david.ncifcrf.gov/) is an open website providing a comprehensive set of functional annotation tools to extrapolate biological meaning from an extensive list of genes. Using DAVID, we identified the main cellular physiological activities reflected by the top 500 differentially expressed genes of each cluster. The KEGG pathways were displayed as a bubble plot by the ggplot2 package in R studio.

Gene Expression Analysis

The expression data of SPI1 and the clinical information of glioma samples were obtained from TCGA, CGGA (26), and Rembrandt databases. The data were sorted into three subgroups according to the WHO grade and used to calculate the mean and 95% confidence interval (CI) of SPI1 expression. The results were visualized as scatter plots.

Correlation Analysis

We utilized TIMER2.0 (Tumor Immune Estimation Resource version 2.0) online web (http://timer.cistrome.org/) (27) to analyze the correlation between the expression of SPI1 and other genes. We input "SPI1" in the "Interested Gene" search box of the "Cene_Corr" module in TIMER2.0 and "C1QA", "C1QB", "C1QC", "SRGN", "TYROBP", "GAP43", "GPM6B", "SEC61G", "PTN", "CX3CR1", "CSF1R", and "IRF8" in the "Gene Expression" box, and obtained the correlation in all tumor types. We picked up the GBM results and saved the scatter plots with rho and p value.

Tumor Purity and Survival Prognosis Analysis

The tumor purity, macrophage infiltration, and survival prognosis analysis were performed as previously described (28).

RESULTS

scRNA Sequencing Reveals the Unique Immune Landscape of Human GBM at a Single-Cell Level

To examine the immune microenvironment of GBM, we obtained 10 × Genomics scRNA sequencing datasets derived from fresh GBM tissues that spanned nine patients, accessed from the Gene Expression Omnibus (GEO) database (accession number GSE131928) (4). A total of nine datasets were integrated and comprehensively analyzed to assess GBM heterogeneity and determine the nature of various associated immune microenvironments. We used t-distributed stochastic neighbor embedding (t-SNE), the unsupervised non linear dimensionality reduction algorithm, to differentiate cell types based on their relative gene expression values. Overall, single-cell transcriptomes for a total of 16,201 cells were retained after initial quality controls and were differentiated into 22 different clusters (cluster 0~-21), visualized as bidimensional t-SNE maps (**Figure S1A**). The distribution of each dataset is displayed in **Figure S1B**. The clusters were sorted into four main cell types by comparing their gene expression characteristics for tumor (light gray), macrophages (green), microglia (blue), and T lymphocyte (purple) (**Figure 1A**). Surprisingly, the number of malignant cells (tumor) accounted for 62.31% (10,095 cells) of the cell population, suggesting that numerous tumor-associated non-malignant cells are a prominent feature of the GBM microenvironment. We observed that TAMs (macrophage and microglia) comprised 36.39% of the tumor tissue cells (the numbers of macrophage and microglia were 3,288 and 2,608 cells, respectively), and the percentage of T cells was only 1.30% (210 cells) of the total cell count (**Figure 1B**). The percentages of cell types in each sample are shown in **Figure S2**.

Heat mapping was performed to examine the expression levels of the top 10 genes in the different clusters. As shown in **Figure 1C** and **Table S1**, each cluster displayed distinct gene expression features. The clusters in the TAM group (particularly clusters 2, 3, 6, 7, 9, and 19) shared a number of similar marker genes, such as complement c1q C chain (*C1QC*), complement c1q B chain (*C1QB*), *Metallothionein 1G* (*MT1G)*, serglycin (*SRGN*), c-c motif chemokine ligand 3 like 3 (*CCL3L3*), major histocompatibility complex class II DR beta 5 (*HLA-DRB5*), and s100 calcium binding protein A8 (*S100A8*). By analyzing the expression of different genes, we observed that TAMs could be identified by the expression of Arachidonate 5-Lipoxygenase Activating Protein (*ALOX5AP*), complement c1q A chain (*C1QA*), *C1QB*, *C1QC*, *SRGN*, and TYRO protein tyrosine kinase binding protein (*TYROBP*), whereas malignant cells expressed the marker genes growth-associated protein 43 (*GAP43*), glycoprotein M6B (*GPM6B*), SEC61 translocon subunit gamma (*SEC61G*), and pleiotrophin (*PTN*)

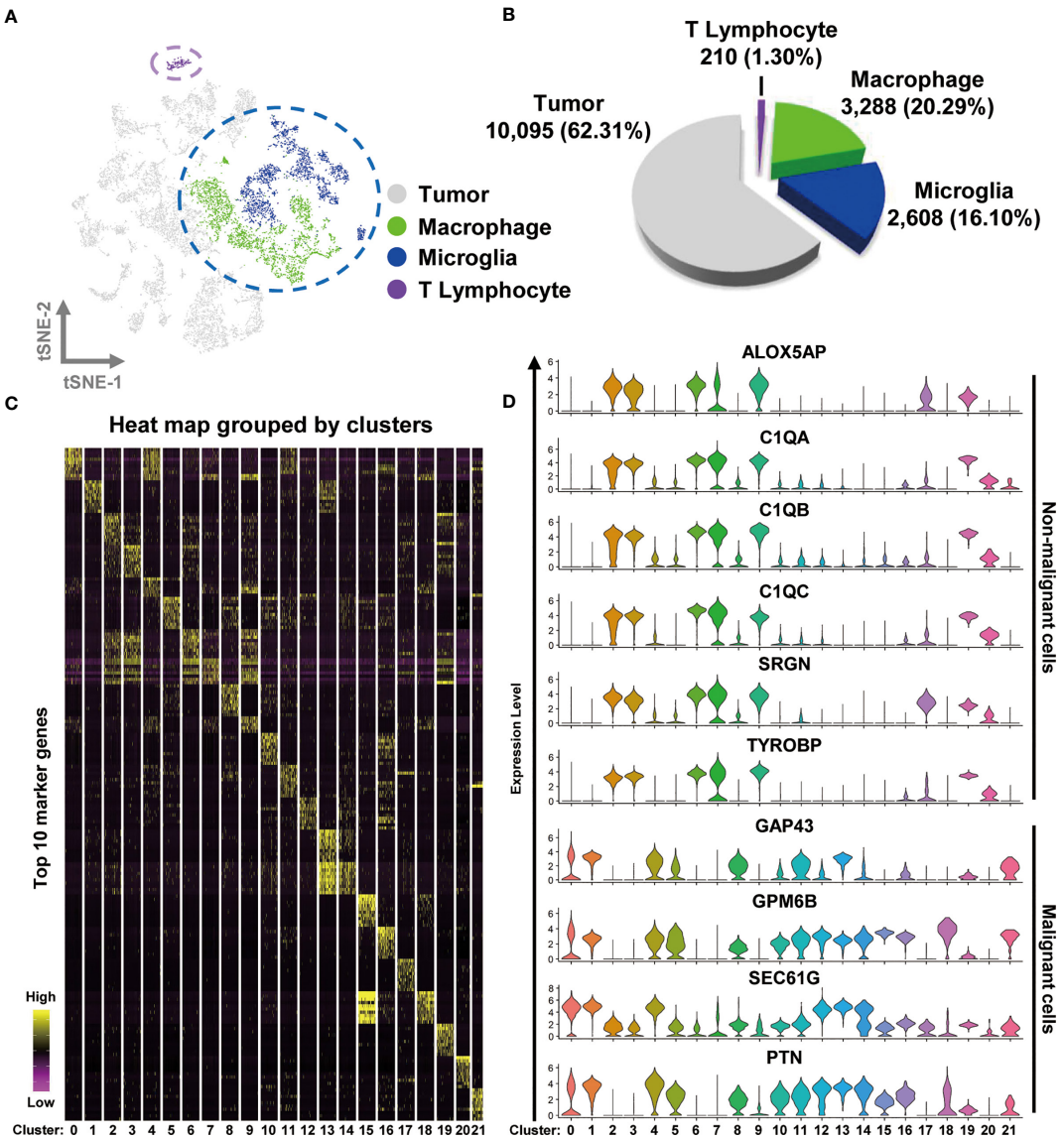

FIGURE 1 | Integrated scRNA-seq analysis from human GBM biopsies. **(A)** A total of 16,201 cells from nine datasets of fresh GBM tissues are visualized by the t-SNE plot. Distinct cell types are represented as follows: light gray indicates tumor cells, green indicates macrophages, cyan indicates microglia, and purple indicates T lymphocytes. **(B)** A pie chart illustrates the proportions of each cell type. **(C)** The expression profiles of the top 10 marker genes of each cluster are displayed as a heat map. **(D)** Distributions of malignant and non malignant cell marker genes are shown as violin plots.

(**Figure 1D**). The non malignant cells were differentiated into T cells and TAMs by the expression of the genes CD3 gamma chain (*CD3G*), granzyme H (*GZMH*), interleukin 2 receptor subunit beta (*IL2RB*), perforin 1 (*PRF1*), and inducible T cell costimulator (*ICOS*) (**Figure S1C**). The non malignant and malignant cells were also easily separated in bidimensional PC maps, which rely on linear principal component analysis (PCA) to reduce dimensionality (**Figure S1D**).

Altogether, our data suggest that TAMs are the most common immune cell type in GBM, comprising over half of the tumor cell population.

Primed and Repressed States of Macrophages/Microglia Characterize the Immune Microenvironment in GBM

To comprehensively characterize the signatures of TAMs in GBM, we subclustered and re analyzed the cells in the macrophage and microglia group. In total, 5,896 cells were sorted and hierarchically sorted into 14 clusters (**Figure S3A**). *CD68* has been widely recognized as a pan-macrophage marker, and we therefore used feature and violin plots to visualize the expression and distribution of *CD68* in these clusters. As shown in **Figures S3B, C**, *CD68* was highly expressed in almost every

cluster, except for cluster 12, which may be tumor cells misdefined as TAMs according to the gene signature above. Then, we further analyzed the *CD68*-positive clusters, which we considered to be TAMs. The macrophage compartment in GBM contains both brain-resident microglia and bone marrow–derived macrophages. *TMEM119* is a reliable microglia marker that discriminates inherent and extrinsic macrophages in the brain (29). Using the violin plot of *TMEM119* expression, we separated the macrophage clusters into two groups. The *TMEM119*-positve clusters (clusters 4, 5, 6, 7, 10, and 11) were identified as resident microglia, and the *TMEM119*-negative clusters (clusters 0, 1, 2, 3, 8, 9, and 13) were defined as bone marrow–derived macrophages (**Figure S3D**). By examining the marker genes defining the *TMEM119*-positive clusters, we selected cytoplasmic fmr1 interacting protein 1 (*CYFIP1*), ectonucleoside triphosphate diphosphohydrolase 1 (*ENTPD1*), and vav guanine nucleotide exchange factor 1 (*VAV1*) as possible microglia marker genes (**Figure S3D**). MHCII is a glycoprotein present on specialized antigen-presenting cells, including macrophages. The elevated expression of MHCII indicates that macrophages have transitioned to a primed state, in which they have acquired the ability to present tumor-specific antigens (30). Macrophages otherwise maintain a repressed state. We therefore examined the expression of *MHCII* by assessing the levels of the human genes, which were HLA-DQ alpha 2 (*HLA-DQA2*) and HLA-DQ beta 2 (*HLA-DQB2*). As shown in **Figure S2E**, HLA-positive expression was confined to clusters 1, 2, 4 5, 6, 8, and 9. Together with their expression of *TMEM119*, the cells were subdivided into four distinct groups as follows: $TMEM119^{+}$-HLA^{+} cells (clusters 4, 5, and 6), $TMEM119^{+}$-HLA^{-} cells (clusters 7, 10, and 11), $TMEM119^{-}$-HLA^{+} cells (clusters 1, 2, 8, and 9), and $TMEM119^{-}$$HLA^{-}$ cells (clusters 0, 3, and 13) (**Figure S3F**).

Next, we wished to determine the precise nature and activation status of TAMs in GBM. In our analysis of the distinctive gene expression profiles of microglia, we found that the cell population of cluster 11 charactered by matrix metallopeptidase 9 (MMP9), MMP25, and periostin (POSTN), which are associated with cell migration, should be more likely microglia with naïve status as an immunological defender in the brain, which has migration and chemotaxis ability. We defined cells with this expressions profile as "microglia: unactivated". Similarly, the expression of cytokine-like 1 (CYTL1) and early growth response 3 (EGR3) were used to define primed microglia. Interferon-induced protein with tetratricopeptide repeats 3 (IFIT3) and interferon alpha inducible protein 27 (IFI27) distinguished microglia in the repressed state. The gene profile analysis of macrophages suggested that cluster 8 represented priming macrophages, owing to the expression of cell cycle-associated genes [aurora kinase B (AURKB), cell division cycle associated 3 (CDCA3), and assembly factor for spindle microtubules (ASPM)]. HLA-positive macrophages could be classified as primed, and HLA-negative macrophages (with the exception of cluster 8) were categorized as repressed, due to the expression of MT1G and ankyrin repeat domain 28 (ANKRD28) (**Figures S4A, B**).

With all of the above characteristics in mind, we redefined the original 14 clusters as seven distinct subsets by comparing the expression of *TMEM119* and *MHCII* with the expression profiles of different clusters (**Figures 2A** and **S4C**). TAMs in GBM consist primarily of bone marrow–derived macrophages, accounting for 60.28% of the cell population, of which 4.55% are undergoing priming, 27.51% are in the primed state, and 28.22% are repressed. Of the remaining cell population, 37.57% consists of resident microglia in unactivated (2.17%), primed (23.74%), and repressed states (11.65%) (**Figure 2B**).

The Orientation and Status of TAM in Different Subtypes of GBM Are Distinctive

To investigate the relationship between the infiltrated TAMs and different GBM subtypes, we assessed the distribution of the cells covered by the nine tumor datasets and selected the MGH105 (40.28%), MGH124 (18.00%), and MGH115 (9.94%) datasets for analysis, as together they covered over half of the total cell number and seven different clusters (**Figures 3A** and **S5**). Fittingly, we found that these datasets represented diverse tumor subtypes previously defined by TCGA (MGH105 was classified as "mixed", MGH115 as "classical", and MGH124 as "proneural") (4), and we therefore examined the characteristics of these distinct GBM subtypes using these three datasets. In the TCGA-mixed tumor, almost all TAMs in the GBM were bone marrow–derived macrophages, with primed state cells occupying 54.95% of the total number (clusters 1 and 2) and repressed state cells accounting for 41.56% (cluster 0) (**Figure 3B**). The TAMs in the TCGA-proneural tumor were characterized by primed microglia (cluster 4; 45.24%), repressed macrophages (cluster 3; 41.19%), and priming macrophages (cluster 8; 10.65%) (**Figure 3C**). A different composition was observed in the TCGA-classical tumor, with repressed microglia (cluster 7) comprising 73.21% of the total cell number and other TAM subtypes, such as repressed macrophages (cluster 3; 15.01%) and priming macrophages (cluster 8; 7.00%), making up the rest of the cell proportion (**Figure 3D**).

Heat map analysis showed that macrophages/microglia in the same activation state possessed distinct gene expression profiles in the different subtypes of GBM (**Figure 3E** and **Table S2**). Each of the clusters included cells present in at least three of the nine datasets (**Figure 4A**). To further clarify the main cellular physiological activities of TAMs, the top 500 differentially expressed genes in each cluster were identified and evaluated by KEGG pathway analysis. As shown in **Figures 4B, E**, "oxidative phosphorylation" was one of the most repressed macrophages from the TCGA-mixed tumor (cluster 0), but "protein processing in ER" was the most enriched set of pathways in the same macrophages from the TCGA-proneural and classical tumors (cluster 3). Primed state macrophages in the TCGA-mixed tumor (clusters 1 and 2) were enriched in the "ribosome" pathway (**Figures 4C, D**). Cluster 4, which represents primed microglia that make up the highest percentage of the cells in the TCGA-proneural tumor, was characterized by the KEGG enrichment term "phagosome" (**Figure 4F**). The pathways associated with "leishmaniasis" were enriched prominently in repressed microglia from the TCGA-classical tumor (cluster 7) (**Figure 4G**). The only TAM cluster present in all three subtypes of GBM was priming macrophages (cluster 8), which were enriched

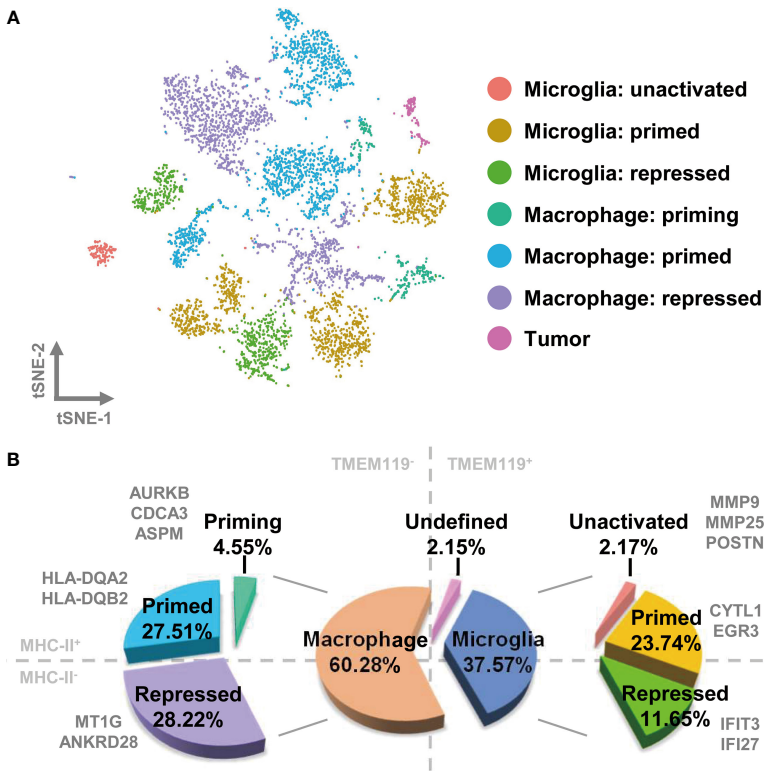

FIGURE 2 | TAMs in GBM comprise different activation states of bone marrow–derived macrophages and brain-resident microglia. **(A)** Each cell type is visualized as a t-SNE plot. **(B)** The relative proportions of macrophages and microglia are 60.28% and 37.57%, respectively. The ratio of detailed TAM states is shown in the pie chart.

for pathways involved in "DNA replication" and the "cell cycle" (**Figure 4H**).

SPI1 Is a Crucial Regulon for TAM Maturation and Polarization and Correlated With Poor Prognosis in GBM

To identify the distinct key transcription factors of different states of macrophages/microglia and compare the regulon differences, Single-Cell rEgulatory Network Inference and Clustering (SCENIC) was employed to draw the gene regulatory network. Based on the calculated regulon activity score (RAS) of transcription factors, we could identify the differences in the activities of regulons among the cell types (**Figure 5A**). The relevance among the regulons was evaluated by connection specificity index (CSI) and visualized in **Figure S6**. Some regulons, such as E2F transcription factor 7 (E2F7) and Cone-Rod Homeobox (CRX), had elevated activities in primed macrophage but decreased activities in repressed macrophage. Meanwhile, some others including SMAD Family Member 1 (SMAD1) and JunD proto-oncogene (JUND) showed low activities in primed but a high activities in repressed state of macrophages. Similarly, high activities of cAMP-responsive element modulator (CREM) and interferon regulatory factor 3 (IRF3) were calculated in primed microglia, but Transcription Factor 7 (TCF7) and interferon regulatory factor 9 (IRF9) in repressed microglia. By calculating the regulon specificity score (RSS), we examined the crucial regulons of each cell type and visualized the top three regulons in sequence diagrams and t-SNE plots (**Figures 5B, C** and **S7A–I**). Surprisingly, we found that SPI1 is picked out in top three of priming macrophages and all states of microglia, and also important for primed and repressed macrophages (**Table S3**). SPI1 is known as a crucial transcription factor for the development of macrophage (31, 32). Our results suggested that the transcription activity of SPI1 is essential for macrophages and microglia maturation and polarization, leading to a tumor-harmful microenvironment formation.

In order to further clarify the vital role of SPI1 in GBM, the expression levels in different grades were measured by analyzing the transcriptome data in TCGA, CGGA, and Rembrandt databases. As shown in **Figure 6A**, grade IV (GBM) samples had the highest level of SPI1. As previously mentioned that marker genes of the TAM group included SPI1, C1QA, C1QB, C1QC, SRGN, and TYROBP (**Figure 1D**), we utilized Spearman's rho value to interrogate the coexpression relationship between the expression level of SPI1 and these genes in GBM. After being analyzed in the TCGA-GBM dataset, the statistical positive correlations were observed between the SPI1 level and the genes expressed in the TAM group (C1QA: $r = 0.823$; C1QB: $r = 0.873$; C1QC: $r = 0.905$; SRGN: $r = 0.687$; TYROBP: $r = 0.774$) (**Figure 6B**), but not in the Tumor group (GAP43: $r = 0.043$; GPM6B: $r = -0.135$; SEC61G: $r = -0.117$; PTN: $r = -0.298$) (**Figure S8**). Meanwhile, we employed the TIMER algorithm to explore if there were

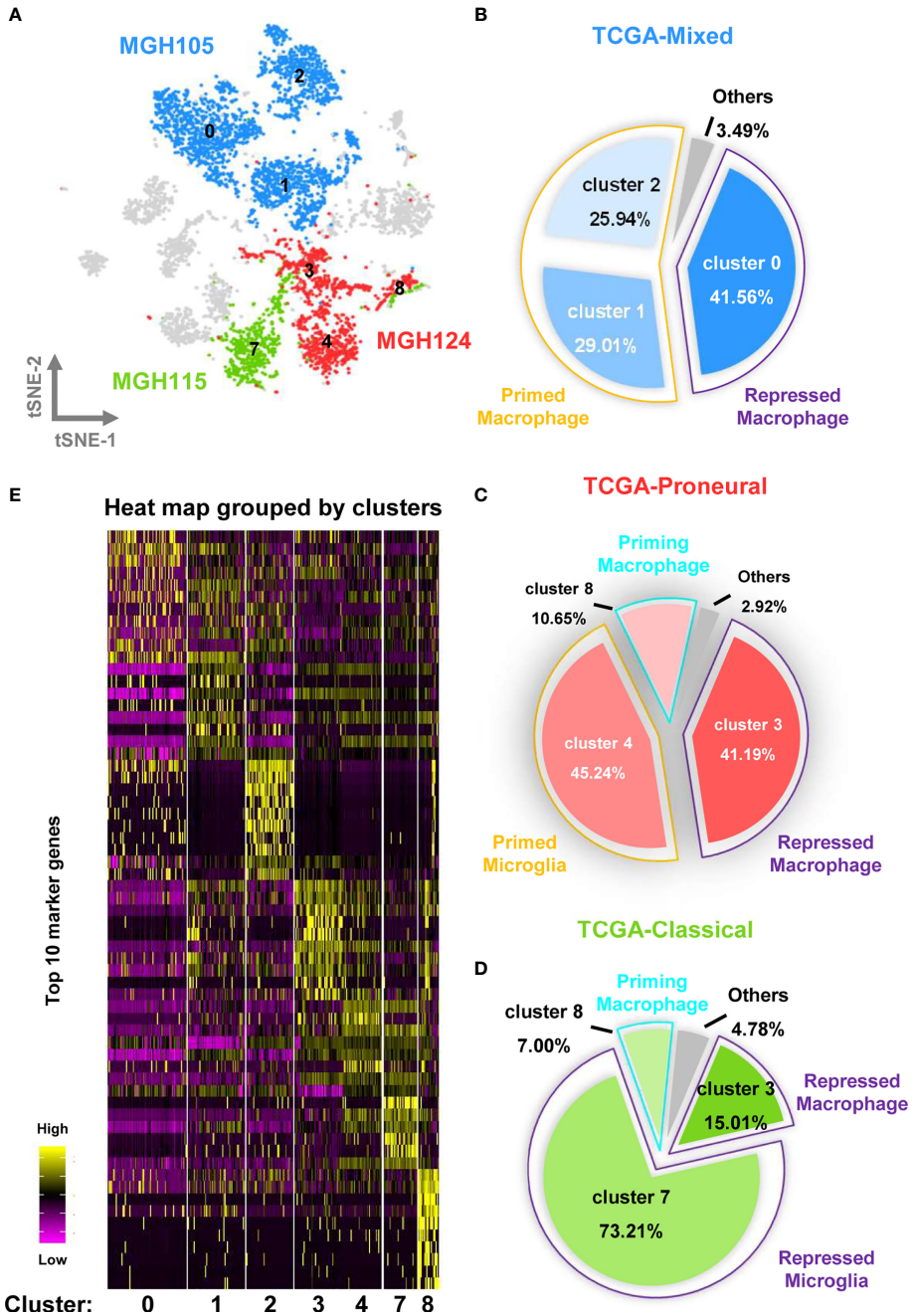

FIGURE 3 | Different molecular subtypes of GBM have distinct TAM composition and characteristics. **(A)** The cell distribution of MGH105, MGH115, and MGH124 are shown by the t-SNE plot. **(B)** TAMs in the TCGA-mixed tumor comprise repressed macrophages, primed macrophages, and others. **(C)** TAMs in the TCGA-proneural tumor comprise repressed macrophage, primed microglia, priming macrophages, and others. **(D)** TAMs in the TCGA-classical tumor contain repressed macrophages, repressed microglia, priming macrophages, and others. **(E)** The expression profiles of the top 10 marker genes of each cluster are displayed as a heat map.

potential relationships between the macrophage infiltration and the expression of these genes. We found that the elevated expression level of SPI1 had lower tumor purity and a higher infiltrating level of macrophage (Tumor purity: r = −0.528; macrophage infiltration: r = 0.687) (**Figure 6C**), so did TAM genes (**Figure S9A**). The tumor genes had no statistical correlation with tumor purity and macrophage infiltration (**Figure S9B**). Moreover, survival analysis using the Kaplan-Meier plotter tool displayed that the upregulated expression of SPI1 in tumor mass was linked to short overall survival (OS) and disease-free survival (DFS) time in patients with GBM (**Figure 6D**). Moreover, we inspected the likely downstream

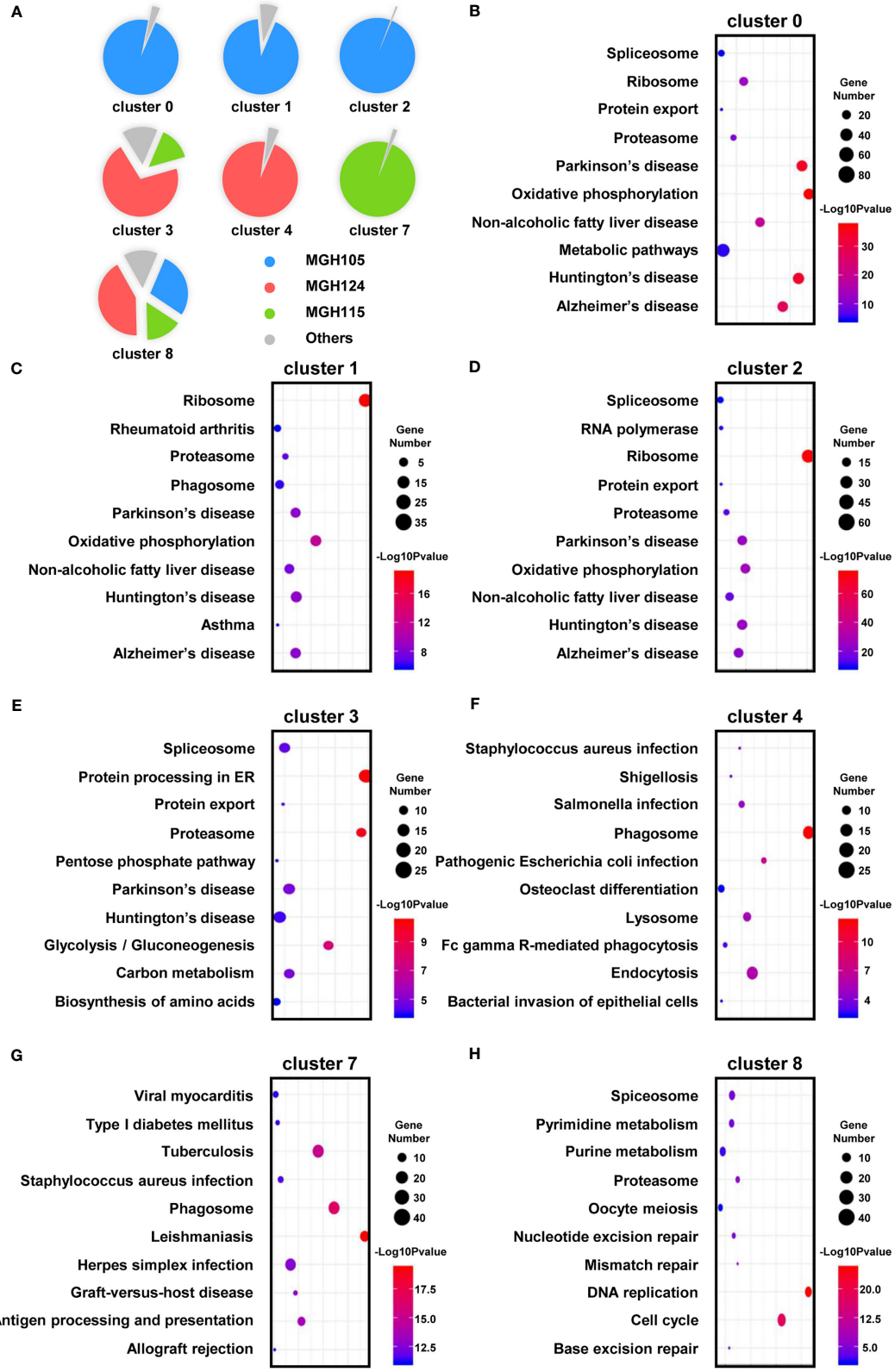

FIGURE 4 | The enriched cellular physiological activities of TAMs differ from each other. **(A)** Each cluster contains at least three of the nine tissues. **(B–H)** The enriched KEGG pathways of each cluster are shown in bubble charts.

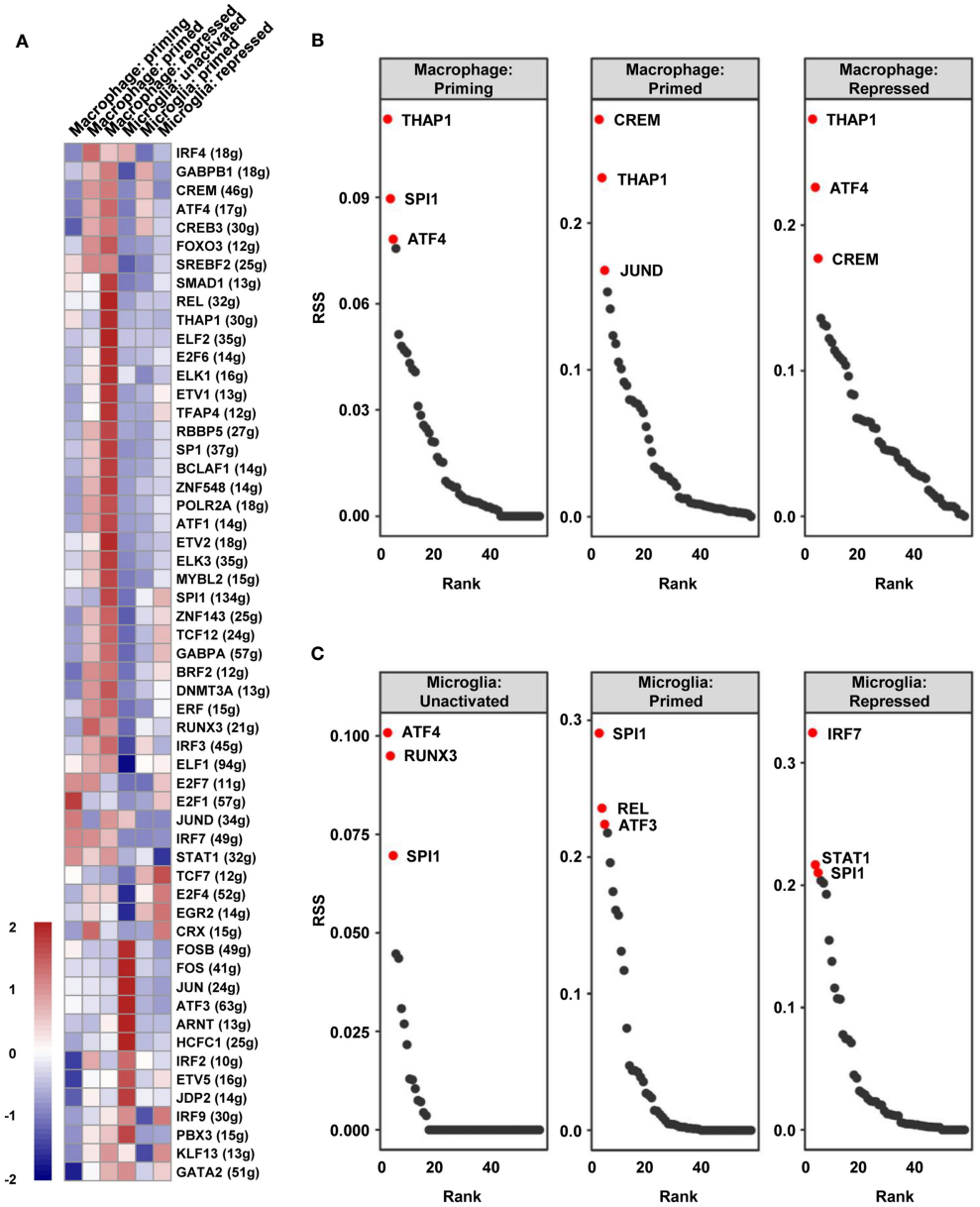

FIGURE 5 | The vital regulons in each cell type of TAMs. **(A)** The RAS of every regulon in different cell types was visualized as a heat map. **(B, C)** The ordered regulons based on the RSS were shown as sequence diagrams.

target genes of SPI1 in TAMs. By analyzing the glioma data in the TCGA database, the expression level of SPI1 displayed a significant positive correlation with target genes (CX3CR1: r = 0.53; CSF1R: r = 0.876; IRF8: r = 0.678) (**Figure S10A**). The co-expression signature was also observed in violin plots in single-cell data (**Figure S10B**).

The above results implied that tumor treatment targeting SPI1 could probably remodel the immune microenvironment of tumor and prolong the life span of GBM patients.

DISCUSSION

The tumor microenvironment (TME) is composed of an extracellular matrix interspersed with various cellular components, which regulates tumor progression *via* crosstalk and interplay with the tumor cells (33, 34). The TME is also associated with tumor metastasis and therapeutic resistance (35–38). Therefore, clarifying the specific characteristics of the TME in various cancers is particularly important in comprehensively

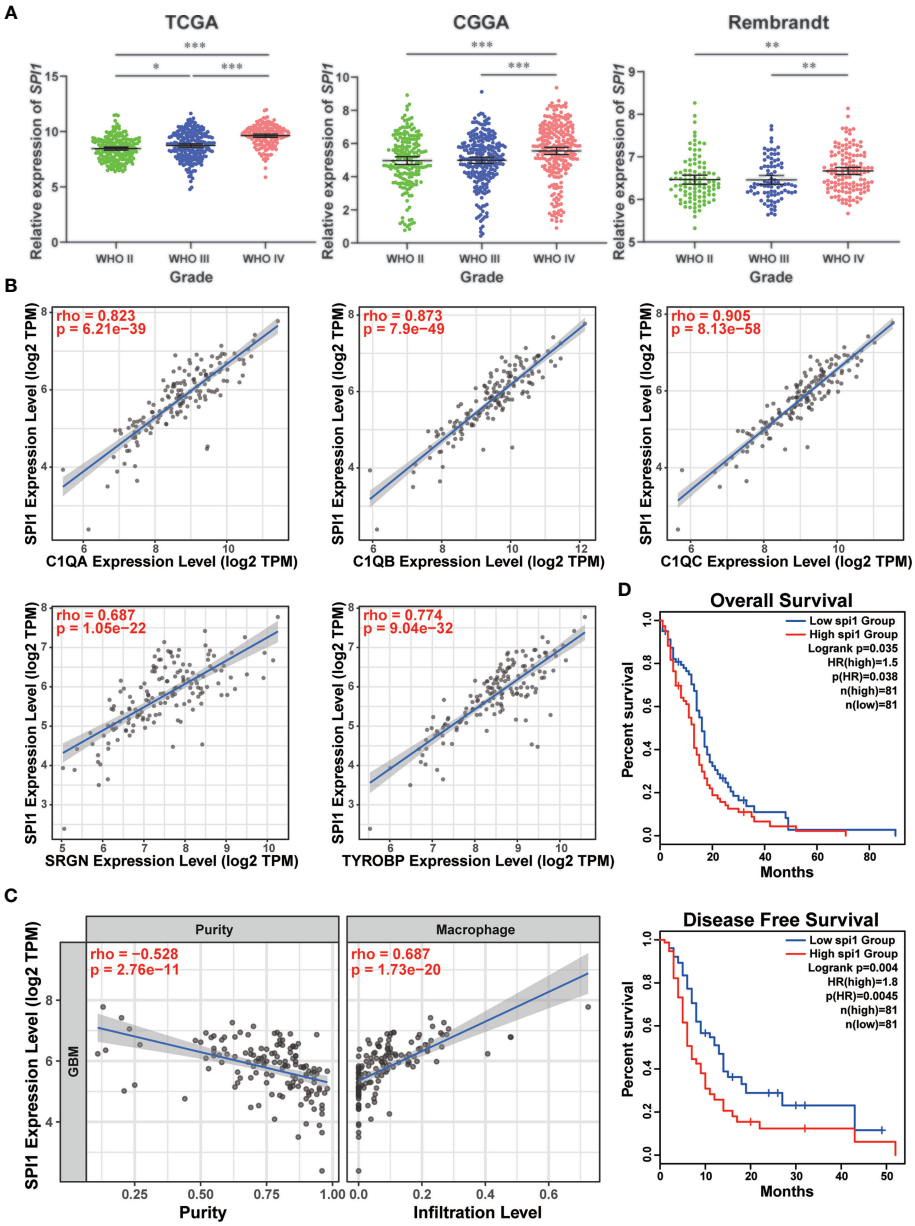

FIGURE 6 | High expression of SPI1 correlated with upper macrophage infiltration and poor prognosis in GBM. **(A)** The expression levels of SPI1 in different WHO groups were calculated and visualized as scatter plots. *p < 0.05, **p < 0.01, ***p < 0.001. **(B)** The expression of SPI1 was positively correlated with marker genes in the TAM group. **(C)** The SPI1 expression was negatively correlated with tumor purity and positively correlated with macrophage infiltration. **(D)** The correlation between SPI1 expression and survival prognosis of GBM in TCGA. The OS and DFS maps were displayed.

understanding and theoretically targeting various tumors. GBM is a malignant neoplasm of the brain with a high heterogeneity and a poor prognosis. The exclusive nature of the brain tissue involved in GBM tumorigenesis determines the unique features of the microenvironment in this cancer (39). In recent years, the immune composition of GBM has emerged as a significant factor in multiple studies, suggesting that TAM populations account for a large number of cells within the tumor mass (19). By utilizing gene expression data from TCGA and GEO databases, Engler et al. discovered an enrichment in immune response–related gene signatures (particularly of TAM genes) in the mesenchymal subtype of GBM, suggesting that TAMs have a subtype-specific role in GBM (40). Another investigation leveraged a mouse model to demonstrate that the majority of GBM-associated macrophages are bone marrow–derived myeloid cells, which infiltrate the tumor during the early stages of oncogenesis and localize to the perivascular niche (41). The use of scRNA-seq to elucidate the gene signatures of *CD11b*-positive

cells from GBM biopsies revealed that individual cells frequently coexpressed of both pro-inflammatory M1 and immune suppressive M2 macrophage genes (42), suggesting that the distinct partitioning of the M1/M2 macrophage subtypes is inadequate to completely represent the TAM expression profiles in GBM (43). However, to our knowledge, this is the first investigation to comprehensively describe the cell composition and transcriptomic characteristics of immune cells in GBM at the single-cell level.

In the present study, we focused on the distinct origin and activation states of TAMs in different subtypes of GBM. In the TCGA-mixed tumor, TAMs were largely composed of primed (clusters 1 and 2) and repressed (cluster 0) macrophages (**Figure 3B**). In the classical subtype, repressed microglia occupied the main proportion of the total (**Figure 3C**). However, in the proneural GBM subtype, the proportions of repressed macrophages and primed microglia were similar, each comprising slightly more than 40% of the total cell population (**Figure 3D**). The classical and proneural subtypes shared TAM cells in the form of repressed macrophages (cluster 3) and priming macrophages (cluster 8). However, each GBM subtype also possessed unique TAMs: the primed microglia (cluster 4) were a prominent feature of the proneural subtype, whereas almost all repressed microglia (cluster 7) originated from the classical subtype. The KEGG pathway analysis also revealed differences in the main cellular biological processes of otherwise similar TAMs, such as the enrichment of "oxidative phosphorylation" pathways in cluster 0 of repressed macrophages but "protein processing in ER" in cluster 3. Unfortunately, the nine datasets analyzed for this study did not include a mesenchymal GBM subtype. However, it is worth emphasizing that GBM is notorious for its high heterogeneity and complex cell components, and different regions of the same tumor have been shown to exhibit features of the different subtypes, with distinct immune cell infiltration. The integrated analysis of the nine samples as a single large tumor mass may thus be a closer reflection of the natural status of GBM *in situ*. This integrated analysis has allowed us to depict the immune landscape of GBM at a single-cell level (**Figure 7**). It should be noted that the batch effect among these datasets still existed because the downloadable matrix is under mathematical manipulation and hard to restore. But in keeping with previous findings (19, 20), our results confirm that TAMs may occupy over one-third of the GBM tumor, with the ratio of the bone marrow–derived macrophages and the brain-resident microglia being 2:1, but infiltrating T lymphocytes comprising less than 2% of the tumor mass. Successful immunotherapy requires substantial infiltration of functional T cells within the tumors (44, 45). The limited number of T lymphocytes in GBM, which is isolated by the blood–brain barrier, means that immunotherapies targeting T cells such as monoclonal antibodies against programmed cell death 1 (PD-1) or cytotoxic T-lymphocyte-associated protein 4 (CTLA-4) are not suitable for treating GBM (46).

Given the large proportion of TAM-infiltrating GBM, the ability to convert immune-suppressed TAMs to a more proinflammatory state has become a promising immunotherapeutic target. The colony-stimulating factor 1 receptor (CSF1R) plays essential roles in the development and function of macrophages and microglia (47). An inhibitor of the CSF1R was able to increase survival and decrease the tumor volume in a

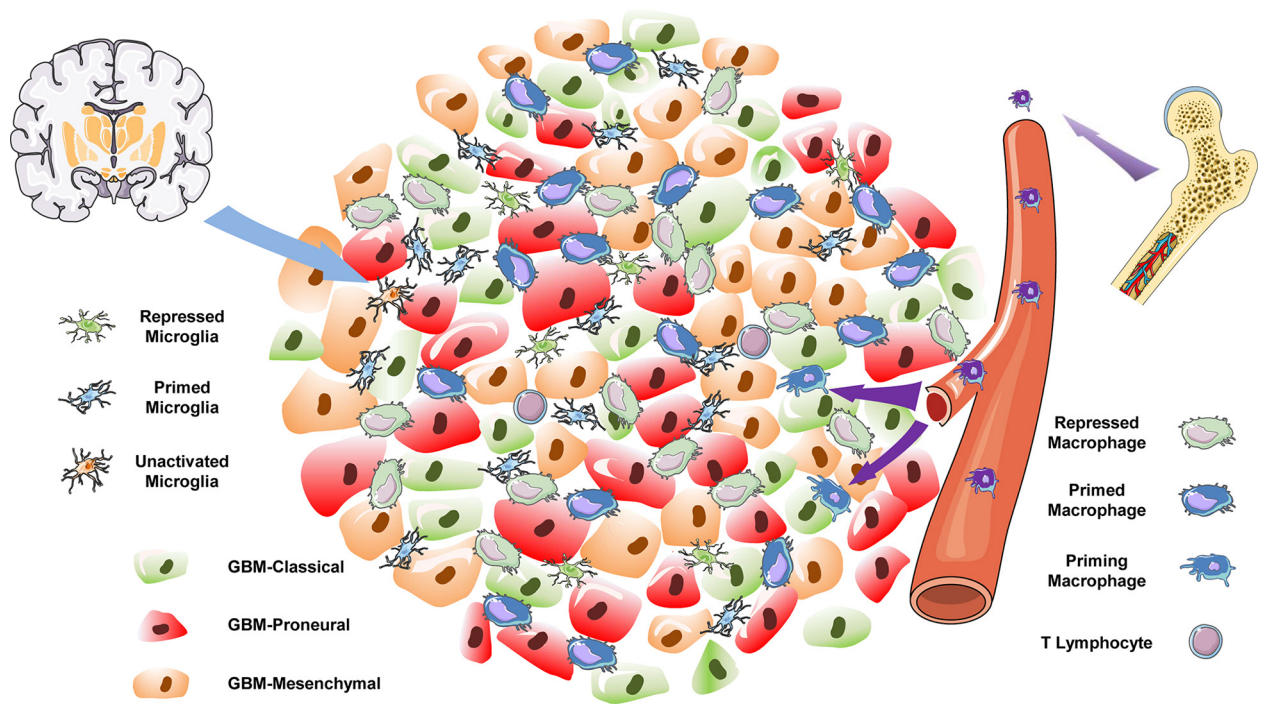

FIGURE 7 | The immune landscape of GBM.

proneural GBM mouse model (48–50). In our study, we observed that *SPI1* was a vital regulon in all states of TAMs (**Figure 5** and **Table S3**). SPI1, also called PU.1, is a member of Ets family transcription factors and specifically expressed in lymphoid and myeloid cell lineages. The continuous high expression of SPI1 in hematopoietic cells results in macrophage differentiation (32). DB1976 is a furan-bisbenzimidazole-diamidine that strongly inhibits the transcription activity of SPI1 (51). We hypothesize that inhibition of SPI1 by utilizing DB1976 could reduce the TAM maturation and polarization, thus eliciting an antitumor effect.

CONCLUSIONS

In summary, our comprehensive characterization of immune cells from a total of nine GBM tissues revealed a unique immune landscape in GBM at the single-cell level and identified SPI1 as a potential immunotherapeutic target against TAMs in GBM.

DATA AVAILABILITY STATEMENT

Publicly available datasets were analyzed in this study. This data can be found here: GSE131928.

AUTHOR CONTRIBUTIONS

Study conception and design: CK and XC. Acquisition of the nine scRNA-seq datasets: XC and FT. Dimensionality reduction and unsupervised clustering: XC, QW, and YW. Deep analysis (cell types and marker genes identification, gene regulatory network, KEGG pathway, etc.): XC, QW, JZ, and CX. Interpretation of data and manuscript writing: XC and CK. Study supervision: CK and HW. Funding acquisition: CK and XC. All authors have read and agreed the published version of the manuscript.

FUNDING

This research was supported by Beijing Tianjin Hebei Basic Research Cooperation Project (Nos. 18JCZDJC45500 and H2018201306), Tianjin Key R&D Plan of Tianjin Science and Technology Plan Project (No. 20YFZCSY00360), National Nature Science Foundation of China (No. 82002657), China Postdoctoral Science Foundation (No. 2020M670673), and Zhao Yi-Cheng Medical Science Foundation (No. ZYYFY2019002).

ACKNOWLEDGMENTS

The authors thank Shanghai OE Biotech Co., Ltd for technical support in scRNA-seq data analysis process.

SUPPLEMENTARY MATERIAL

The Supplementary Material for this article can be found online at: https://www.frontiersin.org/articles/10.3389/fonc.2021.710695/full#supplementary-material

Supplementary Table 1 | All differential expression genes for clusters.

Supplementary Table 2 | All differential expression genes for macrophage clusters.

Supplementary Table 3 | RSS of regulons in each cell type.

Supplementary Figure 1 | Related to **Figure 1**. **(A)** The 22 clusters are identified and visualized as a t-SNE map. **(B)** The distribution of nine samples was displayed as a t-SNE map. **(C)** The expressions of CD3G, GZMH, IL2RB, PRF1, and ICOS distinguish T lymphocytes from the rest of the cell mass. **(D)** Two distinct aggregations are evident in the PCA plot.

Supplementary Figure 2 | Related to **Figure 1**. **(A–I)** The cell types in each sample were identified and visualized as t-SNE plots. **(J)** The relative ratios of each cell type are displayed.

Supplementary Figure 3 | Related to **Figure 2**. **(A)** A t-SNE plot showing the cell clusters. **(B–C)** The distribution of CD68 is visualized by a t-SNE plot and a violin plot. **(D)** Several genes (CYFIP1, ENTPD1, and VAV1) have similar expression signatures in comparison to TMEM119, indicating that these genes might be the marker genes of brain resident microglia. **(E)** The expression of MHC-II, in the form of HLA-DQA2 and HLA-DQB2, is restricted to cluster 1, 2, 4, 5, 6, 8, and 9. **(F)** The expression levels of TMEM119 and MHC-II divide these clusters into 4 main subtypes: TMEM119+-MHC-II+ cells, TMEM119+-MHC-II- cells, TMEM119–MHC-II+ cells, and TMEM119–MHC-II- cells.

Supplementary Figure 4 | Related to **Figure 2**. **(A–B)** Different marker genes in microglia and macrophages. **(C)** The category schemes defining the cell types of TAM in GBM by the expression signatures of TMEM119 and MHC-II.

Supplementary Figure 5 | Related to **Figure 3**. **(A–F)** The cell distributions of MGH102, MGH114, MGH118, MGH 125, MGH126 and MGH143 are displayed in t-SNE plots.

Supplementary Figure 6 | Related to **Figure 5**. **(A)** Heat map display the relevancies among the regulons.

Supplementary Figure 7 | Related to **Figure 5**. **(A–I)** t-SNE map showed the AUCell scores of crucial regulons (THAP1, ATF4, CREM, SPI1, JUND, REL, RUNX3, IRF7, STAT1).

Supplementary Figure 8 | Related to **Figure 6**. The correlation between SPI1 expression and genes in tumor group.

Supplementary Figure 9 | Related to **Figure 6**. **(A)** The expressions of TAM genes were negatively correlated with tumor purity and positively correlated with macrophage infiltration. **(B)** The expressions of tumor genes had no correlation with tumor purity and macrophage infiltration.

Supplementary Figure 10 | Related to **Figure 6**. **(A)** The correlation between SPI1 expression and downstream target genes. **(B)** The distribution of SPI1 and downstream target genes are visualized by violin plots.

REFERENCES

1. Alexander BM, Cloughesy TF. Adult Glioblastoma. *J Clin Oncol* (2017) 35:2402–9. doi: 10.1200/JCO.2017.73.0119
2. Wesseling P, Capper D. Who 2016 Classification of Gliomas. *Neuropathol Appl Neurobiol* (2018) 44:139–50. doi: 10.1111/nan.12432
3. Verhaak RG, Hoadley KA, Purdom E, Wang V, Qi Y, Wilkerson MD, et al. Integrated Genomic Analysis Identifies Clinically Relevant Subtypes of

Glioblastoma Characterized by Abnormalities in Pdgfra, Idh1, EGFR, and Nf1. *Cancer Cell* (2010) 17:98–110. doi: 10.1016/j.ccr.2009.12.020
4. Neftel C, Laffy J, Filbin MG, Hara T, Shore ME, Rahme GJ, et al. An Integrative Model of Cellular States, Plasticity, and Genetics for Glioblastoma. *Cell* (2019) 178:835–49.e21. doi: 10.1016/j.cell.2019.06.024
5. Yuan J, Levitin HM, Frattini V, Bush EC, Boyett DM, Samanamud J, et al. Single-Cell Transcriptome Analysis of Lineage Diversity in High-Grade Glioma. *Genome Med* (2018) 10:57. doi: 10.1186/s13073-018-0567-9
6. Brennan CW, Verhaak RG, McKenna A, Campos B, Noushmehr H, Salama SR, et al. The Somatic Genomic Landscape of Glioblastoma. *Cell* (2013) 155:462–77. doi: 10.1016/j.cell.2013.09.034
7. Sottoriva A, Spiteri I, Piccirillo SG, Touloumis A, Collins VP, Marioni JC, et al. Intratumor Heterogeneity in Human Glioblastoma Reflects Cancer Evolutionary Dynamics. *Proc Natl Acad Sci USA* (2013) 110:4009–14. doi: 10.1073/pnas.1219747110
8. Patel AP, Tirosh I, Trombetta JJ, Shalek AK, Gillespie SM, Wakimoto H, et al. Single-Cell RNA-Seq Highlights Intratumoral Heterogeneity in Primary Glioblastoma. *Science* (2014) 344:1396–401. doi: 10.1126/science.1254257
9. Qazi MA, Vora P, Venugopal C, Sidhu SS, Moffat J, Swanton C, et al. Intratumoral Heterogeneity: Pathways to Treatment Resistance and Relapse in Human Glioblastoma. *Ann Oncol* (2017) 28:1448–56. doi: 10.1093/annonc/mdx169
10. Chen S, Le T, Harley BAC, Imoukhuede PI. Characterizing Glioblastoma Heterogeneity *Via* Single-Cell Receptor Quantification. *Front Bioeng Biotechnol* (2018) 6:92. doi: 10.3389/fbioe.2018.00092
11. Ostrom QT, Gittleman H, Xu J, Kromer C, Wolinsky Y, Kruchko C, et al. Cbtrus Statistical Report: Primary Brain and Other Central Nervous System Tumors Diagnosed in the United States in 2009-2013. *Neuro Oncol* (2016) 18: v1–v75. doi: 10.1093/neuonc/now207
12. Aldape K, Zadeh G, Mansouri S, Reifenberger G, von Deimling A. Glioblastoma: Pathology, Molecular Mechanisms and Markers. *Acta Neuropathol* (2015) 129:829–48. doi: 10.1007/s00401-015-1432-1
13. Okazaki T, Chikuma S, Iwai Y, Fagarasan S, Honjo T. A Rheostat for Immune Responses: The Unique Properties of Pd-1 and Their Advantages for Clinical Application. *Nat Immunol* (2013) 14:1212–8. doi: 10.1038/ni.2762
14. Alsaab HO, Sau S, Alzhrani R, Tatiparti K, Bhise K, Kashaw SK, et al. Pd-1 and Pd-L1 Checkpoint Signaling Inhibition for Cancer Immunotherapy: Mechanism, Combinations, and Clinical Outcome. *Front Pharmacol* (2017) 8:561. doi: 10.3389/fphar.2017.00561
15. Litak J, Mazurek M, Grochowski C, Kamieniak P, Rolinski J. Pd-L1/Pd-1 Axis in Glioblastoma Multiforme. *Int J Mol Sci* (2019) 20(21):5347. doi: 10.3390/ijms20215347
16. Adhikaree J, Moreno-Vicente J, Kaur AP, Jackson AM, Patel PM. Resistance Mechanisms and Barriers to Successful Immunotherapy for Treating Glioblastoma. *Cells* (2020) 9(2):263. doi: 10.3390/cells9020263
17. Wu T, Dai Y. Tumor Microenvironment and Therapeutic Response. *Cancer Lett* (2017) 387:61–8. doi: 10.1016/j.canlet.2016.01.043
18. Nakamura K, Smyth MJ. Myeloid Immunosuppression and Immune Checkpoints in the Tumor Microenvironment. *Cell Mol Immunol* (2020) 17:1–12. doi: 10.1038/s41423-019-0306-1
19. Charles NA, Holland EC, Gilbertson R, Glass R, Kettenmann H. The Brain Tumor Microenvironment. *Glia* (2012) 60:502–14. doi: 10.1002/glia.21264
20. Han S, Ma E, Wang X, Yu C, Dong T, Zhan W, et al. Rescuing Defective Tumor-Infiltrating T-Cell Proliferation in Glioblastoma Patients. *Oncol Lett* (2016) 12:2924–9. doi: 10.3892/ol.2016.4944
21. Ginhoux F, Prinz M. Origin of Microglia: Current Concepts and Past Controversies. *Cold Spring Harb Perspect Biol* (2015) 7:a020537. doi: 10.1101/cshperspect.a020537
22. Hambardzumyan D, Gutmann DH, Kettenmann H. The Role of Microglia and Macrophages in Glioma Maintenance and Progression. *Nat Neurosci* (2016) 19:20–7. doi: 10.1038/nn.4185
23. Tirosh I, Suva ML. Dissecting Human Gliomas by Single-Cell RNA Sequencing. *Neuro Oncol* (2018) 20:37–43. doi: 10.1093/neuonc/nox126
24. Zhang X, Lan Y, Xu J, Quan F, Zhao E, Deng C, et al. CellMarker: A Manually Curated Resource of Cell Markers in Human and Mouse. *Nucleic Acids Res* (2019) 47:D721–8. doi: 10.1093/nar/gky900
25. Aibar S, Gonzalez-Blas CB, Moerman T, Huynh-Thu VA, Imrichova H, Hulselmans G, et al. Scenic: Single-Cell Regulatory Network Inference and Clustering. *Nat Methods* (2017) 14:1083–6. doi: 10.1038/nmeth.4463
26. Zhao Z, Zhang KN, Wang Q, Li G, Zeng F, Zhang Y, et al. Chinese Glioma Genome Atlas (CGGA): A Comprehensive Resource With Functional Genomic Data From Chinese Gliomas. *Genomics Proteomics Bioinf* (2021) S1672-0229(21):00045–0. doi: 10.1016/j.gpb.2020.10.005
27. Li T, Fu J, Zeng Z, Cohen D, Li J, Chen Q, et al. Timer2.0 for Analysis of Tumor-Infiltrating Immune Cells. *Nucleic Acids Res* (2020) 48:W509–14. doi: 10.1093/nar/gkaa407
28. Cui X, Zhang X, Liu M, Zhao C, Zhang N, Ren Y, et al. A Pan-Cancer Analysis of the Oncogenic Role of Staphylococcal Nuclease Domain-Containing Protein 1 (snd1) in Human Tumors. *Genomics* (2020) 112:3958–67. doi: 10.1016/j.ygeno.2020.06.044
29. Satoh J, Kino Y, Asahina N, Takitani M, Miyoshi J, Ishida T, et al. Tmem119 Marks a Subset of Microglia in the Human Brain. *Neuropathology* (2016) 36:39–49. doi: 10.1111/neup.12235
30. Witcher KG, Eiferman DS, Godbout JP. Priming the Inflammatory Pump of the Cns After Traumatic Brain Injury. *Trends Neurosci* (2015) 38:609–20. doi: 10.1016/j.tins.2015.08.002
31. Zhang P, Zhang X, Iwama A, Yu C, Smith KA, Mueller BU, et al. Pu.1 Inhibits Gata-1 Function and Erythroid Differentiation by Blocking Gata-1 DNA Binding. *Blood* (2000) 96:2641–8. doi: 10.1182/blood.V96.8.2641.h8002641_2641_2648
32. McIvor Z, Hein S, Fiegler H, Schroeder T, Stocking C, Just U, et al. Transient Expression of Pu.1 Commits Multipotent Progenitors to a Myeloid Fate Whereas Continued Expression Favors Macrophage Over Granulocyte Differentiation. *Exp Hematol* (2003) 31:39–47. doi: 10.1016/S0301-472X(02)01017-2
33. Hanahan D, Coussens LM. Accessories to the Crime: Functions of Cells Recruited to the Tumor Microenvironment. *Cancer Cell* (2012) 21:309–22. doi: 10.1016/j.ccr.2012.02.022
34. Qian BZ, Pollard JW. Macrophage Diversity Enhances Tumor Progression and Metastasis. *Cell* (2010) 141:39–51. doi: 10.1016/j.cell.2010.03.014
35. Gao D, Joshi N, Choi H, Ryu S, Hahn M, Catena R, et al. Myeloid Progenitor Cells in the Premetastatic Lung Promote Metastases by Inducing Mesenchymal to Epithelial Transition. *Cancer Res* (2012) 72:1384–94. doi: 10.1158/0008-5472.CAN-11-2905
36. Bonde AK, Tischler V, Kumar S, Soltermann A, Schwendener RA. Intratumoral Macrophages Contribute to Epithelial-Mesenchymal Transition in Solid Tumors. *BMC Cancer* (2012) 12:35. doi: 10.1186/1471-2407-12-35
37. Barcellos-Hoff MH, Lyden D, Wang TC. The Evolution of the Cancer Niche During Multistage Carcinogenesis. *Nat Rev Cancer* (2013) 13:511–8. doi: 10.1038/nrc3536
38. Meads MB, Gatenby RA, Dalton WS. Environment-Mediated Drug Resistance: A Major Contributor to Minimal Residual Disease. *Nat Rev Cancer* (2009) 9:665–74. doi: 10.1038/nrc2714
39. Belousov A, Titov S, Shved N, Garbuz M, Malykin G, Gulaia V, et al. The Extracellular Matrix and Biocompatible Materials in Glioblastoma Treatment. *Front Bioeng Biotechnol* (2019) 7:341. doi: 10.3389/fbioe.2019.00341
40. Engler JR, Robinson AE, Smirnov I, Hodgson JG, Berger MS, Gupta N, et al. Increased Microglia/Macrophage Gene Expression in a Subset of Adult and Pediatric Astrocytomas. *PloS One* (2012) 7:e43339. doi: 10.1371/journal.pone.0043339
41. Chen Z, Feng X, Herting CJ, Garcia VA, Nie K, Pong WW, et al. Cellular and Molecular Identity of Tumor-Associated Macrophages in Glioblastoma. *Cancer Res* (2017) 77:2266–78. doi: 10.1158/0008-5472.CAN-16-2310
42. Muller S, Kohanbash G, Liu SJ, Alvarado B, Carrera D, Bhaduri A, et al. Single-Cell Profiling of Human Gliomas Reveals Macrophage Ontogeny as a Basis for Regional Differences in Macrophage Activation in the Tumor Microenvironment. *Genome Biol* (2017) 18:234. doi: 10.1186/s13059-017-1362-4
43. Ransohoff RM. A Polarizing Question: Do M1 and M2 Microglia Exist? *Nat Neurosci* (2016) 19:987–91. doi: 10.1038/nn.4338
44. Iwai Y, Hamanishi J, Chamoto K, Honjo T. Cancer Immunotherapies Targeting the PD-1 Signaling Pathway. *J BioMed Sci* (2017) 24:26. doi: 10.1186/s12929-017-0329-9
45. Fritz JM, Lenardo MJ. Development of Immune Checkpoint Therapy for Cancer. *J Exp Med* (2019) 216:1244–54. doi: 10.1084/jem.20182395
46. Tomaszewski W, Sanchez-Perez L, Gajewski TF, Sampson JH. Brain Tumor Microenvironment and Host State: Implications for Immunotherapy. *Clin Cancer Res* (2019) 25:4202–10. doi: 10.1158/1078-0432.CCR-18-1627

47. Stanley ER, Chitu V. Csf-1 Receptor Signaling in Myeloid Cells. *Cold Spring Harb Perspect Biol* (2014) 6(6):a021857. doi: 10.1101/cshperspect.a021857
48. Coniglio SJ, Eugenin E, Dobrenis K, Stanley ER, West BL, Symons MH, et al. Microglial Stimulation of Glioblastoma Invasion Involves Epidermal Growth Factor Receptor (EGFR) and Colony Stimulating Factor 1 Receptor (csf-1r) Signaling. *Mol Med* (2012) 18:519–27. doi: 10.2119/molmed.2011.00217
49. Elmore MR, Najafi AR, Koike MA, Dagher NN, Spangenberg EE, Rice RA, et al. Colony-Stimulating Factor 1 Receptor Signaling Is Necessary for Microglia Viability, Unmasking a Microglia Progenitor Cell in the Adult Brain. *Neuron* (2014) 82:380–97. doi: 10.1016/j.neuron.2014.02.040
50. Pyonteck SM, Akkari L, Schuhmacher AJ, Bowman RL, Sevenich L, Quail DF, et al. Csf-1r Inhibition Alters Macrophage Polarization and Blocks Glioma Progression. *Nat Med* (2013) 19:1264–72. doi: 10.1038/nm.3337
51. Stephens DC, Kim HM, Kumar A, Farahat AA, Boykin DW, Poon GM. Pharmacologic Efficacy of Pu.1 Inhibition by Heterocyclic Dications: A Mechanistic Analysis. *Nucleic Acids Res* (2016) 44:4005–13. doi: 10.1093/nar/gkw229

Conflict of Interest: The authors declare that the research was conducted in the absence of any commercial or financial relationships that could be construed as a potential conflict of interest.

Publisher's Note: All claims expressed in this article are solely those of the authors and do not necessarily represent those of their affiliated organizations, or those of the publisher, the editors and the reviewers. Any product that may be evaluated in this article, or claim that may be made by its manufacturer, is not guaranteed or endorsed by the publisher.

frontiers in Oncology

ORIGINAL RESEARCH
published: 13 August 2021
doi: 10.3389/fonc.2021.707017

Small RNA Sequencing Identifies PIWI-Interacting RNAs Deregulated in Glioblastoma—piR-9491 and piR-12488 Reduce Tumor Cell Colonies *In Vitro*

Michael Bartos[1], Frantisek Siegl[2], Alena Kopkova[2], Lenka Radova[2], Jan Oppelt[2], Marek Vecera[2], Tomas Kazda[3], Radim Jancalek[4], Michal Hendrych[5], Marketa Hermanova[5], Petra Kasparova[6], Zuzana Pleskacova[7], Vaclav Vybihal[8], Pavel Fadrus[8], Martin Smrcka[8], Radek Lakomy[9], Radim Lipina[10], Tomas Cesak[1], Ondrej Slaby[2,9,11†] and Jiri Sana[2,9,12*†]*

[1] Department of Neurosurgery, University Hospital Hradec Kralove, Hradec Kralove, Czechia, [2] Central European Institute of Technology, Masaryk University, Brno, Czechia, [3] Department of Radiation Oncology, Masaryk Memorial Cancer Institute and Medical Faculty, Masaryk University, Brno, Czechia, [4] Department of Neurosurgery, St. Anne's University Hospital and Medical Faculty, Masaryk University, Brno, Czechia, [5] 1st Department of Pathology, St. Anne's University Hospital and Medical Faculty, Masaryk University, Brno, Czechia, [6] The Fingerland Department of Pathology, University Hospital Hradec Kralove, Hradec Kralove, Czechia, [7] Department of Oncology and Radiotherapy, University Hospital Hradec Kralove, Hradec Kralove, Czechia, [8] Department of Neurosurgery, University Hospital Brno, Brno, Czechia, [9] Department of Comprehensive Cancer Care, Masaryk Memorial Cancer Institute, Brno, Czechia, [10] Department of Neurosurgery, University Hospital Ostrava, Ostrava, Czechia, [11] Department of Biology, Faculty of Medicine, Masaryk University, Brno, Czechia, [12] Department of Pathology, University Hospital Brno, Brno, Czechia

Glioblastoma (GBM) is the most frequently occurring primary malignant brain tumor of astrocytic origin. To change poor prognosis, it is necessary to deeply understand the molecular mechanisms of gliomagenesis and identify new potential biomarkers and therapeutic targets. PIWI-interacting RNAs (piRNAs) help in maintaining genome stability, and their deregulation has already been observed in many tumors. Recent studies suggest that these molecules could also play an important role in the glioma biology. To determine GBM-associated piRNAs, we performed small RNA sequencing analysis in the discovery set of 19 GBM and 11 non-tumor brain samples followed by TaqMan qRT-PCR analyses in the independent set of 77 GBM and 23 non-tumor patients. Obtained data were subsequently bioinformatically analyzed. Small RNA sequencing revealed 58 significantly deregulated piRNA molecules in GBM samples in comparison with non-tumor brain tissues. Deregulation of piR-1849, piR-9491, piR-12487, and piR-12488 was successfully confirmed in the independent groups of patients and controls (all $p < 0.0001$), and piR-9491 and piR-12488 reduced GBM cells' ability to form colonies *in vitro*. In addition, piR-23231 was significantly associated with the overall survival of the GBM patients treated with Stupp regimen ($p = 0.007$). Our results suggest that piRNAs could be a novel promising diagnostic and prognostic biomarker in GBM potentially playing important roles in gliomagenesis.

Keywords: glioblastoma, PIWI-interacting RNA, piRNA, diagnosis, prognosis

OPEN ACCESS

Edited by:
Aleksi Sedo, Charles University, Czechia

Reviewed by:
Bibekanand Mallick, National Institute of Technology Rourkela, India
Mirka Rabajdova, University of Pavol Jozef Šafárik, Slovakia

***Correspondence:**
Jiri Sana
sana.jiri@gmail.com
Ondrej Slaby
on.slaby@gmail.com

†These authors share senior authorship

Specialty section:
This article was submitted to Neuro-Oncology and Neurosurgical Oncology, a section of the journal Frontiers in Oncology

Received: *08 May 2021*
Accepted: *20 July 2021*
Published: *13 August 2021*

Citation:
Bartos M, Siegl F, Kopkova A, Radova L, Oppelt J, Vecera M, Kazda T, Jancalek R, Hendrych M, Hermanova M, Kasparova P, Pleskacova Z, Vybihal V, Fadrus P, Smrcka M, Lakomy R, Lipina R, Cesak T, Slaby O and Sana J (2021) Small RNA Sequencing Identifies PIWI-Interacting RNAs Deregulated in Glioblastoma—piR-9491 and piR-12488 Reduce Tumor Cell Colonies In Vitro. Front. Oncol. 11:707017. doi: 10.3389/fonc.2021.707017

INTRODUCTION

Glioblastoma (GBM) is the most aggressive of the glial tumors and is related to a very poor prognosis with a median survival between 14 and 15 months (1, 2). GBM originates from astrocytes, which have a largely supportive function in the nervous system (1). Based on the genetic pathway of their formation, two types of GBM can be distinguished. Primary GBM arises *de novo* and secondary GBM develops as a continuation of low-grade glioma. Primary GBM has a higher prevalence in elderly people, whereas secondary GBM is more often associated with younger age (1, 3). The most significant prognostic factors are age at the time of diagnosis, size and localization of the tumor, Karnofsky performance status, and the genetic makeup of the tumor (4). Currently, the gold standard of therapy in GBM consists of maximal surgical resection followed by concomitant radiotherapy and chemotherapy with temozolomide (TMZ) (5). In the past two decades, regardless of improvements in general oncological care through intensive research, the recommended treatment in GBM remains largely unchanged and the overall survival (OS) of GBM patients has not significantly improved. Therefore, a great effort is devoted to gaining a better understanding of GBM biology and the research of novel predictive biomarkers as well as potential therapeutic targets. One of the very promising areas of research in potential biomarkers and molecules likely involved in the molecular pathology of GBM are PIWI-interacting RNAs (piRNA). PiRNAs present one of the subclasses of short non-coding RNAs, 24–32 nucleotides in length, which act as regulators of active transposons by induction of heterochromatinization in transposon loci or by direct cleavage of complementary transposon transcripts in piRISC complexes by the associated PIWI proteins [PIWIL1 (HIWI), PIWIL2 (HILI), PIWIL3 (HIWI3), and PIWIL4 (HIWI2)] (6, 7). PiRNA expression was primarily reported in germline cells where they play a crucial role in stem-cell maintenance and cell renewal regulation (7). Although originally thought to be germline-specific, piRNA have subsequently been associated with numerous functions in somatic cells ranging from epigenetic regulation, genome rearrangement, somatic cell development, to gene and protein regulatory functions (6). The aberrant expression of piRNA and PIWI has also recently been described in many cancers including their regulatory roles in tumor biology (8). Nevertheless, to this day, only a few studies have been published on their role in GBM (8, 9).

In this study, we identified a set of piRNAs that are likely closely associated with GBM in comparison to non-tumor brain tissue. These piRNAs may thus play an important role in the pathogenesis of GBM and could present a potential therapeutic target in GBM. Finally, we demonstrated the prognostic potential of piRNAs by showing the ability of piR-23231 to predict OS in GBM patients treated with Stupp regimen independently of the other prognostic markers.

MATERIALS AND METHODS

Patient Cohort and Primary Cell Cultures

The retrospective multi-institutional (University Hospital Brno, University Hospital Hradec Kralove, University Hospital Ostrava, and St Anne's University Hospital Brno) cohort study included 96 patients with histopathologically confirmed primary GBM and 34 non-tumor controls. All patients enrolled in this study gave consent and the study was approved by the local ethics committees. The clinical and pathological characteristics of GBM patients are summarized in **Table 1**. Non-tumor control brain tissues were obtained *via* therapeutic resections in patients with intractable epilepsy—only brain tissue lacking evidence of dysplastic changes from the non-dominant temporal or frontal lobe was used. Forty-one GBM patients underwent adjuvant concomitant chemoradiotherapy (CHRT) according to the Stupp protocol. In summary, 60 Gy of fractionated radiotherapy was administered to the primary site of the tumor, followed by 42 cycles of TMZ chemotherapy. A subset of patients were further indicated to adjuvant TMZ in monotherapy.

Moreover, six primary GBM cell cultures were derived from fresh tumor tissue samples obtained from GBM patients who underwent surgical resection at the Department of Neurosurgery of the University Hospital Brno. The fresh tissue sample was enzymatically dissociated with TrypLE (ThermoFisher Scientific) for 20 min at 37°C with agitation or using the Papain Dissociation System (Worthington) according to the manufacturer's instructions. Single-cell suspensions were seeded into 25 cm^2 tissue culture flasks (Techno Plastic Products AG) and cultured in Dulbecco's modified essential medium supplemented with 10% FBS, 1% Glutamax (both ThermoFisher Scientific), 100 U/ml penicillin and 100 µg/ml streptomycin, 1mM sodium pyruvate and 1% non-essential amino acids (all GE Healthcare). After 1–3 weeks, adherent cells, which covered more than 2/3 of the culture flask in DMEM, were passaged using Trypsin–EDTA solution (Sigma-Aldrich). For the subsequent analyses of selected piRNAs' expression levels, early passage cultures were used (10).

Tissue Sample Preparation and Nucleic Acid Extraction

All tissue samples were frozen and stored at −80°C in RNA stabilization solution—RNAlater (ThermoFisher Scientific, cat. n. AM7021). Fresh-frozen tissues were homogenized with ceramic beads and total RNA enriched with small RNA fractions was isolated using a mirVana miRNA Isolation Kit with phenol (Invitrogen). The concentration of extracted RNA was measured using UV spectrophotometry (NanoDrop 2000 Spectrophotometer, ThermoFisher Scientific) and the integrity of the obtained RNA was assessed *via* electrophoresis on 1% agarose gel. The RNA integrity number (RIN) was assessed with capillary electrophoresis (2200 Tape Station, Agilent).

piRNA Expression Profile Analysis With Next-Generation Sequencing

cDNA libraries for next-generation sequencing were prepared using the CleanTag Small RNA Library Preparation Kit (TriLink Biotechnologies, cat. n. L3206). Concentrations of cDNA libraries were assessed by fluorimetry (Qubit 2.0, ThermoFisher Scientific), and the integrity of libraries was measured by capillary electrophoresis (2200 TapeStation, Agilent). Subsequently, selection of fragments corresponding to a specific length of sncRNA with added adaptors was performed on cDNA libraries using gel electrophoresis (Pippin Prep, Sage Science).

TABLE 1 | Clinical, histopathological, and molecular characteristics of patients included in the study.

Variable	All patients		Patients with concomitant chemoradiotherapy	
	Explorative phase	Validation phase	Explorative phase	Validation phase
Number of patients	19	77	11	30
Age (years; median, range)	64 (42–75)	64 (30–80)	60 (42–71)	61 (33–74)
Gender (men)	11 (58%)	41 (53%)	6 (55%)	19 (63%)
IDH 1/2 mutation	0 (0%)	6 (8%)	0 (0%)	2 (7%)
MGMT methylation	5 (26%)	22 (29%)	3 (27%)	9 (30%)
Concomitant RT with TMZ	11 (58%)	36 (47%)	11 (100%)	30 (100%)

Selected cDNA library fragments underwent next-generation sequencing [NextSeq 500/550 High Output v2 kit (75 cycles)] (Illumina, cat. n. FC-404-2005) on a NextSeq 500 Sequencing System (Illumina). Raw fastq reads were quality checked with FastQC (v0.11.5) and Kraken (v15-065). 3′end adapters were trimmed with Cutadapt (v1.15). The trimmed sequences were size filtered for expected piRNA sizes (24–32 bp), and low-quality ends (Phred < 10) were removed with Cutadapt (v1.15). Statistics from all the preprocessing steps were summarized with MultiQC (v1.4).

Known contaminants (rRNA, tRNA, snoRNA, snRNA, YRNA, and miRNA—stemloop; Ensembl 91) were removed from the preprocessed reads by mapping (end-to-end) the reads to their sequences with Bowtie (v1.2.1.1) with a maximum of 1 mismatch. The preprocessed and cleaned reads were mapped (end-to-end) to human piRNA sequences downloaded from the piRBase database (v1.0) using Bowtie (v1.2.1.1) with a maximum of two mismatches. Raw Bowtie output was converted to SAM format using in-house Perl script and further processed with Samtools (v1.6), Picard (2.8.2), and cgat (v0.3.2). FeatureCounts (v1.5.0) were used to summarize the piRNA counts (minimal overlap of 24 bp). The multimapped reads were equally divided to the mapped references as fractions. Differential expression was calculated in R (v3.4.3) with package DESeq2 (v1.16.1). The criterion of adjusted p-value < 0.05 for differentially expressed piRNAs was considered alone, without any restrictions on logFC. The limma procedure, which does not require any other restrictions, was applied and Benjamini-Hochberg correction was then performed to adjust for multiple comparisons to control for false discovery rate. Only piRNAs with |logFC| > 0.5 were identified as differentially expressed.

Quantification of piRNAs by qRT-PCR

For the synthesis of cDNA from RNA enriched by a fraction of small RNAs, 6.66 ng of RNA was used. For reverse transcription, a TaqMan MicroRNA Reverse Transcription Kit (Applied Biosystems, cat. n. 4366596) was used. A LightCycler 480 Instrument II (Roche) together with a TaqMan MicroRNA Assay protocol (ThermoFisher Scientific) were used for qRT-PCR. The threshold cycle data were determined using the default threshold settings of the machine. All of the performed PCR reactions were made in duplicate, followed by calculation of the average Ct and SD values. For the evaluation of the results, the relative piRNA expression level was calculated by the $2^{-\Delta CT}$ method. ΔCTs were calculated according to the following formula: ΔCT = CT(piRNA of interest) – CT[(CtmiR-103 + CtU6)/2]. As reference molecules, miR-103 and U6 were chosen based on the current literature. GraphPad Prism 8 software (San Diego, CA, USA) was used for the following statistical evaluation including Mann–Whitney non-parametric tests, ROC analysis, and Kaplan–Meier analysis, together with JMP 14.3.0 (Cary, NC, USA), which was used for combined ROC analysis and univariable analysis. As a threshold of significance, a p-value = 0.05 was selected. ROC curve analysis was used to determine the area under the curve (AUC) including 95% confidence interval (CI) values, and cutoff points were set to achieve the highest levels of sensitivity and specificity. In the case of ROC focused on piR-23231 distinguishing the ability between better and poorer prognosis samples, the criterion of division of samples into two groups was set to survival longer or shorter than 15 months. For Kaplan–Meier survival analysis, the log-rank test was used to determine statistical significance. The piR-23231 relative expression value dividing GBM samples/patients into lower and higher piR-23231 expression groups has been determined to be 29.27 using ROC analysis.

Stable Cell Lines and Reagents

For the *in vitro* part of the study, GBM cell line U-251 MG was chosen and maintained in DMEM supplemented with 10% FBS, 1 mM sodium pyruvate, 2 mM glutamine, 100 units/ml of penicillin, and 100 μg/ml of streptomycin. piRNA mimetics with 3'methylated end nucleotides were purchased from IDT—piRNA mimetics piR-hsa-9491—5′UGAAUCUGACAACAGAGGCUUACGACCCCUUmA3′; piR-hsa-12488—5′ CAGAGUGUAGCUUAACACAAAGCACCCAACUmG3′; also, piRNA-like non-targeting RNA sequence was used as scrambled oligonucleotide control 5′ ACGCCACGUCUUAUAUUAACACAACGGUGAGmC3′. For *in vitro* assays, reverse transfection was used using LipofectAMINE RNAiMAX transfection reagent (Invitrogen) according to the manufacturer's protocol. Upregulation of specific piRNA levels was confirmed by qRT-PCR.

Furthermore, commercial stable normal human astrocytes (N7805100, ThermoFisher Scientific) were used for analysis of selected piRNAs' expression levels. These cells are maintained in DMEM supplemented with 10% FBS and 1% N2 supplement (all ThermoFisher Scientific).

MTT Cell Viability Assay

Cells were transfected with piRNA mimetics and scrambled oligonucleotides; also, LipofectAMINE RNAiMAX without RNA oligonucleotides was used as MOCK negative control. MTT (3-(4,5-dimethylthiazol-2-yl)-2,5-diphenyltetrazolium

bromide) was added to the cells after 24 h from transfection and left to metabolize for 2 h. Then, the medium with MTT was aspirated and formazan crystals were dissolved in DMSO (dimethyl sulfoxide). Absorbance was measured using the FLUOstar Omega reader. The method was performed in five independent repetitions in different times; each repetition was performed in hexaplicate.

Colony Formation Assay

One hundred fifty cells per well were seeded and transfected with selected oligonucleotides; also, MOCK was used as control. Cells were left to grow for 10 days and then stained with crystal violet and analyzed using ImageJ v1.8.0 software. Experiments were done in hexaplicate, and five repeated experiments were performed. Colony numbers were analyzed in GraphPad Prism 8 using *t*-test.

RESULTS

Global Expression Analysis of piRNAs in GBM Tissue Samples and Non-Tumor Brain Control

From a set of 595 detected piRNA molecules, 58 molecules accomplished criteria of detection in at least 50% samples with more than 50 reads in GBM tumor tissues (n = 19) and non-tumor samples (n = 11) [median of average expressions = 10.2565; median of log fold change (logFC) = 0.3873] (**Figure 1**). Following statistical evaluation using limma approach identified 15 significantly downregulated piRNAs in GBM samples, whereas 23 of piRNA molecules were significantly upregulated in GBM ($p_{adjust} < 0.05$) (**Table 2**). After the tightening of criteria ($p < 0.0001$), 17 piRNA molecules showed significant dysregulation between tumors and controls.

Validation of the Expression of Selected piRNAs in the Independent Cohort of the GBM Patient Tissue Samples Against Non-Tumor Controls and Primary GBM Cell Lines Against Normal Human Astrocytes

Five piRNAs (piR-hsa-1849, piR-hsa-5938, piR-hsa-9491, piR-hsa-12487, and piR-hsa-12488) selected based on NGS data as the five most significantly dysregulated piRNAs in GBMs were validated on an independent cohort of 77 GBM samples and 23 non-tumor controls. The qRT-PCR analysis using TaqMan stem-loop assays followed by Mann–Whitney analysis confirmed the results from NGS in four piRNAs (piR-1849, piR-9491, piR-12487, and piR-12488) (**Figure 2**). The same results were observed also when comparing primary GBM cell lines and normal human astrocytes (NHA) (**Figure 3**). ROC analyses that differentiate which piRNA/piRNAs have the best distinguishing effect between GBM tissue and non-tumor tissue reveal that the piR-9491 alone shows the best specificity and sensitivity in identifying GBM samples from non-tumor samples (AUC = 0.978) (**Figure 4**); specificity and sensitivity in both other standalone piRNAs and other piRNA combinations were lower.

Tumor Tissue Expression of piR-23231 Is Associated With OS of GBM Patients

Cox regression analysis of OS of GBM patients and global piRNA expression profiles has shown associations with piR-28876, piR-23231, and piR-18709 ($p < 0.1$). Subsequent ROC analysis on the independent cohort of GBM patients who underwent completed Stupp protocol (radiotherapy 60 Gy, 42 cycles of TMZ, and possible adjuvant therapy with TMZ) confirmed that piR-23231 has been able to distinguish patients surviving less and more than 15 months with 75% sensitivity and 66.67% specificity (AUC = 0.7176; **Figure 5A**). Significant association of piR-23231 expression and OS has also been confirmed by Kaplan–Meier analysis ($p = 0.0071$; log-rank test). Specifically, lower expression of piR-23231 has been significantly associated with poorer survival (**Figure 5B**). Finally, univariate Cox regression analysis has confirmed the association of piR-23231 with survival in this examined cohort of GBM patients ($p = 0.02$).

piR-hsa-9491 and piR-hsa-12488 Reduce the Ability to Form Colonies *In Vitro*

We performed *in vitro* transient transfection of piR-hsa-9491 and piR-has-12488 mimics in U-251 MG cell lines to investigate the effect of piR-hsa-9491 and piR-has-12488 levels on GBM cell viability and the ability to form colonies. Colony formation assays showed that both piR-hsa-9491 and piR-has-12488 significantly reduced the ability to form colonies in examined GBM cell line when compared with both control scrambled oligonucleotide and MOCK control (**Figure 6**). MTT viability assay did not show any significant results for selected piRNAs.

DISCUSSION

Despite improvements in oncological care, as well as refinements in neurosurgery and radiodiagnostics, the prognosis of GBM patients remains poor, and in addition, they often suffer from a severely diminished quality of life. This is mostly due to the aggressive and infiltrative character of the disease as well as its cellular and molecular heterogeneity. Brain tissue infiltration by tumor cells exceeds the resection borders; thus, recurrence relatively early into treatment is common. Even compared to other cancers, GBM has a low OS with a median of 14–15 months from diagnosis (1, 11). Treatment of patients with GBM remains an immense challenge; therefore, there is a great need for a better understanding of the molecular background of the disease, its origin, and development. Also, identification of new potential diagnostic and prognostic biomarkers, usable for better patient care management and the prediction of the course of the disease, and novel therapeutic targets could be greatly influential in the future GBM treatment (5). Due to the considerable heterogeneity prevailing between individual GBMs, new molecular markers for better categorization of individual tumors are also in high demand (12).

Dysregulation of short non-coding RNAs was described as a crucial action in the development of most tumors. Moreover, sncRNAs are involved in the vast majority of cellular processes; thus, disruption of their regulation is a crucial step in

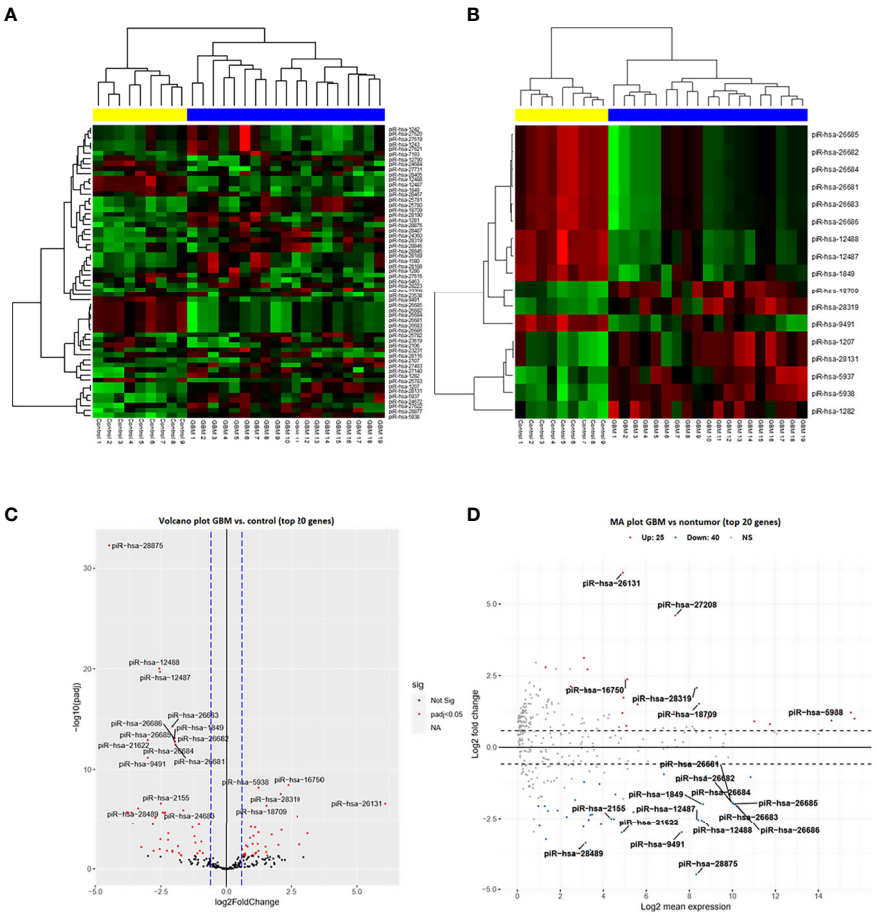

FIGURE 1 | PiRNA expression profiling based on next-generation sequencing data. **(A)** Clustering analysis with heatmap based on the expression of 58 identified piRNAs meeting the criteria of more than 50 reads in at least 50% of samples. Samples were divided into a tumor group (blue) and a control group (yellow) with 100% sensitivity and 100% specificity. Thirty-five piRNAs were upregulated (red) in glioblastoma and 23 were downregulated (green) in glioblastoma. **(B)** Clustering analysis of 17 selected differentially expressed piRNAs (adj. $p < 0.0001$) in glioblastoma compared to non-tumor controls. **(C)** Volcano plot of the dependency of the log2 adjusted p-value on log2 Fold Change of all analyzed ($n = 58$) piRNAs. Red dots represent significantly dysregulated piRNAs (adj. $p < 0.05$); 20 genes with the highest results are described by their names. **(D)** Volcano plot of dependency of the Log2 fold change on Log2 mean expression of all analyzed ($n = 58$) piRNAs. Red dots present significantly dysregulated piRNAs (adj. $p < 0.05$); 20 genes with the highest results are described by their names.

cancerogenesis. A subgroup of sncRNAs—piRNAs, as well as their associated PIWI proteins, were described as aberrantly expressed in many cancers, including GBM. Their dysregulation is often associated with poorer prognosis, which suggests their possible functional role in cancer biogenesis and therefore they present promising diagnostic or prognostic biomarkers, as well as potential therapeutic targets (13). Most of the tumors arise because of epigenetic changes, accumulation of mutations and genome destabilization. The piRNA/PIWI pathway is one of the key regulators in genome stability maintenance. Together, specific piRNA and PIWI proteins form a piRISC complex to control the activity of transposons, including their translocation within the genome. Disruption of the transcriptional and post-transcriptional regulatory role of piRNA molecules could possibly lead to the upregulation of transposons and their uncontrolled incorporation within the genome, leading to increased genome destabilization (14). Moreover, specific piRNAs could be responsible for the regulation of the expression of specific genes, involved in cancer development, growth, or maintenance (15–17). piRNAs with specific protein interactions were also described, extending the possible scoop of action of these molecules (18). Overall, the piRNA/PIWI pathway could play a significant role in cancerogenesis or therapy response of the tumors as significant dysregulation of piRNA molecules has been described in several studies and specific piRNAs as potential biomarkers or therapeutic targets have been proposed (19).

However, studies involving GBM or at least malignant gliomas are rarely seen; therefore, we decided to fill this gap. The aim of this study was to identify piRNAs associated with gliomagenesis, which could be potentially used for the diagnostics or prognosis determination. One of the first studies exploring piRNAs in the context of GBM was done by Jacobs et al., describing approximately 350 piRNA molecules in both tumor and stromal tissue using array-based piRNA expression profiling; among these, piR-8041 (piR-

TABLE 2 | List of the significantly dysregulated PIWI-interacting RNAs in GBM patients compared to non-tumor controls based on next-generation sequencing data.

Upregulated piRNAs in GBM				Downregulated piRNAs in GBM			
piRNA	**logFC**	**AveExpr**	**adj. *p*-value**	**piRNA**	**logFC**	**AveExpr**	**adj. *p*-value**
piR-hsa-5938	**1.429**	**17.409**	**<0.001**	**piR-hsa-12488**	**−2.355**	**10.116**	**<0.001**
piR-hsa-28319	1.851	9.843	<0.001	**piR-hsa-12487**	**−2.335**	**9.971**	**<0.001**
piR-hsa-18709	1.700	10.275	<0.001	**piR-hsa-9491**	**−3.159**	**8.670**	**<0.001**
piR-hsa-5937	1.123	16.535	<0.001	**piR-hsa-1849**	**−1.875**	**10.348**	**<0.001**
piR-hsa-1207	1.342	16.538	<0.001	piR-hsa-26683	−1.953	11.898	<0.001
piR-hsa-28131	1.341	16.538	<0.001	piR-hsa-26686	−1.883	11.842	<0.001
piR-hsa-1282	1.102	12.993	<0.001	piR-hsa-26685	−1.848	11.778	<0.001
piR-hsa-25781	1.189	10.880	<0.001	piR-hsa-26682	−1.844	11.765	<0.001
piR-hsa-28877	1.147	17.55	<0.001	piR-hsa-26684	−1.826	11.748	<0.001
piR-hsa-25780	1.099	10.725	0.001	piR-hsa-26681	−1.825	11.742	<0.001
piR-hsa-24672	0.846	16.164	0.001	piR-hsa-24684	−1.17	9.249	0.001
piR-hsa-28876	0.881	9.845	0.006	piR-hsa-25783	−0.904	12.762	0.002
piR-hsa-27493	0.856	13.67	0.007	piR-hsa-28467	−0.949	10.640	0.007
piR-hsa-28487	0.821	10.189	0.015	piR-hsa-27616	−0.807	8.783	0.01
piR-hsa-1281	0.787	10.073	0.019	piR-hsa-27731	−0.718	9.427	0.052
piR-hsa-1580	0.742	8.714	0.019				
piR-hsa-28189	0.742	8.714	0.019				
piR-hsa-25782	0.614	11.677	0.025				
piR-hsa-23209	1.114	8.802	0.028				
piR-hsa-27622	0.724	15.945	0.025				
piR-hsa-27140	0.774	13.97	0.028				
piR-hsa-7193	0.706	9.222	0.03				
piR-hsa-28188	0.669	8.315	0.04				

Five piRNAs in bold were selected for further validation by qRT-PCR.
log Fold Change = logFC, average expression = AveExpr, adjusted p*-value = adj.* p*-value*

11270 in piRBase, DQ580941) was downregulated, and its upregulation in *in vivo* experiments showed remarkable tumor suppressive effects (9). Nevertheless, limitations of this study are a low number of patients in the piRNA profiling phase; only seven tumors and seven controls were included. Furthermore, the study lacks the validation phase with the independent cohort of patients. In our study, piR-8041 was not found in piRNAs significantly dysregulated in GBM compared to non-tumor controls, as it did not meet the criterion of minimum samples in which it was detected (50 reads at least in 50% samples). This finding could be caused by markedly wider sample size as well as different methodology used for the analysis. Going through glioma studies, Leng et al. described piR-20280 (DQ590027) as an important player in the piR-20280/MIR17HG/miR-153/FOXR2 pathway, playing a crucial role in the regulation of the permeability of glioma-conditioned normal brain–blood barrier (15). Liu et al. described piR-30188 as part of the PIWIL3/OIP5-AS/miR-367-3p/CEBPA pathway, which is downregulated in gliomas, and its overexpression together with overexpression of PIWIL3 and miR-367-3p lead to inhibition of glioma cell progression (16). Shen et al. described piR-23387

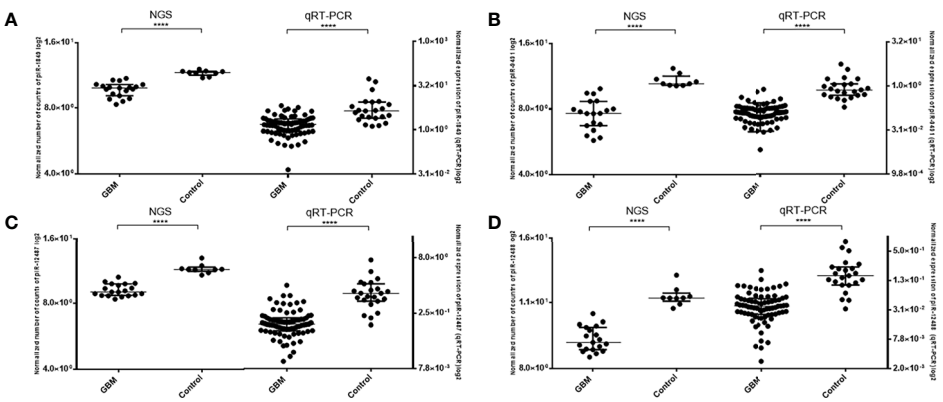

FIGURE 2 | Results of Mann–Whitney analysis of independent validation of selected piRNAs and comparison between obtained results from next-generation sequencing and qRT-PCR. **(A)** piR-1849; **(B)** piR-9491; **(C)** piR-12487; **(D)** piR-12488. ****$p < 0.0001$.

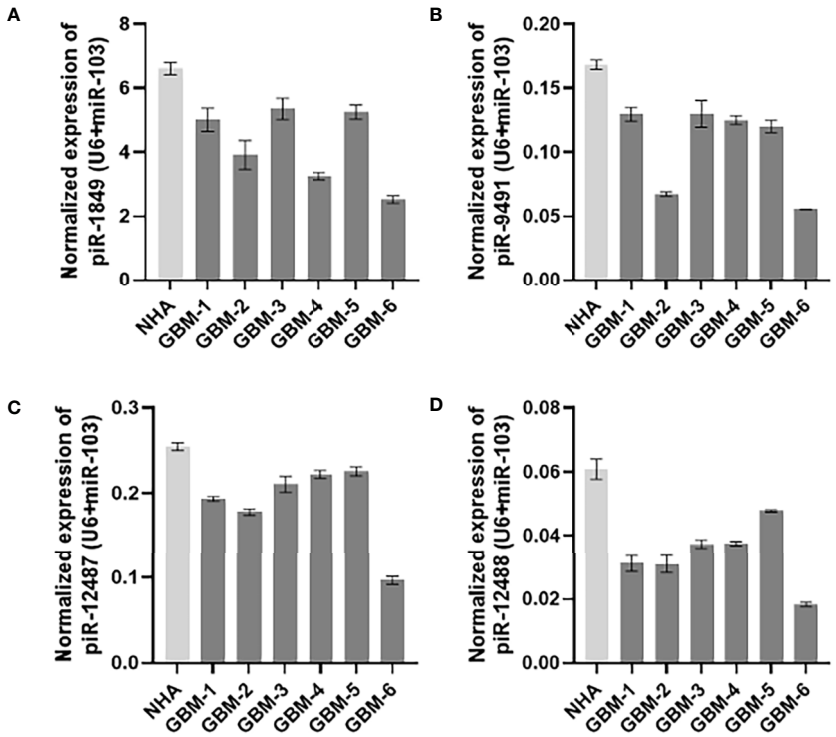

FIGURE 3 | Expression levels of **(A)** piR-1849; **(B)** piR-9491; **(C)** piR-12487; **(D)** piR-12488 in normal human astrocytes (NHA) and primary glioblastoma cell lines analyzed by qRT-PCR.

(DQ593109) as a molecule with an impact on the permeability of the blood–tumor barrier (17). However, those studies aimed different biological processes; specifically, they are not designed for the observation of molecules potentially involved in GBM development or progression of the disease; rather, they focused on the interesting topic of the changes of permeability of blood–brain barrier mediated by the presence of gliomas. This is the basis for the differences between our studies as the authors, mentioned above, use appropriate cell models instead of GBM tissue and different methodology. Despite the different aims of the studies, material, and methodology used, we were able to identify molecules from Shen et al. (piR-DQ593109) and Leng et al. (piR-DQ590027) in our dataset; unfortunately, they did not pass the criterion of at least 50 reads in 50% of the samples, which is completely understandable under the given study conditions and differences.

In the discovery phase of our study, we analyzed 58 piRNAs, selected by strict criteria (50 reads at least in 50% of samples). From this group, we found 23 significantly upregulated piRNAs in GBM in comparison to non-tumor controls and 15 downregulated molecules. From the group of 38 dysregulated piRNAs, several of them were already described as molecules related to cancer. Hashim et al. described piR-28877 (DQ598677) as upregulated, and piR-28467 (DQ598252) and piR-27616 (DQ597341) as downregulated in breast cancer, which corresponds with our results in GBM (20). Also, Huang et al. performed global profiling of piRNAs in breast cancer to find piR-27493 (DQ597218) and piR-7193 (DQ576872) as upregulated, which correspond with our findings in GBM (21). The same tendencies of dysregulation of abovementioned piRNAs possibly suggest cellular roles that could be conserved across different cell types. On the other hand, some of the piRNAs [piR-26682 (DQ596466), piR-26684 (DQ596468)] from the chrM:12206-12237:+ region were also described in a study from Chu et al. On the contrary, those piRNAs were described as upregulated in bladder cancer in contrast to our observation in GBM, suggesting the possible tissue-specific roles of those piRNAs (22). Interestingly, piRNAs from the same region [piR-26681 (DQ596465), piR-26683 (DQ596467), piR-26685 (DQ596469), piR-26686 (DQ596470)] are found to be downregulated in GBM, which may suggest a potential tumor suppressive role of this genomic region. piR-823 (piR-1282, DQ571031) is a well-known molecule described in many cancers with variable expression among different tumors. In multiple myeloma, it is upregulated and connected to *de novo* methylation and angiogenesis (23). However, in gastric cancers, piR-823 is significantly downregulated, contributing to tumor growth, and its increase suppresses tumor growth *in vivo* (24). In the context of GBM, piR-823 was found to be upregulated, corresponding to a case of multiple myeloma, suggesting possible similarities with the role of piR-823 in multiple myeloma. Our finding is also another evidence of the tissue-specific role of piR-823 in various tumors. Interestingly, piR-1849, which is one of the molecules we were interested in, was earlier identified as the molecule that is cargoed into the

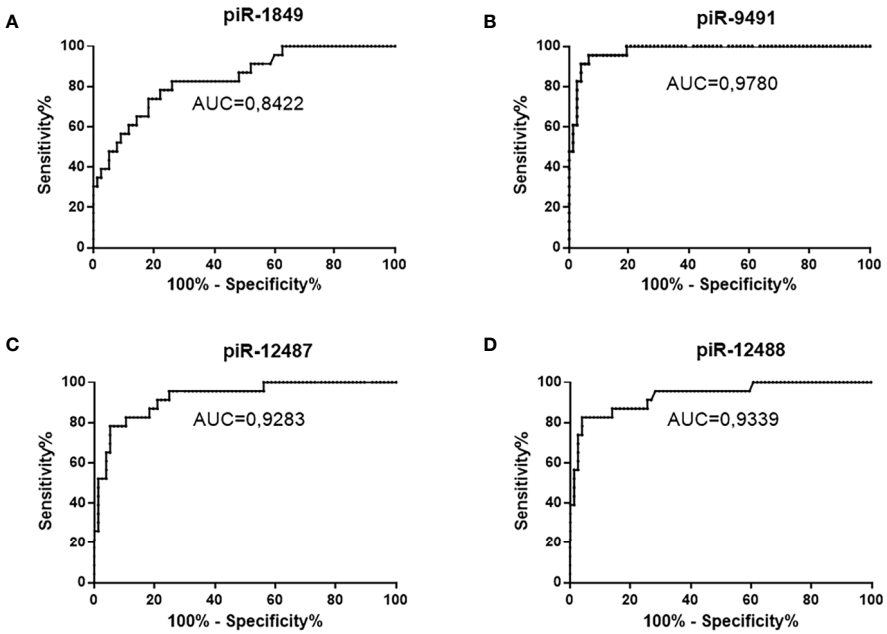

FIGURE 4 | ROC analysis of all successfully validated piRNA molecules and their distinguishing ability between tumors and non-tumor controls. **(A)** piR-1849, AUC 0.8422, sensitivity 82.6%, specificity 74%; **(B)** piR-9491 AUC 0.978, sensitivity 100%, specificity 80.5%; **(C)** piR-12487 AUC 0.9283, sensitivity 91.3%, specificity 79.2%; **(D)** piR-12488 AUC 0.9339, sensitivity 87%, specificity 85.7%.

extracellular vesicles that are released from the GBM cells and could be a potentially promising biomarker of the disease (25).

In the explorative phase, piR-1849 (DQ571526), piR-5983 (DQ575705), piR-9491 (DQ579193), piR-12487 (DQ582264), and piR-12488 (DQ582265) (all adj. p-value < 0.0001) were selected for the validation on the independent cohort of 77 tumor samples and 23 non-tumor controls. We successfully validated piR-1849, piR-9491, piR-12487, and piR-12488 as significantly downregulated molecules in GBM. Subsequently, we performed ROC analyses to identify analytical characteristics of validated piRNAs in distinguishing ability between tumors and non-tumors. It should be mentioned that all selected piRNAs have strong distinguishing abilities alone. However, of all possible combinations of those four piRNAs and the same piRNAs standalone, piR-9491 showed the highest specificity, sensitivity, and AUC.

In search of piRNAs possibly linked to prognosis, we examined obtained data trying to find an association between piRNA expression patterns and OS of GBM patients. In order to increase the validity of our results, we selected only patients who had undergone concomitant chemoradiotherapy in the extent of the Stupp protocol in this part of the study. Kaplan–Meier analyses showed that only piR-23231 (DQ592953) was significantly connected with prognosis (p = 0.0071; log rank test) in GBM patients, and its lower level was associated with a worse prognosis. This coincides with our previous NGS analysis, where piR-23231 was significantly downregulated in GBM and possibly contributing to GBM behavior and poorer survival, which have to

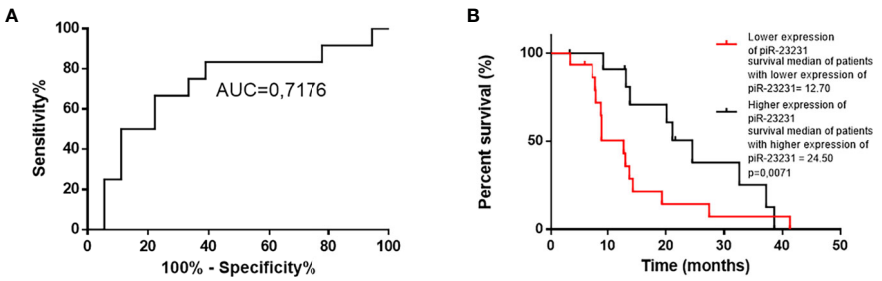

FIGURE 5 | ROC and Kaplan–Meier analysis of piR-23231 on validation cohort of patients. **(A)** ROC analysis to determine the distinguishing ability of piR-23231 between patients with survival shorter and longer than 15 months. **(B)** Kaplan–Meier analysis of lower levels of piR-23231 against higher levels (p = 0.0071).

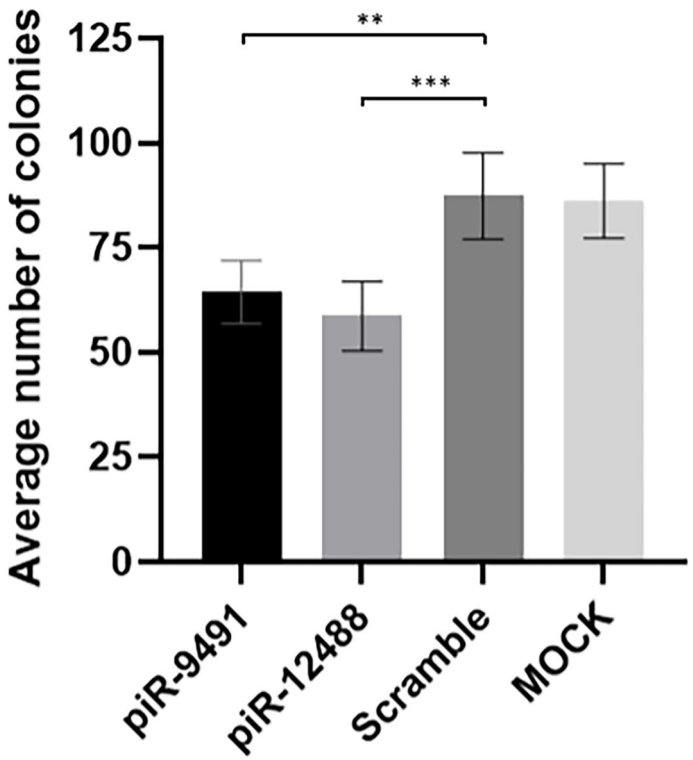

FIGURE 6 | Colony formation analysis results for hsa-piR-9491 and hsa-piR-12488 compared to scrambled oligonucleotide and MOCK negative control. Increased levels of piR-9491 and piR-12488 led to decreased number of colonies compared to scrambled oligonucleotide and U251 MG cells treated with transfection reagent without oligonucleotide (MOCK). $^{**}p < 0.01$, $^{***}p < 0.001$.

be confirmed by appropriate *in vitro* and *in vivo* analyses. Also, Cox regression analyses were performed to distinguish the effect of piR-23231 as a potential prognostic biomarker.

In addition to previously mentioned works, it must be noted that piRNA role in cancer is rather controversial due to the findings of Tosar et al. (26). Based on this study, most of the annotated piRNAs, including some piRNAs described in cancer or other pathophysiological conditions, could be considered as cellular waste or RNA degradation products, originating from rRNA, tRNA, and other RNA species. The main issue is that the large bulk of annotated piRNAs does not meet the main features of this group of molecules, as they lack 1U or 10A. On the other hand, based on the articles mentioned above, it is clear that even molecules lacking 1U can affect cellular qualities and behavior; in fact, two best-described piRNAs—hsa-piR-651 and hsa-piR-823—are lacking 1U. Rather than sequence qualities of each individual piRNA, it would be more convincing to determine whether the particular piRNA binds to PIWI proteins or is able to alter cellular properties or behavior in response to functional analyses.

To answer the previously mentioned issues, functional analyses of selected piRNAs were carried out in U251 MG cells. piRNA expression levels were increased using transient transfection methodology; results were confirmed by qRT-PCR. Analyses showed that higher levels of piR-has-9491 and piR-has-12488 led to the reduced GBM cells' ability to form colonies. Therefore, we assume that these two piRNAs can alter cellular properties and, thus, they are functional molecules rather than degradation fragments of other RNA molecules. However, their specific role in cell biology and ability to bind PIWI proteins must be determined in future studies. Notwithstanding this fact, molecules analyzed in this study provide promising potential GBM biomarkers that could be used for the diagnosis assessment and prognosis determination, if future studies confirm their role in the GBM biology.

CONCLUSIONS

This study presents the largest study so far focused on the global piRNA profiling in GBM tissue samples and non-tumor brain tissue specimens. We identified a set of piRNAs significantly deregulated in GBM from which piR-9491 and piR-12488 were able to reduce the ability to form tumor cell colonies *in vitro*. These two piRNAs seem to be interesting molecules for other investigations, mainly as therapeutic targets in GBM. Finally, expression levels of piR-23231 were associated with patients' OS, suggesting that some piRNAs could also present prognostic biomarkers in GBM. Based on the results, identified piRNAs could be part of the machinery involved in the pathogenesis of gliomas, which needs to be examined in future studies.

DATA AVAILABILITY STATEMENT

The datasets presented in this study can be found in online repositories. The names of the repository/repositories and accession number(s) can be found below: NCBI SRA; PRJNA747758.

ETHICS STATEMENT

The studies involving human participants were reviewed and approved by Local ethics committees at: Masaryk University, Brno; University Hospital Brno, Brno; University Hospital Hradec Kralove, Hradec Kralove. The patients/participants provided their written informed consent to participate in this study.

AUTHOR CONTRIBUTIONS

The proposed study was undertaken at several clinical and academic workplaces. All authors contributed to data acquisition, analyses, and manuscript preparation. Conceptualization: MB, OS, and JS. Data curation: LR, JO, VV, and PF. Formal analysis: FS, LR, and JO. Funding acquisition: OS and JS. Investigation: FS, TK, and MiH. Methodology: AK and MV. Project administration: TK and RLa. Resources: MB, RJ, VV, PF, MS, and RLi. Clinical Data: MaH, PK, ZP, and RLa. Supervision: MV, RJ, MaH, MS, RLi, TC, and JS. Validation: AK and MV. Visualization: FS and JS. Writing—original draft: FS and JS. Writing—review and editing: MB and OS. All authors contributed to the article and approved the submitted version.

FUNDING

This work was financially supported by the Ministry of Health, Czech Republic grant no. NV19-03-00501, conceptual development of research organizations (MOU, 00209805; and FNBr, 65269705); Ministry of Education, Youth and Sports, Czech Republic under the project CEITEC 2020 (LQ1601); and European Regional Development Fund-Project BBMRI-CZ: Biobank network—a versatile platform for the research of the etiopathogenesis of diseases, No. EF16 013/0001674.

ACKNOWLEDGMENTS

We acknowledge the CF Genomics CEITEC MU supported by the NCMG research infrastructure (LM2018132 funded by MEYS CR) for their support with obtaining scientific data presented in this paper.

REFERENCES

1. Sasmita AO, Wong YP, Ling APK. Biomarkers and Therapeutic Advances in Glioblastoma Multiforme. *Asia Pac J Clin Oncol* (2018) 14:40–51. doi: 10.1111/ajco.12756
2. Wesseling P, Capper D. WHO 2016 Classification of Gliomas. *Neuropathol Appl Neurobiol* (2018) 44:139–50. doi: 10.1111/nan.12432
3. Ohgaki H, Kleihues P. The Definition of Primary and Secondary Glioblastoma. *Clin Cancer Res* (2013) 19:764–72. doi: 10.1158/1078-0432.CCR-12-3002
4. Ostrom QT, Bauchet L, Davis FG, Deltour I, Fisher JL, Langer CE, et al. The Epidemiology of Glioma in Adults: A "State of the Science" Review. *Neuro Oncol* (2014) 16:896–913. doi: 10.1093/neuonc/nou087
5. Alexander BM, Cloughesy TF. Adult Glioblastoma. *JCO* (2017) 35:2402–9. doi: 10.1200/JCO.2017.73.0119
6. Ross RJ, Weiner MM, Lin H. PIWI Proteins and PIWI-Interacting RNAs in the Soma. *Nature* (2014) 505:353–9. doi: 10.1038/nature12987
7. Iwasaki YW, Siomi MC, Siomi H. PIWI-Interacting RNA: Its Biogenesis and Functions. *Annu Rev Biochem* (2015) 84:405–33. doi: 10.1146/annurev-biochem-060614-034258
8. Han YN, Li Y, Xia SQ, Zhang YY, Zheng JH, Li W. PIWI Proteins and PIWI-Interacting RNA: Emerging Roles in Cancer. *Cell Physiol Biochem* (2017) 44:1–20. doi: 10.1159/000484541
9. Jacobs DI, Qin Q, Fu A, Chen Z, Zhou J, Zhu Y. piRNA-8041 Is Downregulated in Human Glioblastoma and Suppresses Tumor Growth In Vitro and *In Vivo*. *Oncotarget* (2018) 9:37616–20. doi: 10.18632/oncotarget.26331
10. Sana J, Busek P, Fadrus P, Besse A, Radova L, Vecera M, et al. Identification of microRNAs Differentially Expressed in Glioblastoma Stem-Like Cells and Their Association With Patient Survival. *Sci Rep* (2018) 8:2836. doi: 10.1038/s41598-018-20929-6
11. Omuro A. Glioblastoma and Other Malignant Gliomas: A Clinical Review. *JAMA* (2013) 310:1842. doi: 10.1001/jama.2013.280319
12. Wen PY, Kesari S. Malignant Gliomas in Adults. *N Engl J Med* (2008) 359:492–507. doi: 10.1056/NEJMra0708126
13. Moyano M, Stefani G. piRNA Involvement in Genome Stability and Human Cancer. *J Hematol Oncol* (2015) 8:38. doi: 10.1186/s13045-015-0133-5
14. Assumpção CB, Calcagno DQ, Araújo TMT, dos Santos SEB, dos Santos AKCR, Riggins GJ, et al. The Role of piRNA and Its Potential Clinical Implications in Cancer. *Epigenomics* (2015) 7:975–84. doi: 10.2217/epi.15.37
15. Leng X, Ma J, Liu Y, Shen S, Yu H, Zheng J, et al. Mechanism of piR-DQ590027/MIR17HG Regulating the Permeability of Glioma Conditioned Normal BBB. *J Exp Clin Cancer Res* (2018) 37:246. doi: 10.1186/s13046-018-0886-0
16. Liu X, Zheng J, Xue Y, Yu H, Gong W, Wang P, et al. PIWIL3/OIP5-AS1/miR-367-3p/CEBPA Feedback Loop Regulates the Biological Behavior of Glioma Cells. *Theranostics* (2018) 8:1084–105. doi: 10.7150/thno.21740
17. Shen S, Yu H, Liu X, Chen J, Zhao L, Xue Y, et al. PIWIL1/piRNA-DQ593109 Regulates the Permeability of the Blood-Tumor Barrier *via* the MEG3/miR-330-5p/RUNX3 Axis. *Mol Ther Nucleic Acids* (2018) 10:412–25. doi: 10.1016/j.omtn.2017.12.020
18. Mei Y, Wang Y, Kumari P, Shetty AC, Clark D, MacKerell AD, et al. A piRNA-Like Small RNA Interacts With and Modulates P-ERM Proteins in Human Somatic Cells. *Nat Commun* (2015) 6:7316. doi: 10.1038/ncomms8316
19. Weng W, Li H, Goel A. Piwi-Interacting RNAs (piRNAs) and Cancer: Emerging Biological Concepts and Potential Clinical Implications. *Biochim Biophys Acta (BBA) - Rev Cancer* (2019) 1871:160–9. doi: 10.1016/j.bbcan.2018.12.005
20. Hashim A, Rizzo F, Marchese G, Ravo M, Tarallo R, Nassa G, et al. RNA Sequencing Identifies Specific PIWI-Interacting Small Non-Coding RNA Expression Patterns in Breast Cancer. *Oncotarget* (2014) 5:9901–10. doi: 10.18632/oncotarget.2476
21. Huang G, Hu H, Xue X, Shen S, Gao E, Guo G, et al. Altered Expression of piRNAs and Their Relation With Clinicopathologic Features of Breast Cancer. *Clin Transl Oncol* (2013) 15:563–8. doi: 10.1007/s12094-012-0966-0
22. Chu H, Hui G, Yuan L, Shi D, Wang Y, Du M, et al. Identification of Novel piRNAs in Bladder Cancer. *Cancer Lett* (2015) 356:561–7. doi: 10.1016/j.canlet.2014.10.004
23. Yan H, Wu Q-L, Sun C-Y, Ai L-S, Deng J, Zhang L, et al. piRNA-823 Contributes to Tumorigenesis by Regulating De Novo DNA Methylation and Angiogenesis in Multiple Myeloma. *Leukemia* (2015) 29:196–206. doi: 10.1038/leu.2014.135
24. Cheng J, Deng H, Xiao B, Hou H, Zhou F, Shen Z, et al. piR-823, a Novel Non-Coding Small RNA, Demonstrates In Vitro and *In Vivo* Tumor Suppressive

Activity in Human Gastric Cancer Cells. *Cancer Lett* (2012) 315:12–7. doi: 10.1016/j.canlet.2011.10.004
25. Hallal S, Khani SE, Wei H, Lee MYT, Sim H-W, Sy J, et al. Deep Sequencing of Small RNAs From Neurosurgical Extracellular Vesicles Substantiates miR-486-3p as a Circulating Biomarker That Distinguishes Glioblastoma From Lower-Grade Astrocytoma Patients. *Int J Mol Sci* (2020) 21(14):4954. doi: 10.3390/ijms21144954
26. Tosar JP, Rovira C, Cayota A. Non-Coding RNA Fragments Account for the Majority of Annotated piRNAs Expressed in Somatic Non-Gonadal Tissues. *Commun Biol* (2018) 1:2. doi: 10.1038/s42003-017-0001-7

Conflict of Interest: The authors declare that the research was conducted in the absence of any commercial or financial relationships that could be construed as a potential conflict of interest.

Publisher's Note: All claims expressed in this article are solely those of the authors and do not necessarily represent those of their affiliated organizations, or those of the publisher, the editors and the reviewers. Any product that may be evaluated in this article, or claim that may be made by its manufacturer, is not guaranteed or endorsed by the publisher.

frontiers in Oncology

REVIEW
published: 28 October 2021
doi: 10.3389/fonc.2021.770561

Immunosuppression in Glioblastoma: Current Understanding and Therapeutic Implications

Benjamin T. Himes[1], Philipp A. Geiger[2], Katayoun Ayasoufi[3], Adip G. Bhargav[4], Desmond A. Brown[5] and Ian F. Parney[1,3]*

[1] Department of Neurologic Surgery, Mayo Clinic, Rochester, MN, United States, [2] Department of Neurosurgery, University Hospital Innsbruck, Tirol, Austria, [3] Department of Immunology, Mayo Clinic, Rochester, MN, United States, [4] Department of Neurosurgery, University of Kansas, Kansas City, KS, United States, [5] Surgical Neurology Branch, National Institutes of Neurological Disorders and Stroke, National Institutes of Health, Bethesda, MD, United States

Glioblastoma (GBM) is the most common primary brain tumor in adults an carries and carries a terrible prognosis. The current regiment of surgical resection, radiation, and chemotherapy has remained largely unchanged in recent years as new therapeutic approaches have struggled to demonstrate benefit. One of the most challenging hurdles to overcome in developing novel treatments is the profound immune suppression found in many GBM patients. This limits the utility of all manner of immunotherapeutic agents, which have revolutionized the treatment of a number of cancers in recent years, but have failed to show similar benefit in GBM therapy. Understanding the mechanisms of tumor-mediated immune suppression in GBM is critical to the development of effective novel therapies, and reversal of this effect may prove key to effective immunotherapy for GBM. In this review, we discuss the current understanding of tumor-mediated immune suppression in GBM in both the local tumor microenvironment and systemically. We also discuss the effects of current GBM therapy on the immune system. We specifically explore some of the downstream effectors of tumor-driven immune suppression, particularly myeloid-derived suppressor cells (MDSCs) and other immunosuppressive monocytes, and the manner by which GBM induces their formation, with particular attention to the role of GBM-derived extracellular vesicles (EVs). Lastly, we briefly review the current state of immunotherapy for GBM and discuss additional hurdles to overcome identification and implementation of effective therapeutic strategies.

Keywords: immunosuppression, glioblastoma, myeloid - derived suppressor cell, extracellular vesicles, immunotherapy

OPEN ACCESS

Edited by:
Aleksi Sedo,
Charles University, Czechia

Reviewed by:
Antonio Silvani,
Fondazione Istituto Neurologico Carlo Besta (IRCCS), Italy
Kristin Huntoon,
University of Texas MD Anderson Cancer Center, United States

****Correspondence:***
Benjamin T. Himes
himes.benjamin@mayo.edu

Specialty section:
This article was submitted to Neuro-Oncology and Neurosurgical Oncology, a section of the journal Frontiers in Oncology

Received: *04 September 2021*
Accepted: *24 September 2021*
Published: *28 October 2021*

Citation:
Himes BT, Geiger PA, Ayasoufi K, Bhargav AG, Brown DA and Parney IF (2021) Immunosuppression in Glioblastoma: Current Understanding and Therapeutic Implications. Front. Oncol. 11:770561. doi: 10.3389/fonc.2021.770561

INTRODUCTION

Glioblastoma (GBM) is the most common primary tumor of the central nervous system (CNS) in adults, and carries with a dire prognosis, with median survival of just over 14 months in spite of maximal therapy including surgical resection, radiation, and chemotherapy with temozolomide (1, 2). This paradigm has remained essentially unchanged since 2005 and, while recent advances, including the addition of tumor treating fields (TTF) have shown some modest benefit, the overall

course of the disease remains effectively unchanged (3). Effective new therapies are urgently required.

Immune-modulating therapies are promising for many diseases including cancer. These therapies range from immunotherapies like check point inhibitors where the "brakes" are taken off the immune system in order to induce immune activation, to active immunotherapies like vaccines against cancer antigens, and even the use of oncolytic viruses to simultaneously kill tumor cells and stimulate anti-tumor immune responses. As a whole, immunotherapy has shown tremendous promise in cancer treatment, initially with hematologic malignancies and more recently in solid tumors. This includes several cancer types such as melanoma that previously carried a devastating prognosis (4–6). These therapies hinge on activating and enhancing the immune system's natural role in tumor surveillance and regulation, with specific treatments ranging from antibodies directed against specific tumor antigens, to tumor-derived vaccines, to chimeric-antigen receptor (CAR) T cells, to immune checkpoint inhibitors that seek to disinhibit the immune response against tumor cells (7–10). All of these promising strategies depend upon the underlying integrity of the patient's immune system in order to be of benefit. Successful cancer immunotherapy is dependent on existence of an intact and functional immune system. However, GBM patients frequently exhibit profound local and systemic immunosuppression, limiting the likely efficacy of these therapeutic strategies (**Figure 1**) (11–14). This overt immunosuppression is a critical barrier to improving patient survival through immunotherapy. Without targeting this immunosuppression in GBM, most immunotherapies seem destined to fail. Indeed, several prominent clinical trials of immunotherapies in GBM have failed to demonstrate therapeutic benefit (15–19).

Understanding the mechanisms of immune dysfunction is essential to effectively employing immunotherapies in GBM, yet the nature of these mechanisms remains surprisingly elusive. Tumor-mediated immunosuppression in GBM is unique in that it is severe, multifaceted, and simultaneously affects the tumor-microenvironment and peripheral immune organs even though the tumor itself is limited to the central nervous system (**Figure 1**). In this review, we summarize current knowledge regarding mechanisms of immunosuppression in GBM and offer insights into future immunotherapeutic avenues for this devastating disease.

EPIDEMIOLOGY AND CURRENT TREATMENT

GBM is the most common primary brain tumor, with an annual incidence of 3.19 per 100,000 patients diagnosed annually in the United States (20). Median age of onset is 64 and the disease has a predilection for Caucasian males (20). Current therapy entails maximal safe surgical resection followed by radiation (typically 60Gy over thirty fractions) with adjuvant temozolomide chemotherapy (2). With these maximal interventions, median survival remains just over 14 months with a 2 year survival of under 30% (21, 22). Additional treatments such as the addition of tumor-treating fields (TTF; locally delivered alternating electrical fields) to first line therapy or bevacizumab (anti-angiogenic therapy directed at vascular endothelial growth factor) in recurrent disease provide some modest benefit, but little has changed in the therapeutic paradigm in nearly fifteen years (3, 23). Certain molecular subgroups such as isocitrate dehydrogenase (IDH) mutant or O^6-methylguanine-DNA

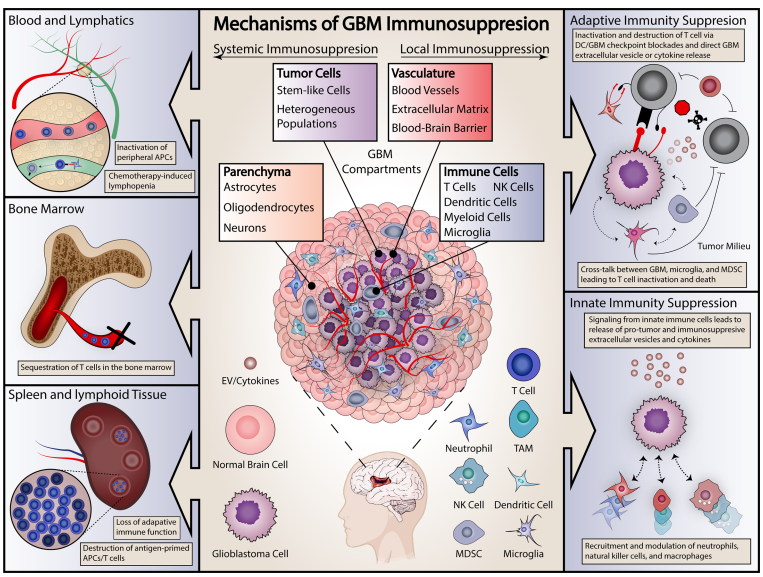

FIGURE 1 | Summary of proposed mechanisms of GBM immunosuppression. Immunosuppressive effects are categorized as either systemic (on left) or local (right). Systemic effects are exerted on either the blood and lymphopoietic systems (including the bone marrow) or secondary lymphoid organs, including the spleen. Local effects include effects on both the adaptive and innate immune systems. Specific examples are included in each panel.

methyltransferase (MGMT) promoter methylated tumors have been correlated with increased survival, but survival in even these cases remains poor long-term (24–26). Occurrence is sporadic, with few environmental or genetic risk factors identified in most cases.

IMMUNE SURVEILLANCE IN CANCER AND GLIOBLASTOMA

Fundamentally, cancer develops in part from a failure of normal immune surveillance. This has traditionally been described as proceeding through three phases: elimination, equilibrium, and escape (27). In the course of normal cell growth and tissue maintenance, cells suffer mutations from mitotic errors or environmental insults, predisposing them to neoplasia. In a healthy immune system, these cells are detected and deleted before tumor formation (the elimination phase) (27, 28). This proceeds through several mechanisms. Mutated cells can present neoantigens on the major histocompatibility complexes (MHC) on their cell surface, failing to register as presenting 'self' antigens by circulating natural killer (NK) or CD8 T cells, resulting in their targeted removal (29). Focal tissue disruption caused by tumor growth causes the release of inflammatory mediators and alarmins, triggering an innate immune response and tissue remodeling, which can create a hostile microenvironment for tumor growth (30).

Historically, the immune system's role in tumor surveillance was considered controversial. Because autoreactive T and B cells are deleted during development to prevent autoimmunity, the idea of beneficial deletion of host cells by mature immune cells in the periphery was considered anathema to basic function of the immune system. However, accumulating evidence such as increased tumor development in immunodeficient animal models lent credence to the idea that the immune system serves as a check on tumorigenesis (27, 31). Similar results were found in immunosuppressed human patients (32). Seminal experiments demonstrating the major histocompatibility complex (MHC)-match dependence for transplantable tumors and the ability of vaccines against tumor antigens to protect from subsequent tumor inoculation further supported the crucial role of the adaptive immune system in anti-tumor immunity (33, 34). Understanding of the importance of this role ultimately led to the discovery that tumors utilize critical immune checkpoint molecules such as programmed death ligand 1 (PD-L1) and cytotoxic T lymphocyte associated protein 4 (CTLA-4) as a means to prevent immune activation towards cancer cells (35, 36). Such inhibitory molecules are one of the key mechanisms by which tumor cells can impede effective immune responses, and hence blocking this inhibition has become a pillar of modern cancer immunotherapy.

IMMUNOSUPPRESSION IN THE TUMOR MICROENVIRONMENT IN GBM

Tumor growth leading to cancer fundamentally requires evasion of and escape from immune surveillance. GBM tumor cells sometimes downregulate MHC expression in order to avoid neoantigen presentation, though this may be more common in other cancer types such as melanoma (37, 38). Tumor cells themselves lose expression of MHC class I, which is expressed nearly ubiquitously by cells and is critical 'self' *versus* 'non-self' distinction by the immune system (39, 40). Loss of MHC class II, which is typically more selectively expressed by antigen presenting cells (APCs) and is essential for cross-presentation of antigens to adaptive immune cells, has also been described in GBM, particularly microglia, underscoring the broader immunosuppressive effects of the tumor (41, 42). The GBM microenvironment is rich in immunomodulatory factors, including transforming growth factor β (TGF-β), interleukin 10 (IL-10), and prostaglandin E-2 (PGE2) (43–46). Increasing evidence suggests that these immunosuppressive factors, particularly TGF-β derived from the GBM cells themselves, support transition of brain resident/infiltrating immune cells such as microglia and tumor infiltrating myeloid cells to an immunosuppressive phenotype that allows aggressive tumor growth and progression while blocking anti-tumor immune responses (47, 48). Immunomodulatory surface ligands including PD-L1 are also frequently expressed by tumor cells, including GBM, reducing anti-tumor immunity and promoting T cell exhaustion and anergy (49). Other immunomodulatory signals, including IDO and MIF, have also been reported in GBM (50–52). Additional GBM-derived factors such as interleukin 6 (IL-6) help recruit myeloid cells, prompt a shift in the immune response from inflammatory anti-tumor responses to anti-inflammatory and wound-healing type responses, reduce the ability of immune cells to effectively destroy tumor cells, and can lead to tissue remodeling to create a site of relative immune privilege and thereby preventing immunologic access to the tumor cells (14, 53, 54).

In GBM particularly, this is associated with a large amount of vascular remodeling and abnormal angiogenesis promoted by vascular endothelial growth factor (VEGF), which has extensively been investigated as a therapeutic target in GBM resulting in the regular use of the anti-VEGF antibody bevacizumab in GBM treatment, though this may have only modest impact on overall survival (if any impact at all) (23, 55–57). Hypoxia within the tumor microenvironment has also been implicated in impairing immune cell function, particularly through increased expression of hypoxia-inducible factor 1-α (HIF1-α), whose upregulation is associated expression of immunomodulatory proteins including PD-L1 in other cancers (58–60). In GBM, exposure to GBM cell conditioned-media in the presence of hypoxia has been shown to induce the formation of immunosuppressive myeloid-derived suppressive cells at a higher rate than normoxic conditions (61). With tumor cell division and a shift in the microenvironment, a stable nidus of tumor cells is able to persist in spite of immune surveillance (the equilibrium phase).

Finally, immunologic control ultimately breaks down as tumor cell proliferation overwhelms the ability of the immune response to remove cancerous cells, especially as this response is attenuated by the aforementioned factors. This final stage is

termed 'escape,' and tumor growth proceeds relatively unchecked. In many cancers this manifests as distant metastasis formation in addition to continued growth at the primary tumor site. In GBM only local growth is typically seen, through leptomeningeal spread does occasionally occur (62). For GBM, unchecked disease manifests by uncontrolled tumor growth, which entails a persistent and expansive failure of the immune response to the tumor.

These local effects serve to suppress both the innate and adaptive components of the immune system. The GBM microenvironment, particularly through the release of IL-6 and the expression of PD-L1 and IDO-1, has been shown to induce the formation of regulatory T cells (Tregs) that blunt the anti-tumor T cell response (52, 63–66). Tregs release the immunosuppressive cytokine IL-10, inhibiting T cell proliferation and blocking anti-tumor immune responses, which further attenuates T cell cytotoxic activity and allows tumor growth. Recently, Miska and colleagues demonstrated that HIF-1α expression by Tregs was critical for their immunosuppressive functions within the GBM microenvironment (67). At the innate level, the microenvironment has similar effects on microglia and tumor-associated macrophages (TAMs), reducing their antigen-presenting capability and promoting a shift towards an immunosuppressive macrophage phenotype (68). A significant part to the tumor bulk in GBM has been identified as infiltrating neutrophils, and the have been proposed as an additional source of immune suppression through the expression of arginase 1 (69, 70). Finally, monocytic cells are associated with a pronounced immunosuppressive phenotype induced by the tumor, as discussed in further detail below.

SYSTEMIC IMMUNOSUPPRESSION IN GBM

Broadly, the phenomenological evidence of tumor-mediated immune suppression can be divided into local and systemic effects. Despite the absence of systemic metastases, GBM patients frequently exhibit profound systemic immunosuppression (14). This is reflected in multiple ways, including reduced T cell counts and functionality. Indeed, CD4 T cell numbers in some GBM patients approach lows seen in patients with acquired immunodeficiency syndrome (AIDS) (12, 13, 71). In addition, GBM patients present with small secondary lymphoid organs compared to healthy volunteers (as measured by spleen volumes) and their blood-derived monocytes have lower class II MHC expression levels (12, 13). Smaller spleens, smaller thymi, reduced MHCII levels, and reduced CD4 T cell counts have been reproduced in both GL261 and CTIIA murine GBM models (11, 12). Moreover, sera isolated from glioma-bearing mice potently inhibits immune cells activation *in vitro* demonstrating presence of profound systemic immunosuppression in GBM (11). The thymus significantly involutes in glioma-bearing mice and bone marrow homeostasis is disrupted by accumulation of mature T cells within the niche (11, 12). Ayasoufi et al. demonstrated that serum isolated from glioma-bearing mice harbors a potent non-steroid factor that inhibits T cell proliferation *in vitro* (11). In short, GBM patients and glioma-bearing mice demonstrate a multifaceted systemic immunosuppression that affects both primary and secondary lymphoid organs.

The precise mechanisms underlying systemic immunosuppression in GBM are not well understood. It has been postulated that circulating tumor-derived cytokines could account for such overt immunosuppression. However, efforts quantifying circulating cytokines in GBM patients have failed to reveal levels sufficient to explain this profound systemic immunosuppression (13, 72). Others have suggested that systemic immunosuppression in GBM is simply a result of cytotoxic chemotherapy and other standard medications such corticosteroids used to treat cerebral edema. However, immunosuppression is seen in untreated GBM patients before receiving corticosteroids or chemotherapy (13). Additionally, untreated GBM-bearing mice exhibit the exact facets of immunosuppression observed in patients. While we do not know the exact mechanisms underlying systemic immunosuppression in this population, it remains a major barrier to effective immunotherapy in GBM patients. Simultaneously, this immunosuppression is a barrier to the success of any immune-modulating therapies introduced into this system. In order to get rid of the tumor, we must first reverse the immunosuppression.

EFFECTS OF STANDARD THERAPIES ON LOCAL AND SYSTEMIC IMMUNOSUPPRESSION IN GBM

Immunosuppression both systemically and locally can be increased by standard therapies for GBM. Temozolomide in particular is associated with myelosuppression which contributes to decreased lymphocyte counts (2). However, the effects of temozolomide on immune function are complex and several groups have suggested possible synergistic effects with immunotherapies, possibly through selective reductions in immunosuppressive regulatory T cells (73–75). Corticosteroids have immunosuppressive effects and are ubiquitous in the treatment of symptomatic cerebral edema in GBM patients. However, steroids are not the sole mechanism of immunosuppression as treatment naïve GBM patients also exhibit similar immunosuppression. Radiation therapy can potentially have negative in-field immunomodulatory effects, such as impaired wound healing post-surgery (76, 77). The effects of radiation therapy in the GBM microenvironment are also somewhat controversial. Radiation theoretically improves the accessibility of tumor neoantigens as tumor cells die, and in some cases may potentiate a systemic response to immunotherapy (78, 79). However, radiation also has multiple effects on immune cells in the tumor microenvironment. While some studies have suggested that radiotherapy increases T cell infiltration in GBM, Wang and colleagues recently noted an increase in M2 (anti-inflammatory-pro tumor growth) tumor-associated macrophages that correlates with relapse following radiation and likely contributes to an immunosuppressive microenvironment as well as resistance to radiation therapy (80–82). Radiation necrosis post-treatment, which involves formation of fibrotic tissue and vascular abnormalities, can also present an additional barrier for immune cells to traverse to effectively encounter residual tumor cells (83).

Circulating immunosuppressive cytokines are not sufficiently elevated in GBM patients to account for their systemic immunosuppression (13, 14, 72). This is particularly curious in GBM where, unlike many cancers, the primary tumor virtually never metastasizes. This suggests that systemic effects result either from previously unappreciated tumor-secreted and/or brain derived factors, or by the local induction of immunosuppressive cells that subsequently exert systemic effects.

IMMUNOSUPPRESSIVE MONOCYTES INCLUDING MYELOID-DERIVED SUPPRESSOR CELLS IN GBM

While the precise mechanisms of tumor-mediated immune suppression remain an area of active investigation, many studies have pointed to the induction of immunosuppressive monocytes such as myeloid-derived suppressor cells (MDSCs) as a key immunosuppressive mechanism in GBM (13, 72, 84). MDSCs are a heterogenous population of monocytic cells that have been implicated in tumor-mediated immune suppression in multiple cancers including glioblastoma (85–88). These cells exert their effects locally through the release of immunomodulatory cytokines including IL-10, TGF-β, IDO-1, and arginase, curtailing the adaptive immune response (52, 72, 84–86). Precise definitions of MDSCs remain in flux, with most definitions combining surface marker profile and a functional measure of immune suppression such as inhibiting T cell activation/proliferation or release of immunosuppressive cytokines such as IL-10 (61, 72, 84). The current key MDSC categories include monocytic (mMDSCs) and granulocytic (gMDSCs). In addition, a number of other types of immunosuppressive monocytes including early MDSCs and non-classical monocytes have been described.

A growing literature has been concerned with mMDSCs in glioblastoma, which have a surface marker profile in humans characterized by CD14 expression combined with low HLA-DR expression (13). Loss of CD14 and CD15 expression is also frequently used to help differentiate mMDSCs from gMDSCs (89). Both mMDSCs and gMDSCs are derived from CD14+ monocytes. Increased populations of these cells have been described in the tumor microenvironment in a number of cancers, including breast, ovarian, and lung cancers (90–92). They have also been reported in glioblastoma, where Woichiechowsy and colleagues initially described reduced HLA-DR expression and cytokine release in monocytes collected from GBM patients (93, 94). These cells induce immune suppression by inhibiting conventional T cells, releasing immunosuppressive cytokines including IL-10 and TGF-B, and upregulating immunosuppressive PD-L1 and IDO-1. They have been found systemically as well as within the tumor microenvironment (72, 95). A similar population of cells is defined in mice by high levels of Ly6-C expression and absent Ly6-G expression in Gr-1+ myeloid cells (96).

Granulocytic MDSCs (also called polymorphonuclear MDSCs, or PMN-MDSCs) are frequently discussed, albeit less well-defined, in GBM. They typically lose CD14 expression while retaining high levels of HLA-DR and expressing CD15 and CD33 (86, 97). These cells have also been described in a number of cancers and induce functional immune suppression (98). Some studies have speculated that these cells are of neutrophilic rather than monocytic origin, however other evidence points more strongly to these cells also deriving from monocytes (99–101). Immunosuppressive neutrophils may be a separate, distinct entity or may overlap with gMDSCs but overall neutrophilia has long been described in multiple cancers, including GBM (69). Significant challenges in defining specific markers to effectively distinguish neutrophils from gMDSCs (both express CD15, which is commonly used to distinguish gMDSCs from mMDSCs) has led to significant ambiguity to the relative contributions of these cell types in immune suppression, with a recent study by Negorev and colleagues suggesting that common techniques used to isolate peripheral blood mononuclear cells (PBMCs) for the study of circulating MDSCs may be susceptible to high levels of neutrophil contamination (102). Another recent study has put forth LOX-1 as a potential gMDSC-specific marker (99). The murine analog of gMDSCs express low levels of Ly6-C and high levels of Ly6-G (96).

The relative importance of mMDSCs and gMDSCs in glioblastoma, and in cancer in general, is the subject of debate. The relative fractions of MDSCs induced seem to differ in human disease and murine models, with the latter having a strong predilection for gMDSC development, while the relative proportion in human disease has been more ambiguous (103, 104). This may be related to some evidence of sexual dimorphism in MDSC responses in GBM, as some immunocompetent murine models require the use of female mice (105). A recent study by McKelvey and colleagues also suggests a temporal evolution in MDSC populations infiltrating tumor, with an initial peak of gMDSC following tumor implantation and then an accumulation of mMDSCs (106). gMDSCs may make up the bulk of tumor-infiltrating MDSCs in GBM, while mMDSCs can be detected in the peripheral blood of GBM patients (89). The tumor microenvironment likely plays a significant role on a case or disease-specific basis, as the relative presence of granulocyte colony-stimulating factor (G-CSF) and granulocyte-macrophage colony-stimulating factor (GBM-CSF) influences the development of gMDSCs or mMDSCs, respectively (104, 107, 108). Distinguishing gMDSCs from tumor-infiltrating neutrophils remains an area of debate as well, and distinguishing MDSCs in general from tumor-associated macrophages or microglia remain an ongoing challenge.

While mMDSCs and gMDSCs have been traditionally discussed as predominant types of immunosuppressive cells in cancer, there is an increasing understanding that immunosuppressive monocytes as a group are likely far more heterogenous than these categories would imply. A number of recent studies have described early MDSCs (eMDSCs), which may represent a traditional state into a mature MDSC subtype (96, 109). A growing body of evidence, including work by our own group, has pointed toward programed death ligand 1 (PD-1) positive non-classical monocytes, (previously defined as CD14 mid-to-high, CD16+ cells) as an important

mediator of tumor-derived immune suppression (84). A recent murine study by Strauss and colleagues demonstrated that selective deletion of PD-1 in myeloid cells, in contrast to T cells, lead to better tumor control in a melanoma model (110). Given the heterogeneity of these populations of immunosuppressive monocytes, it may prove difficult to precisely define the relative importance of each in systemic immune suppression, and indeed, this could vary from cancer to cancer and even from patient to patient depending on the precise biology of the tumor. There is significant overlap in the means by which different types of immunosuppressive monocytes exert their effects. Ultimately, an appreciation of the diversity of immunosuppressive monocytes is critical for developing effective therapeutic strategies, as an effective approach need to adequately address multiple potential sources of immune suppression, rather than focusing exclusively on a given MDSC subtype.

MECHANISMS OF TUMOR-MEDIATED INDUCTION OF IMMUNOSUPPRESSIVE MONOCYTES

The tumor microenvironment in GBM is inherently immunosuppressive. GBM tumors release immunosuppressive cytokines including TGF-B, prostaglandin E_2, and other immunosuppressive cytokines (14). PD-L1 expression is frequently elevated in tumors, preventing an effective anti-tumor immune response (49). This milieu causes a shift in the profile of resident immune cells towards a more permissive Type 2 response or in some cases a frankly immunosuppressive phenotype (111). This behavior applies to monocytes/macrophages, as detailed above, but has also been described in T cells (112). In many cases the exact mechanisms are not yet well understood (**Figure 2**).

Increasing evidence suggests that tumor-derived extracellular vesicles (EVs) are major mediators of tumor-induced immune suppression in GBM (84, 113). EVs are small lipid bilayer-encapsulated particles shed from the surface of all cells. These are released through several mechanisms, including direct membrane budding (microvesicles or large EVs, > 100 nm) and endocytotic/Golgi apparatus-derived exocytotic pathways (exosomes or small EVs, < 100nm). These particles are shed in large volumes by tumor cells, are present within the local microenvironment, and have the potential to enter systemic circulation. EVs are biologically active particles carrying both membrane-bound receptors and soluble proteins which can be functionally delivered to target cells, either through cell surface interactions, endocytotic uptake, or direct membrane fusion. EVs also carry coding mRNA and short non-coding RNAs including microRNAs, pi-RNAs and y-RNAs, that can carry out biological functions when delivered to target cells (**Figure 2**) (114). Our group has recently described the role of PD-L1 expression in GBM-derived EVs in the induction of PD-1+ non-classical monocytes, and demonstrated that EV-conditioning of healthy monocytes leads to the induction of an immunosuppressive phenotype (**Figure 2**) (84). Other groups have explored the role of GBM-derived EVs in direct inhibition of T cells (113). An increasing body of work from studies in other cancers points to EVs as a critical mechanism of tumor-derived immune suppression (115). All in all, EVs serve as an important immunosuppressive liaison between the tumor microenvironment and the peripheral immune system (**Figure 3**).

Immunosuppressive monocytes, similar to EVs, likely have the ability to exert immunosuppressive effects both locally and

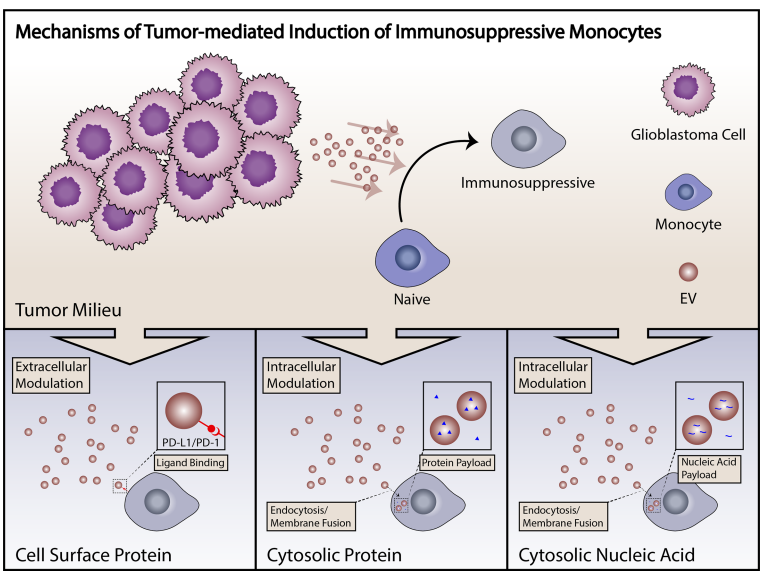

FIGURE 2 | Summary of mechanisms of induction of immunosuppressive monocytes. Induction of immunosuppressive monocytes by GBM tumor cells can proceed through a number of different mechanisms, including direct cell surface-mediated signaling, uptake of proteins with subsequent cytosolic effects, or signaling by tumor-derived small RNAs. Tumor-derived EVs are capable of signaling by any of these mechanisms.

systemically, migrating from the tumor bed and entering systemic circulation, where they can influence T cell maturation and activation in the secondary lymphoid tissues (**Figure 3**) (116). MDSCs have been identified in the circulation of GBM patients, as well as in the bulk tumor.

IMMUNOTHERAPY IN GBM

Current anti-tumor immunotherapies range from highly specific strategies to more general approaches. For example, antibodies directed against specific tumor fusion proteins or chimeric antigen receptor T cells (CAR T cells) provide specific and active immunity against specific cell types or tumor neoantigens, while checkpoint blockade inhibitors such as anti PD-1/PD-L1 or anti-CTLA4 increase the overall activity of the T cell response which consequently increases anti-tumor immunity (117). Additionally, vaccinations against tumor antigens and use of oncolytic viruses have also been put forward as immune-modulatory therapies for GBM.

GBM has particular features in addition to tumor-mediated immune suppression that present unique hurdles to effective immunotherapy. The mutational burden of GBM is middling on the spectrum of mutational burdens in cancer, meaning that it both lacks a defining mutation that presents a clear candidate for targeted therapy (the EGFRvIII mutation, which is frequently associated with GBM, is present in only 30% of tumors) and lacks the extensive genetic instability of high mutation burden tumors (e.g. melanoma) that present a range of immunogenic neoantigens and have shown a propensity for response to checkpoint blockade therapy (118, 119).

Drug (and immunotherapy) delivery also poses a challenge in GBM. The brain is no longer viewed as an immune privileged site. Microglia function as resident antigen presenting cells, T cells can traffic in and out of the brain, and recently-described lymphatic drainage allows for T cell surveillance of the central nervous system. However, the brain is certainly immunologically distinct site (120, 121). The blood-brain barrier (BBB) limits the penetration of both therapeutic agents and immune cells, making it difficult to deliver both drugs and cell-based therapies. Immune cell penetration into tumor most certainly occurs in GBM, but numbers of T cells seen infiltrating the tumor is relatively small. In parallel, neutrophils and myeloid-lineage cells make up the bulk of the tumor-associated immune cells (122–124). Direct delivery of therapeutic agents to the tumor through mechanisms including convection-enhanced delivery is one potential strategy for circumventing these anatomic challenges, and this technique could extend to the application of immunotherapies (125). Additionally, all immune-modulatory therapies rely on existence of an intact and functional innate and adaptive immune system. GBM patients are systemically immunosuppressed. These patients have very few T cells in circulations, small spleens, and their remaining T cells lack responsiveness against novel antigens. In fact, GBM patients do not respond strongly to flu vaccinations when compared to healthy controls demonstrating a challenge in vaccine design (126). Innate immune cells are also not optimally functional in these patients. The latter was demonstrated by lower levels of MHCII expression on blood-derived monocytes and the presence of suppressive MDSCs and neutrophils in circulations as discussed at length in the above section. In addition, serum isolated from mice with glioma was demonstrated by Ayasoufi et al. to potently inhibit proliferation of T cell *in vitro* (11). This further suggests that not only existing immune system in GBM patients is not functional, but also that putting healthy immune cells (i.e. CAR T cells) in the GBM patients' circulation may render these cells not functional, as well. These together present even greater challenges to success of immunotherapies in GBM.

In spite of these challenges, a number of clinical trials have been undertaking exploring the efficacy of different immunotherapies for

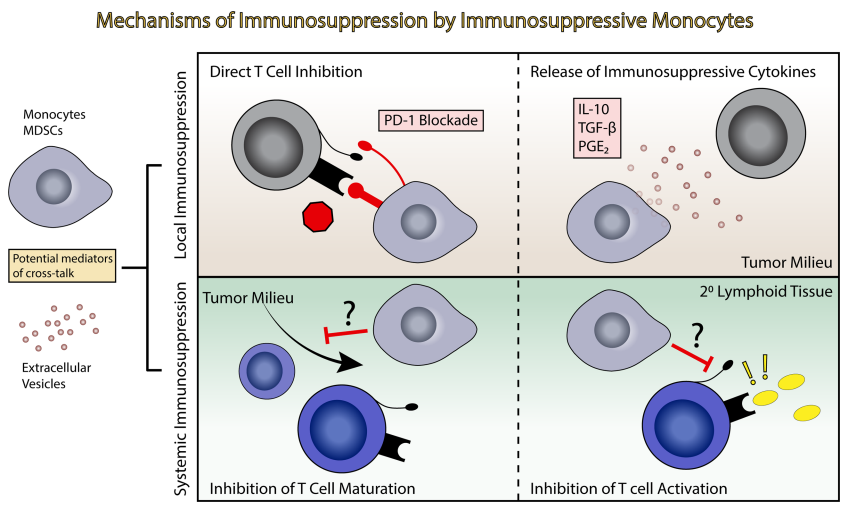

FIGURE 3 | Induction of immunosuppression by immunosuppressive monocytes. Immunosuppressive monocytes and MDSCs potentially exert both local and systemic effects leading to immune suppression. This can include direct T cell inhibition and release of immunosuppressive cytokines in the tumor milieu (top panels), or inhibition of T cell maturation or inhibition in the primary and secondary lymphoid tissues (bottom panels).

the treatment of GBM. These have been reviewed extensively elsewhere. However, in light of immunosuppression in GBM, it is perhaps not surprising that overall results from these studies have been disappointing (17, 127). Multiple studies involving checkpoint blockade inhibitors, most recently the CheckMate 143 study, which considered the use of the anti PD-1 antibody nivolumab *versus* bevacizumab for the treatment of recurrent GBM, failed to show a benefit (18). The only completed Phase III tumor vaccine study for GBM (ACT IV), which consisted of an EGFRvIII peptide in addition to treatment with GM-CSF and temozolomide, failed to show improvement in overall survival (17, 19). Earlier (Phase II) trials involving the use of oncolytic viral therapy, such as recombinant polio virus, have shown some promise, but more extensive trials are still required (128). These failed trials together with extensive accumulating evidence demonstrating multifaceted and systemic immunosuppression in GBM demonstrates that we must first reverse the immunosuppression before attempting to treat GBM patients with immune-modulating therapies. In the absence of such overt immunosuppression, endogenous anti-tumor-responses in combination with immunotherapies will likely produce successful results. Therefore, reversal of both local and systemic immunosuppression in GBM is the first step in designing a successful immunotherapy.

CONCLUSION

Novel therapies for GBM remain urgently needed in order to improve prognosis for this uniformly fatal disease. Immunotherapy holds tremendous promise for revolutionizing cancer therapies, but results thus far in the treatment of GBM have been underwhelming. The reasons for this are multifactorial, ranging from the relative mutational burden of GBM to the unique physiology of the brain, but the significant immunosuppression seen in GBM patients undoubtedly plays a significant role. Indeed, it is impossible to rule out the potential efficacy of any trialed immunotherapies to date, as all have been tested in the context of patients with an abnormal immune system, setting them up for failure. Understanding and reversing this tumor-mediated immune suppression is critical to effective deployment of immunotherapies for GBM, whether it be checkpoint blockade or a tumor-derived vaccine. The mechanisms of this immune suppression remain an active area of investigation, but a growing body of evidence points to the induction of immunosuppressive immune cells, including MDSCs and non-classical monocytes, as essential mediators of immune suppression in GBM. Clearly understanding the induction of these cell types and therapeutically targeting their formation may be a critical avenue to treating GBM-mediated immune suppression. Following reversal of both local and systemic immunosuppression, endogenous anti-tumor responses and immunotherapies will undoubtedly produce favorable results.

AUTHOR CONTRIBUTIONS

BH contributed conception, design, and primary authorship of the manuscript. PG contributed writing, research, and revision support. KA and AB contributed writing, figure design, and revisions. DB contributed writing and revision support. IP contributed to conception and design as well as critical revisions. All authors approved the final version of the manuscript.

REFERENCES

1. Koshy M, Villano JL, Dolecek TA, Howard A, Mahmood U, Chmura SJ, et al. Improved Survival Time Trends for Glioblastoma Using the SEER 17 Population-Based Registries. *J Neurooncol* (2012) 107:207–12. doi: 10.1007/s11060-011-0738-7
2. Stupp R, Mason WP, van den Bent MJ, Weller M, Fisher B, Taphoorn MJ, et al. Radiotherapy Plus Concomitant and Adjuvant Temozolomide for Glioblastoma. *N Engl J Med* (2005) 352:987–96. doi: 10.1056/NEJMoa043330
3. Stupp R, Taillibert S, Kanner A, Read W, Steinberg D, Lhermitte B, et al. Effect of Tumor-Treating Fields Plus Maintenance Temozolomide vs Maintenance Temozolomide Alone on Survival in Patients With Glioblastoma: A Randomized Clinical Trial. *JAMA* (2017) 318:2306–16. doi: 10.1001/jama.2017.18718
4. Hamid O, Robert C, Daud A, Hodi FS, Hwu WJ, Kefford R, et al. Safety and Tumor Responses With Lambrolizumab (Anti-PD-1) in Melanoma. *N Engl J Med* (2013) 369:134–44. doi: 10.1056/NEJMoa1305133
5. Robert C, Long GV, Brady B, Dutriaux C, Maio M, Mortier L, et al. Nivolumab in Previously Untreated Melanoma Without BRAF Mutation. *N Engl J Med* (2015) 372:320–30. doi: 10.1056/NEJMoa1412082
6. Weber J, Mandala M, Del Vecchio M, Gogas HJ, Arance AM, Cowey CL, et al. Adjuvant Nivolumab Versus Ipilimumab in Resected Stage III or IV Melanoma. *N Engl J Med* (2017) 377:1824–35. doi: 10.1056/NEJMoa1709030
7. Carreno BM, Magrini V, Becker-Hapak M, Kaabinejadian S, Hundal J, Petti AA, et al. Cancer Immunotherapy. A Dendritic Cell Vaccine Increases the Breadth and Diversity of Melanoma Neoantigen-Specific T Cells. *Science* (2015) 348:803–8. doi: 10.1126/science.aaa3828
8. Hauschild A, Grob JJ, Demidov LV, Jouary T, Gutzmer R, Millward M, et al. Dabrafenib in BRAF-Mutated Metastatic Melanoma: A Multicentre, Open-Label, Phase 3 Randomised Controlled Trial. *Lancet* (2012) 380:358–65. doi: 10.1016/S0140-6736(12)60868-X
9. Neelapu SS, Locke FL, Bartlett NL, Lekakis LJ, Miklos DB, Jacobson CA, et al. Axicabtagene Ciloleucel CAR T-Cell Therapy in Refractory Large B-Cell Lymphoma. *N Engl J Med* (2017) 377:2531–44. doi: 10.1056/NEJMoa1707447
10. Postow MA, Callahan MK, Wolchok JD. Immune Checkpoint Blockade in Cancer Therapy. *J Clin Oncol* (2015) 33:1974–82. doi: 10.1200/JCO.2014.59.4358
11. Ayasoufi K, Pfaller CK, Evgin L, Khadka RH, Tritz ZP, Goddery EN, et al. Brain Cancer Induces Systemic Immunosuppression Through Release of Non-Steroid Soluble Mediators. *Brain* (2020) 143(12):3629–52. doi: 10.1093/brain/awaa343
12. Chongsathidkiet P, Jackson C, Koyama S, Loebel F, Cui X, Farber SH, et al. Sequestration of T Cells in Bone Marrow in the Setting of Glioblastoma and Other Intracranial Tumors. *Nat Med* (2018) 24:1459–68. doi: 10.1038/s41591-018-0135-2
13. Gustafson MP, Lin Y, New KC, Bulur PA, O'Neill BP, Gastineau DA, et al. Systemic Immune Suppression in Glioblastoma: The Interplay Between CD14+HLA-DRlo/neg Monocytes, Tumor Factors, and Dexamethasone. *Neuro Oncol* (2010) 12:631–44. doi: 10.1093/neuonc/noq001
14. Parney IF. Basic Concepts in Glioma Immunology. *Adv Exp Med Biol* (2012) 746:42–52. doi: 10.1007/978-1-4614-3146-6_4
15. Fecci PE, Sampson JH. The Current State of Immunotherapy for Gliomas: An Eye Toward the Future. *J Neurosurg* (2019) 131:657–66. doi: 10.3171/2019.5.JNS181762
16. Goff SL, Morgan RA, Yang JC, Sherry RM, Robbins PF, Restifo NP, et al. Pilot Trial of Adoptive Transfer of Chimeric Antigen Receptor-Transduced T Cells Targeting EGFRvIII in Patients With Glioblastoma. *J Immunother* (2019) 42:126–35. doi: 10.1097/CJI.0000000000000260

17. Lim M, Xia Y, Bettegowda C, Weller M. Current State of Immunotherapy for Glioblastoma. *Nat Rev Clin Oncol* (2018) 15:422–42. doi: 10.1038/s41571-018-0003-5
18. Reardon DA, Brandes AA, Omuro A, Mulholland P, Lim M, Wick A, et al. Effect of Nivolumab vs Bevacizumab in Patients With Recurrent Glioblastoma: The CheckMate 143 Phase 3 Randomized Clinical Trial. *JAMA Oncol* (2020) 6:1003–10. doi: 10.1001/jamaoncol.2020.1024
19. Weller M, Butowski N, Tran DD, Recht LD, Lim M, Hirte H, et al. Rindopepimut With Temozolomide for Patients With Newly Diagnosed, EGFRvIII-Expressing Glioblastoma (ACT IV): A Randomised, Double-Blind, International Phase 3 Trial. *Lancet Oncol* (2017) 18:1373–85. doi: 10.1016/S1470-2045(17)30517-X
20. S De Vleeschouwer ed. *Glioblastoma*. Brisbane: Codon Publications (AU (2017).
21. Omuro A, DeAngelis LM. Glioblastoma and Other Malignant Gliomas: A Clinical Review. *JAMA* (2013) 310:1842–50. doi: 10.1001/jama.2013.280319
22. Stupp R, Hegi ME, Mason WP, van den Bent MJ, Taphoorn MJ, Janzer RC, et al. Effects of Radiotherapy With Concomitant and Adjuvant Temozolomide Versus Radiotherapy Alone on Survival in Glioblastoma in a Randomised Phase III Study: 5-Year Analysis of the EORTC-NCIC Trial. *Lancet Oncol* (2009) 10:459–66. doi: 10.1016/S1470-2045(09)70025-7
23. Friedman HS, Prados MD, Wen PY, Mikkelsen T, Schiff D, Abrey LE, et al. Bevacizumab Alone and in Combination With Irinotecan in Recurrent Glioblastoma. *J Clin Oncol* (2009) 27:4733–40. doi: 10.1200/JCO.2008.19.8721
24. Hegi ME, Diserens AC, Gorlia T, Hamou MF, de Tribolet N, Weller M, et al. MGMT Gene Silencing and Benefit From Temozolomide in Glioblastoma. *N Engl J Med* (2005) 352:997–1003. doi: 10.1056/NEJMoa043331
25. Turcan S, Rohle D, Goenka A, Walsh LA, Fang F, Yilmaz E, et al. IDH1 Mutation Is Sufficient to Establish the Glioma Hypermethylator Phenotype. *Nature* (2012) 483:479–83. doi: 10.1038/nature10866
26. Yan H, Parsons DW, Jin G, McLendon R, Rasheed BA, Yuan W, et al. IDH1 and IDH2 Mutations in Gliomas. *N Engl J Med* (2009) 360:765–73. doi: 10.1056/NEJMoa0808710
27. Swann JB, Smyth MJ. Immune Surveillance of Tumors. *J Clin Invest* (2007) 117:1137–46. doi: 10.1172/JCI31405
28. Dunn GP, Old LJ, Schreiber RD. The Three Es of Cancer Immunoediting. *Annu Rev Immunol* (2004) 22:329–60. doi: 10.1146/annurev.immunol.22.012703.104803
29. Schumacher TN, Scheper W, Kvistborg P. Cancer Neoantigens. *Annu Rev Immunol* (2019) 37:173–200. doi: 10.1146/annurev-immunol-042617-053402
30. Woo SR, Corrales L, Gajewski TF. Innate Immune Recognition of Cancer. *Annu Rev Immunol* (2015) 33:445–74. doi: 10.1146/annurev-immunol-032414-112043
31. Finn OJ. Cancer Immunology. *N Engl J Med* (2008) 358:2704–15. doi: 10.1056/NEJMra072739
32. Roithmaier S, Haydon AM, Loi S, Esmore D, Griffiths A, Bergin P, et al. Incidence of Malignancies in Heart and/or Lung Transplant Recipients: A Single-Institution Experience. *J Heart Lung Transplant* (2007) 26:845–9. doi: 10.1016/j.healun.2007.05.019
33. Jaffee EM, Pardoll DM. Murine Tumor Antigens: Is it Worth the Search? *Curr Opin Immunol* (1996) 8:622–7. doi: 10.1016/S0952-7915(96)80077-X
34. Murphy K, Weaver C. *Janeway's Immunobiology: Garland Science*. New York and London: Garland Science, Taylor and Francis Group (2016).
35. Dong H, Zhu G, Tamada K, Chen L. B7-H1, a Third Member of the B7 Family, Co-Stimulates T-Cell Proliferation and Interleukin-10 Secretion. *Nat Med* (1999) 5:1365–9. doi: 10.1038/70932
36. Walunas TL, Lenschow DJ, Bakker CY, Linsley PS, Freeman GJ, Green JM, et al. CTLA-4 can Function as a Negative Regulator of T Cell Activation. *Immunity* (1994) 1:405–13. doi: 10.1016/1074-7613(94)90071-X
37. Kageshita T, Hirai S, Ono T, Hicklin DJ, Ferrone S. Down-Regulation of HLA Class I Antigen-Processing Molecules in Malignant Melanoma: Association With Disease Progression. *Am J Pathol* (1999) 154:745–54. doi: 10.1016/S0002-9440(10)65321-7
38. Razavi SM, Lee KE, Jin BE, Aujla PS, Gholamin S, Li G. Immune Evasion Strategies of Glioblastoma. *Front Surg* (2016) 3:11. doi: 10.3389/fsurg.2016.00011
39. Mehling M, Simon P, Mittelbronn M, Meyermann R, Ferrone S, Weller M, et al. WHO Grade Associated Downregulation of MHC Class I Antigen-Processing Machinery Components in Human Astrocytomas: Does it Reflect a Potential Immune Escape Mechanism? *Acta Neuropathol* (2007) 114:111–9. doi: 10.1007/s00401-007-0231-8
40. Zagzag D, Salnikow K, Chiriboga L, Yee H, Lan L, Ali MA, et al. Downregulation of Major Histocompatibility Complex Antigens in Invading Glioma Cells: Stealth Invasion of the Brain. *Lab Invest* (2005) 85:328–41. doi: 10.1038/labinvest.3700233
41. Qian J, Luo F, Yang J, Liu J, Liu R, Wang L, et al. TLR2 Promotes Glioma Immune Evasion by Downregulating MHC Class II Molecules in Microglia. *Cancer Immunol Res* (2018) 6:1220–33. doi: 10.1158/2326-6066.CIR-18-0020
42. Schartner JM, Hagar AR, Van Handel M, Zhang L, Nadkarni N, Badie B. Impaired Capacity for Upregulation of MHC Class II in Tumor-Associated Microglia. *Glia* (2005) 51:279–85. doi: 10.1002/glia.20201
43. Hishii M, Nitta T, Ishida H, Ebato M, Kurosu A, Yagita H, et al. Human Glioma-Derived Interleukin-10 Inhibits Antitumor Immune Responses *In Vitro*. *Neurosurgery* (1995) 37:1160–6; discussion 1166-1167. doi: 10.1227/00006123-199512000-00016
44. Ikushima H, Todo T, Ino Y, Takahashi M, Miyazawa K, Miyazono K. Autocrine TGF-Beta Signaling Maintains Tumorigenicity of Glioma-Initiating Cells Through Sry-Related HMG-Box Factors. *Cell Stem Cell* (2009) 5:504–14. doi: 10.1016/j.stem.2009.08.018
45. Joseph JV, Balasubramaniyan V, Walenkamp A, Kruyt FA. TGF-Beta as a Therapeutic Target in High Grade Gliomas - Promises and Challenges. *Biochem Pharmacol* (2013) 85:478–85. doi: 10.1016/j.bcp.2012.11.005
46. Nduom EK, Weller M, Heimberger AB. Immunosuppressive Mechanisms in Glioblastoma. *Neuro Oncol* (2015) 17(Suppl 7):vii9–14. doi: 10.1093/neuonc/nov151
47. Gabrusiewicz K, Ellert-Miklaszewska A, Lipko M, Sielska M, Frankowska M, Kaminska B. Characteristics of the Alternative Phenotype of Microglia/Macrophages and Its Modulation in Experimental Gliomas. *PloS One* (2011) 6:e23902. doi: 10.1371/journal.pone.0023902
48. Wesolowska A, Kwiatkowska A, Slomnicki L, Dembinski M, Master A, Sliwa M, et al. Microglia-Derived TGF-Beta as an Important Regulator of Glioblastoma Invasion–an Inhibition of TGF-Beta-Dependent Effects by shRNA Against Human TGF-Beta Type II Receptor. *Oncogene* (2008) 27:918–30. doi: 10.1038/sj.onc.1210683
49. Nduom EK, Wei J, Yaghi NK, Huang N, Kong LY, Gabrusiewicz K, et al. PD-L1 Expression and Prognostic Impact in Glioblastoma. *Neuro Oncol* (2016) 18:195–205. doi: 10.1093/neuonc/nov172
50. Avril T, Saikali S, Vauleon E, Jary A, Hamlat A, De Tayrac M, et al. Distinct Effects of Human Glioblastoma Immunoregulatory Molecules Programmed Cell Death Ligand-1 (PDL-1) and Indoleamine 2,3-Dioxygenase (IDO) on Tumour-Specific T Cell Functions. *J Neuroimmunol* (2010) 225:22–33. doi: 10.1016/j.jneuroim.2010.04.003
51. Mittelbronn M, Platten M, Zeiner P, Dombrowski Y, Frank B, Zachskorn C, et al. Macrophage Migration Inhibitory Factor (MIF) Expression in Human Malignant Gliomas Contributes to Immune Escape and Tumour Progression. *Acta Neuropathol* (2011) 122:353–65. doi: 10.1007/s00401-011-0858-3
52. Wainwright DA, Balyasnikova IV, Chang AL, Ahmed AU, Moon KS, Auffinger B, et al. IDO Expression in Brain Tumors Increases the Recruitment of Regulatory T Cells and Negatively Impacts Survival. *Clin Cancer Res* (2012) 18:6110–21. doi: 10.1158/1078-0432.CCR-12-2130
53. Tchirkov A, Rolhion C, Bertrand S, Dore JF, Dubost JJ, Verrelle P. IL-6 Gene Amplification and Expression in Human Glioblastomas. *Br J Cancer* (2001) 85:518–22. doi: 10.1054/bjoc.2001.1942
54. Van Meir E, Sawamura Y, Diserens AC, Hamou MF, de Tribolet N. Human Glioblastoma Cells Release Interleukin 6 *In Vivo* and *In Vitro*. *Cancer Res* (1990) 50:6683–8.
55. Chinot OL, Wick W, Mason W, Henriksson R, Saran F, Nishikawa R, et al. Bevacizumab Plus Radiotherapy-Temozolomide for Newly Diagnosed Glioblastoma. *N Engl J Med* (2014) 370:709–22. doi: 10.1056/NEJMoa1308345
56. Keunen O, Johansson M, Oudin A, Sanzey M, Rahim SA, Fack F, et al. Anti-VEGF Treatment Reduces Blood Supply and Increases Tumor Cell Invasion in Glioblastoma. *Proc Natl Acad Sci USA* (2011) 108:3749–54. doi: 10.1073/pnas.1014480108

57. Turkowski K, Brandenburg S, Mueller A, Kremenetskaia I, Bungert AD, Blank A, et al. VEGF as a Modulator of the Innate Immune Response in Glioblastoma. *Glia* (2018) 66:161–74. doi: 10.1002/glia.23234
58. Kumar V, Gabrilovich DI. Hypoxia-Inducible Factors in Regulation of Immune Responses in Tumour Microenvironment. *Immunology* (2014) 143:512–9. doi: 10.1111/imm.12380
59. Shi Y. Regulatory Mechanisms of PD-L1 Expression in Cancer Cells. *Cancer Immunol Immunother* (2018) 67:1481–9. doi: 10.1007/s00262-018-2226-9
60. Wei J, Wu A, Kong LY, Wang Y, Fuller G, Fokt I, et al. Hypoxia Potentiates Glioma-Mediated Immunosuppression. *PloS One* (2011) 6:e16195. doi: 10.1371/journal.pone.0016195
61. Kumar R, de Mooij T, Peterson TE, Kaptzan T, Johnson AJ, Daniels DJ, et al. Modulating Glioma-Mediated Myeloid-Derived Suppressor Cell Development With Sulforaphane. *PloS One* (2017) 12:e0179012. doi: 10.1371/journal.pone.0179012
62. Lawton CD, Nagasawa DT, Yang I, Fessler RG, Smith ZA. Leptomeningeal Spinal Metastases From Glioblastoma Multiforme: Treatment and Management of an Uncommon Manifestation of Disease. *J Neurosurg Spine* (2012) 17:438–48. doi: 10.3171/2012.7.SPINE12212
63. Crane CA, Ahn BJ, Han SJ, Parsa AT. Soluble Factors Secreted by Glioblastoma Cell Lines Facilitate Recruitment, Survival, and Expansion of Regulatory T Cells: Implications for Immunotherapy. *Neuro Oncol* (2012) 14:584–95. doi: 10.1093/neuonc/nos014
64. DiDomenico J, Lamano JB, Oyon D, Li Y, Veliceasa D, Kaur G, et al. The Immune Checkpoint Protein PD-L1 Induces and Maintains Regulatory T Cells in Glioblastoma. *Oncoimmunology* (2018) 7:e1448329. doi: 10.1080/2162402X.2018.1448329
65. Lamano JB, Lamano JB, Li YD, DiDomenico JD, Choy W, Veliceasa D, et al. Glioblastoma-Derived IL6 Induces Immunosuppressive Peripheral Myeloid Cell PD-L1 and Promotes Tumor Growth. *Clin Cancer Res* (2019) 25:3643–57. doi: 10.1158/1078-0432.CCR-18-2402
66. Zhai L, Lauing KL, Chang AL, Dey M, Qian J, Cheng Y, et al. The Role of IDO in Brain Tumor Immunotherapy. *J Neurooncol* (2015) 123:395–403. doi: 10.1007/s11060-014-1687-8
67. Miska J, Lee-Chang C, Rashidi A, Muroski ME, Chang AL, Lopez-Rosas A, et al. HIF-1alpha Is a Metabolic Switch Between Glycolytic-Driven Migration and Oxidative Phosphorylation-Driven Immunosuppression of Tregs in Glioblastoma. *Cell Rep* (2019) 27:226–37.e224. doi: 10.1016/j.celrep.2019.03.029
68. See AP, Parker JJ, Waziri A. The Role of Regulatory T Cells and Microglia in Glioblastoma-Associated Immunosuppression. *J Neurooncol* (2015) 123:405–12. doi: 10.1007/s11060-015-1849-3
69. Massara M, Persico P, Bonavita O, Mollica Poeta V, Locati M, Simonelli M, et al. Neutrophils in Gliomas. *Front Immunol* (2017) 8:1349. doi: 10.3389/fimmu.2017.01349
70. Sippel TR, White J, Nag K, Tsvankin V, Klaassen M, Kleinschmidt-DeMasters BK, et al. Neutrophil Degranulation and Immunosuppression in Patients With GBM: Restoration of Cellular Immune Function by Targeting Arginase I. *Clin Cancer Res* (2011) 17:6992–7002. doi: 10.1158/1078-0432.CCR-11-1107
71. Fecci PE, Mitchell DA, Whitesides JF, Xie W, Friedman AH, Archer GE, et al. Increased Regulatory T-Cell Fraction Amidst a Diminished CD4 Compartment Explains Cellular Immune Defects in Patients With Malignant Glioma. *Cancer Res* (2006) 66:3294–302. doi: 10.1158/0008-5472.CAN-05-3773
72. Rodrigues JC, Gonzalez GC, Zhang L, Ibrahim G, Kelly JJ, Gustafson MP, et al. Normal Human Monocytes Exposed to Glioma Cells Acquire Myeloid-Derived Suppressor Cell-Like Properties. *Neuro Oncol* (2010) 12:351–65. doi: 10.1093/neuonc/nop023
73. Karachi A, Dastmalchi F, Mitchell DA, Rahman M. Temozolomide for Immunomodulation in the Treatment of Glioblastoma. *Neuro Oncol* (2018) 20:1566–72. doi: 10.1093/neuonc/noy072
74. Learn CA, Fecci PE, Schmittling RJ, Xie W, Karikari I, Mitchell DA, et al. Profiling of CD4+, CD8+, and CD4+CD25+CD45RO+FoxP3+ T Cells in Patients With Malignant Glioma Reveals Differential Expression of the Immunologic Transcriptome Compared With T Cells From Healthy Volunteers. *Clin Cancer Res* (2006) 12:7306–15. doi: 10.1158/1078-0432.CCR-06-1727
75. Sampson JH, Aldape KD, Archer GE, Coan A, Desjardins A, Friedman AH, et al. Greater Chemotherapy-Induced Lymphopenia Enhances Tumor-Specific Immune Responses That Eliminate EGFRvIII-Expressing Tumor Cells in Patients With Glioblastoma. *Neuro Oncol* (2011) 13:324–33. doi: 10.1093/neuonc/noq157
76. Cheng YK, Weng HH, Yang JT, Lee MH, Wang TC, Chang CN. Factors Affecting Graft Infection After Cranioplasty. *J Clin Neurosci* (2008) 15:1115–9. doi: 10.1016/j.jocn.2007.09.022
77. Golas AR, Boyko T, Schwartz TH, Stieg PE, Boockvar JA, Spector JA. Prophylactic Plastic Surgery Closure of Neurosurgical Scalp Incisions Reduces the Incidence of Wound Complications in Previously-Operated Patients Treated With Bevacizumab (Avastin(R)) and Radiation. *J Neurooncol* (2014) 119:327–31. doi: 10.1007/s11060-014-1482-6
78. Park SS, Dong H, Liu X, Harrington SM, Krco CJ, Grams MP, et al. PD-1 Restrains Radiotherapy-Induced Abscopal Effect. *Cancer Immunol Res* (2015) 3:610–9. doi: 10.1158/2326-6066.CIR-14-0138
79. Yan Y, Kumar AB, Finnes H, Markovic SN, Park S, Dronca RS, et al. Combining Immune Checkpoint Inhibitors With Conventional Cancer Therapy. *Front Immunol* (2018) 9:1739. doi: 10.3389/fimmu.2018.01739
80. Deng L, Liang H, Burnette B, Beckett M, Darga T, Weichselbaum RR, et al. Irradiation and Anti-PD-L1 Treatment Synergistically Promote Antitumor Immunity in Mice. *J Clin Invest* (2014) 124:687–95. doi: 10.1172/JCI67313
81. Ruffell B, Coussens LM. Macrophages and Therapeutic Resistance in Cancer. *Cancer Cell* (2015) 27:462–72. doi: 10.1016/j.ccell.2015.02.015
82. Wang Q, Hu B, Hu X, Kim H, Squatrito M, Scarpace L, et al. Tumor Evolution of Glioma-Intrinsic Gene Expression Subtypes Associates With Immunological Changes in the Microenvironment. *Cancer Cell* (2017) 32:42–56.e46. doi: 10.1016/j.ccell.2017.06.003
83. Siu A, Wind JJ, Iorgulescu JB, Chan TA, Yamada Y, Sherman JH. Radiation Necrosis Following Treatment of High Grade Glioma–a Review of the Literature and Current Understanding. *Acta Neurochir (Wien)* (2012) 154:191–201; discussion 201. doi: 10.1007/s00701-011-1228-6
84. Himes BT, Peterson TE, de Mooij T, Garcia M, Jung MY, Uhm S, et al. The Role of Extracellular Vesicles and PD-L1 in Glioblastoma-Mediated Immunosuppressive Monocyte Induction. *Neuro-Oncol* (2020) 22(7):967–78. doi: 10.1093/neuonc/noaa029
85. Mirghorbani M, Van Gool S, Rezaei N. Myeloid-Derived Suppressor Cells in Glioma. *Expert Rev Neurother* (2013) 13:1395–406. doi: 10.1586/14737175.2013.857603
86. Raychaudhuri B, Rayman P, Ireland J, Ko J, Rini B, Borden EC, et al. Myeloid-Derived Suppressor Cell Accumulation and Function in Patients With Newly Diagnosed Glioblastoma. *Neuro Oncol* (2011) 13:591–9. doi: 10.1093/neuonc/nor042
87. Talmadge JE, Gabrilovich DI. History of Myeloid-Derived Suppressor Cells. *Nat Rev Cancer* (2013) 13:739–52. doi: 10.1038/nrc3581
88. Umansky V, Blattner C, Gebhardt C, Utikal J. The Role of Myeloid-Derived Suppressor Cells (MDSC) in Cancer Progression. *Vaccines (Basel)* (2016) 4:36. doi: 10.3390/vaccines4040036
89. Gielen PR, Schulte BM, Kers-Rebel ED, Verrijp K, Petersen-Baltussen HM, ter Laan M, et al. Increase in Both CD14-Positive and CD15-Positive Myeloid-Derived Suppressor Cell Subpopulations in the Blood of Patients With Glioma But Predominance of CD15-Positive Myeloid-Derived Suppressor Cells in Glioma Tissue. *J Neuropathol Exp Neurol* (2015) 74:390–400. doi: 10.1097/NEN.0000000000000183
90. Limagne E, Richard C, Thibaudin M, Fumet JD, Truntzer C, Lagrange A, et al. Tim-3/Galectin-9 Pathway and mMDSC Control Primary and Secondary Resistances to PD-1 Blockade in Lung Cancer Patients. *Oncoimmunology* (2019) 8:e1564505. doi: 10.1080/2162402X.2018.1564505
91. Santegoets S, de Groot AF, Dijkgraaf EM, Simoes AMC, van der Noord VE, van Ham JJ, et al. The Blood mMDSC to DC Ratio Is a Sensitive and Easy to Assess Independent Predictive Factor for Epithelial Ovarian Cancer Survival. *Oncoimmunology* (2018) 7:e1465166. doi: 10.1080/2162402X.2018.1465166
92. Speigl L, Burow H, Bailur JK, Janssen N, Walter CB, Pawelec G, et al. CD14+ HLA-DR-/Low MDSCs are Elevated in the Periphery of Early-Stage Breast Cancer Patients and Suppress Autologous T Cell Proliferation. *Breast Cancer Res Treat* (2018) 168:401–11. doi: 10.1007/s10549-017-4594-9
93. Waziri A. Glioblastoma-Derived Mechanisms of Systemic Immunosuppression. *Neurosurg Clin N Am* (2010) 21:31–42. doi: 10.1016/j.nec.2009.08.005
94. Woiciechowsky C, Asadullah K, Nestler D, Schoning B, Glockner F, Docke WD, et al. Diminished Monocytic HLA-DR Expression and *Ex Vivo*

Cytokine Secretion Capacity in Patients With Glioblastoma: Effect of Tumor Extirpation. *J Neuroimmunol* (1998) 84:164–71. doi: 10.1016/S0165-5728(97)00236-1
95. Zou JP, Morford LA, Chougnet C, Dix AR, Brooks AG, Torres N, et al. Human Glioma-Induced Immunosuppression Involves Soluble Factor(s) That Alters Monocyte Cytokine Profile and Surface Markers. *J Immunol* (1999) 162:4882–92.
96. Bronte V, Brandau S, Chen SH, Colombo MP, Frey AB, Greten TF, et al. Recommendations for Myeloid-Derived Suppressor Cell Nomenclature and Characterization Standards. *Nat Commun* (2016) 7:12150. doi: 10.1038/ncomms12150
97. Gielen PR, Schulte BM, Kers-Rebel ED, Verrijp K, Bossman SA, Ter Laan M, et al. Elevated Levels of Polymorphonuclear Myeloid-Derived Suppressor Cells in Patients With Glioblastoma Highly Express S100A8/9 and Arginase and Suppress T Cell Function. *Neuro Oncol* (2016) 18:1253–64. doi: 10.1093/neuonc/now034
98. Condamine T, Dominguez GA, Youn JI, Kossenkov AV, Mony S, Alicea-Torres K, et al. Lectin-Type Oxidized LDL Receptor-1 Distinguishes Population of Human Polymorphonuclear Myeloid-Derived Suppressor Cells in Cancer Patients. *Sci Immunol* (2016) 1(2):aaf8943. doi: 10.1126/sciimmunol.aaf8943
99. Chai E, Zhang L, Li C. LOX-1+ PMN-MDSC Enhances Immune Suppression Which Promotes Glioblastoma Multiforme Progression. *Cancer Manag Res* (2019) 11:7307–15. doi: 10.2147/CMAR.S210545
100. Millrud CR, Bergenfelz C, Leandersson K. On the Origin of Myeloid-Derived Suppressor Cells. *Oncotarget* (2017) 8:3649–65. doi: 10.18632/oncotarget.12278
101. Pillay J, Tak T, Kamp VM, Koenderman L. Immune Suppression by Neutrophils and Granulocytic Myeloid-Derived Suppressor Cells: Similarities and Differences. *Cell Mol Life Sci* (2013) 70:3813–27. doi: 10.1007/s00018-013-1286-4
102. Negorev D, Beier UH, Zhang T, Quatromoni JG, Bhojnagarwala P, Albelda SM, et al. Human Neutrophils can Mimic Myeloid-Derived Suppressor Cells (PMN-MDSC) and Suppress Microbead or Lectin-Induced T Cell Proliferation Through Artefactual Mechanisms. *Sci Rep* (2018) 8:3135. doi: 10.1038/s41598-018-21450-6
103. Dubinski D, Wolfer J, Hasselblatt M, Schneider-Hohendorf T, Bogdahn U, Stummer W, et al. CD4+ T Effector Memory Cell Dysfunction Is Associated With the Accumulation of Granulocytic Myeloid-Derived Suppressor Cells in Glioblastoma Patients. *Neuro Oncol* (2016) 18:807–18. doi: 10.1093/neuonc/nov280
104. Waight JD, Hu Q, Miller A, Liu S, Abrams SI. Tumor-Derived G-CSF Facilitates Neoplastic Growth Through a Granulocytic Myeloid-Derived Suppressor Cell-Dependent Mechanism. *PloS One* (2011) 6:e27690. doi: 10.1371/journal.pone.0027690
105. Bayik D, Zhou Y, Park C, Hong C, Vail D, Silver DJ, et al. Myeloid-Derived Suppressor Cell Subsets Drive Glioblastoma Growth in a Sex-Specific Manner. *Cancer Discov* (2020) 10:1210–25. doi: 10.1158/2159-8290.CD-19-1355
106. McKelvey KJ, Hudson AL, Prasanna Kumar R, Wilmott JS, Attrill GH, Long GV, et al. Temporal and Spatial Modulation of the Tumor and Systemic Immune Response in the Murine Gl261 Glioma Model. *PloS One* (2020) 15:e0226444. doi: 10.1371/journal.pone.0226444
107. Kohanbash G, McKaveney K, Sakaki M, Ueda R, Mintz AH, Amankulor N, et al. GM-CSF Promotes the Immunosuppressive Activity of Glioma-Infiltrating Myeloid Cells Through Interleukin-4 Receptor-Alpha. *Cancer Res* (2013) 73:6413–23. doi: 10.1158/0008-5472.CAN-12-4124
108. Wei WC, Lin SY, Lan CW, Huang YC, Lin CY, Hsiao PW, et al. Inhibiting MDSC Differentiation From Bone Marrow With Phytochemical Polyacetylenes Drastically Impairs Tumor Metastasis. *Sci Rep* (2016) 6:36663. doi: 10.1038/srep36663
109. Fleming V, Hu X, Weber R, Nagibin V, Groth C, Altevogt P, et al. Targeting Myeloid-Derived Suppressor Cells to Bypass Tumor-Induced Immunosuppression. *Front Immunol* (2018) 9:398. doi: 10.3389/fimmu.2018.00398
110. Strauss L, Mahmoud MAA, Weaver JD, Tijaro-Ovalle NM, Christofides A, Wang Q, et al. Targeted Deletion of PD-1 in Myeloid Cells Induces Antitumor Immunity. *Sci Immunol* (2020) 5(43). doi: 10.1126/sciimmunol.aay1863
111. Prosniak M, Harshyne LA, Andrews DW, Kenyon LC, Bedelbaeva K, Apanasovich TV, et al. Glioma Grade Is Associated With the Accumulation and Activity of Cells Bearing M2 Monocyte Markers. *Clin Cancer Res* (2013) 19:3776–86. doi: 10.1158/1078-0432.CCR-12-1940
112. Wainwright DA, Dey M, Chang A, Lesniak MS. Targeting Tregs in Malignant Brain Cancer: Overcoming IDO. *Front Immunol* (2013) 4:116. doi: 10.3389/fimmu.2013.00116
113. Ricklefs FL, Alayo Q, Krenzlin H, Mahmoud AB, Speranza MC, Nakashima H, et al. Immune Evasion Mediated by PD-L1 on Glioblastoma-Derived Extracellular Vesicles. *Sci Adv* (2018) 4:eaar2766. doi: 10.1126/sciadv.aar2766
114. de Mooij T, Peterson TE, Evans J, McCutcheon B, Parney IF. Short non-Coding RNA Sequencing of Glioblastoma Extracellular Vesicles. *J Neurooncol* (2020) 146:253–63. doi: 10.1007/s11060-019-03384-9
115. Vader P, Breakefield XO, Wood MJ. Extracellular Vesicles: Emerging Targets for Cancer Therapy. *Trends Mol Med* (2014) 20:385–93. doi: 10.1016/j.molmed.2014.03.002
116. Chae M, Peterson TE, Balgeman A, Chen S, Zhang L, Renner DN, et al. Increasing Glioma-Associated Monocytes Leads to Increased Intratumoral and Systemic Myeloid-Derived Suppressor Cells in a Murine Model. *Neuro Oncol* (2015) 17:978–91. doi: 10.1093/neuonc/nou343
117. Farkona S, Diamandis EP, Blasutig IM. Cancer Immunotherapy: The Beginning of the End of Cancer? *BMC Med* (2016) 14:73. doi: 10.1186/s12916-016-0623-5
118. Gan HK, Kaye AH, Luwor RB. The EGFRvIII Variant in Glioblastoma Multiforme. *J Clin Neurosci* (2009) 16:748–54. doi: 10.1016/j.jocn.2008.12.005
119. Martincorena I, Campbell PJ. Somatic Mutation in Cancer and Normal Cells. *Science* (2015) 349:1483–9. doi: 10.1126/science.aab4082
120. Brioschi S, Colonna M. The CNS Immune-Privilege Goes Down the Drain (Age). *Trends Pharmacol Sci* (2019) 40:1–3. doi: 10.1016/j.tips.2018.11.006
121. Louveau A, Smirnov I, Keyes TJ, Eccles JD, Rouhani SJ, Peske JD, et al. Structural and Functional Features of Central Nervous System Lymphatic Vessels. *Nature* (2015) 523:337–41. doi: 10.1038/nature14432
122. Fossati G, Ricevuti G, Edwards SW, Walker C, Dalton A, Rossi ML. Neutrophil Infiltration Into Human Gliomas. *Acta Neuropathol* (1999) 98:349–54. doi: 10.1007/s004010051093
123. Gabrusiewicz K, Rodriguez B, Wei J, Hashimoto Y, Healy LM, Maiti SN, et al. Glioblastoma-Infiltrated Innate Immune Cells Resemble M0 Macrophage Phenotype. *JCI Insight* (2016) 1(2). doi: 10.1172/jci.insight.85841
124. Orrego E, Castaneda CA, Castillo M, Bernabe LA, Casavilca S, Chakravarti A, et al. Distribution of Tumor-Infiltrating Immune Cells in Glioblastoma. *CNS Oncol* (2018) 7:CNS21. doi: 10.2217/cns-2017-0037
125. Zhou J, Atsina KB, Himes BT, Strohbehn GW, Saltzman WM. Novel Delivery Strategies for Glioblastoma. *Cancer J* (2012) 18:89–99. doi: 10.1097/PPO.0b013e318244d8ae
126. Strowd RE, Swett K, Harmon M, Carter AF, Pop-Vicas A, Chan M, et al. Influenza Vaccine Immunogenicity in Patients With Primary Central Nervous System Malignancy. *Neuro Oncol* (2014) 16:1639–44. doi: 10.1093/neuonc/nou051
127. Preusser M, Lim M, Hafler DA, Reardon DA, Sampson JH. Prospects of Immune Checkpoint Modulators in the Treatment of Glioblastoma. *Nat Rev Neurol* (2015) 11:504–14. doi: 10.1038/nrneurol.2015.139
128. Desjardins A, Gromeier M, Herndon JE2nd, Beaubier N, Bolognesi DP, Friedman AH, et al. Recurrent Glioblastoma Treated With Recombinant Poliovirus. *N Engl J Med* (2018) 379:150–61. doi: 10.1056/NEJMoa1716435

Conflict of Interest: The authors declare that the research was conducted in the absence of any commercial or financial relationships that could be construed as a potential conflict of interest.

Publisher's Note: All claims expressed in this article are solely those of the authors and do not necessarily represent those of their affiliated organizations, or those of the publisher, the editors and the reviewers. Any product that may be evaluated in this article, or claim that may be made by its manufacturer, is not guaranteed or endorsed by the publisher.

frontiers in Oncology

REVIEW
published: 21 January 2022
doi: 10.3389/fonc.2021.805628

Mechanical Properties in the Glioma Microenvironment: Emerging Insights and Theranostic Opportunities

Adip G. Bhargav[1], *Joseph S. Domino*[1], *Roukoz Chamoun*[1] *and Sufi M. Thomas*[2*]

[1] Department of Neurological Surgery, University of Kansas Medical Center, Kansas City, KS, United States, [2] Department of Otolaryngology, University of Kansas Medical Center, Kansas City, KS, United States

OPEN ACCESS

Edited by:
Bozena Kaminska, Nencki Institute of Experimental Biology (PAS), Poland

Reviewed by:
Serena Pellegatta, IRCCS Carlo Besta Neurological Institute Foundation, Italy
Ignacio Ochoa, University of Zaragoza, Spain

***Correspondence:**
Sufi M. Thomas
sthomas7@kumc.edu

Specialty section:
This article was submitted to Neuro-Oncology and Neurosurgical Oncology, a section of the journal Frontiers in Oncology

Received: *30 October 2021*
Accepted: *29 December 2021*
Published: *21 January 2022*

Citation:
Bhargav AG, Domino JS, Chamoun R and Thomas SM (2022) Mechanical Properties in the Glioma Microenvironment: Emerging Insights and Theranostic Opportunities. Front. Oncol. 11:805628. doi: 10.3389/fonc.2021.805628

Gliomas represent the most common malignant primary brain tumors, and a high-grade subset of these tumors including glioblastoma are particularly refractory to current standard-of-care therapies including maximal surgical resection and chemoradiation. The prognosis of patients with these tumors continues to be poor with existing treatments and understanding treatment failure is required. The dynamic interplay between the tumor and its microenvironment has been increasingly recognized as a key mechanism by which cellular adaptation, tumor heterogeneity, and treatment resistance develops. Beyond ongoing lines of investigation into the peritumoral cellular milieu and microenvironmental architecture, recent studies have identified the growing role of mechanical properties of the microenvironment. Elucidating the impact of these biophysical factors on disease heterogeneity is crucial for designing durable therapies and may offer novel approaches for intervention and disease monitoring. Specifically, pharmacologic targeting of mechanical signal transduction substrates such as specific ion channels that have been implicated in glioma progression or the development of agents that alter the mechanical properties of the microenvironment to halt disease progression have the potential to be promising treatment strategies based on early studies. Similarly, the development of technology to measure mechanical properties of the microenvironment *in vitro* and *in vivo* and simulate these properties in bioengineered models may facilitate the use of mechanical properties as diagnostic or prognostic biomarkers that can guide treatment. Here, we review current perspectives on the influence of mechanical properties in glioma with a focus on biophysical features of tumor-adjacent tissue, the role of fluid mechanics, and mechanisms of mechanical signal transduction. We highlight the implications of recent discoveries for novel diagnostics, therapeutic targets, and accurate preclinical modeling of glioma.

Keywords: glioma, heterogeneity, tumor microenvironment, biophysical properties, tissue mechanics

INTRODUCTION

Contemporary Management of Malignant Glioma and Biological Considerations

Mortality due to cancer continues to rise worldwide with improving medical management of other disease processes. Brain cancer, specifically, represents one of the most lethal cancer subtypes. Malignant gliomas are a group of primary brain tumors that harbor a poor prognosis for afflicted patients (1, 2). Though there is some variation in survival rates ranging from months to decades among the different histological and molecular categories and grades of gliomas, in general, current therapies are not curative. Within this group is a subset of particularly high-grade tumors including glioblastoma which portend the worst survival with recent estimates of median survival at 8 to 14 months and a 7.2% 5-year survival rate post-diagnosis (1, 3). Unfortunately, this group also comprises the most common type of malignant glioma accounting for approximately 48.6% of all primary malignant brain tumors (1).

The standard of care and outcomes for glioblastoma have been largely unchanged since the development of the Stupp protocol (4, 5). Contemporary management of glioblastoma aims for maximal cytoreductive surgery while preserving critical neurologic function that is followed by adjunctive chemotherapy with temozolomide and fractionated radiotherapy (6). In certain cases, this treatment algorithm is limited by patient and disease factors including fitness to undergo aggressive therapy and tumor location, respectively. In such cases, intervention is directed towards establishing a definitive diagnosis as with biopsy and mitigating symptoms (6).

In light of poor outcomes in patients with glioblastoma, several lines of investigation are ongoing in order to develop novel therapeutics and treatment strategies (7–12). Importantly, advances in the understanding of tumor biology and influences of the microenvironment have begun to inform emerging paradigms for management of glioma. Glioma stem cells or brain tumor-initiating cells (BTICs) have been established as a subset of cells within glioma that contribute to treatment resistance and recurrence of disease. These cells exhibit properties including chemoresistance and radioresistance as well as considerable heterogeneity and plasticity on multiple levels which has posed a therapeutic challenge (13–18). Heterogeneity of BTICs encompasses variation in tumor characteristics over time—temporal heterogeneity, variation in tumor and cellular characteristics depending on location within a tumor—locoregional heterogeneity, and variation in disease characteristics from patient to patient—population heterogeneity which can impact response to treatment. As a result, current investigations are transitioning from single-agent or single-target therapies to treatment modalities with robust mechanisms of action that may overcome disease heterogeneity. Similarly, robust mechanisms of action are required to bypass tumor plasticity and changes in response to unimodal therapies (8, 17, 19–21). Examples of such efforts include cell-based therapies, immunotherapy approaches, and bioengineering strategies such as gene therapy, and excellent overviews of these topics can be found elsewhere (8, 9, 11, 22–24).

Improved understanding of plasticity and heterogeneity of BTICs has also led to further study of the tumor microenvironment and its inherent heterogeneity and plasticity. Similar to BTICs, studies have demonstrated that cellular and vascular components of the microenvironment respond to tumorigenesis and treatment in ways that may be facilitating malignant adaptation in tumor cells (16, 25–27). The potential bidirectional interaction between tumor cells and tumor microenvironment is particularly evident when considering the influence of immune-active cells such as myeloid-derived suppressor cells on immunosuppression *via* immune cell dysregulation (16, 17, 25, 28). Although cellular and vascular niches in the tumor microenvironment are now known to be a key player in the tumor milieu, the study of the mechanical properties of the microenvironment is relatively new. As with other components of the microenvironment, evidence suggests an important evolving role for mechanical properties in the context of treatment resistance and disease.

Tissue Mechanics in the Brain

Tissue mechanics broadly comprise cellular and tissue stiffness properties as well as stresses transmitted by fluid including cerebrospinal fluid (CSF) dynamics and interstitial fluid pressures. The influence of tissue mechanics on normal brain development and homeostasis has been well-described (29, 30). In the developing brain, stiffness gradients arise during various stages of embryogenesis and migration of neural precursors and neural stem cell populations particularly in the subventricular zones of the brain. Gradients have been attributed to maturation of cellular cytoarchitecture and changes in extracellular matrix (ECM) composition that facilitate normal migratory and tissue organization in development (31–34). As a result, a general trend towards increased global brain stiffness is seen with notable regions of 'softer' brain such as the hippocampus in the adult brain (35–38). In addition to spatial organization of cells and tissue, heterogeneity of tissue mechanics in non-disease states is important for directing differentiation and cell-type determination of embryonic neural stem cells as well as adult stem cells. Notably, aberrant mechanical signaling from the microenvironment has tremendous implications for regulating the behavior and plasticity of BTICs and preclinical models of BTICs that is discussed in detail in subsequent sections (29, 30).

Tissue Mechanics in Disease and Cancer

Alteration of the inherent spatiotemporal heterogeneity during development and maturation contributes to various disease states including traumatic brain injury, neurodegenerative diseases, and cancer (29, 39, 40). Briefly, studies demonstrate a progressive loss of global brain stiffness in the context of neurodegenerative disease that is contrary to generalized stiffening of the brain in aging, and this is secondary to cellular injury and compromise of cell-intrinsic mechanical factors as well as cell-extrinsic factors such as breakdown of the basement membrane in certain disease processes and changes in the composition of the ECM (29, 41–44). Conversely, preliminary studies demonstrate elevation in pro-stiffening factors such as

Tenascin-C (TNC) in the setting of traumatic brain injury with evidence suggesting enhancement of mechanical signaling likely owing to changes in intracranial pressure, injury from intracranial hemorrhage, and direct injury to areas of adult neurogenesis that may affect long-term outcomes and neurodegeneration (29, 39, 40).

The study of physical traits and microenvironmental mechanics in cancer is a relatively young field compared to research surrounding the traditional hallmarks of cancer. In recent years, the importance of physical characteristics in addition to biological factors has been increasingly recognized and extensively investigated in several cancers including breast cancer and carcinomas of the gastrointestinal system. From this work, ECM stiffness has emerged as a physical hallmark of many cancers that contributes to tumorigenesis, metastasis, metabolism, immune response and numerous additional processes (45–50). Though discussion of tissue mechanics in other cancer types is beyond the scope of this review, we highlight important principles gleaned from work in other cancers that may offer a template for further investigation of tissue mechanics in glioma, which is comparatively in its early stages. Comprehensive reviews of these fundamental discoveries and the work leading to these findings can be found elsewhere (46, 47, 51, 52). Investigation of tissue mechanics of the cancer microenvironment in various models has illuminated three biophysical concepts: 1) solid stress 2) fluid stress and 3) stiffness. Solid stress refers to amount of force per area present in the region of interest whether it is the tumor or the surrounding milieu (52, 51). The key factor influencing solid stress is derived from tumor tissue and cellular properties, though there is also contribution from ECM and surrounding components. Increased proliferation of cells within a tumor transmits increased stress through the space-limited tumor microenvironment. In addition, spatial and geometric considerations can also exacerbate regional solid stress based on the alignment of cellular cytoskeletal components relative to ECM matrix components as well as through a mechanism referred to as "jamming" whereby cumulative stress is increased after a critical cell population is reached that augments cell to cell contact and force (46, 51, 52). Fluid stress is the result of perturbation of interstitial fluid pressure as well as shear flow in certain microenvironments such as adjacent to the ventricles of the brain. Leaky tumor vasculature, impaired lymphatic drainage, and vascular compression secondary to solid stress can all contribute to increased interstitial pressure (51, 52).Global elevation in fluid stress as in the case of increased intracranial pressure in the fixed volume of the cranium can also exacerbate fluid stress at the tissue level. Finally, stiffness refers to the resistance to deformation as a result of stress and can be used to describe the tumor as a whole, individual cells, or the microenvironment and its components including the ECM. Global tissue stiffness is affected by ECM deposition or degradation, ECM cross-linking and changes in microarchitecture, and at the cellular level by cytoskeletal remodeling and cell contraction (45, 51, 52).

Interdependence between certain hallmarks of cancer and physical traits in the microenvironment is a relatively unexplored area in brain cancer but has been described in other cancer types (47–49, 52). Recent studies have revealed a potential link between immune escape and tissue mechanics where regional stress may impair vascular and lymphatic channels (49, 51, 52). This results in reduced migration of immune effector cells to the tumor site and effectively creates a functional immune escape phenomenon. Relatedly, cellular deformation secondary to solid and fluid stress may affect the integrity of intracellular structures including the nucleus and alter expression of immune soluble factors through direct physical perturbation as well as through mechanisms of mechanotransduction that affect downstream genetic and epigenetic regulation (49, 51, 52). A similar type of interdependence is observed with tumor metabolism and tissue mechanics; it is possible that solid and fluid stress may significantly predispose tumor cells towards aberrant metabolism in a feed-forward mechanism that continues to progress as the tumor grows and microenvironmental stress increases. One example of this is the Warburg effect and the interplay between stress and aerobic glycolysis: increased regional stress may promote hypoxia *via* vascular compression within the tumor and thereby apply selection towards aerobic glycolysis to facilitate tumor growth and progression (48). Overarching these overlapping mechanisms is the concept of mechanoreciprocity which mirrors the dynamic seen between cancer cells and the biological factors of the microenvironment such as the dynamic interactions between BTICs and immune cells or BTICs and neurons in the tumor milieu (17, 46). In the same way, the interaction between cancer cell and physical properties of the microenvironment is also dynamic and has been most extensively documented in the process of cancer migration where reciprocal signal transduction and physical changes at the cellular level and tissue level enable the requisite cellular geometric changes, elasticity, and focal adhesions to achieve metastasis (47, 51, 52). This dynamic interaction acts as the substrate for heterogeneity and plasticity in the physical traits of the tumor and microenvironment much like biological receptor- or soluble factor-mediated cell communication and therapy-induced changes to the cellular phenotype or genetics.

BIOPHYSICAL FEATURES OF GLIOMA-ADJACENT TISSUE

Current Understanding of Tissue Mechanics in the Glioma Microenvironment

Tissue mechanics in the glioma microenvironment primarily refers to solid stress from contributions by the surrounding ECM and tissue architecture as well as the cellular compartment in the tumor milieu which includes glioma cells. Unlike many other systemic cancers where the causative factors of solid stress may be more intuitive owing to typical growth patterns characterized by displacement of surrounding tissue *via* mass effect, gliomas tend to exhibit an infiltrative growth pattern. The components of physical stress generation in the microenvironment were unknown until recently. These are summarized in **Figure 1**.

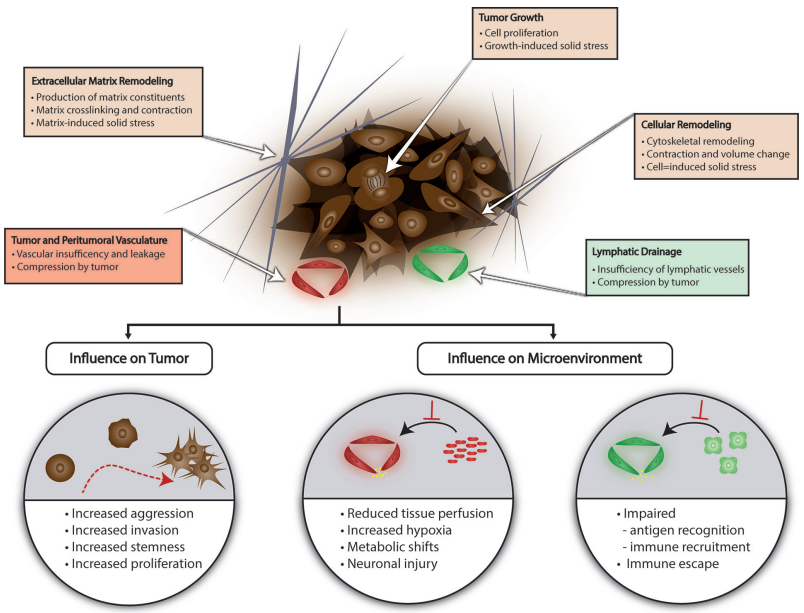

FIGURE 1 | Tissue Mechanics in Glioma. Several factors contribute to generation of solid stress in the glioma microenvironment including lymphatic or vascular insufficiency, tumor growth, and ECM or cellular remodeling. Solid stress can promote glioma aggression and create a microenvironment conducive for immune escape and BTIC selection. ECM, extracellular matrix; BTIC, brain tumor-initiating cell.

Stylianopoulos et al. developed a mathematical model to calculate growth-induced solid stress in a tumor by measuring the extent of deformation of tumor as stress is released from the tumor microenvironment after a cut is made along the long axis of the tumor (53). Various orthotopic cancer lines were employed to assess tumor-related solid stress and notably the U87 human glioblastoma cell line. Briefly, inoculation of tumor was performed in the flank of immunocompromised mice, and tumor was excised after reaching a tumor size of $1cm^3$. The solid stress-release assay was performed in different iterations after treatment with agents to selectively deplete individual components of the tumor microenvironment and thereby identify the contributory factors to solid stress. Selective depletion of U87 cancer cells or collagen in the ECM produced almost a two-fold decrease in tumor opening, a surrogate measurement for solid stress compared to control tumor. Importantly, no relationship between interstitial fluid pressure and solid stress was noted suggesting that cellular and ECM factors are the primary contributors (53). Nia et al. later developed an alternate method to characterize growth-induced solid stress *in situ* as well as *ex vivo* measurement (54). For *ex vivo* measurement, following tumor excision in the manner aforementioned, tumor was embedded in agarose gel. A planar cut is then performed, and the 2-dimensional planar deformation of the tumor is measured using an ultrasound probe. *In situ* assessment of solid stress in a murine orthotopic model of U87 GBM was subsequently performed by using a cylindrical punch to excavate a component of the tumor through the cranial window and measuring deformation with ultrasound. Interestingly, initial *ex vivo* 2-dimensional mapping of embedded U87 GBM demonstrated greater compressive stress at the periphery compared to the central core. Additionally, these tumors experienced less solid stress compared to other tumor types (maximum stress of 0.21 kPa versus 7 kPa in pancreatic tumors) (54). *In situ* measurement of solid stress revealed a significant influence of the surrounding tumor microenvironment—the cranial vault with fixed volume and surrounding normal tissue. Lesser degree of deformation was observed *ex vivo* compared to *in situ* measurement and approximately 0.02 kPa and 0.1 kPa compressive forces, respectively (54). This finding confirms the importance of considering the cranial vault as a fixed volume and accounting for the consequences when examining tissue mechanics in brain tumors. For example, states with increased intracranial pressure due to ancillary causes such as obstructive hydrocephalus may impact glioma microenvironment solid stress. Stylianopoulos et al. utilizing the previously described tumor relaxation model and mathematical model that the amount of deformation in U87 GBM tumors is proportional to the stored solid stress in the tumor microenvironment, and that solid stress forces in the periphery contribute to vascular and lymphatic collapse (55). This represents a possible mechanism based in the mechanical properties of the tumor microenvironment for BTIC selection and plasticity; impaired perfusion and lymphatic drainage may promote hypoxia within the tumor and a milieu conducive for aggressive, resistant cellular phenotypes as well as secondarily creating a physical barrier for potential cellular therapy or conventional chemotherapy (**Figure 1**). Seano and Nia et al.

relate tumor growth pattern to the amount of solid stress imposed on surrounding normal brain tissue using *in situ*, ultrasound-based measurement of stress (56). They utilize two distinct GBM cell lines U87 and MGG8 which exhibit nodular and infiltrative growth, respectively in an orthotopic murine model. Analysis of solid stress in these groups revealed qualitative deformation of surrounding tissue on histology with U87 nodular tumors, but not MGG8 tumors. This was corroborated with stress measurements that showed lesser radial and circumferential stress in the MGG8 infiltrative tumors compared to U87 nodular tumors (MGG8: radial stress 0.014 +/- 0.001 kPa, circumferential stress 0.063 +/- 0.004 kPa; U87: radial stress 0.020 +/- 0.001 kPa, circumferential stress 0.110 +/- 0.005 kPa) (56).

Although the fundamental mechanisms of growth-induced solid stress and the variables affecting this has been elucidated over the past decade, investigating these features in humans within a complex biophysical system continues to be a challenge. In large part due to limitations of current technologies, noninvasive methods of assessing physical properties of intracranial tumors are still being optimized by several groups (57–61). Initial studies have begun to define the biophysical properties of glioma, albeit with some discrepancy among groups. Specifically, the stiffness of glioma tissue and the microenvironment is debated, contrary to other systemic cancers where tumor stiffness is a hallmark. Schregel et al. characterized physical parameters of orthotopic G30 BTIC cell line using magnetic resonance elastography (MRE) (62). Analysis of MRE parameters revealed significant heterogeneity within tumor tissue as indicated by viscoelastic modulus and shear wave speed; stiffer areas on MRE corresponded to regions of high cell density on histology, and softer areas corresponded to regions necrosis and lower cell density (62). *In vivo*, intraoperative MRE of brain tumors performed by some groups suggested increased stiffness of brain tumor compared to normal brain as well as a trend of increasing stiffness with lower grade tumors (57, 58). Notably, these were the only studies to utilize MRE intraoperatively. Chauvet et al. report young's modulus ranging from 11.4 kPa to 33.1 kPa by shear wave elastography including meningiomas, low-grade gliomas, high-grade gliomas, and metastases. Meningiomas exhibited the greatest stiffness (33.1 +/- 5.9 kPa) whereas high-grade gliomas exhibited the least stiffness (11.4 +/- 4.9 kPa); however, tumors on average were stiffer than normal brain stiffness of 7.3 +/- 3.6 kPa (58). Other groups report similar trends with tumor grade, but report glioma tissue as softer than normal brain tissue though there is a small subset of gliomas that are stiffer in these studies (59–61). Reiss-Zimmerman et al. observe no significant difference in the elasticity parameter with MRE among tumor types whereas the elasticity component reflects the trend reported in the other studies—meningiomas exhibiting the least elasticity likely owing to higher cellular density compared to infiltrative gliomas. In this study, average young's modulus for all tumors was 1.43 +/- 0.33 kPa while the average for normal white matter was 1.62 +/- 0.27 (59). Moreover, intertumoral heterogeneity and intratumoral heterogeneity in viscoelastic properties were evident among gliomas as well as meningiomas to a lesser degree and may be due to high rates of cell turnover and heterogeneous distribution of cell density in gliomas (59).

The biological substrate of tissue stiffness also requires special consideration in the context of gliomas. Typical constituents of the ECM found elsewhere in the body are absent in the brain, namely collagen, fibronectin, and laminin (63–65). Instead, proteoglycans as well as heparin sulfate and hyaluronic acid are present. Proteins involved in cellular adhesion, particularly TNC, are also present and these constituents are frequently enriched in gliomas which can contribute to ECM stiffness (63–65). The orchestration of changes in glioma microenvironment stiffness and the subsequent mechano-transduction remains unclear. Although aberrant production of ECM constituents, even in the absence of typical proteins such as collagen in the brain, likely plays a role in promoting glioma tissue stiffness, other mechanisms have also been described. Pogoda et al. report a phenomenon of compression stiffening in glioma tissue obtained from biopsy specimens of patients with GBM (66). They demonstrate that the young's moduli measured in patient GBM tissue is not significantly different from the viscoelasticity of normal mouse brain tissue which was used as a proxy for normal human brain. With the addition of compressive force, the relative young's modulus for GBM tissue compared to normal brain tissue increased significantly with increasing compressive force to a relative young's modulus of approximately 1.8 at 20% compression of tissue (66). Additionally, using the LN229 GBM cell line, Pogoda et al. showed cell stiffness and morphology was dependent on substrate stiffness which was assessed by gel cultures of varying stiffness (66). Compared to normal astrocytes, a monotonic dependence of cell adherent area on substrate shear modulus ranging from 300 to 14,000 Pa was observed. A similar relationship was observed with cell stiffness with a maximal cell stiffness of approximately 5 kPa achieved at 14 kPa of substrate stiffness after which no further changes in cellular stiffness was observed (66). Taken together, these findings suggests that although glioma tissue may be softer at baseline compared to surrounding tissue, regional normal brain stiffness can stimulate local changes in glioma stiffness signifying cytoskeletal remodeling and motility. A compression-driven mechanism of focal glioma stiffness may complement previously recognized mechanisms of primary ECM stiffening due to changes in ECM composition and deposition which is likely not the sole mediator of glioma stiffness. Compression from surrounding normal brain tissue can arise from various processes including increased intracranial pressure or interstitial pressures which are not uncommon in intracranial malignancy.

A recent MRE-based study and mathematical analysis by Streitberger et al. offer further reconciliation of relative glioma "softness" compared to normal brain and tumor progression and invasion (67). The authors first devised a phantom model mimicking the ECM and cytoarchitecture of meningioma and glioma using amalgamations of agar, heparin, and tofu. Viscoelastic properties were measured using MRE at varying

solid composition ratios of the model and varying water content to determine how the viscoelastic properties of an intracranial tumor may change in response to increased fluid due to disrupted blood-brain barrier in surrounding vasculature (67). In their phantom models, different substrates functionally recapitulated different components of glioma ECM—abundant glucosaminoglycans (GAGs), absence of significant fibrosis in the case of heparin while the tofu phantom mimicked an entanglement of proteins governed by hydrophobic interactions with the high collagen content observed in meningioma with relatively high viscosity and increased fluidity (67). With glioma and the heparin phantom model, an inverse relationship between water absorption and viscosity was observed (67). Indeed, this was corroborated with MRE imaging studies in patients where T2 signal reflected higher water content and this corresponded to lower viscosity, i.e. lower phase angle and consequently decreased fluidity. Interestingly, other groups have also shown that increased ADC signal in GBM corresponding to higher water content may be associated with worse outcomes (68, 69). Based on these findings, the authors posit that GBM behaves functionally as a low viscosity, low fluidity solid secondary to the ability of significant, hydrophilic GAGs in the ECM to bind to water without meaningful perturbation of viscosity (67). On the other hand, meningioma behaves like a high viscosity, high fluidity fluid with ECM consisting of entangled proteins with hydrophobic aggregation. In the case of meningioma, the variation in focal shear stress can steeply increase stiffness due to local drainage of water followed by direct solid-solid contact of ECM constituents and protein coagulation (67). With regards to glioma infiltrative growth and tumor progression, viscous fingering. Briefly, in viscous fingering, the less viscous glioma with lower regional surface tension is pushed into the higher viscosity surrounding producing the characteristic microinvasive infiltration without clear margins (67). Overall, these studies suggest a unifying theory though additional work is required to elucidate the impact of tumor subtype, tumor location such as proximity to the ventricle, tumor/microenvironment heterogeneity, among other factors.

Influence of Microenvironmental Tissue Mechanics on Glioma Malignancy

Though studies examining the impact of tissue mechanics are limited, this is an area of considerable interest and active research with themes beginning to emerge. Unsurprisingly, given discoveries in tissue mechanics in other types of cancers, tissue mechanics in glioma tend to regulate hallmarks of cancer. Here we highlight representative studies that have uncovered these mechanisms (**Figure 1**).

Several studies have linked alterations in microenvironmental rigidity to enhanced glioma aggression, and some have also identified certain microenvironmental features as prognostic markers for survival at the patient level (70–73). Miroshnikova et al. established the importance of HIF1α signaling, IDH status, and ECM components in GBM (70). Using *in vitro* models as well as human tumor samples, the authors show that increasing in ECM stiffness is observed with increasing grade of tumor in glioma ranging from 50-1,400 Pa in low grade gliomas to 70-13,500 in higher grade gliomas; analysis of human samples revealed worst patient prognosis with tumors with a high proportion of stiff ECM >1,400 Pa (70). Mechanistically, they define TNC and hyaluronic acid (HA) as key contributors to ECM stiffness in glioma and show increased levels of these constituents is associated with worse survival and stiffer tumor ECM. Finally, they describe the downstream effects of HIF1α expression in a hypoxic tumor microenvironment (70). HIF1α serves as a regulator of TNC expression and ultimately glioma microenvironment mechanical properties through stiffening of the ECM. At the tumor level, the authors show that perturbation of TNC-mediated ECM stiffening or at a point in the regulatory pathway with HIF1α or one of its regulators miR-203 improved survival is observed in murine xenograft models of GBM. Notably, wild-type IDH *via* onco-metabolite (R)-2-hydroxyglutarate is implicated in HIF1α regulation and consequently ECM stiffness regulation; in patients with recurrent IDH-mutant tumor, ECM stiffness was noted to increase comparing initial diagnosis and associated increased TNC expression suggesting a mechanosignaling-induced tumor aggression (70). Chen et al. similarly define a key mechanosignaling axis involving the PIEZO1 ion channel that has been shown to be overexpressed in a variety of cancers including all subtypes and grades of glioma signifying a potential common, evolutionarily conserved mechanosensation mechanism in cancer (71). Beginning with a *Drosophila* model of glioma and subsequently utilizing GBM and BTIC cell lines, the authors demonstrated that the PIEZO1 channel is necessary for tumor growth *in vitro and in vivo* and abrogation of the ion channel resulted in significantly longer survival and reduced tumor growth in mouse models (71). Further characterization of PIEZO1 as a central hub in a mechanotransduction cascade revealed subcellular location of the channel at sites of focal adhesion and a feed-forward mechanism whereby PIEZO1 was shown to be essential for ECM stiffening *via* regulation of other ECM remodeling genes including TAZ and FHL3 as well as glioma cell mechanotransduction (71). In experiments with PIEZO1 knockdown, stiffness-dependent glioma cell growth was not observed, and in experiments assessing the stiffness-dependent growth of glioma cells in response to varying stiffness hydrogels, increased expression of PIEZO1 was observed (71). Other groups have also confirmed the influence of microenvironmental stiffness on glioma growth and proliferation in the context of other signaling pathways including the EGFR and Rho/GTPase signaling pathways (72–74).

In addition to promoting glioma growth and proliferation, mechanical cues from the microenvironment also enhance other aspects of glioma stemness, specifically migration and invasion which enables diffuse spread through brain parenchyma (75–77). Zhang et al. elucidate a mechanism involving the cytokine IL-33 and receptor ST2 in the tumor milieu that stimulates expression and accumulation of TNC *via* NF-κB signaling in the microenvironment (76). Using a transwell migration assay, they demonstrate that IL-33 treatment produces a nearly 3-fold

increase in invaded cells in a TNC-dependent matter; the authors observed enhanced migration on *in vivo* histologic analysis as well (76). Kim et al. identify another mechanosensation mediator in the CD44-HA interaction that also enhances glioma cell invasion (77). Aberrant and increased expression of CD44 and HA is present in the glioma microenvironment, and Kim et al. show that this ligand-mediated interaction is distinct from other adhesion interactions as with integrins and is stiffness-dependent (77). Using U373-MG glioma cells in transwell invasion assay and time-lapse microscopy, the authors show that the migration speed and invasion properties of these cells in the presence of CD44/HA improves with increasing stiffness of the HA hydrogel in which they are cultured (77). Integrin-mediated interaction between glioma cells and microenvironment components such as the glycocalyx or BCL9L have also been described and shown to enhance glioma stemness (75, 78, 79). Notably, in these studies, glioma stemness also incorporates the treatment-resistant quality of this phenotype and the authors show treatment sensitization employing gain- or loss-of-function methodologies to disturb the specific integrin-mediated mechanosensation (78, 79). Barnes et al. specifically examine recurrent GBM and determine that a bulky glycocalyx in the tumor microenvironment, that is frequently seen in recurrent GBM, interacts with integrins with mechanoreciprocity whereby downstream signaling enhances stemness of the cell which in turn effects increased tension in the glycocalyx to form a feedback loop (79).

Interestingly, in investigations by Miroshnikova et al. and others, GBM tumor tissue was observed to be stiffer than normal tissue and a trend was observed towards increased stiffness with high grade; in contrast, previously discussed studies found gliomas to be softer compared to normal brain and to exhibit the opposite trend with grade (59, 60, 66, 67, 70, 78). This underscores the complexity of measuring mechanical properties of the glioma microenvironments and requires further study to elucidate with consideration of standardized measurement techniques and preclinical modeling. Moreover, this may also be an indicator of the challenge associated with defining features of a heterogeneous disease process including sampling bias of the tumor as well as other confounders such as patient comorbidities and history of treatment.

Microenvironmental tissue properties also induce changes in tumor-adjacent tissue compartments in addition to glioma cells **(Figure 1)**. Seano and Nia et al. show that glioma tumor growth in an orthotopic murine model compresses tumor-adjacent vasculature and decreases perfusion (56). They note that this effect is more pronounced in glioma cell lines characteristic for nodular growth pattern—U87, GL261, and BT474 compared with cell lines that exhibit infiltrative growth. For example, at a 20-day timepoint, the authors demonstrate that the nodular cell line U87 resulted in a significantly reduced intravital perfused blood volume fraction compared to baseline (0.35 to 0.2) in surrounding vasculature whereas no significant changes were observed in the infiltrative cell line MGG8 in the same time frame (56). In tumors models with nodular growth, perfusion in the surrounding vasculature is also inversely correlated with tumor growth (56). MRI-based analysis of perfusion in tumor adjacent regions, not including peritumoral T2/FLAIR signal in a cohort of patients with GBM confirmed reduced perfusion in up to 53% of patients (56). Histological and behavioral analysis after tumor-related brain compression in the intracranial tumor mouse models also revealed evidence of neuronal injury and neuroinflammation as well as concordant significant changes in locomotion and gait suggesting deleterious neuronal sequelae from the physical effects of tumor growth (56). Tumor-related mechanical changes in the microenvironment can also promote local immune dysfunction. This type of microenvironment-mediated immunosuppression has been characterized in a variety of cancers and may result from tumor-related solid stress transmitted through the microenvironment as well as soluble factors and interactions with tumor-associated vasculature (80). In glioma specifically, Huang et al. show GBM ECM-based inhibition of T cell migration into the tumor milieu. Furthermore, they define an inverse correlation between TNC expression in the ECM and T cell transmigration (81). Increased levels of TNC *in vivo* in a mouse model of GBM was associated with reduced T cell enrichment in tumor tissue on histologic analysis, and assessment of *in vivo* transmigration using a mouse air pouch model demonstrated TNC-mediated transmigration of T cells (81). Pathway analysis *in vitro* using co-cultures of Jurkat cells with U118MG glioma tumor cells or tumor ECM identified phosphorylation of focal adhesion kinase (FAK) and migration-related kinase ERK which was shown to be required for transmigration through a cancer monolayer (81). Interestingly, a potential relationship between tumor ECM constituents and peritumoral edema was also observed in a study by Qu et al. analyzing the expression of GBM PIEZO1 relative to normal peritumoral tissue in patients; quantification of PIEZO1 expression and image analysis revealed a positive relationship between expression and extent of peritumoral edema where higher expression was observed in patients with severe edema that was defined as an edema index >3 (calculated as the ratio of tumor and edema volume to tumor volume) (82). Lastly, it is well known that GBM and the tumor microenvironment present numerous challenges to adequate and effective delivery of therapeutics, and this concept also extends to the physical properties of the tumor and microenvironment. Recent efforts have included innovative strategies to create therapeutics that account for and accommodate the rheological features to engineer adaptive therapeutics (83). Detailed overview of recent trends and advances in overcoming physical barriers to drug delivery can be found elsewhere (84).

Mechanisms of Mechanical Stimuli Transduction in Glioma

Mechanistic understanding of mechanical stimuli transduction in glioma is lacking, though recent advances have shed some light on the microenvironment and cellular network interactions that underlie the effects of mechanical properties on disease progression. Hubs of mechanical stimuli transduction in gliomas can be generally categorized as either *via* mechanosensitive ion channels or non-ion channel-based mechanotransduction which encompasses a complex swath of poorly understood signaling pathways including integrin signaling, ligand-mediated signaling

through interaction with ECM components, or receptor-mediated signaling through interaction with ECM components (85). Here, we briefly summarize representative mechanisms in the evolving framework of glioma mechanotransduction **(Table 1)**.

Three main classes of mechanosensitive ion channels have been implicated in gliomas: PIEZO, TRP, and ENaC **(Table 1)**. Of these, mechanotransduction *via* PIEZO and TRP channels have been the most well characterized (85). PIEZO1 specifically in glioblastoma serves as an intermediary for a variety of downstream affects including cytoskeletal remodeling, ECM remodeling as well as directly regulating stemness and aggression of cancer cells (71, 85, 88, 89). Studies have described colocalization of PIEZO1 to regions of cell membrane stress such as those with focal adhesions and signaling *via* the integrin-FAK pathway (71, 88, 89). Different subtypes of TRP channels have been implicated in glioma including TRPC1, TRPC6, and TRPM7 **(Table 1)** (85, 86, 90–94). Similarly, mechanotransduction of physical microenvironmental stimuli through these channels influences downstream regulation of disease progression through effects key cellular structure and function ranging from motility and migration to proliferation and metabolism (86, 90–94). TRP channels in GBM have been associated with activation of Notch signaling and JAK/STAT signaling pathways (94). Ross et al. also identified a potential role for the ENaC channel which has primarily been shown to regulate cell volume, presumably to facilitate cell motility and migration in complex microenvironments **(Table 1)** (87). Study of mechanosensitive ion channels has centered largely on those located on the cell membrane, and intracellular or nuclear ion channels in the context of mechanotransduction may represent a new frontier that could improve understanding of downstream signal transduction.

Non-ion channel-based mechanotransduction in glioma is poorly defined and represents an active area of investigation. In recent years, groups have been able to thoroughly characterize a few signal transduction pathways that utilize ligand-mediated, receptor-mediated, and integrin-mediated mechanosensation (45, 76, 77, 79, 95). Other studies in this area have focused on defining downstream components of signaling mediators following the initial mechanosensation event, and this has led to the identification YAP/TAZ, PHIP, and MGAT, among others that play a role in glioma stemness and disease progression; however, a unifying mechanism that considers heterogeneity in mechanical properties of the glioma microenvironment as well genetic and treatment-related drivers of plasticity is lacking and requires further investigation (96–104). Kim et al. describe a ligand-mediated mechanotransduction mechanism in gliomas that leverages the interaction between HA that is overexpressed in the ECM and CD44 **(Table 1)** (77). In this study, the authors observe a temporal component to mechanotransduction where HA-CD44-mediated signaling and consequent enhanced glioma adhesion appears to occur earlier than integrin-mediated signaling and adhesion in glioma cells cultured in modified hydrogels (77). This suggests that early mechanotransduction may occur *via* an CD44-independent ligand-mediated mechanism whereas the well-described ECM-integrin interactions in glioma may occur later. Temporal cues that define these mechanisms as well as the molecular implications of this phenomenon are unknown. Moreover, this finding adds another potential layer of complexity to mechanotransduction mechanisms in glioma in that our current framework does not clearly define whether temporal heterogeneity exists in this mechanism or the previously described mechanisms and whether this is of functional significance. Several groups have described the mechanotransduction scheme and downstream effects of integrin-mediated signaling (45, 79, 95). TNC has been established as a protein mediator of microenvironment and glioma cell interaction ultimately facilitating and converging on integrin-mediated signaling (70, 76, 105–108). A possible receptor-mediated mechanism for the regulation of mechanosensation has been described by Zhang et al. who show that binding of IL-33 to the ST2 receptor is associated with TNC accumulation and subsequent alteration in the GBM phenotype **(Table 1)** (76). TNC is an important mediator of mechanical cues in the microenvironment, and these findings suggest that interactions (in this case a receptor-mediated interaction) that alter the availability of such mediators can have implications for mechanotransduction, though further investigation is required to elucidate these potential links.

ROLE OF FLUID MECHANICS IN GLIOMA

Fluid Shear Stress and Interstitial Fluid Dynamics

Alteration of brain fluid mechanics in patients with glioma, specifically cerebrospinal fluid (CSF) dynamics is not uncommon (109). This can occur secondary to tumor-related obstruction of natural CSF drainage pathways or dysfunction of CSF resorption. Bloodstream-related fluid shear stress and other fluid stresses has been extensively studied in the context of metastatic cancer as well as other disease processes; however, studies characterizing these forces in glioma and examining the impact on the disease process are sparse. Further investigation in this area may provide a more complete view of the stresses at play

TABLE 1 | Representative Substrates of Mechanical Signal Transduction in Glioma.

Class	Substrate	Effect	Model	Ref.
Mechanosensitive Ion Channel	PIEZO1	Promotes glioma aggression, growth; reduces survival *in vivo*	Murine, Xenograft	(71)
	TRP1	Cell migration, chemotaxis	Cell Culture	(86)
	ENaC	Cell volume regulation	Cell Culture	(87)
Non-Ion Channel-Based Mechanosensation	HA/CD44	Cell adhesion, migration, invasion	Cell Culture	(77)
	IL-33/ST2-R/TNC	Cell invasion	Cell Culture	(76)

HA, hyaluronic acid; TNC, Tenascin-C; ST2-R, ST2 receptor.

in the tumor bulk and microenvironment, and early studies suggest that the influence fluid-related stresses may be clinically significant (85, 110–116).

Interstitial fluid flow refers to fluid flow generally through a 3-dimensional matrix and interstitial fluid pressure (IFP) refers to the biophysical manifestation of the pressure gradient typically between a capillary and a draining lymphatic vessel. In the context of cancer and glioma, an elevated IFP is observed due to increased vessel permeability, i.e., leaky vasculature, secondary to tumor-mediated angiogenesis and dysplastic tumor vessels (**Figure 2**). The resultant high IFP has several effects on the tumor and tumor microenvironment. First, elevated IFP is transmitted through the tumor milieu and ECM of the glioma subjecting glioma cells and ECM components to various forces including normal force and shear stress. Much of the current understanding of the sequelae of these fluid-based forces in glioma and in the brain in general are extrapolated from studies in other organ systems and disease contexts; this is in part due to the difficulty to accurately measure these stress forces in a complex microenvironment (**Figure 2**) (117–119). It is presumable that shear stress-mediated deformation of either the cancer cell cytoarchitecture directly or ECM components promotes changes in stemness, migration, and other features of cancer through mechanotransduction as discussed in previous sections, but this is yet to be investigated comprehensively. Qazi et al. examined the effect of simulated fluid shear stress on the migratory activity of glioma cell lines in a modified Boyden chamber (116). The authors demonstrated that both time of exposure to shear stress and magnitude of shear stress diminished migration in two of three cell lines by 92% and 58%, but the third cell line was not affected by shear stress (116). Quantification of MMP levels showed a concomitant downregulation of active and total MMP with exposure to shear stress that was confirmed with MMP inhibitor assays. Interestingly, the third cell line that was not affected by shear stress also exhibited minimal change in MMP levels. They observed differential migratory activity in the presence of or absence of a TGF-α flow gradient suggesting enhanced cell migration due to a flow-induced chemotaxis—89%, 566%, and 101% enhancement in migratory capacity with TGF-α (116). In similar studies by Li et al. and Namba et al., simulated fluid shear stress applied to U87 glioma cells and BTICs in a microfluidic apparatus produced an increase cellular adhesion strength and differential invasion based on differentiation—less differentiated nestin-positive BTICs tended to invade first under interstitial flow (115, 120). In addition to mechanical effects of fluid shear stress and IFP, these forces in various cancer models including have been shown to produce flow-induced gradients of soluble factors in the microenvironments including chemokines that influence directionality and invasion through chemical signaling (**Figure 2**) (85, 114, 118, 119, 121). Although initial studies of interstitial fluid flow and IFP posited a radial IFP emanating from the tumor core outward because of the arrangement of leaky vasculature, Spin echo-MRI analysis by Kingsmore et al. of xenograft mouse glioma tumors revealed heterogenous interstitial flow dynamics (110, 111, 122–124). They noted a general trend of outward flow of interstitial fluid but observed significant intratumoral heterogeneity in interstitial flow

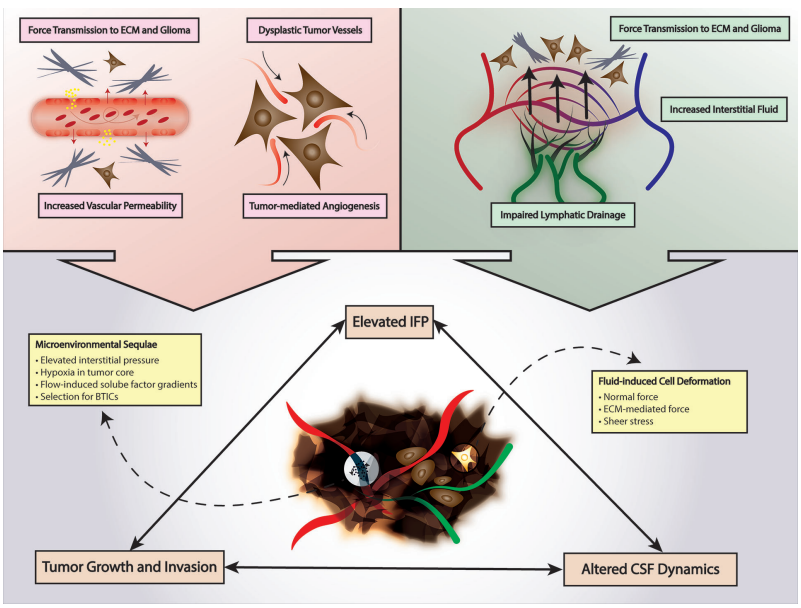

FIGURE 2 | Fluid Mechanics in Glioma. Tumor-mediated angiogenesis and tumor-mediated increased vascular permeability increases interstitial fluid pressure and force transmission to glioma cells and ECM. Lymphatic insufficiency also contributes to increased interstitial fluid pressure. Increased mechanical stimuli from elevated interstitial fluid pressure can promote a tumor environment selective for BTICs and alter CSF dynamics. CSF, cerebrospinal fluid; ECM, extracellular matrix; BTICs, brain tumor-initiating cells; IFP, interstitial fluid pressure.

velocities which correlated with Evans blue assessment of drainage (111). Taken together with the work by Qazi et al. it is evident that fluid dynamics and the response to local fluid dynamics is not uniform but rather heterogenous (111, 113, 116). Further investigation of interstitial fluid dynamics and shear stress in glioma will not only improve our understanding of tumoral and microenvironment heterogeneity but also potentially uncover new therapeutic targets that can be modulated to either slow disease progression or perhaps facilitate enhanced drug delivery to sites of disease (113).

Lymphatic Flow Dynamics

Lymphatic flow dynamics and drainage effectively link microenvironmental properties such as IFP and interstitial fluid flow with the local immunosuppression that is observed in glioma. In brain tumors such as GBM, draining lymphatic vessels of the tumor are typically compromised, and the tumor milieu is inadequately drained. This produces a dual mechanical and immunological effect in the microenvironment. As a result of compromised lymphatics, interstitial fluid accumulates in certain regions of the microenvironment resulting in elevated IFP with its associated mechanical and chemical signaling as previously discussed **(Figure 2)** (49, 117, 125–127). Secondly, impaired lymphatic drainage from the tumor simultaneously hinders antigen presentation and immune cell recruitment at peripheral sites as well as preventing migration of immune effector cells into the tumor tissue ultimately producing a function immune escape phenomenon **(Figure 1)** (49, 125–127). Studies have demonstrated that pharmacologic restoration of these meningeal lymphatic vessels can sensitize GBM to the host immune response and synergize with immunotherapy effectively (117, 125–128). This new class of targeted therapies such as VEGF-C is promising in that it represents a priming of cellular immunotherapy, if successful, can reach infiltrative disease in addition to the primary disease site while concurrently ameliorating malignant mechanical stimuli-induced changes in glioma cells by relieving IFP in areas of impaired lymphatic drainage (49, 125–129).

THERANOSTIC OPPORTUNITIES AND MODELING

Therapeutic Targets

Several potential therapeutic targets follow from the present overview of the current understanding of mechanical properties in the glioma microenvironment. Given the crucial role of mechanotransducers such as mechanosensitive ion channels in promoting glioma malignancy, pharmacologic inhibition of signal transduction is attractive. Known inhibitors exist already for some of these channels such as the PIEZO, mechanically gated ion channels; however, non-specificity poses a hurdle as well as the perpetual barrier of achieving effective delivery of any therapeutic to the primary tumor site and invasive BTICs (130–134). Drug pharmacology surrounding the PIEZO channels is still in its infancy, with the majority of studies employing non-specific inhibitors for the purposes of interrogation of channel properties and mechanism of action (130, 133). Groups have identified inhibitors of the PIEZO1 and PIEZO2 channel including the polycation ruthenium red, gadolinium, and the peptide GsMTx-4, but these agents are yet to be tested in translational studies. Activators such as Yoda1, Jedi1, and Jedi have also been described and these agents have been similarly leveraged to elucidate the mechanism of these channels in the glioma microenvironment (71, 133, 135). For example, Chen et al. utilize Yoda1 to further define the relationship between surrounding tissue stiffness and PIEZO1 activity in glioma by showing that beyond a certain level of expression of the channel that is necessary for growth, overactivation of the PIEZO1 channels with Yoda1 do not enhance glioma cell proliferation *in vitro* (71). As *Xiao* outlines in his excellent review of the prospects for future therapeutics targeting PIEZO channels, with increasing recognition of the influence of such ion channels on glioma cell phenotype and disease progression, studies directed towards drug discovery and targeted inactivators of mechanosensitive ion channels for clinical application are forthcoming (133). This is supported by the recent elucidation of the crystal structure of such channels that have paved the path for high-throughput, targeted drug development (136, 137).

In addition to directly inhibiting mechanical signal transduction, another feasible approach is to target the downstream molecular mechanisms and cellular processes that promote disease progression. One such target is autophagy which has been implicated in treatment resistance in various cancers including GBM (138–140). Recent studies have shown that the process of autophagy is altered by mechanical stimuli and signal transduction primarily through two mechanisms: 1) crosstalk between the shared regulatory proteins in autophagy and mechanical signal transduction pathway or 2) competition for molecular substrates utilized in both processes such as cytoskeletal elements (138). Several common pathways have been described in the literature and include the YAP/TAZ axis, JAK-mediated signal transduction, and the expression of EGFR (138, 141, 142). Dupont et al. demonstrate in a series of experiments that the transcriptional regulators YAP/TAZ are required for transducing mechanical cues from the microenvironment and specifically the elasticity of the ECM (96). Using a stem cell model, they demonstrate that altering ECM stiffness and geometry of the growth substrate differentially regulates both proliferation and cell differentiation in a YAP/TAZ-dependent manner (96). Interestingly, YAP/TAZ is also observed to facilitate the fusion of autophagolysosomes and promote autophagic flux *via* a downstream protein target, Armus, in a study by Totaro et al. (101, 143) When this effect was pharmacologically dampened with autophagy inhibitors or through knockdown of autophagy genes, growth of breast cancer cells *in vitro* decreased. The opposite effect was observed when YAP/TAZ was overexpressed, and cancer stem cell features such as plasticity as measured by differentiation potential were enhanced (143). This data suggests that the YAP/TAZ axis may be one of several common pathways between mechanical signal transduction and other aberrant cellular

processes in cancer that can be simultaneously targeted (143). Taken together, development of therapeutics that interfere with the cytoprotective effects of autophagy in cancer cells may represent a potential treatment modality and serve as an example for identifying points of convergence between mechanical signal transduction and other known processes in cancer progression amenable to therapeutic targeting (139, 140).

Alternatively, a therapeutic strategy that alters the mechanical properties of the microenvironment, i.e., manipulating solid stress and fluid stress in the tumor milieu, to engineer an anti-glioma environment may be plausible (71, 83, 113, 144, 145). The advantage with such an approach may be the ability to create "smart" or responsive therapies that can either effect mechanical changes locoregionally—in the area of radiographic disease or visible tumor or global changes to target invisible, infiltrative disease (71, 83, 113, 144, 145). Many of the studies discussed in this review as well as other studies examining mechanical properties in the cancer microenvironment have used some type of bioengineering approach to create a microenvironment-mimetic substrate to alter the physical forces that are felt by the cell or tissue of interest. In these studies, modulation of the substrate whether it is a 3D hydrogel or 2D suspension has resulted in elimination of malignant properties. This concept can be theoretically applied as a treatment whereby engineered materials may be implanted into tumor resection cavities after surgical removal of visible tumor. The material or scaffold could be engineered to respond to chemical and physical stimuli from surrounding brain tissue and to alter local physical properties to promote an anti-glioma microenvironment (114, 116, 146–149). This paradigm requires further study and is yet to be developed for clinical application in glioma. Although bioengineering technologies have evolved to meet these needs, this type of approach is hindered by our current rudimentary understanding of biophysical dynamics and their ramifications in brain cancer and in normal brain. Another approach to achieve the same effect is with the use of pharmacologic agents that can alter mechanical properties in the microenvironment such as with the angiotensin inhibitor Losartan. Chauhan et al. show that in models of breast and prostate cancer, administration of Losartan decreases solid stress in the tumor microenvironment by reducing the production of profibrotic components in the ECM such as collagen and hyaluronan (150). The use of Losartan with the intent to target mechanical properties in the context of brain tumors has not been well-studied, but a Phase 2 clinical trial is currently ongoing within this area (NCT03951142). Even in the absence of therapeutics targeted at tissue mechanics, improved understanding of these properties may pave the way for designing adjunctive therapies that can mitigate the biophysical barriers to other treatments such as drug delivery of conventional chemotherapeutics or effective immune cell infiltration of disease sites and successful immunotherapy-based approaches (11, 23, 84, 151).

Diagnostics

Unique mechanical properties of glioma and its microenvironment provide a basis for the development of novel diagnostics to address two unmet needs in clinical medicine: 1) accurate identification of infiltrative disease in nervous tissue that is radiographically and microscopically occult and 2) characterization disease heterogeneity and plasticity towards predictive analytics for treatment response or prognosis. Fundamental technologies are available as were described in the studies presented in this review such as MRE and other tools for rheological phenotyping, and these have the potential to be adapted and refined as possible intraoperative adjuncts or as supplements to the conventional imaging obtained for patients with GBM to better guide treatment choices (57, 59, 61, 62, 67, 152–154). Briefly, techniques can be categorized based on the substrate assessed—either cells and tissue or more macroscopically a region of the brain (**Table 2**). MRE as discussed previously, is now a well-studied imaging technique that can characterize tissue stiffness on a global scale in the brain. In this technique, vibrations through the brain are coupled with magnetic resonance imaging (MRI) sequences to create a landscape of tissue stiffness in the brain (59–62, 85, 155). This is particularly useful when trying to evaluate a mass in the brain as the tissue stiffness within the mass and surrounding regions may offer insights into the tumor type, grade, and propensity for malignant transformation (59, 60, 67). Investigations are ongoing to optimize the imaging protocols for this technique and to develop iterations that can be used at the point-of-care in the operating room. Intraoperative imaging with this technology could provide information regarding prognostication, response to therapy, growth rate in addition to the other intraoperative imaging tools available currently such as Raman spectroscopy, brain mapping, fluorescence-guidance, and optical coherence tomography (156). Further research is needed to establish and validate MRE as a reliable surrogate for such clinical

TABLE 2 | Representative Methods of Measuring Mechanical Tissue Properties in Glioma.

Method	Substrate	Mechanism	Ref.
MRE	Brain/Tissue	Stiffness map of ROI	(59, 60, 67)
US	Brain/Tissue	Stiffness based on permeability to ultrasonic waves	(85)
SWE	Brain/Tissue	Stiffness based on propagation of ultrasonic waves and tissue displacement	(58)
Needle biopsy	Tissue	Solid stress based on tissue deformation	(54–56, 85)
Serial slices	Tissue	Solid stress based on tissue deformation	(54–56, 85)
Planar cut	Tissue	Solid stress based on tissue deformation	(54–56, 85)
AFM	Tissue/Cell	Stiffness based on force measurement between probe and tissue	(47, 85)
Particle tracking	Tissue/Cell	Live imaging and measurement of particle movement, viscosity measurement	(85)

MRE, Magnetic Resonance Elastography; US, ultrasound; SWE, shear wave elastography.
AFM, Atomic Force Microscopy; ROI, region of interest.

parameters. Ultrasound-based imaging technologies can also be used at the point-of-care, and the two general modalities are traditional ultrasound-based imaging and shear wave elastography **(Table 2)**. In traditional ultrasound, the ultrasound probe can be placed on the tissue of interest during surgery and an interpretation of physical characteristics is made based on the radiolucency of the area of interest. In shear wave elastography, a device is used to measure the propagation of ultrasonic waves through the region of interest and also measure the displacement of the tissue to calculate physical parameters such as shear modulus (47, 58, 85) **(Table 2)**. Many methods have been described to study the physical properties of cells and tissue, and these include atom force microscopy, particle-tracking techniques, and measurements of tissue deformation (53–55, 110, 122, 124) **(Table 2)**. The latter technique consists of lesioning a piece of tissue typically with a needle biopsy, serial slicing, or a single planar cut and subsequently measuring the magnitude of deformation or displacement of the tissue into the lesioned area. Comprehensive reviews of methodologies used to study mechanical properties *in vitro* and *in vivo* can be found elsewhere (47, 85, 155). Advances in bioengineering in the fields of microfluidics, biomimetics, and hydrogel may also enable the development of high-throughput, point-of-care methods to define disease features such as the mechanophenotype that may aid in clinical-decision making (84, 147, 152, 157).

Preclinical Modeling

Veritable preclinical models of glioma that accurately recapitulate important aspects of the disease are essential for successful clinical translation of innovative therapeutics. Our growing understanding of all the layers of disease heterogeneity and plasticity is now further complicated by heterogeneity and plasticity of the mechanical properties of glioma and its microenvironment (17, 25, 84, 147, 157, 158). Recent work also highlights clinically significant sexual dimorphism in many facets of the glioma disease process, and this feature of glioma has yet to be studied rigorously from the biophysical perspective which will be an important consideration for therapy development (20, 158–160). For example, it is unknown whether sex differences affect solid stress or fluid stress components within a glioma and its microenvironment. Similarly, the influence of other tumor characteristics on the biophysical properties of the tumor microenvironment are also poorly understood. These include factors such as proximity to the cerebrospinal fluid spaces of the brain and the response of tumor to surgical resection and chemoradiation which have been shown to play a role in other processes, but further investigation is needed with regards to mechanical properties (161, 162). Once again, the application of bioengineering to model mechanical features of the microenvironment may be several in dissecting mechanisms of mechanotransduction, mechanoreciprocity, and plasticity. Current models attempt to incorporate different features of heterogeneity in the tumor microenvironment that may impact its mechanical properties such as varying the composition of the ECM constituents as well as the type of model—3D versus 2D (147). Other groups have recreated heterogeneity in stiffness, elasticity, and soluble factor gradients (147, 149, 163, 164). These models will be crucial for effective drug development because they may offer useful information about pharmacokinetic and pharmacodynamic properties of proposed therapeutics as well as uncover additional therapeutic targets or treatment resistance mechanisms. As new variables are identified that can influence the mechanical properties of the microenvironment, the models that attempt to recapitulate these features will likely continue to become more sophisticated (114, 116, 147–149, 165–167).

CONCLUSION

The study of mechanical properties in the glioma microenvironment holds considerable promise. Further elucidation of the biophysical features of the microenvironment will enable a more comprehensive understanding of glioma as a disease process, and this may create novel theranostic opportunities while also informing preclinical modeling.

AUTHOR CONTRIBUTIONS

AB: conceptualization, investigation, writing - original draft, writing – review and editing, visualization, and management. JD: writing – review and editing. RC: writing – review and editing, and supervision. ST: conceptualization, writing – review and editing and supervision. All authors contributed to the article and approved the submitted version.

FUNDING

ST received funding from the National Institutes of Health (R01CA227838) and a pilot project award from the University of Kansas Cancer Center, NCI support grant P30 CA168524.

ACKNOWLEDGMENTS

The authors thank Dr. Paul Camarata, MD, Chair, Department of Neurosurgery for supporting the publication costs.

REFERENCES

1. Ostrom QT, Patil N, Cioffi G, Waite K, Kruchko C, Barnholtz-Sloan JS, et al. CBTRUS Statistical Report: Primary Brain and Other Central Nervous System Tumors Diagnosed in the United States in 2013-2017. *Neuro Oncol* (2020) 22:iv1–iv96. doi: 10.1093/neuonc/noaa200
2. ReFaey K, Tripathi S, Grewal SS, Bhargav AG, Quinones DJ, Chaichana KL, et al. Cancer Mortality Rates Increasing vs Cardiovascular Disease Mortality Decreasing in the World: Future Implications. *Mayo Clin Proc Innov Qual Outcomes* (2021) 5:645–53. doi: 10.1016/j.mayocpiqo.2021.05.005
3. Louis DN, Perry A, Wesseling P, Brat DJ, Cree IA, Figarella-Branger D, et al. The 2021 WHO Classification of Tumors of the Central Nervous System: A Summary. *Neuro Oncol* (2021) 23:1231–51. doi: 10.1093/neuonc/noab106

4. Stupp R, Mason WP, van den Bent MJ, Weller M, Fisher B, Taphoorn MJ, et al. Radiotherapy Plus Concomitant and Adjuvant Temozolomide for Glioblastoma. *N Engl J Med* (2005) 352:987–96. doi: 10.1056/NEJMoa043330
5. Stupp R, Taillibert S, Kanner A, Read W, Steinberg D, Lhermitte B, et al. Effect of Tumor-Treating Fields Plus Maintenance Temozolomide vs Maintenance Temozolomide Alone on Survival in Patients With Glioblastoma: A Randomized Clinical Trial. *JAMA* (2017) 318:2306–16. doi: 10.1001/jama.2017.18718
6. Sanai N, Berger MS. Surgical Oncology for Gliomas: The State of the Art. *Nat Rev Clin Oncol* (2018) 15:112–25. doi: 10.1038/nrclinonc.2017.171
7. Lara-Velazquez M, Al-Kharboosh R, Jeanneret S, Vazquez-Ramos C, Mahato D, Tavanaiepour D, et al. Advances in Brain Tumor Surgery for Glioblastoma in Adults. *Brain Sci* (2017) 7:1–16. doi: 10.3390/brainsci7120166
8. Bhargav AG, Mondal SK, Garcia CA, Green JJ, Quinones-Hinojosa A. Nanomedicine Revisited: Next Generation Therapies for Brain Cancer. *Adv Ther-Germany* (2020) 3:ARTN 2000118. doi: 10.1002/adtp.202000118
9. Dunn GP, Cloughesy TF, Maus MV, Prins RM, Reardon DA, Sonabend AM, et al. Emerging Immunotherapies for Malignant Glioma: From Immunogenomics to Cell Therapy. *Neuro Oncol* (2020) 22:1425–38. doi: 10.1093/neuonc/noaa154
10. Lim M, Xia Y, Bettegowda C, Weller M. Current State of Immunotherapy for Glioblastoma. *Nat Rev Clin Oncol* (2018) 15:422–42. doi: 10.1038/s41571-018-0003-5
11. Shah K. Stem Cell-Based Therapies for Tumors in the Brain: Are We There Yet? *Neuro Oncol* (2016) 18:1066–78. doi: 10.1093/neuonc/now096
12. Stuckey DW, Shah K. Stem Cell-Based Therapies for Cancer Treatment: Separating Hope From Hype. *Nat Rev Cancer* (2014) 14:683–91. doi: 10.1038/nrc3798
13. Quinones-Hinojosa A, Sanai N, Soriano-Navarro M, Gonzalez-Perez O, Mirzadeh Z, Gil-Perotin S, et al. Cellular Composition and Cytoarchitecture of the Adult Human Subventricular Zone: A Niche of Neural Stem Cells. *J Comp Neurol* (2006) 494:415–34. doi: 10.1002/cne.20798
14. Sanai N, Tramontin AD, Quinones-Hinojosa A, Barbaro NM, Gupta N, Kunwar S, et al. Unique Astrocyte Ribbon in Adult Human Brain Contains Neural Stem Cells But Lacks Chain Migration. *Nature* (2004) 427:740–4. doi: 10.1038/nature02301
15. Lathia J, Liu H, Matei D. The Clinical Impact of Cancer Stem Cells. *Oncologist* (2020) 25:123–31. doi: 10.1634/theoncologist.2019-0517
16. Lathia JD, Mack SC, Mulkearns-Hubert EE, Valentim CL, Rich JN. Cancer Stem Cells in Glioblastoma. *Genes Dev* (2015) 29:1203–17. doi: 10.1101/gad.261982.115
17. Mitchell K, Troike K, Silver DJ, Lathia JD. The Evolution of the Cancer Stem Cell State in Glioblastoma: Emerging Insights Into the Next Generation of Functional Interactions. *Neuro Oncol* (2021) 23:199–213. doi: 10.1093/neuonc/noaa259
18. Saygin C, Matei D, Majeti R, Reizes O, Lathia JD. Targeting Cancer Stemness in the Clinic: From Hype to Hope. *Cell Stem Cell* (2019) 24:25–40. doi: 10.1016/j.stem.2018.11.017
19. Comba A, Faisal SM, Varela ML, Hollon T, Al-Holou WN, Umemura Y, et al. Uncovering Spatiotemporal Heterogeneity of High-Grade Gliomas: From Disease Biology to Therapeutic Implications. *Front Oncol* (2021) 11:703764. doi: 10.3389/fonc.2021.703764
20. Gimple RC, Bhargava S, Dixit D, Rich JN. Glioblastoma Stem Cells: Lessons From the Tumor Hierarchy in a Lethal Cancer. *Genes Dev* (2019) 33:591–609. doi: 10.1101/gad.324301.119
21. Prager BC, Bhargava S, Mahadev V, Hubert CG, Rich JN. Glioblastoma Stem Cells: Driving Resilience Through Chaos. *Trends Cancer* (2020) 6:223–35. doi: 10.1016/j.trecan.2020.01.009
22. Fecci PE, Sampson JH. The Current State of Immunotherapy for Gliomas: An Eye Toward the Future. *J Neurosurg* (2019) 131:657–66. doi: 10.3171/2019.5.JNS181762
23. Yeini E, Ofek P, Albeck N, Ajamil DR, Neufeld L, Eldar-Boock A, et al. Targeting Glioblastoma: Advances in Drug Delivery and Novel Therapeutic Approaches. *Adv Ther-Germany* (2021) 4:ARTN 2000124. doi: 10.1002/adtp.202000124
24. Ma YF, Yang ZG, Huntoon K, Jiang W, Kim BYS. Advanced Immunotherapy Approaches for Glioblastoma. *Adv Ther-Germany* (2021) 4:ARTN 2100046. doi: 10.1002/adtp.202100046
25. Lathia JD, Heddleston JM, Venere M, Rich JN. Deadly Teamwork: Neural Cancer Stem Cells and the Tumor Microenvironment. *Cell Stem Cell* (2011) 8:482–5. doi: 10.1016/j.stem.2011.04.013
26. Bonavia R, Inda MM, Cavenee WK, Furnari FB. Heterogeneity Maintenance in Glioblastoma: A Social Network. *Cancer Res* (2011) 71:4055–60. doi: 10.1158/0008-5472.CAN-11-0153
27. Gilbertson RJ, Rich JN. Making a Tumour's Bed: Glioblastoma Stem Cells and the Vascular Niche. *Nat Rev Cancer* (2007) 7:733–6. doi: 10.1038/nrc2246
28. Andersen BM, Faust Akl C, Wheeler MA, Chiocca EA, Reardon DA, Quintana FJ. Glial and Myeloid Heterogeneity in the Brain Tumour Microenvironment. *Nat Rev Cancer* (2021) 23:199–213. doi: 10.1038/s41568-021-00397-3
29. Barnes JM, Przybyla L, Weaver VM. Tissue Mechanics Regulate Brain Development, Homeostasis and Disease. *J Cell Sci* (2017) 130:71–82. doi: 10.1242/jcs.191742
30. Kaushik S, Persson AI. Unlocking the Dangers of a Stiffening Brain. *Neuron* (2018) 100:763–5. doi: 10.1016/j.neuron.2018.11.011
31. Iwashita M, Kataoka N, Toida K, Kosodo Y. Systematic Profiling of Spatiotemporal Tissue and Cellular Stiffness in the Developing Brain. *Development* (2014) 141:3793–8. doi: 10.1242/dev.109637
32. Heisenberg CP, Bellaiche Y. Forces in Tissue Morphogenesis and Patterning. *Cell* (2013) 153:948–62. doi: 10.1016/j.cell.2013.05.008
33. Sawamoto K, Wichterle H, Gonzalez-Perez O, Cholfin JA, Yamada M, Spassky N, et al. New Neurons Follow the Flow of Cerebrospinal Fluid in the Adult Brain. *Science* (2006) 311:629–32. doi: 10.1126/science.1119133
34. Alvarez-Buylla A, Lim DA. For the Long Run: Maintaining Germinal Niches in the Adult Brain. *Neuron* (2004) 41:683–6. doi: 10.1016/s0896-6273(04)00111-4
35. Saha K, Keung AJ, Irwin EF, Li Y, Little L, Schaffer DV, et al. Substrate Modulus Directs Neural Stem Cell Behavior. *Biophys J* (2008) 95:4426–38. doi: 10.1529/biophysj.108.132217
36. Georges PC, Miller WJ, Meaney DF, Sawyer ES, Janmey PA. Matrices With Compliance Comparable to That of Brain Tissue Select Neuronal Over Glial Growth in Mixed Cortical Cultures. *Biophys J* (2006) 90:3012–8. doi: 10.1529/biophysj.105.073114
37. Leipzig ND, Shoichet MS. The Effect of Substrate Stiffness on Adult Neural Stem Cell Behavior. *Biomaterials* (2009) 30:6867–78. doi: 10.1016/j.biomaterials.2009.09.002
38. Guo J, Bertalan G, Meierhofer D, Klein C, Schreyer S, Steiner B, et al. Brain Maturation is Associated With Increasing Tissue Stiffness and Decreasing Tissue Fluidity. *Acta Biomater* (2019) 99:433–42. doi: 10.1016/j.actbio.2019.08.036
39. Chang EH, Adorjan I, Mundim MV, Sun B, Dizon MLV, Szele FG. Traumatic Brain Injury Activation of the Adult Subventricular Zone Neurogenic Niche. *Front Neurosci* (2016) 10:332. doi: 10.3389/fnins.2016.00332
40. Laywell ED, Dorries U, Bartsch U, Faissner A, Schachner M, Steindler DA, et al. Enhanced Expression of the Developmentally Regulated Extracellular Matrix Molecule Tenascin Following Adult Brain Injury. *Proc Natl Acad Sci USA* (1992) 89:2634–8. doi: 10.1073/pnas.89.7.2634
41. Murphy MC, Jones DT, Jack CR Jr, Glaser KJ, Senjem ML, Manduca A, et al. Decreased Brain Stiffness in Alzheimer's Disease Determined by Magnetic Resonance Elastography. *J Magn Reson Imaging* (2011) 34:494–8. doi: 10.1002/jmri.22707
42. Murphy MC, Jones DT, Jack CR Jr, Glaser KJ, Senjem ML, Manduca A, et al. Regional Brain Stiffness Changes Across the Alzheimer's Disease Spectrum. *NeuroImage Clin* (2016) 10:283–90. doi: 10.1016/j.nicl.2015.12.007
43. Lau LW, Cua R, Keough MB, Haylock-Jacobs S, Yong VW. Pathophysiology of the Brain Extracellular Matrix: A New Target for Remyelination. *Nat Rev Neurosci* (2013) 14:722–9. doi: 10.1038/nrn3550
44. Bonneh-Barkay D, Wiley CA. Brain Extracellular Matrix in Neurodegeneration. *Brain Pathol* (2009) 19:573–85. doi: 10.1111/j.1750-3639.2008.00195.x
45. Levental KR, Yu H, Kass L, Lakins JN, Egeblad M, Erler JT, et al. Matrix Crosslinking Forces Tumor Progression by Enhancing Integrin Signaling. *Cell* (2009) 139:891–906. doi: 10.1016/j.cell.2009.10.027
46. Katira P, Bonnecaze RT, Zaman MH. Modeling the Mechanics of Cancer: Effect of Changes in Cellular and Extra-Cellular Mechanical Properties. *Front Oncol* (2013) 3:145. doi: 10.3389/fonc.2013.00145

47. Kumar S, Weaver VM. Mechanics, Malignancy, and Metastasis: The Force Journey of a Tumor Cell. *Cancer Metastasis Rev* (2009) 28:113–27. doi: 10.1007/s10555-008-9173-4
48. Tung JC, Barnes JM, Desai SR, Sistrunk C, Conklin MW, Schedin P, et al. Tumor Mechanics and Metabolic Dysfunction. *Free Radic Biol Med* (2015) 79:269–80. doi: 10.1016/j.freeradbiomed.2014.11.020
49. Swartz MA, Lund AW. Lymphatic and Interstitial Flow in the Tumour Microenvironment: Linking Mechanobiology With Immunity. *Nat Rev Cancer* (2012) 12:210–9. doi: 10.1038/nrc3186
50. Quail DF, Joyce JA. Microenvironmental Regulation of Tumor Progression and Metastasis. *Nat Med* (2013) 19:1423–37. doi: 10.1038/nm.3394
51. Mohammadi H, Sahai E. Mechanisms and Impact of Altered Tumour Mechanics. *Nat Cell Biol* (2018) 20:766–74. doi: 10.1038/s41556-018-0131-2
52. Nia HT, Munn LL, Jain RK. Physical Traits of Cancer. *Science* (2020) 370:1–9. doi: 10.1126/science.aaz0868
53. Stylianopoulos T, Martin JD, Chauhan VP, Jain SR, Diop-Frimpong B, Bardeesy N, et al. Causes, Consequences, and Remedies for Growth-Induced Solid Stress in Murine and Human Tumors. *Proc Natl Acad Sci USA* (2012) 109:15101–8. doi: 10.1073/pnas.1213353109
54. Nia HT, Liu H, Seano G, Datta M, Jones D, Rahbari N, et al. Solid Stress and Elastic Energy as Measures of Tumour Mechanopathology. *Nat BioMed Eng* (2016) 1:1–11. doi: 10.1038/s41551-016-0004
55. Stylianopoulos T, Martin JD, Snuderl M, Mpekris F, Jain SR, Jain RK, et al. Coevolution of Solid Stress and Interstitial Fluid Pressure in Tumors During Progression: Implications for Vascular Collapse. *Cancer Res* (2013) 73:3833–41. doi: 10.1158/0008-5472.CAN-12-4521
56. Seano G, Nia HT, Emblem KE, Datta M, Ren J, Krishnan S, et al. Solid Stress in Brain Tumours Causes Neuronal Loss and Neurological Dysfunction and can be Reversed by Lithium. *Nat BioMed Eng* (2019) 3:230–45. doi: 10.1038/s41551-018-0334-7
57. Xu L, Lin Y, Han JC, Xi ZN, Shen H, Gao PY, et al. Magnetic Resonance Elastography of Brain Tumors: Preliminary Results. *Acta Radiol* (2007) 48:327–30. doi: 10.1080/02841850701199967
58. Chauvet D, Imbault M, Capelle L, Demene C, Mossad M, Karachi C, et al. *In Vivo* Measurement of Brain Tumor Elasticity Using Intraoperative Shear Wave Elastography. *Ultraschall Med* (2016) 37:584–90. doi: 10.1055/s-0034-1399152
59. Reiss-Zimmermann M, Streitberger KJ, Sack I, Braun J, Arlt F, Fritzsch D, et al. High Resolution Imaging of Viscoelastic Properties of Intracranial Tumours by Multi-Frequency Magnetic Resonance Elastography. *Clin Neuroradiol* (2015) 25:371–8. doi: 10.1007/s00062-014-0311-9
60. Streitberger KJ, Reiss-Zimmermann M, Freimann FB, Bayerl S, Guo J, Arlt F, et al. High-Resolution Mechanical Imaging of Glioblastoma by Multifrequency Magnetic Resonance Elastography. *PloS One* (2014) 9: e110588. doi: 10.1371/journal.pone.0110588
61. Simon M, Guo J, Papazoglou S, Scholand-Engler H, Erdmann C, Melchert U, et al. Non-Invasive Characterization of Intracranial Tumors by Magnetic Resonance Elastography. *New J Phys* (2013) 15:Artn 085024. doi: 10.1088/1367-2630/15/8/085024
62. Schregel K, Nazari N, Nowicki MO, Palotai M, Lawler SE, Sinkus R, et al. Characterization of Glioblastoma in an Orthotopic Mouse Model With Magnetic Resonance Elastography. *NMR BioMed* (2018) 31:e3840. doi: 10.1002/nbm.3840
63. Reinhard J, Brosicke N, Theocharidis U, Faissner A. The Extracellular Matrix Niche Microenvironment of Neural and Cancer Stem Cells in the Brain. *Int J Biochem Cell Biol* (2016) 81:174–83. doi: 10.1016/j.biocel.2016.05.002
64. Ruoslahti E. Brain Extracellular Matrix. *Glycobiology* (1996) 6:489–92. doi: 10.1093/glycob/6.5.489
65. Quail DF, Joyce JA. The Microenvironmental Landscape of Brain Tumors. *Cancer Cell* (2017) 31:326–41. doi: 10.1016/j.ccell.2017.02.009
66. Pogoda K, Chin L, Georges PC, Byfield FJ, Bucki R, Kim R, et al. Compression Stiffening of Brain and its Effect on Mechanosensing by Glioma Cells. *New J Phys* (2014) 16:75002. doi: 10.1088/1367-2630/16/7/075002
67. Streitberger KJ, Lilaj L, Schrank F, Braun J, Hoffmann KT, Reiss-Zimmermann M, et al. How Tissue Fluidity Influences Brain Tumor Progression. *P Natl Acad Sci USA* (2020) 117:128–34. doi: 10.1073/pnas.1913511116
68. Pope WB, Kim HJ, Huo J, Alger J, Brown MS, Gjertson D, et al. Recurrent Glioblastoma Multiforme: ADC Histogram Analysis Predicts Response to Bevacizumab Treatment. *Radiology* (2009) 252:182–9. doi: 10.1148/radiol.2521081534
69. Pope WB, Mirsadraei L, Lai A, Eskin A, Qiao J, Kim HJ, et al. Differential Gene Expression in Glioblastoma Defined by ADC Histogram Analysis: Relationship to Extracellular Matrix Molecules and Survival. *AJNR Am J Neuroradiol* (2012) 33:1059–64. doi: 10.3174/ajnr.A2917
70. Miroshnikova YA, Mouw JK, Barnes JM, Pickup MW, Lakins JN, Kim Y, et al. Tissue Mechanics Promote IDH1-Dependent HIF1alpha-Tenascin C Feedback to Regulate Glioblastoma Aggression. *Nat Cell Biol* (2016) 18:1336–45. doi: 10.1038/ncb3429
71. Chen X, Wanggou S, Bodalia A, Zhu M, Dong W, Fan JJ, et al. A Feedforward Mechanism Mediated by Mechanosensitive Ion Channel PIEZO1 and Tissue Mechanics Promotes Glioma Aggression. *Neuron* (2018) 100:799–815 e797. doi: 10.1016/j.neuron.2018.09.046
72. Ulrich TA, de Juan Pardo EM, Kumar S. The Mechanical Rigidity of the Extracellular Matrix Regulates the Structure, Motility, and Proliferation of Glioma Cells. *Cancer Res* (2009) 69:4167–74. doi: 10.1158/0008-5472.CAN-08-4859
73. Umesh V, Rape AD, Ulrich TA, Kumar S. Microenvironmental Stiffness Enhances Glioma Cell Proliferation by Stimulating Epidermal Growth Factor Receptor Signaling. *PloS One* (2014) 9:e101771. doi: 10.1371/journal.pone.0101771
74. Pajic M, Herrmann D, Vennin C, Conway JRW, Chin VT, Jonhsson A-KE, et al. The Dynamics of Rho GTPase Signaling and Implications for Targeting Cancer and the Tumor Microenvironment. *Small GTPases* (2015) 6:123–33. doi: 10.4161/21541248.2014.973749
75. Northey JJ, Przybyla L, Weaver VM. Tissue Force Programs Cell Fate and Tumor Aggression. *Cancer Discovery* (2017) 7:1224–37. doi: 10.1158/2159-8290.Cd-16-0733
76. Zhang JF, Tao T, Wang K, Zhang GX, Yan Y, Lin HR, et al. IL-33/ST2 Axis Promotes Glioblastoma Cell Invasion by Accumulating Tenascin-C. *Sci Rep* (2019) 9:20276. doi: 10.1038/s41598-019-56696-1
77. Kim Y, Kumar S. CD44-Mediated Adhesion to Hyaluronic Acid Contributes to Mechanosensing and Invasive Motility. *Mol Cancer Res* (2014) 12:1416–29. doi: 10.1158/1541-7786.MCR-13-0629
78. Tao B, Song Y, Wu Y, Yang X, Peng T, Peng L, et al. Matrix Stiffness Promotes Glioma Cell Stemness by Activating BCL9L/Wnt/beta-Catenin Signaling. *Aging (Albany NY)* (2021) 13:5284–96. doi: 10.18632/aging.202449
79. Barnes JM, Kaushik S, Bainer RO, Sa JK, Woods EC, Kai F, et al. A Tension-Mediated Glycocalyx-Integrin Feedback Loop Promotes Mesenchymal-Like Glioblastoma. *Nat Cell Biol* (2018) 20:1203–14. doi: 10.1038/s41556-018-0183-3
80. Joyce JA, Fearon DT. T Cell Exclusion, Immune Privilege, and the Tumor Microenvironment. *Science* (2015) 348:74–80. doi: 10.1126/science.aaa6204
81. Huang JY, Cheng YJ, Lin YP, Lin HC, Su CC, Juliano R, et al. Extracellular Matrix of Glioblastoma Inhibits Polarization and Transmigration of T Cells: The Role of Tenascin-C in Immune Suppression. *J Immunol* (2010) 185:1450–9. doi: 10.4049/jimmunol.0901352
82. Qu S, Hu T, Qiu O, Su Y, Gu J, Xia Z, et al. Effect of Piezo1 Overexpression on Peritumoral Brain Edema in Glioblastomas. *AJNR Am J Neuroradiol* (2020) 41:1423–9. doi: 10.3174/ajnr.A6638
83. Parkins CC, MCAbee JH, Ruff L, Wendler A, Mair R, Gilbertson RJ, et al. Mechanically Matching the Rheological Properties of Brain Tissue for Drug-Delivery in Human Glioblastoma Models. *Biomaterials* (2021) 276:120919. doi: 10.1016/j.biomaterials.2021.120919
84. Stylianopoulos T, Munn LL, Jain RK. Reengineering the Physical Microenvironment of Tumors to Improve Drug Delivery and Efficacy: From Mathematical Modeling to Bench to Bedside. *Trends Cancer* (2018) 4:292–319. doi: 10.1016/j.trecan.2018.02.005
85. Momin A, Bahrampour S, Min HK, Chen X, Wang X, Sun Y, et al. Channeling Force in the Brain: Mechanosensitive Ion Channels Choreograph Mechanics and Malignancies. *Trends Pharmacol Sci* (2021) 42:367–84. doi: 10.1016/j.tips.2021.02.006
86. Bomben VC, Turner KL, Barclay TT, Sontheimer H. Transient Receptor Potential Canonical Channels are Essential for Chemotactic Migration of Human Malignant Gliomas. *J Cell Physiol* (2011) 226:1879–88. doi: 10.1002/jcp.22518

87. Ross SB, Fuller CM, Bubien JK, Benos DJ. Amiloride-Sensitive Na+ Channels Contribute to Regulatory Volume Increases in Human Glioma Cells. *Am J Physiol Cell Physiol* (2007) 293:C1181–1185. doi: 10.1152/ajpcell.00066.2007
88. De Felice D, Alaimo A. Mechanosensitive Piezo Channels in Cancer: Focus on Altered Calcium Signaling in Cancer Cells and in Tumor Progression. *Cancers (Basel)* (2020) 12:1–14. doi: 10.3390/cancers12071780
89. Zhou W, Liu X, van Wijnbergen JWM, Yuan L, Liu Y, Zhang C, et al. Identification of PIEZO1 as a Potential Prognostic Marker in Gliomas. *Sci Rep* (2020) 10:16121. doi: 10.1038/s41598-020-72886-8
90. Chigurupati S, Venkataraman R, Barrera D, Naganathan A, Madan M, Paul L, et al. Receptor Channel TRPC6 is a Key Mediator of Notch-Driven Glioblastoma Growth and Invasiveness. *Cancer Res* (2010) 70:418–27. doi: 10.1158/0008-5472.CAN-09-2654
91. Cuddapah VA, Turner KL, Sontheimer H. Calcium Entry *via* TRPC1 Channels Activates Chloride Currents in Human Glioma Cells. *Cell Calcium* (2013) 53:187–94. doi: 10.1016/j.ceca.2012.11.013
92. Ding X, He Z, Zhou K, Cheng J, Yao H, Lu D, et al. Essential Role of TRPC6 Channels in G2/M Phase Transition and Development of Human Glioma. *J Natl Cancer Inst* (2010) 102:1052–68. doi: 10.1093/jnci/djq217
93. Lepannetier S, Zanou N, Yerna X, Emeriau N, Dufour I, Masquelier J, et al. Sphingosine-1-Phosphate-Activated TRPC1 Channel Controls Chemotaxis of Glioblastoma Cells. *Cell Calcium* (2016) 60:373–83. doi: 10.1016/j.ceca.2016.09.002
94. Liu M, Inoue K, Leng T, Guo S, Xiong ZG. TRPM7 Channels Regulate Glioma Stem Cell Through STAT3 and Notch Signaling Pathways. *Cell Signal* (2014) 26:2773–81. doi: 10.1016/j.cellsig.2014.08.020
95. Lathia JD, Gallagher J, Heddleston JM, Wang J, Eyler CE, MacSwords J, et al. Integrin Alpha 6 Regulates Glioblastoma Stem Cells. *Cell Stem Cell* (2010) 6:421–32. doi: 10.1016/j.stem.2010.02.018
96. Dupont S, Morsut L, Aragona M, Enzo E, Giulitti S, Cordenonsi M, et al. Role of YAP/TAZ in Mechanotransduction. *Nature* (2011) 474:179–83. doi: 10.1038/nature10137
97. Elosegui-Artola A, et al. Force Triggers YAP Nuclear Entry by Regulating Transport Across Nuclear Pores. *Cell* (2017) 171:1397–1410 e1314. doi: 10.1016/j.cell.2017.10.008
98. Halder G, Dupont S, Piccolo S. Transduction of Mechanical and Cytoskeletal Cues by YAP and TAZ. *Nat Rev Mol Cell Biol* (2012) 13:591–600. doi: 10.1038/nrm3416
99. Novev JK, Heltberg ML, Jensen MH, Doostmohammadi A. Spatiotemporal Model of Cellular Mechanotransduction *via* Rho and YAP. *Integr Biol (Camb)* (2021) 13:197–209. doi: 10.1093/intbio/zyab012
100. Panciera T, Azzolin L, Cordenonsi M, Piccolo S. Mechanobiology of YAP and TAZ in Physiology and Disease. *Nat Rev Mol Cell Biol* (2017) 18:758–70. doi: 10.1038/nrm.2017.87
101. Totaro A, Panciera T, Piccolo S. YAP/TAZ Upstream Signals and Downstream Responses. *Nat Cell Biol* (2018) 20:888–99. doi: 10.1038/s41556-018-0142-z
102. Zhang Y, Xie P, Wang X, Pan P, Wang Y, Zhang H, et al. YAP Promotes Migration and Invasion of Human Glioma Cells. *J Mol Neurosci* (2018) 64:262–72. doi: 10.1007/s12031-017-1018-6
103. de Semir D, Bezrookove V, Nosrati M, Scanlon KR, Singer E, Judkins J, et al. PHIP Drives Glioblastoma Motility and Invasion by Regulating the Focal Adhesion Complex. *Proc Natl Acad Sci USA* (2020) 117:9064–73. doi: 10.1073/pnas.1914505117
104. Marhuenda E, Fabre C, Zhang C, Martin-Fernandez M, Iskratsch T, Saleh A, et al. Glioma Stem Cells Invasive Phenotype at Optimal Stiffness is Driven by MGAT5 Dependent Mechanosensing. *J Exp Clin Cancer Res* (2021) 40:139. doi: 10.1186/s13046-021-01925-7
105. Sivasankaran B, et al. Tenascin-C is a Novel RBPJkappa-Induced Target Gene for Notch Signaling in Gliomas. *Cancer Res* (2009) 69:458–65. doi: 10.1158/0008-5472.CAN-08-2610
106. Xia S, Lal B, Tung B, Wang S, Goodwin CR, Laterra J, et al. Tumor Microenvironment Tenascin-C Promotes Glioblastoma Invasion and Negatively Regulates Tumor Proliferation. *Neuro Oncol* (2016) 18:507–17. doi: 10.1093/neuonc/nov171
107. Garcion E, Halilagic A, Faissner Affrench-Constant, C. Generation of an Environmental Niche for Neural Stem Cell Development by the Extracellular Matrix Molecule Tenascin C. *Development* (2004) 131:3423–32. doi: 10.1242/dev.01202
108. Sarkar S, Nuttall RK, Liu S, Edwards DR, Yong VW. Tenascin-C Stimulates Glioma Cell Invasion Through Matrix Metalloproteinase-12. *Cancer Res* (2006) 66:11771–80. doi: 10.1158/0008-5472.CAN-05-0470
109. Bir SC, Patra DP, Maiti TK, Sun H, Guthikonda B, Notarianni C, et al. Epidemiology of Adult-Onset Hydrocephalus: Institutional Experience With 2001 Patients. *Neurosurg Focus* (2016) 41:E5. doi: 10.3171/2016.7.FOCUS16188
110. Boucher Y, Baxter LT, Jain RK. Interstitial Pressure Gradients in Tissue-Isolated and Subcutaneous Tumors: Implications for Therapy. *Cancer Res* (1990) 50:4478–84. doi: 10.1158/0008-5472.CAN-05-0470
111. Kingsmore KM, Vaccari A, Abler D, Cui SX, Epstein FH, Rockne RC, et al. MRI Analysis to Map Interstitial Flow in the Brain Tumor Microenvironment. *APL Bioeng* (2018) 2:1–12. doi: 10.1063/1.5023503
112. Mitchell MJ, King MR. Computational and Experimental Models of Cancer Cell Response to Fluid Shear Stress. *Front Oncol* (2013) 3:44. doi: 10.3389/fonc.2013.00044
113. Munson JM. Interstitial Fluid Flow Under the Microscope: Is it a Future Drug Target for High Grade Brain Tumours Such as Glioblastoma? *Expert Opin Ther Targets* (2019) 6:1–13. doi: 10.1080/14728222.2019.1647167
114. Munson JM, Bellamkonda RV, Swartz MA. Interstitial Flow in a 3D Microenvironment Increases Glioma Invasion by a CXCR4-Dependent Mechanism. *Cancer Res* (2013) 73:1536–46. doi: 10.1158/0008-5472.CAN-12-2838
115. Namba N, Chonan Y, Nunokawa T, Sampetrean O, Saya H, Sudo R, et al. Heterogeneous Glioma Cell Invasion Under Interstitial Flow Depending on Their Differentiation Status. *Tissue Eng Part A* (2021) 27:467–78. doi: 10.1089/ten.TEA.2020.0280
116. Qazi H, Shi ZD, Tarbell JM. Fluid Shear Stress Regulates the Invasive Potential of Glioma Cells *via* Modulation of Migratory Activity and Matrix Metalloproteinase Expression. *PloS One* (2011) 6:e20348. doi: 10.1371/journal.pone.0020348
117. Ahn JH, Cho H, Kim J-H, Kim SH, Ham J-S, Park I, et al. Meningeal Lymphatic Vessels at the Skull Base Drain Cerebrospinal Fluid. *Nature* (2019) 572:62–6. doi: 10.1038/s41586-019-1419-5
118. Butcher DT, Alliston T, Weaver VM. A Tense Situation: Forcing Tumour Progression. *Nat Rev Cancer* (2009) 9:108–22. doi: 10.1038/nrc2544
119. DuFort CC, Paszek MJ, Weaver VM. Balancing Forces: Architectural Control of Mechanotransduction. *Nat Rev Mol Cell Biol* (2011) 12:308–19. doi: 10.1038/nrm3112
120. Li W, Mao S, Khan M, Zhang Q, Huang Q, Feng S, et al. Responses of Cellular Adhesion Strength and Stiffness to Fluid Shear Stress During Tumor Cell Rolling Motion. *ACS Sens* (2019) 4:1710–5. doi: 10.1021/acssensors.9b00678
121. Polacheck WJ, Charest JL, Kamm RD. Interstitial Flow Influences Direction of Tumor Cell Migration Through Competing Mechanisms. *Proc Natl Acad Sci USA* (2011) 108:11115–20. doi: 10.1073/pnas.1103581108
122. Netti PA, Roberge S, Boucher Y, Baxter LT, Jain RK. Effect of Transvascular Fluid Exchange on Pressure-Flow Relationship in Tumors: A Proposed Mechanism for Tumor Blood Flow Heterogeneity. *Microvasc Res* (1996) 52:27–46. doi: 10.1006/mvre.1996.0041
123. Rutkowski JM, Swartz MA. A Driving Force for Change: Interstitial Flow as a Morphoregulator. *Trends Cell Biol* (2007) 17:44–50. doi: 10.1016/j.tcb.2006.11.007
124. Boucher Y, Jain RK. Microvascular Pressure is the Principal Driving Force for Interstitial Hypertension in Solid Tumors: Implications for Vascular Collapse. *Cancer Res* (1992) 52:5110–4. doi: 10.1016/j.tcb.2006.11.007
125. Hu X, Deng Q, Ma L, Li Q, Chen Y, Liao Y, et al. Meningeal Lymphatic Vessels Regulate Brain Tumor Drainage and Immunity. *Cell Res* (2020) 30:229–43. doi: 10.1038/s41422-020-0287-8
126. Kanamori M, Kipnis J. Meningeal Lymphatics "Drain" Brain Tumors. *Cell Res* (2020) 30:191–2. doi: 10.1038/s41422-020-0286-9
127. Song E, Mao T, Dong H, Boisserand LSB, Antila S, Bosenberg M, et al. VEGF-C-Driven Lymphatic Drainage Enables Immunosurveillance of Brain Tumours. *Nature* (2020) 577:689–94. doi: 10.1038/s41586-019-1912-x

128. Dafni H, Israely T, Bhujwalla ZM, Benjamin LE, Neeman M. Overexpression of Vascular Endothelial Growth Factor 165 Drives Peritumor Interstitial Convection and Induces Lymphatic Drain: Magnetic Resonance Imaging, Confocal Microscopy, and Histological Tracking of Triple-Labeled Albumin. *Cancer Res* (2002) 62:6731–9. doi: 10.1038/s41586-019-1912-x
129. Louveau A, Herz J, Alme MN, Salvador AF, Dong MQ, Viar KE, et al. CNS Lymphatic Drainage and Neuroinflammation are Regulated by Meningeal Lymphatic Vasculature. *Nat Neurosci* (2018) 21:1380–91. doi: 10.1038/s41593-018-0227-9
130. Bae C, Sachs F, Gottlieb PA. The Mechanosensitive Ion Channel Piezo1 is Inhibited by the Peptide Gsmtx4. *Biochemistry* (2011) 50:6295–300. doi: 10.1021/bi200770q
131. Coste B, Mathur J, Schmidt M, Eraley TJ, Ranade S, Petrus MJ, et al. Piezo1 and Piezo2 are Essential Components of Distinct Mechanically Activated Cation Channels. *Science* (2010) 330:55–60. doi: 10.1126/science.1193270
132. Syeda R, Xu J, Dubin AE, Coste B, Mathur J. Chemical Activation of the Mechanotransduction Channel Piezo1. *Elife* (2015) 4:6295–300. doi: 10.7554/eLife.07369
133. Xiao B. Levering Mechanically Activated Piezo Channels for Potential Pharmacological Intervention. *Annu Rev Pharmacol Toxicol* (2020) 60:195–218. doi: 10.1146/annurev-pharmtox-010919-023703
134. Gnanasambandam R, Ghatak C, Yasmann A, Nishizawa K, Sachs F, Ladokhin AS, et al. GsMTx4: Mechanism of Inhibiting Mechanosensitive Ion Channels. *Biophys J* (2017) 112:31–45. doi: 10.1016/j.bpj.2016.11.013
135. Wang Y, Chi S, Guo H, Li G, Wang L, Zhao Q, et al. A Lever-Like Transduction Pathway for Long-Distance Chemical- and Mechano-Gating of the Mechanosensitive Piezo1 Channel. *Nat Commun* (2018) 9:1300. doi: 10.1038/s41467-018-03570-9
136. Zhao Q, Zhou H, Chi S, Wang Y, Wang J, Geng J, et al. Structure and Mechanogating Mechanism of the Piezo1 Channel. *Nature* (2018) 554:487–92. doi: 10.1038/nature25743
137. Saotome K, Murthy SE, Kefauver JM, Whitwam T, Patapoutian. Structure of the Mechanically Activated Ion Channel Piezo1. *Nature* (2018) 554:481–6. doi: 10.1038/nature25453
138. Hernandez-Caceres MP, Munoz L, Pradenas JM, Pena F, Lagos P, Aceiton P, et al. Mechanobiology of Autophagy: The Unexplored Side of Cancer. *Front Oncol* (2021) 11:632956. doi: 10.3389/fonc.2021.632956
139. Kanzawa T, Germano IM, Komata T, Ito H, Kondo Y, Kondo S. Role of Autophagy in Temozolomide-Induced Cytotoxicity for Malignant Glioma Cells. *Cell Death Differ* (2004) 11:448–57. doi: 10.1038/sj.cdd.4401359
140. Ulasov I, Fares J, Timashev P, Lesniak MS. Editing Cytoprotective Autophagy in Glioma: An Unfulfilled Potential for Therapy. *Trends Mol Med* (2020) 26:252–62. doi: 10.1016/j.molmed.2019.11.001
141. Pavel M, Renna M, Park SJ, Menzies FM, Ricketts T, Füllgrabe J, et al. Contact Inhibition Controls Cell Survival and Proliferation *via* YAP/TAZ-Autophagy Axis. *Nat Commun* (2018) 9:2961. doi: 10.1038/s41467-018-05388-x
142. Jutten B, Keulers TG, Schaaf MBE, Savelkouls K, Theys J, Span PN, et al. EGFR Overexpressing Cells and Tumors are Dependent on Autophagy for Growth and Survival. *Radiother Oncol* (2013) 108:479–83. doi: 10.1016/j.radonc.2013.06.033
143. Totaro A, Zhuang Q, Panciera T, Battilana G, Azzolin L, Brumana G, et al. Cell Phenotypic Plasticity Requires Autophagic Flux Driven by YAP/TAZ Mechanotransduction. *Proc Natl Acad Sci USA* (2019) 116:17848–57. doi: 10.1073/pnas.1908228116
144. Sivakumar H, Strowd R, Skardal A. Exploration of Dynamic Elastic Modulus Changes on Glioblastoma Cell Populations With Aberrant EGFR Expression as a Potential Therapeutic Intervention Using a Tunable Hyaluronic Acid Hydrogel Platform. *Gels* (2017) 3:479–83. doi: 10.3390/gels3030028
145. Lian S, Shi R, Huang X, Hu X, Song S, Bai Y, et al. Artesunate Attenuates Glioma Proliferation, Migration and Invasion by Affecting Cellular Mechanical Properties. *Oncol Rep* (2016) 36:984–90. doi: 10.3892/or.2016.4847
146. Brusatin G, Panciera T, Gandin A, Citron A, Piccolo S. Biomaterials and Engineered Microenvironments to Control YAP/TAZ-Dependent Cell Behaviour. *Nat Mater* (2018) 17:1063–75. doi: 10.1038/s41563-018-0180-8
147. Wolf KJ, Chen J, Coombes J, Aghi MK, Kumar S. Dissecting and Rebuilding the Glioblastoma Microenvironment With Engineered Materials. *Nat Rev Mater* (2019) 4:651–68. doi: 10.1038/s41578-019-0135-y
148. Baruffaldi D, Palmara G, Pirri C, Frascella F. 3d Cell Culture: Recent Development in Materials With Tunable Stiffness. *ACS Appl Bio Materials* (2021) 4:2233–50. doi: 10.1021/acsabm.0c01472
149. Pedron S, Harley BA. Impact of the Biophysical Features of a 3D Gelatin Microenvironment on Glioblastoma Malignancy. *J BioMed Mater Res A* (2013) 101:3404–15. doi: 10.1002/jbm.a.34637
150. Chauhan VP, Martin JD, Liu H, Lacorre DA, Jain SR, Kozin SV, et al. Angiotensin Inhibition Enhances Drug Delivery and Potentiates Chemotherapy by Decompressing Tumour Blood Vessels. *Nat Commun* (2013) 4:2516. doi: 10.1038/ncomms3516
151. Munson JM, Shieh AC. Interstitial Fluid Flow in Cancer: Implications for Disease Progression and Treatment. *Cancer Manag Res* (2014) 6:317–28. doi: 10.2147/CMAR.S65444
152. Sengul E, Elitas M. Single-Cell Mechanophenotyping in Microfluidics to Evaluate Behavior of U87 Glioma Cells. *Micromachines (Basel)* (2020) 11:1–11. doi: 10.3390/mi11090845
153. Jamin Y, Boult JKR, Li J, Popov S, Garteiser P, Ulloa JL, et al. Exploring the Biomechanical Properties of Brain Malignancies and Their Pathologic Determinants *In Vivo* With Magnetic Resonance Elastography. *Cancer Res* (2015) 75:1216–24. doi: 10.1158/0008-5472.CAN-14-1997
154. Tanner K, Boudreau A, Bissell MJ, Kumar S. Dissecting Regional Variations in Stress Fiber Mechanics in Living Cells With Laser Nanosurgery. *Biophys J* (2010) 99:2775–83. doi: 10.1016/j.bpj.2010.08.071
155. Budday S, Ovaert TC, Holzapfel GA, Steinmann P, Kuhl E. Fifty Shades of Brain: A Review on the Mechanical Testing and Modeling of Brain Tissue. *Arch Comput Methods Eng* (2020) 27:1187–230. doi: 10.1007/s11831-019-09352-w
156. Yecies D, Liba O, Zerda A, Grant GA. Intraoperative Imaging Modalities and the Potential Role of Speckle Modulating Optical Coherence Tomography. *Neurosurgery* (2018) 65:74–7. doi: 10.1093/neuros/nyy199
157. Logun M, Zhao W, Mao L, Karumbaiah L. Microfluidics in Malignant Glioma Research and Precision Medicine. *Adv Biosyst* (2018) 2:1187–230. doi: 10.1002/adbi.201700221
158. Garcia CA, Bhargav AG, Brooks M, Suárez-Meade P, Mondal SK, Zarco N, et al. Functional Characterization of Brain Tumor-Initiating Cells and Establishment of GBM Preclinical Models That Incorporate Heterogeneity, Therapy, and Sex Differences. *Mol Cancer Ther* (2021) 65:74–7. doi: 10.1158/1535-7163.MCT-20-0547
159. Lee J, Kay K, Troike K, Ahluwalia MS, Lathia JD. Sex Differences in Glioblastoma Immunotherapy Response. *Neuromolecular Med* (2021) 2:1–43. doi: 10.1007/s12017-021-08659-x
160. Sun T, Plutynski A, Ward S, Rubin JB. An Integrative View on Sex Differences in Brain Tumors. *Cell Mol Life Sci* (2015) 72:3323–42. doi: 10.1007/s00018-015-1930-2
161. Lathia JD. Fountain of Chaos: Cerebrospinal Fluid Enhancement of Cancer Stem Cells in Glioblastoma. *Neuro Oncol* (2021) 23:530–2. doi: 10.1093/neuonc/noab026
162. Lara-Velazquez M, Zarco N, Carrano A, Phillipps J, S Norton E, Schiapparelli P, et al. Alpha 1-Antichymotrypsin Contributes to Stem Cell Characteristics and Enhances Tumorigenicity of Glioblastoma. *Neuro Oncol* (2021) 23:599–610. doi: 10.1093/neuonc/noaa264
163. Rao SS, Bentil S, De Jesus J, Larison J, Hissong A, Dupaix R, et al. Inherent Interfacial Mechanical Gradients in 3D Hydrogels Influence Tumor Cell Behaviors. *PloS One* (2012) 7:e35852. doi: 10.1371/journal.pone.0035852
164. Pedron S, Becka E, Harley BA. Spatially Gradated Hydrogel Platform as a 3D Engineered Tumor Microenvironment. *Adv Mater* (2015) 27:1567–72. doi: 10.1002/adma.201404896
165. Schneider CS, Bhargav AG, Perez JG, Wadajkar AS, Winkles JA, Woodworth GF, et al. Surface Plasmon Resonance as a High Throughput Method to Evaluate Specific and non-Specific Binding of Nanotherapeutics. *J Control Release* (2015) 219:331–44. doi: 10.1016/j.jconrel.2015.09.048
166. Pedron S, Becka E, Harley BA. Regulation of Glioma Cell Phenotype in 3D Matrices by Hyaluronic Acid. *Biomaterials* (2013) 34:7408–17. doi: 10.1016/j.biomaterials.2013.06.024

167. Momin A, Bahrampour S, Min H-K, Chen X, Wang X, Sun Y, et al. Channeling Force in the Brain: Mechanosensitive Ion Channels Choreograph Mechanics and Malignancies. *Trends Pharmacol Sci* (2021) 42:367–84. doi: 10.1016/j.tips.2021.02.006

Conflict of Interest: The authors declare that the research was conducted in the absence of any commercial or financial relationships that could be construed as a potential conflict of interest.

Publisher's Note: All claims expressed in this article are solely those of the authors and do not necessarily represent those of their affiliated organizations, or those of the publisher, the editors and the reviewers. Any product that may be evaluated in this article, or claim that may be made by its manufacturer, is not guaranteed or endorsed by the publisher.

frontiers in Oncology

REVIEW
published: 02 March 2022
doi: 10.3389/fonc.2022.852950

Glioblastoma Microenvironment: From an Inviolable Defense to a Therapeutic Chance

Vincenzo Di Nunno[1†], *Enrico Franceschi*[2*†], *Alicia Tosoni*[2], *Lidia Gatto*[1], *Stefania Bartolini*[2] *and Alba Ariela Brandes*[2†]

[1] Department of Oncology, AUSL Bologna, Bologna, Italy, [2] Nervous System Medical Oncology Department, IRCCS Istituto delle Scienze Neurologiche di Bologna, Bologna, Italy

OPEN ACCESS

Edited by:
Alireza Mansouri,
The Pennsylvania State University (PSU), United States

Reviewed by:
Maksim Sinyuk,
Abeona Therapeutics, United States
Ryota Tamura,
Keio University School of Medicine, Japan

***Correspondence:**
Enrico Franceschi
enricofra@yahoo.it

†ORCID:
Vincenzo Di Nunno
orcid.org/0000-0003-4441-9834
Enrico Franceschi
orcid.org/0000-0001-9332-4677
Alba Ariela Brandes
orcid.org/0000-0002-2503-9089

Specialty section:
This article was submitted to Neuro-Oncology and Neurosurgical Oncology, a section of the journal Frontiers in Oncology

Received: *11 January 2022*
Accepted: *09 February 2022*
Published: *02 March 2022*

Citation:
Di Nunno V, Franceschi E, Tosoni A, Gatto L, Bartolini S and Brandes AA (2022) Glioblastoma Microenvironment: From an Inviolable Defense to a Therapeutic Chance. Front. Oncol. 12:852950. doi: 10.3389/fonc.2022.852950

Glioblastoma is an aggressive tumor and is associated with a dismal prognosis. The availability of few active treatments as well as the inexorable recurrence after surgery are important hallmarks of the disease. The biological behavior of glioblastoma tumor cells reveals a very complex pattern of genomic alterations and is partially responsible for the clinical aggressiveness of this tumor. It has been observed that glioblastoma cells can recruit, manipulate and use other cells including neurons, glial cells, immune cells, and endothelial/stromal cells. The final result of this process is a very tangled net of interactions promoting glioblastoma growth and progression. Nonetheless, recent data are suggesting that the microenvironment can also be a niche in which glioblastoma cells can differentiate into glial cells losing their tumoral phenotype. Here we summarize the known interactions between micro-environment and glioblastoma cells highlighting possible therapeutic implications.

Keywords: microenvironment, glioblastoma, macrophages, neurons, immune-system

INTRODUCTION

The 2021 World Health Organization (WHO) Classification defines glioblastoma (GBM) as a diffuse astrocytic glioma without IDH (Isocitrate dehydrogenase) and H3R gene mutations, with enhanced microvascular proliferation, necrosis, and specific alterations like gain of chromosome 7/chromosome 10 loss, EGFR (Epidermal Growth Factor Receptor) amplification, and/or TERT (Telomerase Reverse Transcriptase) mutations (1, 2).

GBM is one of the most fatal primary central nervous system (CNS) malignancies with an estimated 5-years overall survival (OS) of only 6.8% (3, 4). In particular, the prognosis of patients with newly diagnosed GBM ranged from 12 to 18 months (5) while the recurrent disease is associated with a very poor outcome with an estimated OS of 5-10 months (6).

Several efforts have been spent to improve clinical outcomes of patients with GBM, nonetheless, none of the investigated agents have replaced the standard of care represented by maximal safe surgery followed by chemoradiation and adjuvant temozolomide, which has been adopted in 2005 (4). Even in the management of recurrent GBM, few systemic compounds demonstrated clinical efficacy (6).

There are several reasons behind these failures. First, the enrollment of GBM patients within clinical trials is limited only to10% of all GBM patients (7, 8).

However, the major cause explaining the difficult development of effective agents is certainly the complex biology of the disease. Indeed, GBM is associated with specific features which can be summarized in 1) the extremely high heterogeneity presented by tumor cells requiring combined treatment for different subtypes of GBM cancer cells; 2) the lack of biological models able to replicate or at least estimate the interaction between human tumor cells and the surrounding tissue; 3) the complex microenvironment surrounding the tumor (9–12). Furthermore, the presence of glioblastoma cancer stem cells (CSCs) has been employed to explain the impressive recurrence rate and regenerative proprieties of this tumor (13).

Of note, it has been demonstrated that GBM cells can manipulate the microenvironment surrounding themselves developing a niche sustaining tumor growth and development (14). This process involves immune cells, astrocytes, glial cells, neurons, extra-cellular matrix (ECM), vascular cells, and other cell types (15–20). There are several ways by which GBM can communicate with the surrounding tissue. The secretion of soluble factors able to modulate genomic expression and biological behaviors of tumor-associated cells is one of the most obvious and described systems.

Of interest, GBM cells can develop a nuclear and cytoplasmatic ''continuum'' with neighboring cells. These nanotubes mediate the transfer of protein and inorganic elements (21). Moreover, this also non-secretable molecules such as RNAs, DNA and also mitochondria, and nuclei can be transported from the tumoral to a surrounding cell by these nano-tubules (22–24). Notably, this system is also probably responsible for acquired resistance to radiation and systemic temozolomide (TMZ) (23).

GBM cells can also promote the creation of gap junction and cytoplasmatic connections (15–20). Finally, the secretion of microvesicles, extracellular vesicles, and exosomes can promote communication with also very distant cells or tissues (15–20).

The interactions between tumor cells and immune cells have acquired an increased interest due to the availability of agents able to promote immune-system reactivation. Nonetheless, other interactions have been only partially investigated and could hide novel promising targets for tumor treatment. Here we performed a review summarizing the identified interactions between GBM and its associated microenvironment. We also focused our attention on possible novel treatments targeting these complex interactions.

IMMUNE CELLS AND GLIOBLASTOMA

Immune-contexture assumes a very important role within the GBM microenvironment. It can stimulate the progression and development of tumor cells (25).

In contrast to what was supposed in the past, it has been largely demonstrated that glioblastoma is not an immune ''cold tumor'' (26, 27). Similar to other tissue, the CNS has its resident immune tissue represented mainly from microglia (28). Furthermore, like other solid tumors, GBM can activate and recall migrating immune cells from systemic tissues and lymphatic vessels (28). Indeed, there is a connection between deep cervical nodes, dural sinus, and lymphatic vessels allowing systemic immune cells to move into the CNS reaching the target site (29, 30). CNS is regulated by several molecular mechanisms able to enhance or suppress the immune response. However, the main difference with other peripheral non-CNS tissues is that the balance between inhibitory and stimulating mechanisms is biased in favor of immune suppression (31–35). One of the most important factors mediating an immune-inhibition is the TGFβ2 (transforming growth factor β2) (36, 37). This factor can mediate inhibition of Interleukin 2 mediated T cell survival and reduce the production of critical effector proteins by lymphocytes and other immune cells (36, 37). An increased intracranial pressure, such as that observed during an inflammation response, could be catastrophic and associated with irreparable damage to the neurological tissues. Thus, CNS protects itself preventing prolonged immune response with activation of several mechanisms supporting an immune-depressive status (31–35).

Recently, two transcription factors showed to mediate several immune-depressive effects in GBM (38). These factors are represented by SRY-Box Transcription Factor 2 (Sox2) and octamer-binding transcription factor 4 (Oct4) whose activation promotes the suppression of both innate and adaptive immune responses maintaining glioma cell stemness and tumor-propagating potential (38). In particular, the co-expression of Oct4/Sox2 inhibits the expression of CCL5 (C-C Motif Chemokine Ligand 5), CXCL9 (C-X-C Motif Chemokine Ligand 9), CXCL10, and CXCL11 which are essential to induce lymphocyte CD8 effector (Th1 response) attraction (38). Furthermore, they promote the secretion of SPP (signal peptide peptidase), IL8 (Interleukin 8), CXCL5, CCL20, IL6 (interleukin 6) inducing Treg (immune-inhibitory) response and shifting macrophage differentiation toward an immune-regulatory profile more than an immune-active one (38). Several immune checkpoints such as PD-L1 (Programmed Death Receptor Ligand 1), CD70 (Cluster of differentiation 70), A2aR (adenosine A2A receptor), and TDO (Tryptophan 2,3-dioxygenase) are also overexpressed in cells with Sox2/Oct4 overexpression (38). The effects promoted by Sox2/Oct4 are directly mediated by overexpression of the BRD3 (Bromodomain containing protein 3) and BRD4 (Bromodomain containing protein 4) proteins which belong to the Bromodomain and extra terminal motif (BET) proteins family. The BRD3 and BRD4 proteins act modulating the activity of the histone 3 (H3) acetylation mediated by the H3K27Ac enzyme. This mechanism appears of particular interest considering the availability of pan BET inhibitors.

Another recent research investigated RNA expression of GBM-derived sphere-line treated with the BET inhibitor JQ1. The inhibition of BET resulted in a significant modulation of genes responding to Interferon-alpha (enhanced in about 50% of GBM) through a direct transcriptional inhibition more than interference to the JAK (Janus Kinase) -STAT (Signal transducer and activator of transcription) pathway (39).

BET inhibitors have recently been assessed on phase I clinical studies and further trials assessing their clinical efficacy are needed (40–47).

In conclusion, differently from other tissues, CNS physiologically employs signals able to reduce an immune innate and adaptive response. This happened to prevent catastrophic effects associated with an uncontrolled inflammation in a dedicated system such as the brain or the spinal cord. In this context, GBM cells adopt several mechanisms to reinforce this inhibition. Glioblastoma stem cells (GSCs) are probably an important component of this complex mechanism as they express important transcription factors such as Sox2 and Oct4 (38). Nonetheless, it is also likely that other pathways converge on the same inhibition suggesting that the inhibition of a singular cascade could not be associated with an effective immune response reactivation.

GBM – Microglia, Myeloid Cells, and Macrophages

Immune resident cells of the CNS are microglia and macrophages including perivascular, meningeal, choroid plexus, and circumventricular macrophages (28). These cells cover over 50% of the GBM tumor load and their composition change during the time and tumor progression (48). In the early phases of GBM development, the microglia is the most represented infiltrating cell subtype while macrophages and myeloid cells composed a large part of GBM volume in advanced phases (49, 50). Differently from macrophages, microglia constitute the resident immune system of the CNS. These cells can move within the CNS but they do not circulate in other tissues. Both microglia and macrophages are ineffective against tumors as their immune response is suppressed by the presence of an immune-depressive cytokines storm (11, 51). Indeed, GBM cells can directly mediate the production of several immune-depressive cytokines. Furthermore, cancer cells can manipulate the secretion and phenotype of surrounding immune cells shifting their phenotype toward an immune-suppressive one and initiating positive feedback leading to an immune-suppressive contexture. Notably, macrophages and myeloid cells are important protagonists of this process.

Myeloid cells constitute a large part of the immune-contexture of GBM. These cells are recruited directly from tumors cells and then can differentiate toward macrophages and monocyte phenotypes (52).

Myeloid cells have been classified into monocytic and granulocytic subtypes. Both these cells inhibit T cell and NK activities. Curiously, some data seem to confirm a negative prognostic role of these cells in males while these same cells can positively activate an immune response in female patients (52).

The main stimulation for macrophages and microglia accrual around the tumor is mediated by the same glioblastoma cells through the production of CCL2 (C-C Motif Chemokine Ligand 2), CCL7 (C-C Motif Chemokine Ligand 7), GDNF (Glial Cell-Derived Neurotrophic Factor), SDF1 (stromal cell-derived factor 1), TNF (tumor necrosis factor), VEGF (vascular endothelial growth factor), ATP (adenosine triphosphate), CSF-1 (Colony-stimulating factor 1), GM-CSF (Granulocyte-Macrophage Colony-Stimulating Factor), and expression of OLIG2 (Oligodendrocyte transcription factor 2) (48, 51, 53). Macrophages and microglia can perpetuate themselves accrual through the production of CCL2 resulting in a positive feedback loop (53). In advanced phases, microglia are localized mainly around tumor tissue while macrophages are localized in perivascular regions (54).

The differentiation of macrophages ranges from two specific phenotypes which are: M1 (immune-response enhancer) or M2 (immune-regulator inhibiting immune response) (55, 56). Although explicative, this classification is not definitive as macrophages can reach an intermediate grade of differentiation activating both genes of the M1 and M2 subtypes (57). In GBM, the resulting phenotype can inhibit immune response through secretion of transforming growth factor β1 (TGFβ1), arginase 1 (ARG1), or interleukin 10 (IL-10) enhancing neo-angiogenesis through VEGF production and extracellular matrix modeling by metalloproteases (MP) (38). On the other hand, these macrophages also produce pro-inflammatory molecules such as IL-β1 (interleukin β1), TNF, IL-5 (interleukin 5), and IL-12 (interleukin 12) which are molecules stimulating the immune response (38).

It has been demonstrated that macrophages promote GBM growth and progression in different ways (11).

First, the macrophage tumor suppression phenotype inhibits the response of other immune cells surrounding the tumor. This immune inhibition is mainly explicated by myeloid cells and differentiated macrophages which miss the activation of natural killer (NK) cells, the production of interferon γ (INF γ) and TGFβ (55). These same cells can induce lymphocytes differentiation toward an immune-regulatory (Th2) profile by TGFβ, reactive oxygen species (ROS), cysteine depletion, L-selectin downregulation, ARG1, and inducible nitric oxide synthase (iNOS2) production (36, 37).

The remodeling of ECM is essential for tumor migration and is mediated by the production of inactive metalloproteases enzymes by GBM cells (48, 58). These pro-Metalloproteases are then activated by enzymes produced by microglia. Moreover, the production of CSF1 by glioblastoma induces the release of the insulin-like growth factor-binding protein 1 (IGFBP1) by microglia which Is essential to promote vascularization and angiogenesis (48, 58, 59).

The administration of macrophages able to restore immune response would be a promising strategy able to partially restore immune-response against the tumor. The development of engineered macrophages (car-M) is at an early stage of assessment but it could be a promising strategy for GBM treatment (60).

Similar to macrophages and microglia also neutrophils and other innate immune cells are attracted by the tumor. In particular, inflammatory factors secreted after a surgical intervention such as IL-8, TNF, and CCL2 can promote neutrophil infiltration in addition to SDF1 and plasminogen activator inhibitor 1 secreted by tumor cells (61, 62). These innate immune cells can facilitate further accrual of macrophages and contribute to microenvironment remodeling.

Lymphocytes and Antigen-Presenting Cells

Antigens exposure can start an adaptive immune response in the CNS like observed in other organs.

The presence of lymphocytes surrounding the tumor has been largely reported in GBM where their concentration correlates positively with survival (63, 64).

When an antigen is recognized by the immune system, a specific lymphocyte clone targeting the same antigen expands itself starting an adaptive immune response. The antigen-presenting cells (APCs) are essential to start the clonal expansion as these cells mediate the presentation of the antigen to the lymphocytes initiating the immune response (29, 30). Antigens captured within the CNS are processed by APC and then presented to lymphocytes probably in deep cervical nodes. Activated lymphocytes can move into the brain directly thanks to the increased permeability resulting from inflammation and neo-vessels or after exposure to antigen by APCs on the meningeal surface (29, 30).

Even if lymphocytes can move around GBM mass their ability to start an immune response against tumor is strongly inhibited by several factors. Once lymphocytes come to the peritumoral tissue they are invested by strong immune-depressive signaling mediated tumor cells and GBM associated microenvironment. The TGFβ1 and TGFβ2 molecules are the main characters for this inhibition (11, 37, 65).

It is important to observe that immune-inhibitory signals are largely provided by the microenvironment more than directly by GBM cells. This is a concrete example of how GBM cells manipulate the microenvironment to sustain their growth and expansion (11). Notably, it has been reported that GBM cells can induce pericytes to produce TGFβ and IL-10 (an inhibitory interleukin) (66).

GBM cells can also release directly inhibitory signals such Fas antigen ligand (FASLG), and other inhibitory molecules. Lymphocytes assume the classical exhaustion phenotype expressing several-inhibitory receptors including the PD-1, T cell membrane protein 3 (TIM3), lymphocyte activation gene 3 protein (LAG3), and T cell immunoreceptor with immunoglobulin and ITIM domains (TIGIT) (67).

As already specified, it is interesting to observe that a large part of inhibitory molecules released by GBM cells can be mediated by the Sox2/Oct4 (38).

The complex network of immune-inhibitory signals can partially explain the failure of clinical trials exploring immune-checkpoint inhibitors (ICIs). To date, three different phases III trials failed to show a clinical benefit from the addition of nivolumab in newly diagnosed and recurrent GBM (68–70).

In the last years, a novel immune strategy employing engineered T-cells (car-T) has been investigated with favorable preliminary results. In GBM the introduction of reprogrammed T-cells could be ineffective due to the immune shield provided by the tumor microenvironment (70). Strategies aimed to switch the composition of cancer-associated immune cells from an immune-suppressive to an immune-active one are of critical importance. Combinatory strategies employing more immune targets are under investigation (70).

NEURONS AND GLIOBLASTOMA

The brain is composed of over 60% of the white matter which is largely composed of myelinic axons. Neurons, astrocytes, and oligodendrocytes with other glial cells (including microglia) are the most represented cells in the brain and CNS (71).

The study of the interactions between these components and glioblastoma appears of extreme interest as these are strictly related to some of the most important biological and clinical features of GBM cells.

Indeed, connexons between white matter, neurons, and tumors can partially explain the high recurrence rate of the disease as well as the ability to relapse also in a distant site such as the contralateral hemisphere (71–74). Of interest, the interaction between neurons and GBCs assumes a particular interest in recent years.

Indeed, the biological niche composed of GBM cells, GSCs, peritumoral oligodendrocytes, astrocytes, and also neuronal axons can both drive differentiation of a GSCs cell toward a tumoral phenotype or, surprisingly, toward a differentiated non-tumoral cell subtype (75). On the other hand, also GBM cells can induce the dedifferentiation of astrocytic cells while astrocytes and oligodendrocytes can support tumor growth in different ways. In particular, astrocytes can support tumor growth and development through the secretion of several cytokines and other soluble factors stimulating directly GBM growth and maintaining an immune-suppressive contexture (76, 77).

Astrocytes

Tumor-associated astrocytes (TAAs) can contribute to GBM growth in different ways. During early phases of tumor development, TAAs respond to initial injury with the secretion of TGFβ, IL-6, and Insulin growth factor 1 (IGF-1) which could contribute to GBM sustainment (76, 77). These same TAAs express the sonic hedgehog (SHH) gene and are concentrated in the perivascular niche of GBM (78–80). In early and advanced phases communications between GBM and TAAs occurred especially through the secretion of extracellular vesicles which contribute to stimulating several growth factors by TAAs (81). These include the vascular endothelial growth factor (VEGF), fibroblast growth factor (FGF), hepatocyte growth factor (HGF), and epidermal growth factor (EGF) (81).

The contribution of TAAs is of key importance as these cells can stimulate neo-angiogenesis through secretion of VEGF and hypoxia-inducible factor -1 (HIF-1) (82, 83).

Of interest, it has been demonstrated that astrocytes actively participate in chemotherapy resistance by GBM (84). The exact mechanism by which this is possible is still unclear but *in vitro* studies identified that chemoprotection performed by TAAs is possible only when these cells are connected to cancer cells by gap junctions. Indeed, apoptosis and GBM cells death increased when the development of gap junctions was inhibited by the administration of carbenoxolone (a gap junctions communication inhibitor) (84).

One of the most surprising behaviors of astrocytes is the capacity to be transformed in tumor-initiating cells. *In vivo* studies demonstrated that several oncogenes including MYC,

RAS, and EGFR variant III can dedifferentiate astrocytes in tumoral cells (85, 86). This close relationship suggests a common phenotype shared by GBM and astrocyte supporting the hypothesis that astrocytes are the precursor normal cells by which gliomas originate. It is still unknown the exact mechanism, but it has been observed that glioma cells inhibit the expression of the onco-suppressor p53 in normal astrocytes (87, 88). The malignant transformation of astrocytes required the miR-10b which is silenced in TAAs but is largely expressed and secreted by GBM cells using extracellular vesicles (89).

Although the already cited oncogene (MYC, RAS, and EGFR) can mediate the transformation of astrocyte into malignant glioma cells it is still unclear the exact mechanism by which GBM cells can initiate this process in humans (85, 86). However, the manipulation and conversion of surrounding astrocytes into neoplastic cells can be another issue explaining the well-known recurrence and regeneration proprieties of this tumor

Neurons

Neurons can be manipulated by glioma cells to stimulate tumor progression and invasion. One of the first documented interactions between neurons and GBM is associated with the release of glutamate which could be enhanced in patients with GBM resulting in seizure onset and increased vascular permeability mediated by the N-methyl-D-aspartate receptors (NMDA) (90, 91). Of interest, synapsing signaling of cortical neurons can directly stimulate GBM growth. Neurons and oligodendrocyte precursor cells can secrete the postsynaptic adhesion molecule neuroligin 3 which mediated the activation of several key pathways including the mammalian target of rapamycin (mTOR), phosphoinositide-3-kinase (PI3K), and focal adhesion kinase (FAK) (92). Also, the brain-derived neurotrophic factor chaperone Bip (HSPA5) has been identified as an agent able to stimulate mitosis and cell division (92).

Oligodendrocytes and White Matter

Oligodendrocytes may absolve an inhibitory function against GBM cells. Indeed, these cells can activate the WNT inhibitory factor 1 leading to the inhibition of GBM growth and proliferation (93, 94). In CNS, Oligodendrocytes modulate neural plasticity, metabolic support, and axon activity through myelination. It is well known that GBM can spread through myelinic axons (75). The butterfly shape commonly observed in GBM indicates that tumor cells can invade the contralateral side following the commissure fibers of the corpus callosum (75). Similarly, GBM can spread through the arcuate fasciculus and using the radiation of the corpus callosum (75). It has been supposed that GBM cells adopted myelinated axons as scaffolds and tracks however a recently published study could drastically modify this concept (75). Glioblastoma stem cells are contained in a specific biological niche composed of their microenvironment which influences GSCs fate and differentiation. It is easy to think that GSCs differentiate into cancer cells but it is not always true as in some conditions these cells can differentiate into normal cells without tumorigenicity. It seems that a biological niche composed of white matter can induce GSCs to differentiate toward a pre-oligodendrocyte phenotype losing oncogenic potential (75). This mechanism is similar to that happening during the response to injury (75). Thus, this is an important discovery demonstrating that GSCs can differentiate toward a normal cell phenotype.

The mechanism by which this happens involves the white matter destruction which leads to upregulation of the SOX10 transcription factor. The SOX10 mediates oligodendrocyte differentiation also by cancer cells (75).

Further investigation of this pathway will probably provide new therapeutic insights for the clinical management of GBM.

CANCER STEM CELLS

Glioblastoma stem cells explain the extreme clinical aggressiveness of GBM. In GSCs are associated with the high recurrence rate of the tumor even after complete resection (72). These cells are also associated with tumor renewal and resistance to treatment (73). Finally, the ability to spread and relapse in a distant site of the brain such as the contralateral hemisphere could be partially explained by GSCs an interaction between tumors and neurons (71–74). As already discussed, the differentiation of GSCs could be shifted toward a tumoral or non-tumoral phenotype according to the biological niche in which these cells are located (75).

Glioblastoma stem cells are localized in a specific niche localized in the perivascular and hypoxic regions of the tumor. These cells are similar to normal neural stem cells (NSCs) which are localized mainly in the subventricular zone of the brain which is a common site of origin for glioblastoma (95–97).

It is still unclear if GSCs derived from altered NSCs or mutated glioma cells (98). Glioblastoma Stem Cells are surely associated with GBM progression and recurrence after surgery (99, 100). The surface marker CD133 is one of the most adopted markers to recognize GSCs.

The expression of CD133 is regulated by Sox2 and agents targeting or interfering with this transcription factor can reduce tumor-initiating ability, resistance to chemotherapy, and recurrence (101). Nestin is another upregulated factor reported on GSCs that is directly correlated with poorer survival (98) (102).

Notably, the specific position of GSCs leads to an interaction with Endothelial cells (ECs) and pericytes. It has been supposed that GSCs directly respond to hypoxia stimulating vessels creation and neo-angiogenesis through the production of VEGF (103, 104). Moreover, GSCs can differentiate into ECs and pericytes (103–105). The most surprising finding related to GSCs is that these cells can be located at a distance of up to 3 cm from the primary tumor (106). Moreover, their histological identification is almost impossible as these cells are indistinguishable from normal tissue cells (72). Nonetheless, some studies suggest that GSCs derived from the GBM core are different from those isolated by peritumoral tissue presenting different behaviors in terms of proliferative potential and expression of stem-cell markers (72, 107, 108). Even if peritumoral GSCs are less aggressive compared to GSCs from the core of GBM these same cells are also more resistant to temozolomide and radiation therapy (72, 107, 108). As

discussed in a previous paragraph, the transcription factors Sox2 and Oct4 are activated in GSCs promoting glioma cell stemness and stimulating several mechanisms leading to innate and adaptive immune response inhibition (38). Curiously, recent data suggest a strong interaction between glioblastoma cancer cells and GSCs (109). This is mainly mediated by the cascade activated by the brain-derived neurotrophic factor (BDNF) secreted by GBM cells and the receptor neurotrophic receptor tyrosine kinase 2 (NTRK2) localized on stem cells. This interaction leads to a paracrine effect resulting in tumor growth and development (109).

ENDOTHELIAL CELLS

Neovascularization and new vessels development are both hallmarks of GBM. The fast growth of the tumor mass required high blood intake thus there are several identified pathways by which GBM cells can interact and manipulate ECs activity (110).

Hypoxia is one of the most important stimulations for tumor growth, vessels development, and acquisition of more aggressive pathological features by tumor cells (111–113). In general, hypoxia leads to a metabolic switch by tumor cells which are more likely to promote aerobic glycolysis. Hypoxia induces also an attenuated expression of DNA repair enzymes and impedes the formation of Reactive Oxygen Species (ROS) reducing the cytotoxic effect of radiation therapy (111–113).

Notably, ROS can assume a different biological role according to their concentration. Low levels of ROS are associated with stimulation of hormone secretion, synaptic plasticity, and immune response (114, 115). High levels of ROS are instead associated with DNA damage and in particular p53 damage (116). The DNA damage promoted by ROS could partially explain the switch from low to high-grade gliomas (117). The NADPH oxidase (NOX) 4 is activated by PDGF and TGF-β and is a key enzyme associated with ROS production (H2O2) (118). The inhibition of this enzyme could be a promising target in patients with GBM.

One of the most established pathways for new vessels development is the recruitment of EC progenitors by the bone marrow. This is a process occurring during embryogenesis or after an ischemic insult which is also adopted by GBM cells (119, 120). Tumor cells or microenvironments manipulated by GBM cells can secrete the SDF-1 which is the ligand of the CXCR4 receptor expressed by EC progenitors (121, 122). The interaction between SDF-1/CXCR-4 resulted in EC activation and recruitment of novel EC (121, 122).

It has been well established that GBM cells and the surrounding microenvironment can stimulate the production of the VEGF. This factor can drive EC toward the development of novel vessels in a process known as sprouting angiogenesis. Notably, the neoangiogenic promotion carried out by VEGF can be inhibited by the interaction between the Notch receptor and Delta-like canonical Notch ligand 4 (DLL4) (123). Curiously, novel vessels development can originate also through a process known as vasculogenic mimicry (124–126). This phenomenon is mediated by the same tumor cells which can differentiate to create a vessels-like structure. In particular, macrophages surrounding tumors can mediate cyclooxygenase-2 (COX-2) activation stimulating vasculogenic mimicry (127). Other supposed mechanisms involved in this pathway are the expression of VE-Cadherin by GBM stem cells resulting from hypoxia and the HIF 1 and HIF 2 secretion. Also, the mTOR expression seems to be involved in this pathway (128).

Vascular co-option is another mechanism by which tumor cells move around pre-existing vessels gaining the access to oxygen and nutrients. Curiously GBM cells can induce secretion of bradykinin by EC cells. Bradykinin plays a chemotaxis effect on GBM cells (129, 130). The interaction between SDF1/CXCR4 (129, 130) and the expression of the EGFRvIII are also involved in this mechanism (129–131).

A well-described mechanism associated with neo-angiogenesis is the interaction between VEGF and VEGFR2 and VEGFR1 (132). The interaction between VEGF and VEGFR1 or VEGFR2 induces the phosphorylation and activation of the ERK 1/2 (extracellular signal-regulated kinases 1 and 2) and p38 MAPK (mitogen-activated protein kinase) which together mediated transcription of pro-angiogenic factors (132).

This interaction also results in blood vessels permeability, and proteins lost from blood (110) explaining an increased permeability, edema onset, and increased intracranial pressure. This can explain the clinical benefit experienced by patients treated with the anti-VEGF agent bevacizumab (133–136). Even if the administration of bevacizumab is associated with reduced edema and vascularization within tumor masses it failed to show a significant survival benefit among patients with GBM (133–136).

The lack of the survival benefit observed could reflect the co-existence of several mechanisms resulting in angiogenesis and vessels development. In this optic, the inhibition of the VEGF mediated by bevacizumab can activate or reinforce other molecular pathways converging on angiogenesis promotion resulting in resistance to the anti-VEGF.

The study of the interactions between immune cells in tumor-associated microenvironment assumes an increased interest (137). Increasing data seem to indicate that hypoxia induces secretion of the VEGF which is one of the main molecules mediating this signaling. In particular Regulatory T lymphocytes (T reg) mediate the production of IL-10, IL-4, and IL-13 inducing differentiation of macrophages into M2 phenotype and stimulating expression of inhibitory B7-H receptor on their membranes (137).

Thus, the inhibition of VEGF could also result in an enhanced immune response against the tumor. This supposed synergic effect has led to the assessment of combination strategies in the clinical setting. Unfortunately, a phase II study assessing the combination between bevacizumab and pembrolizumab (a PD-1 inhibitor) failed to show a significant clinical efficacy on patients with GBM (138).

TARGETING THE MICROENVIRONMENT IN GLIOBLASTOMA

There are very few systemic agents showing clinical efficacy in patients with glioblastoma (139–142). As already discussed in

previous paragraphs, a great interest in the immune contexture of GBM is explained by the availability of active compounds able to restore immune response against tumors. Nonetheless, immune-checkpoint inhibitors failed to improve the survival of patients with GBM (68). The reason for this failure can be partially explained by the lack of uniformly expressed tumor-specific antigen due to the high heterogeneity of tumor GBM cells as well as the presence of an immune-depressive microenvironment which impairs the ability of immunotherapy to work. Also, GSCs can mediate immune escape (38).

Novel combination strategies are under investigation to overcome these limitations.

For example, it has been demonstrated that other immune checkpoints co-exist with PD-1. These are the indoleamine 2,3-dioxygenase (IDO1), T cell immunoglobulin-mucin-domain containing-3 (TIM-3), and lymphocyte activation gene 3 (LAG3) (143). Novel trials exploring combinations between PD-1 and LAG3 (NCT02658981) or IDO1 (NCT03707457) are under investigation. Similarly, the combination between temozolomide and IDO1 inhibitors is under investigation (NCT02052648).

Previous trials investigating neoantigen vaccination showed that vaccines can induce a significant increase of tumors infiltrating lymphocytes (144). Unfortunately, these infiltrating lymphocytes assume an exhausted phenotype. Thus the co-administration of multi-epitope vaccines and immune-checkpoint inhibitors could be another promising approach (NCT02149225 GAPVAC trial) (144). Strategies assessing co-administration of vaccines and CAR-T engineered with EGFRvIII and PD-1 are also under investigation (NCT04003649, NCT04201873, NCT02529072, NCT02287428) (145–147). Also, the administration of co-stimulatory agonists able to enhance T cell function is under investigation. Agonists such as CD27, 4-1BB, OX40 or CD40 are under investigation (NCT04547777, NCT02658981, NCT03688178, NCT04440943) (145–147).

Since macrophages are strongly associated with the development of an immune-depressive microenvironment the possibility to develop an engineered cell type of macrophage could be a promising strategy allowing a microenvironment to switch toward an immune-active phenotype (60). This Car-M strategy is still under early assessment however this appears a very promising approach.

As already specified SOX2 and Oct4 are two transcription factors able to modulate a very large amount of genes involved in the immune response. These two factors act through proteins belonging to the BET family. To date, BET inhibitors have been assessed on phase I trials with more of them showing a safety profile (39–47). A further investigation of these agents could be important for patients with GBM.

The inhibition of the CSF1 receptor can inhibit the interaction between GBM and cells of the immune innate system including tumor-associated macrophages. Studies on murine models showed that macrophages develop resistance to CSF1 inhibition through the expression of the insulin growth factor 1 (148). The co-administration of CSF1 and IGF1 inhibitors could be an interesting approach as associated to restored immune-active microenvironment resulting from macrophages activation (148).

In the last years, several agents targeting angiogenesis have been tested in GBM without significant results. The only FDA-approved drug is bevacizumab which has been associated with prolonged progression-free survival, a reduction of symptoms related to the tumor but failed to show a significant impact on overall survival (133–136). Several efforts are spent to understand the reason for bevacizumab resistance. The very high hypoxia level described inside the tumor can partially explain this failure. Indeed, hypoxia is associated with upregulation of the hypoxia-inducible protein 2 (HIG2) gene with downregulation of the CYLD gene expression. The overexpression of HIG2 resulted in HIF-1β, VEGF expression, and bevacizumab resistance through direct stimulation of hypoxia-inducible factor. Nonetheless, agents targeting HIG2 products failed to improve the clinical outcomes of patients with GBM (149). Novel approaches are aimed to target the angiotensin II receptors (AngII-R) and VEGF (150). However, this approach has been evaluated only in murine models thus assessments on humans are necessary to further assess this approach.

Since GBM cells adopt extracellular vesicles to communicate with surrounding tissue, a system able to reduce vesicles uptake and synthesis can be a promising target. Pre-clinical studies showed that inhibitors of neutral sphingomyelinase (GW4869) can reduce the production of extracellular vesicles while heparin and annexin A1 inhibitors can reduce vesicles intake by target cells (151–153).

Direct inhibition of junctions between GBM and microenvironment is also a strategy under investigation. Inhibition of connexin 43 is essential to inhibit the interaction between GBM and astrocytes (154). Another interaction between oligodendrocytes, astrocytes, and GBM cells is the interaction between neuroligin 3/ADAM10 (155). Indeed, GBM cells produce neuroligin 3 which is cleaved from the ADAM10 secreted by neurons and oligodendrocytes (156). The effect is a stimulation of GBM growth and development (11). Thus inhibitors of the ADAM10 appear a promising strategy for GBM which should be further assessed among clinical trials in humans.

CONCLUSION

GBM remains a fatal disease with limited treatments. The reason for this failure could be partially explained by the development of a complex and effective net of interactions between tumor cells and surrounding tissue cells. The microenvironment resulting from the manipulation carried out by cancer cells can feed and stimulate GBM proliferation hiding and protecting tumor cells from systemic treatments.

Interactions between tumor, endothelial and immune cells are under careful assessment due to the availability of drugs targeting these pathways. Recently, also the associations between glioblastoma and astrocytes, oligodendrocytes, white matter, and neurons come out from the shadow offering novel promising targets with therapeutic implications.

Due to the presence of deep communications between tumor cells and the microenvironment the use of agents targeting more than one altered intracellular cascade at the same time appears a promising approach.

In this optic novel immune-combination including immune checkpoint inhibitors) targeting PD-1/PD-L1, IDO1, TIM3, LAG3), engineered immune cells (CAR-T and CAR M), immune agonists (targeting OX40, CD27,4-1BB, CD40), and BET inhibitors are under investigation. Notably, tumor-associated macrophages are one of the most important cell-associated with the development of an immune-depressive habitat. Thus, a strategy able to reverse this effect such as CAR M assumes a particular interest.

Strategies aimed to inhibit the signaling between GBM cells and the microenvironment are also of key importance as able to inhibit the manipulation carried out by tumor cells on surrounding tissues. Inhibitors of sphingomyelinase, annexin A1 can act on extracellular vesicles secretion and intake while other agents such as ADAM10 inhibitors could directly interfere with the jap junctions connecting GBM to other cells.

Finally, it should be noted that a specific microenvironment composition (such as that described on the white matter) can promote GBM differentiation and convert a tumor cell into an oligodendrocyte well-differentiated element. This surprising finding suggests that there are some elements inside the microenvironment that can provide inhibitory messages to GBM reversing its natural course. Interactions between neurons and glia (especially oligodendrocyte) appear of particular interest and should be further assessed as could hide important targets for novel drugs development. In conclusion, GBM should be considered as a network of interactions in which an action perpetuates against tumor cells result in a response of the associated microenvironment and vice versa. The role of the microenvironment should be always considered during pre-clinical studies and would offer novel targets for patients with GBM.

AUTHOR CONTRIBUTIONS

VN and LG: writing and draft. EF, AB, AT, and SB: project conception and reviewing. All authors contributed to the article and approved the submitted version.

REFERENCES

1. Louis DN, Perry A, Wesseling P, Brat DJ, Cree IA, Figarella-Branger D, et al. The 2021 WHO Classification of Tumors of the Central Nervous System: A Summary. *Neuro Oncol* (2021) 23(8):1231–51. doi: 10.1093/neuonc/noab106
2. Weller M, van den Bent M, Preusser M, Le Rhun E, Tonn JC, Minniti G, et al. EANO Guidelines on the Diagnosis and Treatment of Diffuse Gliomas of Adulthood. *Nat Rev Clin Oncol* (2021) 18(3):170–86. doi: 10.1038/s41571-020-00447-z
3. Stupp R, Hegi ME, Mason WP, van den Bent MJ, Taphoorn MJ, Janzer RC, et al. Effects of Radiotherapy With Concomitant and Adjuvant Temozolomide Versus Radiotherapy Alone on Survival in Glioblastoma in a Randomised Phase III Study: 5-Year Analysis of the EORTC-NCIC Trial. *Lancet Oncol* (2009) 10(5):459–66. doi: 10.1016/s1470-2045(09)70025-7
4. Stupp R, Mason WP, van den Bent MJ, Weller M, Fisher B, Taphoorn MJ, et al. Radiotherapy Plus Concomitant and Adjuvant Temozolomide for Glioblastoma. *N Engl J Med* (2005) 352(10):987–96. doi: 10.1056/NEJMoa043330
5. Brandes AA, Franceschi E, Paccapelo A, Tallini G, De Biase D, Ghimenton C, et al. Role of MGMT Methylation Status at Time of Diagnosis and Recurrence for Patients With Glioblastoma: Clinical Implications. *Oncologist* (2017) 22(4):432–7. doi: 10.1634/theoncologist.2016-0254
6. Di Nunno V, Franceschi E, Tosoni A, Di Battista M, Gatto L, Lamperini C, et al. Treatment of Recurrent Glioblastoma: State-of-the-Art and Future Perspectives. *Expert Rev Anticancer Ther* (2020) 20(9):785–95. doi: 10.1080/14737140.2020.1807949
7. Di Nunno V, Franceschi E, Tosoni A, Gatto L, Lodi R, Bartolini S, et al. Glioblastoma: Emerging Treatments and Novel Trial Designs. *Cancers (Basel)* (2021) 13(15). doi: 10.3390/cancers13153750
8. Vanderbeek AM, Rahman R, Fell G, Ventz S, Chen T, Redd R, et al. The Clinical Trials Landscape for Glioblastoma: Is it Adequate to Develop New Treatments? *Neuro Oncol* (2018) 20(8):1034–43. doi: 10.1093/neuonc/noy027
9. McLendon R, Friedman A, Bigner D, Van Meir EG, Brat DJ, Mastrogianakis GM. Comprehensive Genomic Characterization Defines Human Glioblastoma Genes and Core Pathways. *Nature* (2008) 455(7216):1061–8. doi: 10.1038/nature07385
10. Brennan CW, Verhaak RG, McKenna A, Campos B, Noushmehr H, Salama SR, et al. The Somatic Genomic Landscape of Glioblastoma. *Cell* (2013) 155(2):462–77. doi: 10.1016/j.cell.2013.09.034
11. Broekman ML, Maas SLN, Abels ER, Mempel TR, Krichevsky AM, Breakefield XO. Multidimensional Communication in the Microenvirons of Glioblastoma. *Nat Rev Neurol* (2018) 14(8):482–95. doi: 10.1038/s41582-018-0025-8
12. Zhao J, Chen AX, Gartrell RD, Silverman AM, Aparicio L, Chu T, et al. Immune and Genomic Correlates of Response to Anti-PD-1 Immunotherapy in Glioblastoma. *Nat Med* (2019) 25(3):462–9. doi: 10.1038/s41591-019-0349-y
13. Bradley CA. Glioblastoma: Stem Cells - Masters of Their Fates. *Nat Rev Cancer* (2017) 17(10):574–5. doi: 10.1038/nrc.2017.88
14. Roesch S, Rapp C, Dettling S, Herold-Mende C. When Immune Cells Turn Bad-Tumor-Associated Microglia/Macrophages in Glioma. *Int J Mol Sci* (2018) 19(2). doi: 10.3390/ijms19020436
15. Balça-Silva J, Matias D, Dubois LG, Carneiro B, do Carmo A, Girão H, et al. The Expression of Connexins and SOX2 Reflects the Plasticity of Glioma Stem-Like Cells. *Transl Oncol* (2017) 10(4):555–69. doi: 10.1016/j.tranon.2017.04.005
16. Hong X, Sin WC, Harris AL, Naus CC. Gap Junctions Modulate Glioma Invasion by Direct Transfer of Microrna. *Oncotarget* (2015) 6(17):15566–77. doi: 10.18632/oncotarget.3904
17. Joseph JV, Magaut CR, Storevik S, Geraldo LH, Mathivet T, Latif MA, et al. TGF-β Promotes Microtube Formation in Glioblastoma Through Thrombospondin 1. *Neuro Oncol* (2021). doi: 10.1093/neuonc/noab212
18. Thuringer D, Boucher J, Jego G, Pernet N, Cronier L, Hammann A, et al. Transfer of Functional Micrornas Between Glioblastoma and Microvascular Endothelial Cells Through Gap Junctions. *Oncotarget* (2016) 7(45):73925–34. doi: 10.18632/oncotarget.12136
19. Tkach M, Théry C. Communication by Extracellular Vesicles: Where We are and Where We Need to Go. *Cell* (2016) 164(6):1226–32. doi: 10.1016/j.cell.2016.01.043
20. Weil S, Osswald M, Solecki G, Grosch J, Jung E, Lemke D, et al. Tumor Microtubes Convey Resistance to Surgical Lesions and Chemotherapy in Gliomas. *Neuro Oncol* (2017) 19(10):1316–26. doi: 10.1093/neuonc/nox070
21. Osswald M, Jung E, Sahm F, Solecki G, Venkataramani V, Blaes J, et al. Brain Tumour Cells Interconnect to a Functional and Resistant Network. *Nature* (2015) 528(7580):93–8. doi: 10.1038/nature16071
22. Pinto G, Saenz-de-Santa-Maria I, Chastagner P, Perthame E, Delmas C, Toulas C, et al. Patient-Derived Glioblastoma Stem Cells Transfer Mitochondria Through Tunneling Nanotubes in Tumor Organoids. *Biochem J* (2021) 478(1):21–39. doi: 10.1042/bcj20200710
23. Valdebenito S, Audia A, Bhat KPL, Okafo G, Eugenin EA. Tunneling Nanotubes Mediate Adaptation of Glioblastoma Cells to Temozolomide

and Ionizing Radiation Treatment. *iScience* (2020) 23(9):101450. doi: 10.1016/j.isci.2020.101450
24. Valdebenito S, Malik S, Luu R, Loudig O, Mitchell M, Okafo G, et al. Tunneling Nanotubes, TNT, Communicate Glioblastoma With Surrounding Non-Tumor Astrocytes to Adapt Them to Hypoxic and Metabolic Tumor Conditions. *Sci Rep* (2021) 11(1):14556. doi: 10.1038/s41598-021-93775-8
25. Ostrom QT, Edelson J, Byun J, Han Y, Kinnersley B, Melin B, et al. Partitioned Glioma Heritability Shows Subtype-Specific Enrichment in Immune Cells. *Neuro Oncol* (2021) 23(8):1304–14. doi: 10.1093/neuonc/noab072
26. Chen Z, Hambardzumyan D. Immune Microenvironment in Glioblastoma Subtypes. *Front Immunol* (2018) 9:1004. doi: 10.3389/fimmu.2018.01004
27. Daubon T, Hemadou A, Romero Garmendia I, Saleh M. Glioblastoma Immune Landscape and the Potential of New Immunotherapies. *Front Immunol* (2020) 11:585616:585616. doi: 10.3389/fimmu.2020.585616
28. Li Q, Barres BA. Microglia and Macrophages in Brain Homeostasis and Disease. *Nat Rev Immunol* (2018) 18(4):225–42. doi: 10.1038/nri.2017.125
29. Aspelund A, Antila S, Proulx ST, Karlsen TV, Karaman S, Detmar M, et al. A Dural Lymphatic Vascular System That Drains Brain Interstitial Fluid and Macromolecules. *J Exp Med* (2015) 212(7):991–9. doi: 10.1084/jem.20142290
30. Rua R, McGavern DB. Advances in Meningeal Immunity. *Trends Mol Med* (2018) 24(6):542–59. doi: 10.1016/j.molmed.2018.04.003
31. Basu A, Krady JK, Enterline JR, Levison SW. Transforming Growth Factor Beta1 Prevents IL-1beta-Induced Microglial Activation, Whereas Tnfalpha- and IL-6-Stimulated Activation Are Not Antagonized. *Glia* (2002) 40 (1):109–20. doi: 10.1002/glia.10118
32. Irani DN. How Much Control Does the Brain Exert Over the Immune System? *Curr Opin Neurol* (2002) 15(3):323–6. doi: 10.1097/00019052-200206000-00016
33. Lobo-Silva D, Carriche GM, Castro AG, Roque S, Saraiva M. Balancing the Immune Response in the Brain: IL-10 and its Regulation. *J Neuroinflamm* (2016) 13(1):297. doi: 10.1186/s12974-016-0763-8
34. Teeling JL, Perry VH. Systemic Infection and Inflammation in Acute CNS Injury and Chronic Neurodegeneration: Underlying Mechanisms. *Neuroscience* (2009) 158(3):1062–73. doi: 10.1016/j.neuroscience.2008.07.031
35. Vitkovic L, Maeda S, Sternberg E. Anti-Inflammatory Cytokines: Expression and Action in the Brain. *Neuroimmunomodulation* (2001) 9(6):295–312. doi: 10.1159/000059387
36. Masson F, Calzascia T, Di Berardino-Besson W, de Tribolet N, Dietrich PY, Walker PR. Brain Microenvironment Promotes the Final Functional Maturation of Tumor-Specific Effector CD8+ T Cells. *J Immunol* (2007) 179(2):845–53. doi: 10.4049/jimmunol.179.2.845
37. Thomas DA, Massagué J. TGF-Beta Directly Targets Cytotoxic T Cell Functions During Tumor Evasion of Immune Surveillance. *Cancer Cell* (2005) 8(5):369–80. doi: 10.1016/j.ccr.2005.10.012
38. Ma T, Hu C, Lal B, Zhou W, Ma Y, Ying M, et al. Reprogramming Transcription Factors Oct4 and Sox2 Induce a BRD-Dependent Immunosuppressive Transcriptome in GBM-Propagating Cells. *Cancer Res* (2021) 81(9):2457–69. doi: 10.1158/0008-5472.Can-20-2489
39. Gusyatiner O, Bady P, Pham MDT, Lei Y, Park J, Daniel RT, et al. BET Inhibitors Repress Expression of Interferon-Stimulated Genes and Synergize With HDAC Inhibitors in Glioblastoma. *Neuro Oncol* (2021) 23(10):1680–92. doi: 10.1093/neuonc/noab115
40. Ameratunga M, Braña I, Bono P, Postel-Vinay S, Plummer R, Aspegren J, et al. First-in-Human Phase 1 Open Label Study of the BET Inhibitor ODM-207 in Patients With Selected Solid Tumours. *Br J Cancer* (2020) 123 (12):1730–6. doi: 10.1038/s41416-020-01077-z
41. Amorim S, Stathis A, Gleeson M, Iyengar S, Magarotto V, Leleu X, et al. Bromodomain Inhibitor OTX015 in Patients With Lymphoma or Multiple Myeloma: A Dose-Escalation, Open-Label, Pharmacokinetic, Phase 1 Study. *Lancet Haematol* (2016) 3(4):e196–204. doi: 10.1016/s2352-3026(16)00021-1
42. Berthon C, Raffoux E, Thomas X, Vey N, Gomez-Roca C, Yee K, et al. Bromodomain Inhibitor OTX015 in Patients With Acute Leukaemia: A Dose-Escalation, Phase 1 Study. *Lancet Haematol* (2016) 3(4):e186–95. doi: 10.1016/s2352-3026(15)00247-1
43. Falchook G, Rosen S, LoRusso P, Watts J, Gupta S, Coombs CC, et al. Development of 2 Bromodomain and Extraterminal Inhibitors With Distinct Pharmacokinetic and Pharmacodynamic Profiles for the Treatment of Advanced Malignancies. *Clin Cancer Res* (2020) 26(6):1247–57. doi: 10.1158/1078-0432.Ccr-18-4071
44. Moreno V, Sepulveda JM, Vieito M, Hernández-Guerrero T, Doger B, Saavedra O, et al. Phase I Study of CC-90010, a Reversible, Oral BET Inhibitor in Patients With Advanced Solid Tumors and Relapsed/Refractory Non-Hodgkin's Lymphoma. *Ann Oncol* (2020) 31(6):780–8. doi: 10.1016/j.annonc.2020.03.294
45. Piha-Paul SA, Sachdev JC, Barve M, LoRusso P, Szmulewitz R, Patel SP, et al. First-in-Human Study of Mivebresib (ABBV-075), an Oral Pan-Inhibitor of Bromodomain and Extra Terminal Proteins, in Patients With Relapsed/Refractory Solid Tumors. *Clin Cancer Res* (2019) 25(21):6309–19. doi: 10.1158/1078-0432.Ccr-19-0578
46. Postel-Vinay S, Herbschleb K, Massard C, Woodcock V, Soria JC, Walter AO, et al. First-in-Human Phase I Study of the Bromodomain and Extraterminal Motif Inhibitor BAY 1238097: Emerging Pharmacokinetic/Pharmacodynamic Relationship and Early Termination Due to Unexpected Toxicity. *Eur J Cancer* (2019) 109:103–10. doi: 10.1016/j.ejca.2018.12.020
47. Shapiro GI, LoRusso P, Dowlati A, TD K, Jacobson CA, Vaishampayan U, et al. A Phase 1 Study of RO6870810, a Novel Bromodomain and Extra-Terminal Protein Inhibitor, in Patients With NUT Carcinoma, Other Solid Tumours, or Diffuse Large B-Cell Lymphoma. *Br J Cancer* (2021) 124 (4):744–53. doi: 10.1038/s41416-020-01180-1
48. Hambardzumyan D, Gutmann DH, Kettenmann H. The Role of Microglia and Macrophages in Glioma Maintenance and Progression. *Nat Neurosci* (2016) 19(1):20–7. doi: 10.1038/nn.4185
49. Bowman RL, Klemm F, Akkari L, Pyonteck SM, Sevenich L, Quail DF, et al. Macrophage Ontogeny Underlies Differences in Tumor-Specific Education in Brain Malignancies. *Cell Rep* (2016) 17(9):2445–59. doi: 10.1016/j.celrep.2016.10.052
50. Müller A, Brandenburg S, Turkowski K, Müller S, Vajkoczy P. Resident Microglia, and Not Peripheral Macrophages, are the Main Source of Brain Tumor Mononuclear Cells. *Int J Cancer* (2015) 137(2):278–88. doi: 10.1002/ijc.29379
51. Li W, Graeber MB. The Molecular Profile of Microglia Under the Influence of Glioma. *Neuro Oncol* (2012) 14(8):958–78. doi: 10.1093/neuonc/nos116
52. Bayik D, Zhou Y, Park C, Hong C, Vail D, Silver DJ, et al. Myeloid-Derived Suppressor Cell Subsets Drive Glioblastoma Growth in a Sex-Specific Manner. *Cancer Discov* (2020) 10(8):1210–25. doi: 10.1158/2159-8290.Cd-19-1355
53. Chang AL, Miska J, Wainwright DA, Dey M, Rivetta CV, Yu D, et al. CCL2 Produced by the Glioma Microenvironment is Essential for the Recruitment of Regulatory T Cells and Myeloid-Derived Suppressor Cells. *Cancer Res* (2016) 76(19):5671–82. doi: 10.1158/0008-5472.Can-16-0144
54. Brandenburg S, Müller A, Turkowski K, Radev YT, Rot S, Schmidt C, et al. Resident Microglia Rather Than Peripheral Macrophages Promote Vascularization in Brain Tumors and are Source of Alternative Pro-Angiogenic Factors. *Acta Neuropathol* (2016) 131(3):365–78. doi: 10.1007/s00401-015-1529-6
55. Mantovani A, Sozzani S, Locati M, Allavena P, Sica A. Macrophage Polarization: Tumor-Associated Macrophages as a Paradigm for Polarized M2 Mononuclear Phagocytes. *Trends Immunol* (2002) 23(11):549–55. doi: 10.1016/s1471-4906(02)02302-5
56. Ransohoff RM. A Polarizing Question: Do M1 and M2 Microglia Exist? *Nat Neurosci* (2016) 19(8):987–91. doi: 10.1038/nn.4338
57. Xue J, Schmidt SV, Sander J, Draffehn A, Krebs W, Quester I, et al. Transcriptome-Based Network Analysis Reveals a Spectrum Model of Human Macrophage Activation. *Immunity* (2014) 40(2):274–88. doi: 10.1016/j.immuni.2014.01.006
58. Du R, Petritsch C, Lu K, Liu P, Haller A, Ganss R, et al. Matrix Metalloproteinase-2 Regulates Vascular Patterning and Growth Affecting Tumor Cell Survival and Invasion in GBM. *Neuro Oncol* (2008) 10(3):254–64. doi: 10.1215/15228517-2008-001
59. Nijaguna MB, Patil V, Urbach S, Shwetha SD, Sravani K, Hegde AS, et al. Glioblastoma-Derived Macrophage Colony-Stimulating Factor (MCSF) Induces Microglial Release of Insulin-Like Growth Factor-Binding Protein 1 (IGFBP1) to Promote Angiogenesis. *J Biol Chem* (2015) 290(38):23401–15. doi: 10.1074/jbc.M115.664037

60. Gatto L, Nunno VD, Franceschi E, Brandes AA. Chimeric Antigen Receptor Macrophage for Glioblastoma Immunotherapy: The Way Forward. *Immunotherapy* (2021) 13(11):879–83. doi: 10.2217/imt-2021-0054
61. Sionov RV, Fridlender ZG, Granot Z. The Multifaceted Roles Neutrophils Play in the Tumor Microenvironment. *Cancer Microenviron* (2015) 8 (3):125–58. doi: 10.1007/s12307-014-0147-5
62. Attarha S, Roy A, Westermark B, Tchougounova E. Mast Cells Modulate Proliferation, Migration and Stemness of Glioma Cells Through Downregulation of GSK3β Expression and Inhibition of STAT3 Activation. *Cell Signal* (2017) 37:81–92. doi: 10.1016/j.cellsig.2017.06.004
63. Han S, Zhang C, Li Q, Dong J, Liu Y, Huang Y, et al. Tumour-Infiltrating CD4(+) and CD8(+) Lymphocytes as Predictors of Clinical Outcome in Glioma. *Br J Cancer* (2014) 110(10):2560–8. doi: 10.1038/bjc.2014.162
64. Lohr J, Ratliff T, Huppertz A, Ge Y, Dictus C, Ahmadi R, et al. Effector T-Cell Infiltration Positively Impacts Survival of Glioblastoma Patients and is Impaired by Tumor-Derived TGF-β. *Clin Cancer Res* (2011) 17(13):4296–308. doi: 10.1158/1078-0432.Ccr-10-2557
65. D'Alessio A, Proietti G, Sica G, Scicchitano BM. Pathological and Molecular Features of Glioblastoma and its Peritumoral Tissue. *Cancers (Basel)* (2019) 11(4). doi: 10.3390/cancers11040469
66. Valdor R, García-Bernal D, Bueno C, Ródenas M, Moraleda JM, Macian F, et al. Glioblastoma Progression is Assisted by Induction of Immunosuppressive Function of Pericytes Through Interaction With Tumor Cells. *Oncotarget* (2017) 8(40):68614–26. doi: 10.18632/oncotarget.19804
67. Wherry EJ, Kurachi M. Molecular and Cellular Insights Into T Cell Exhaustion. *Nat Rev Immunol* (2015) 15(8):486–99. doi: 10.1038/nri3862
68. Reardon DA, Brandes AA, Omuro A, Mulholland P, Lim M, Wick A, et al. Effect of Nivolumab vs Bevacizumab in Patients With Recurrent Glioblastoma: The Checkmate 143 Phase 3 Randomized Clinical Trial. *JAMA Oncol* (2020) 6(7):1003–10. doi: 10.1001/jamaoncol.2020.1024
69. Di Nunno V, Franceschi E, Gatto L, Bartolini S, Brandes AA. Predictive Markers of Immune Response in Glioblastoma: Hopes and Facts. *Future Oncol* (2020) 16(15):1053–63. doi: 10.2217/fon-2020-0047
70. Chan HY, Choi J, Jackson C, Lim M. Combination Immunotherapy Strategies for Glioblastoma. *J Neurooncol* (2021) 151(3):375–91. doi: 10.1007/s11060-020-03481-0
71. Cuddapah VA, Robel S, Watkins S, Sontheimer H. A Neurocentric Perspective on Glioma Invasion. *Nat Rev Neurosci* (2014) 15(7):455–65. doi: 10.1038/nrn3765
72. Piccirillo SG, Combi R, Cajola L, Patrizi A, Redaelli S, Bentivegna A, et al. Distinct Pools of Cancer Stem-Like Cells Coexist Within Human Glioblastomas and Display Different Tumorigenicity and Independent Genomic Evolution. *Oncogene* (2009) 28(15):1807–11. doi: 10.1038/onc.2009.27
73. Molina JR, Hayashi Y, Stephens C, Georgescu MM. Invasive Glioblastoma Cells Acquire Stemness and Increased Akt Activation. *Neoplasia* (2010) 12 (6):453–63. doi: 10.1593/neo.10126
74. Vehlow A, Cordes N. Invasion as Target for Therapy of Glioblastoma Multiforme. *Biochim Biophys Acta* (2013) 1836(2):236–44. doi: 10.1016/j.bbcan.2013.07.001
75. Brooks LJ, Clements MP, Burden JJ, Kocher D, Richards L, Devesa SC, et al. The White Matter is a Pro-Differentiative Niche for Glioblastoma. *Nat Commun* (2021) 12(1):2184. doi: 10.1038/s41467-021-22225-w
76. Seike T, Fujita K, Yamakawa Y, Kido MA, Takiguchi S, Teramoto N, et al. Interaction Between Lung Cancer Cells and Astrocytes *via* Specific Inflammatory Cytokines in the Microenvironment of Brain Metastasis. *Clin Exp Metastasis* (2011) 28(1):13–25. doi: 10.1007/s10585-010-9354-8
77. Placone AL, Quiñones-Hinojosa A, Searson PC. The Role of Astrocytes in the Progression of Brain Cancer: Complicating the Picture of the Tumor Microenvironment. *Tumour Biol* (2016) 37(1):61–9. doi: 10.1007/s13277-015-4242-0
78. Clement V, Sanchez P, de Tribolet N, Radovanovic I, Ruiz i Altaba A. HEDGEHOG-GLI1 Signaling Regulates Human Glioma Growth, Cancer Stem Cell Self-Renewal, and Tumorigenicity. *Curr Biol* (2007) 17(2):165–72. doi: 10.1016/j.cub.2006.11.033
79. Brandao M, Simon T, Critchley G, Giamas G. Astrocytes, the Rising Stars of the Glioblastoma Microenvironment. *Glia* (2019) 67(5):779–90. doi: 10.1002/glia.23520
80. Becher OJ, Hambardzumyan D, Fomchenko EI, Momota H, Mainwaring L, Bleau AM, et al. Gli Activity Correlates With Tumor Grade in Platelet-Derived Growth Factor-Induced Gliomas. *Cancer Res* (2008) 68(7):2241–9. doi: 10.1158/0008-5472.Can-07-6350
81. Pink RC, Elmusrati AA, Lambert D, Carter DRF. Royal Society Scientific Meeting: Extracellular Vesicles in the Tumour Microenvironment. *Philos Trans R Soc Lond B Biol Sci* (2018) 373(1737). doi: 10.1098/rstb.2017.0066
82. Vasudev NS, Reynolds AR. Anti-Angiogenic Therapy for Cancer: Current Progress, Unresolved Questions and Future Directions. *Angiogenesis* (2014) 17(3):471–94. doi: 10.1007/s10456-014-9420-y
83. Quail DF, Joyce JA. The Microenvironmental Landscape of Brain Tumors. *Cancer Cell* (2017) 31(3):326–41. doi: 10.1016/j.ccell.2017.02.009
84. Chen W, Wang D, Du X, He Y, Chen S, Shao Q, et al. Glioma Cells Escaped From Cytotoxicity of Temozolomide and Vincristine by Communicating With Human Astrocytes. *Med Oncol* (2015) 32(3):43. doi: 10.1007/s12032-015-0487-0
85. Li F, Liu X, Sampson JH, Bigner DD, Li CY. Rapid Reprogramming of Primary Human Astrocytes Into Potent Tumor-Initiating Cells With Defined Genetic Factors. *Cancer Res* (2016) 76(17):5143–50. doi: 10.1158/0008-5472.Can-16-0171
86. Jahani-Asl A, Yin H, Soleimani VD, Haque T, Luchman HA, Chang NC, et al. Control of Glioblastoma Tumorigenesis by Feed-Forward Cytokine Signaling. *Nat Neurosci* (2016) 19(6):798–806. doi: 10.1038/nn.4295
87. Khwaja FW, Svoboda P, Reed M, Pohl J, Pyrzynska B, Van Meir EG. Proteomic Identification of the Wt-P53-Regulated Tumor Cell Secretome. *Oncogene* (2006) 25(58):7650–61. doi: 10.1038/sj.onc.1209969
88. Biasoli D, Sobrinho MF, da Fonseca AC, de Matos DG, Romão L, de Moraes Maciel R, et al. Glioblastoma Cells Inhibit Astrocytic P53-Expression Favoring Cancer Malignancy. *Oncogenesis* (2014) 3(10):e123. doi: 10.1038/oncsis.2014.36
89. El Fatimy R, Subramanian S, Uhlmann EJ, Krichevsky AM. Genome Editing Reveals Glioblastoma Addiction to Microrna-10b. *Mol Ther* (2017) 25 (2):368–78. doi: 10.1016/j.ymthe.2016.11.004
90. Vazana U, Veksler R, Pell GS, Prager O, Fassler M, Chassidim Y, et al. Glutamate-Mediated Blood-Brain Barrier Opening: Implications for Neuroprotection and Drug Delivery. *J Neurosci* (2016) 36(29):7727–39. doi: 10.1523/jneurosci.0587-16.2016
91. Sattler R, Tyler B, Hoover B, Coddington LT, Recinos V, Hwang L, et al. Increased Expression of Glutamate Transporter GLT-1 in Peritumoral Tissue Associated With Prolonged Survival and Decreases in Tumor Growth in a Rat Model of Experimental Malignant Glioma. *J Neurosurg* (2013) 119(4):878–86. doi: 10.3171/2013.6.Jns122319
92. Venkatesh HS, Johung TB, Caretti V, Noll A, Tang Y, Nagaraja S, et al. Neuronal Activity Promotes Glioma Growth Through Neuroligin-3 Secretion. *Cell* (2015) 161(4):803–16. doi: 10.1016/j.cell.2015.04.012
93. Peferoen L, Kipp M, van der Valk P, van Noort JM, Amor S. Oligodendrocyte-Microglia Cross-Talk in the Central Nervous System. *Immunology* (2014) 141(3):302–13. doi: 10.1111/imm.12163
94. Asslaber M, Schauer S, Gogg-Kamerer M, Bernhart E, Quehenberger F, Haybaeck J. Native Oligodendrocytes in Astrocytomas Might Inhibit Tumor Proliferation by WIF1 Expression. *J Neuropathol Exp Neurol* (2017) 76 (1):16–26. doi: 10.1093/jnen/nlw098
95. Calabrese C, Poppleton H, Kocak M, Hogg TL, Fuller C, Hamner B, et al. A Perivascular Niche for Brain Tumor Stem Cells. *Cancer Cell* (2007) 11 (1):69–82. doi: 10.1016/j.ccr.2006.11.020
96. Hambardzumyan D, Bergers G. Glioblastoma: Defining Tumor Niches. *Trends Cancer* (2015) 1(4):252–65. doi: 10.1016/j.trecan.2015.10.009
97. Li Z, Bao S, Wu Q, Wang H, Eyler C, Sathornsumetee S, et al. Hypoxia-Inducible Factors Regulate Tumorigenic Capacity of Glioma Stem Cells. *Cancer Cell* (2009) 15(6):501–13. doi: 10.1016/j.ccr.2009.03.018
98. Singh SK, Hawkins C, Clarke ID, Squire JA, Bayani J, Hide T, et al. Identification of Human Brain Tumour Initiating Cells. *Nature* (2004) 432 (7015):396–401. doi: 10.1038/nature03128
99. Berg TJ, Marques C, Pantazopoulou V, Johansson E, von Stedingk K, Lindgren D, et al. The Irradiated Brain Microenvironment Supports Glioma Stemness and Survival *via* Astrocyte-Derived Transglutaminase 2. *Cancer Res* (2021) 81(8):2101–15. doi: 10.1158/0008-5472.Can-20-1785

100. Sharifzad F, Ghavami S, Verdi J, Mardpour S, Mollapour Sisakht M, Azizi Z, et al. Glioblastoma Cancer Stem Cell Biology: Potential Theranostic Targets. *Drug Resist Update* (2019) 42:35–45. doi: 10.1016/j.drup.2018.03.003
101. Ahmed SI, Javed G, Laghari AA, Bareeqa SB, Farrukh S, Zahid S, et al. CD133 Expression in Glioblastoma Multiforme: A Literature Review. *Cureus* (2018) 10(10):e3439. doi: 10.7759/cureus.3439
102. Zhang M, Song T, Yang L, Chen R, Wu L, Yang Z, et al. Nestin and CD133: Valuable Stem Cell-Specific Markers for Determining Clinical Outcome of Glioma Patients. *J Exp Clin Cancer Res* (2008) 27(1):85. doi: 10.1186/1756-9966-27-85
103. D'Alessio A, Proietti G, Lama G, Biamonte F, Lauriola L, Moscato U, et al. Analysis of Angiogenesis Related Factors in Glioblastoma, Peritumoral Tissue and Their Derived Cancer Stem Cells. *Oncotarget* (2016) 7 (48):78541–56. doi: 10.18632/oncotarget.12398
104. Lemée JM, Clavreul A, Menei P. Intratumoral Heterogeneity in Glioblastoma: Don't Forget the Peritumoral Brain Zone. *Neuro Oncol* (2015) 17(10):1322–32. doi: 10.1093/neuonc/nov119
105. Mei X, Chen YS, Chen FR, Xi SY, Chen ZP. Glioblastoma Stem Cell Differentiation Into Endothelial Cells Evidenced Through Live-Cell Imaging. *Neuro Oncol* (2017) 19(8):1109–18. doi: 10.1093/neuonc/nox016
106. Burger PC, Dubois PJ, Schold SCJr., Smith KRJr., Odom GL, Crafts DC, et al. Computerized Tomographic and Pathologic Studies of the Untreated, Quiescent, and Recurrent Glioblastoma Multiforme. *J Neurosurg* (1983) 58 (2):159–69. doi: 10.3171/jns.1983.58.2.0159
107. Piccirillo SG, Dietz S, Madhu B, Griffiths J, Price SJ, Collins VP, et al. Fluorescence-Guided Surgical Sampling of Glioblastoma Identifies Phenotypically Distinct Tumour-Initiating Cell Populations in the Tumour Mass and Margin. *Br J Cancer* (2012) 107(3):462–8. doi: 10.1038/bjc.2012.271
108. Ruiz-Ontañon P, Orgaz JL, Aldaz B, Elosegui-Artola A, Martino J, Berciano MT, et al. Cellular Plasticity Confers Migratory and Invasive Advantages to a Population of Glioblastoma-Initiating Cells That Infiltrate Peritumoral Tissue. *Stem Cells* (2013) 31(6):1075–85. doi: 10.1002/stem.1349
109. Wang X, Prager BC, Wu Q, Kim LJY, Gimple RC, Shi Y, et al. Reciprocal Signaling Between Glioblastoma Stem Cells and Differentiated Tumor Cells Promotes Malignant Progression. *Cell Stem Cell* (2018) 22(4):514–28.e5. doi: 10.1016/j.stem.2018.03.011
110. Peleli M, Moustakas A, Papapetropoulos A. Endothelial-Tumor Cell Interaction in Brain and CNS Malignancies. *Int J Mol Sci* (2020) 21(19). doi: 10.3390/ijms21197371
111. Beppu T, Kamada K, Yoshida Y, Arai H, Ogasawara K, Ogawa A. Change of Oxygen Pressure in Glioblastoma Tissue Under Various Conditions. *J Neurooncol* (2002) 58(1):47–52. doi: 10.1023/a:1015832726054
112. Colwell N, Larion M, Giles AJ, Seldomridge AN, Sizdahkhani S, Gilbert MR, et al. Hypoxia in the Glioblastoma Microenvironment: Shaping the Phenotype of Cancer Stem-Like Cells. *Neuro Oncol* (2017) 19(7):887–96. doi: 10.1093/neuonc/now258
113. Mihaylova VT, Bindra RS, Yuan J, Campisi D, Narayanan L, Jensen R, et al. Decreased Expression of the DNA Mismatch Repair Gene Mlh1 Under Hypoxic Stress in Mammalian Cells. *Mol Cell Biol* (2003) 23(9):3265–73. doi: 10.1128/mcb.23.9.3265-3273.2003
114. Görlach A, Dimova EY, Petry A, Martínez-Ruiz A, Hernansanz-Agustín P, Rolo AP, et al. Reactive Oxygen Species, Nutrition, Hypoxia and Diseases: Problems Solved? *Redox Biol* (2015) 6:372–85. doi: 10.1016/j.redox.2015.08.016
115. Zuo L, Zhou T, Pannell BK, Ziegler AC, Best TM. Biological and Physiological Role of Reactive Oxygen Species–the Good, the Bad and the Ugly. *Acta Physiol (Oxf)* (2015) 214(3):329–48. doi: 10.1111/apha.12515
116. Lo HW. Targeting Ras-RAF-ERK and its Interactive Pathways as a Novel Therapy for Malignant Gliomas. *Curr Cancer Drug Targets* (2010) 10 (8):840–8. doi: 10.2174/156800910793357970
117. Ohgaki H, Kleihues P. Genetic Alterations and Signaling Pathways in the Evolution of Gliomas. *Cancer Sci* (2009) 100(12):2235–41. doi: 10.1111/j.1349-7006.2009.01308.x
118. Li Y, Han N, Yin T, Huang L, Liu S, Liu D, et al. Lentivirus-Mediated Nox4 Shrna Invasion and Angiogenesis and Enhances Radiosensitivity in Human Glioblastoma. *Oxid Med Cell Longev* (2014) 2014:581732. doi: 10.1155/2014/581732
119. Moschetta M, Mishima Y, Sahin I, Manier S, Glavey S, Vacca A, et al. Role of Endothelial Progenitor Cells in Cancer Progression. *Biochim Biophys Acta* (2014) 1846(1):26–39. doi: 10.1016/j.bbcan.2014.03.005
120. Orlic D, Kajstura J, Chimenti S, Jakoniuk I, Anderson SM, Li B, et al. Bone Marrow Cells Regenerate Infarcted Myocardium. *Nature* (2001) 410 (6829):701–5. doi: 10.1038/35070587
121. Duda DG, Cohen KS, Kozin SV, Perentes JY, Fukumura D, Scadden DT, et al. Evidence for Incorporation of Bone Marrow-Derived Endothelial Cells Into Perfused Blood Vessels in Tumors. *Blood* (2006) 107(7):2774–6. doi: 10.1182/blood-2005-08-3210
122. Wang SC, Yu CF, Hong JH, Tsai CS, Chiang CS. Radiation Therapy-Induced Tumor Invasiveness is Associated With SDF-1-Regulated Macrophage Mobilization and Vasculogenesis. *PloS One* (2013) 8(8):e69182. doi: 10.1371/journal.pone.0069182
123. Hellström M, Phng LK, Hofmann JJ, Wallgard E, Coultas L, Lindblom P, et al. Dll4 Signalling Through Notch1 Regulates Formation of Tip Cells During Angiogenesis. *Nature* (2007) 445(7129):776–80. doi: 10.1038/nature05571
124. Fernández-Cortés M, Delgado-Bellido D, Oliver FJ. Vasculogenic Mimicry: Become an Endothelial Cell "But Not So Much". *Front Oncol* (2019) 9:803. doi: 10.3389/fonc.2019.00803
125. Hendrix MJ, Seftor EA, Meltzer PS, Gardner LM, Hess AR, Kirschmann DA, et al. Expression and Functional Significance of VE-Cadherin in Aggressive Human Melanoma Cells: Role in Vasculogenic Mimicry. *Proc Natl Acad Sci U.S.A.* (2001) 98(14):8018–23. doi: 10.1073/pnas.131209798
126. Ricci-Vitiani L, Pallini R, Biffoni M, Todaro M, Invernici G, Cenci T, et al. Tumour Vascularization *via* Endothelial Differentiation of Glioblastoma Stem-Like Cells. *Nature* (2010) 468(7325):824–8. doi: 10.1038/nature09557
127. Rong X, Huang B, Qiu S, Li X, He L, Peng Y. Tumor-Associated Macrophages Induce Vasculogenic Mimicry of Glioblastoma Multiforme Through Cyclooxygenase-2 Activation. *Oncotarget* (2016) 7(51):83976–86. doi: 10.18632/oncotarget.6930
128. Mao XG, Xue XY, Wang L, Zhang X, Yan M, Tu YY, et al. CDH5 is Specifically Activated in Glioblastoma Stemlike Cells and Contributes to Vasculogenic Mimicry Induced by Hypoxia. *Neuro Oncol* (2013) 15(7):865–79. doi: 10.1093/neuonc/not029
129. Krusche B, Ottone C, Clements MP, Johnstone ER, Goetsch K, Lieven H, et al. Ephrinb2 Drives Perivascular Invasion and Proliferation of Glioblastoma Stem-Like Cells. *Elife* (2016) 5. doi: 10.7554/eLife.14845
130. Seifert S, Sontheimer H. Bradykinin Enhances Invasion of Malignant Glioma Into the Brain Parenchyma by Inducing Cells to Undergo Amoeboid Migration. *J Physiol* (2014) 592(22):5109–27. doi: 10.1113/jphysiol.2014.274498
131. Lindberg OR, McKinney A, Engler JR, Koshkakaryan G, Gong H, Robinson AE, et al. GBM Heterogeneity as a Function of Variable Epidermal Growth Factor Receptor Variant III Activity. *Oncotarget* (2016) 7(48):79101–16. doi: 10.18632/oncotarget.12600
132. Szabo E, Schneider H, Seystahl K, Rushing EJ, Herting F, Weidner KM, et al. Autocrine VEGFR1 and VEGFR2 Signaling Promotes Survival in Human Glioblastoma Models *in Vitro* and in Vivo. *Neuro Oncol* (2016) 18(9):1242–52. doi: 10.1093/neuonc/now043
133. Wick W, Gorlia T, Bendszus M, Taphoorn M, Sahm F, Harting I, et al. Lomustine and Bevacizumab in Progressive Glioblastoma. *N Engl J Med* (2017) 377(20):1954–63. doi: 10.1056/NEJMoa1707358
134. Wefel JS, Armstrong TS, Pugh SL, Gilbert MR, Wendland MM, Brachman DG, et al. Neurocognitive, Symptom, and Health-Related Quality of Life Outcomes of a Randomized Trial of Bevacizumab for Newly Diagnosed Glioblastoma (NRG/RTOG 0825). *Neuro Oncol* (2021) 23(7):1125–38. doi: 10.1093/neuonc/noab011
135. Gilbert MR, Dignam JJ, Armstrong TS, Wefel JS, Blumenthal DT, Vogelbaum MA, et al. A Randomized Trial of Bevacizumab for Newly Diagnosed Glioblastoma. *N Engl J Med* (2014) 370(8):699–708. doi: 10.1056/NEJMoa1308573
136. Chinot OL, Wick W, Mason W, Henriksson R, Saran F, Nishikawa R, et al. Bevacizumab Plus Radiotherapy-Temozolomide for Newly Diagnosed Glioblastoma. *N Engl J Med* (2014) 370(8):709–22. doi: 10.1056/NEJMoa1308345

137. Tamura R, Tanaka T, Akasaki Y, Murayama Y, Yoshida K, Sasaki H. The Role of Vascular Endothelial Growth Factor in the Hypoxic and Immunosuppressive Tumor Microenvironment: Perspectives for Therapeutic Implications. *Med Oncol* (2019) 37(1):2. doi: 10.1007/s12032-019-1329-2
138. Nayak L, Molinaro AM, Peters K, Clarke JL, Jordan JT, de Groot J, et al. Randomized Phase II and Biomarker Study of Pembrolizumab Plus Bevacizumab Versus Pembrolizumab Alone for Patients With Recurrent Glioblastoma. *Clin Cancer Res* (2021) 27(4):1048–57. doi: 10.1158/1078-0432.Ccr-20-2500
139. Brandes AA, Tosoni A, Franceschi E, Blatt V, Santoro A, Faedi M, et al. Fotemustine as Second-Line Treatment for Recurrent or Progressive Glioblastoma After Concomitant and/or Adjuvant Temozolomide: A Phase II Trial of Gruppo Italiano Cooperativo Di Neuro-Oncologia (GICNO). *Cancer Chemother Pharmacol* (2009) 64(4):769–75. doi: 10.1007/s00280-009-0926-8
140. Franceschi E, Bartolotti M, Tosoni A, Bartolini S, Sturiale C, Fioravanti A, et al. The Effect of Re-Operation on Survival in Patients With Recurrent Glioblastoma. *Anticancer Res* (2015) 35(3):1743–8.
141. Tosoni A, Franceschi E, Ermani M, Bertorelle R, Bonaldi L, Blatt V, et al. Temozolomide Three Weeks on and One Week Off as First Line Therapy for Patients With Recurrent or Progressive Low Grade Gliomas. *J Neurooncol* (2008) 89(2):179–85. doi: 10.1007/s11060-008-9600-y
142. Van Den Bent M, Eoli M, Sepulveda JM, Smits M, Walenkamp A, Frenel JS, et al. INTELLANCE 2/EORTC 1410 Randomized Phase II Study of Depatux-M Alone and With Temozolomide vs Temozolomide or Lomustine in Recurrent EGFR Amplified Glioblastoma. *Neuro Oncol* (2020) 22(5):684–93. doi: 10.1093/neuonc/noz222
143. Woroniecka K, Chongsathidkiet P, Rhodin K, Kemeny H, Dechant C, Farber SH, et al. T-Cell Exhaustion Signatures Vary With Tumor Type and are Severe in Glioblastoma. *Clin Cancer Res* (2018) 24(17):4175–86. doi: 10.1158/1078-0432.Ccr-17-1846
144. Singh K, Batich KA, Wen PY, Tan AC, Bagley SJ, Lim M, et al. Designing Clinical Trials for Combination Immunotherapy: A Framework for Glioblastoma. *Clin Cancer Res* (2021). doi: 10.1158/1078-0432.Ccr-21-2681
145. Wainwright DA, Chang AL, Dey M, Balyasnikova IV, Kim CK, Tobias A, et al. Durable Therapeutic Efficacy Utilizing Combinatorial Blockade Against IDO, CTLA-4, and PD-L1 in Mice With Brain Tumors. *Clin Cancer Res* (2014) 20(20):5290–301. doi: 10.1158/1078-0432.Ccr-14-0514
146. Scott EM, Duffy MR, Freedman JD, Fisher KD, Seymour LW. Solid Tumor Immunotherapy With T Cell Engager-Armed Oncolytic Viruses. *Macromol Biosci* (2018) 18(1). doi: 10.1002/mabi.201700187
147. Gedeon PC, Schaller TH, Chitneni SK, Choi BD, Kuan CT, Suryadevara CM, et al. A Rationally Designed Fully Human Egfrviii : CD3-Targeted Bispecific Antibody Redirects Human T Cells to Treat Patient-Derived Intracerebral Malignant Glioma. *Clin Cancer Res* (2018) 24(15):3611–31. doi: 10.1158/1078-0432.Ccr-17-0126
148. Quail DF, Bowman RL, Akkari L, Quick ML, Schuhmacher AJ, Huse JT, et al. The Tumor Microenvironment Underlies Acquired Resistance to CSF-1R Inhibition in Gliomas. *Science* (2016) 352(6288):aad3018. doi: 10.1126/science.aad3018
149. Lombardi G, Pambuku A, Bellu L, Farina M, Della Puppa A, Denaro L, et al. Effectiveness of Antiangiogenic Drugs in Glioblastoma Patients: A Systematic Review and Meta-Analysis of Randomized Clinical Trials. *Crit Rev Oncol Hematol* (2017) 111:94–102. doi: 10.1016/j.critrevonc.2017.01.018
150. Levin VA, Chan J, Datta M, Yee JL, Jain RK. Effect of Angiotensin System Inhibitors on Survival in Newly Diagnosed Glioma Patients and Recurrent Glioblastoma Patients Receiving Chemotherapy and/or Bevacizumab. *J Neurooncol* (2017) 134(2):325–30. doi: 10.1007/s11060-017-2528-3
151. Asai H, Ikezu S, Tsunoda S, Medalla M, Luebke J, Haydar T, et al. Depletion of Microglia and Inhibition of Exosome Synthesis Halt Tau Propagation. *Nat Neurosci* (2015) 18(11):1584–93. doi: 10.1038/nn.4132
152. Atai NA, Balaj L, van Veen H, Breakefield XO, Jarzyna PA, Van Noorden CJ, et al. Heparin Blocks Transfer of Extracellular Vesicles Between Donor and Recipient Cells. *J Neurooncol* (2013) 115(3):343–51. doi: 10.1007/s11060-013-1235-y
153. Jansen F, Yang X, Hoyer FF, Paul K, Heiermann N, Becher MU, et al. Endothelial Microparticle Uptake in Target Cells is Annexin I/Phosphatidylserine Receptor Dependent and Prevents Apoptosis. *Arterioscler Thromb Vasc Biol* (2012) 32(8):1925–35. doi: 10.1161/atvbaha.112.253229
154. Hitomi M, Deleyrolle LP, Mulkearns-Hubert EE, Jarrar A, Li M, Sinyuk M, et al. Differential Connexin Function Enhances Self-Renewal in Glioblastoma. *Cell Rep* (2015) 11(7):1031–42. doi: 10.1016/j.celrep.2015.04.021
155. Fridman JS, Caulder E, Hansbury M, Liu X, Yang G, Wang Q, et al. Selective Inhibition of ADAM Metalloproteases as a Novel Approach for Modulating Erbb Pathways in Cancer. *Clin Cancer Res* (2007) 13(6):1892–902. doi: 10.1158/1078-0432.Ccr-06-2116
156. Jimenez-Pascual A, Hale JS, Kordowski A, Pugh J, Silver DJ, Bayik D, et al. ADAMDEC1 Maintains a Growth Factor Signaling Loop in Cancer Stem Cells. *Cancer Discov* (2019) 9(11):1574–89. doi: 10.1158/2159-8290.Cd-18-1308

Conflict of Interest: The authors declare that the research was conducted in the absence of any commercial or financial relationships that could be construed as a potential conflict of interest.

GLOSSARY

ADAM10	Adam metallopeptidase domain 10
APC	Antigen Presenting Cell
ARG1	arginase 1
A2aR	adenosine A2A receptor
ATP	adenosine triphosphate
BDNF	brain derived neurotrophic factor
BET	Bromodomain and extra terminal motif proteins family
BRD3	Bromodomain containing protein 3
BRD4	Bromodomain containing protein 4
CD70	Cluster of differentiation 70
CD133	prominin-1
CCL2	C-C Motif Chemokine Ligand 2
CCL5	C-C Motif Chemokine Ligand 5
CCL7	C-C Motif Chemokine Ligand 7
COX 2	cyclooxygenase-2
CCL20	C-C Motif Chemokine Ligand 20
CXCL3	C-X-C Motif Chemokine Ligand 3
CXCL5	C-X-C Motif Chemokine Ligand 5
CXCL9	C-X-C Motif Chemokine Ligand 9
CXCL10	C-X-C Motif Chemokine Ligand 10
CXCL11	C-X-C Motif Chemokine Ligand 11
CNS	Central Nervous System
CSF-1	Colony stimulating factor 1
DLL4	Delta-like canonical Notch ligand 4
EC	Endothelial cell
ECM	Extra-cellular matrix
EGF	Epiderma growth factor
EGFR	Epidermal growth factor receptor
ERK 1/2	extracellular signal-regulated kinases 1 and 2
FAK	focal adhesion kinase
FGF	Fibroblast Growth factor
GBM	Glioblastoma
GDNF	Glial Cell Derived Neutrophic Factor
GM-CSF	Granulocyte-Macrophage Colony-Stimulating Factor
GSC	Glioblastoma stem cell
JAK	Jasus Kinase
HGF	Hepatocyte growth factor
HIF-1	hypoxia inducible factor 1
HIF-2	hypoxia inducible factor 2
HIG-2	hypoxia inducible protein 2
HSPA5	brain-derived neurotrophic factor chaperone Bip
IDH	Isocitrate dehydrogenase
IDO1	Indoleamine 2,3-dioxygenase
IGF1	insulin growth factor 1
IGFBP1	insulin-like growth factor-binding protein 1
IL5	Interleukin 5
IL6	Interleukin 6
IL8	Interleukin 8
IL10	Interleukin 10
INF γ	interferon γ
iNOS	inducible nitric oxide synthase
LAG 3	lymphocyte activation gene 3
MAPK	mitogen-activated protein kinase
MGMT	O^6 – methylguanine DNA methyltransferase
MP	Metalloprotease
mTOR	mammalian target of rapamycin
NMDA	N-methyl-D-aspartate receptors
NOX 4	NADPH oxidase 4
NSC	Neural stem cell
NTRK2	neurotrophic receptor tyrosine kinase 2
Oct4	Octamer-binding transcription factor 4
OLIG2	Oligodendrocyte transcription factor 2
OS	Overall survival
PD-1	Programmed Death Receptor 1
PD-L1	Programmed Death Receptor Ligand 1
PI3K	phosphoinositide-3-kinase
ROS	reactive oxygen species
SDF1	stromal cell-derived factor 1
SHH	Sonic Hedgehog
SOX2	SRY-Box Transcription Factor 2
SOX10	SRY-Box Transcription Factor 10
SPP	Signal Peptide Peptidase
STAT	Signal transducer and activator of transcription
TAA	Tumor associated astrocytes
TDO	Tryptophan 2,3-dioxygenase
TERT	Telomerase Reverse Transcriptase
TGFβ1	transforming growth factor β1
TIM-3	T cell immunoglobulin-mucin-domain containing3
TMZ	Temozolomide
TNF	tumor necrosis factor
VEGF	vascular endothelial growth factor
WHO	World Health Organization

frontiers in Oncology

ORIGINAL RESEARCH
published: 15 March 2022
doi: 10.3389/fonc.2022.826273

The Metalloprotease-Disintegrin ADAM8 Alters the Tumor Suppressor miR-181a-5p Expression Profile in Glioblastoma Thereby Contributing to Its Aggressiveness

Agnes Schäfer[1†], Lara Evers[1†], Lara Meier[1], Uwe Schlomann[1], Miriam H. A. Bopp[1,2], Gian-Luca Dreizner[1], Olivia Lassmann[1], Aaron Ben Bacha[1], Andreea-Cristina Benescu[1], Mirza Pojskic[1], Christian Preußer[3], Elke Pogge von Strandmann[3], Barbara Carl[1], Christopher Nimsky[1,2] and Jörg W. Bartsch[1,2]*

[1] Department of Neurosurgery, Philipps University Marburg, Marburg, Germany, [2] Marburg Center for Mind, Brain and Behavior (MCMBB), Marburg, Germany, [3] Core Facility Extracellular Vesicles, Philipps University of Marburg – Medical Faculty, Marburg, Germany

Glioblastoma (GBM) as the most common and aggressive brain tumor is characterized by genetic heterogeneity, invasiveness, radio-/chemoresistance, and occurrence of GBM stem-like cells. The metalloprotease-disintegrin ADAM8 is highly expressed in GBM tumor and immune cells and correlates with poor survival. In GBM, ADAM8 affects intracellular kinase signaling and increases expression levels of osteopontin/SPP1 and matrix metalloproteinase 9 (MMP9) by an unknown mechanism. Here we explored whether microRNA (miRNA) expression levels could be regulators of MMP9 expression in GBM cells expressing ADAM8. Initially, we identified several miRNAs as dysregulated in ADAM8-deficient U87 GBM cells. Among these, the tumor suppressor miR-181a-5p was significantly upregulated in ADAM8 knockout clones. By inhibiting kinase signaling, we found that ADAM8 downregulates expression of miR-181a-5p *via* activation of signal transducer and activator of transcription 3 (STAT3) and mitogen-activated protein kinase (MAPK) signaling suggesting an ADAM8-dependent silencing of miR-181a-5p. In turn, mimic miR-181a-5p transfection caused decreased cell proliferation and lower MMP9 expression in GBM cells. Furthermore, miR-181a-5p was detected in GBM cell-derived extracellular vesicles (EVs) as well as patient serum-derived EVs. We identified miR-181a-5p downregulating MMP9 expression *via* targeting the MAPK pathway. Analysis of patient tissue samples (n=22) revealed that in GBM, miR-181a-5p is strongly downregulated compared to *ADAM8* and *MMP9* mRNA expression, even in localized tumor areas. Taken together, we provide evidence for a functional axis involving ADAM8/miR-181a-5p/MAPK/MMP9 in GBM tumor cells.

Keywords: glioblastoma, tumor microenvironment, extracellular vesicles, miRNA, MR spectroscopy, ADAM8, miR-181a-5p, MMP9

OPEN ACCESS

Edited by:
Bozena Kaminska, Nencki Institute of Experimental Biology (PAS), Poland

Reviewed by:
Katarzyna Rolle, Institute of Bioorganic Chemistry (PAS), Poland
Francesca Peruzzi, Louisiana State University, United States

***Correspondence:**
Jörg W. Bartsch
jbartsch@med.uni-marburg.de

†These authors have contributed equally to this work

Specialty section:
This article was submitted to Neuro-Oncology and Neurosurgical Oncology, a section of the journal Frontiers in Oncology

Received: *30 November 2021*
Accepted: *16 February 2022*
Published: *15 March 2022*

Citation:
Schäfer A, Evers L, Meier L, Schlomann U, Bopp MHA, Dreizner G-L, Lassmann O, Ben Bacha A, Benescu A-C, Pojskic M, Preußer C, von Strandmann EP, Carl B, Nimsky C and Bartsch JW (2022) The Metalloprotease-Disintegrin ADAM8 Alters the Tumor Suppressor miR-181a-5p Expression Profile in Glioblastoma Thereby Contributing to Its Aggressiveness. Front. Oncol. 12:826273. doi: 10.3389/fonc.2022.826273

INTRODUCTION

Glioblastoma multiforme (GBM) is the most common malignant primary brain tumor in adults. Despite a standard multimodal therapeutic strategy combining maximum safe surgical resection and radio-/chemotherapy with temozolomide, the median survival remains low between 12 and 15 months (1). To improve the poor prognosis of GBM patients it is crucial to identify new therapeutic targets and their underlying dysregulated signaling pathways.

GBM is characterized as a highly invasive, heterogeneously composed, and rapidly growing tumor (2). At the molecular level, a disintegrin and metalloproteinases (ADAMs) mediate tumor cell adhesion and migration as well as intracellular signaling (3). One such proteolytically active family member is the metalloproteinase-disintegrin 8 (ADAM8), strongly associated with tumor aggressiveness, progression, and reduced survival in various cancers including breast cancer, pancreatic ductal adenocarcinoma (PDAC), and GBM (4–7). ADAM8, in particular, the cytoplasmic domain (CD) and the disintegrin/cysteine-rich domain (DC) can activate central signaling pathways in carcinogenesis. First, ADAM8 activates the mitogen-activated protein kinase (MAPK) signaling cascade, epidermal growth factor receptor (EGFR) independently (8, 9). Second, ADAM8 mediates angiogenesis by inducing the expression of osteopontin (*SPP1*) *via* STAT3 signaling (10). Moreover, ADAM8 interacts with integrin ß1 (ITGB1) and thereby activates its downstream targets focal adhesion kinase (FAK), and the PI3K/AKT pathway (9, 11). Interestingly, ADAM8 dependent activation of the MAPK pathway as well the PI3K/AKT pathway enhanced temozolomide-chemoresistance in GBM cell lines (12). Considering these diverse functions of ADAM8 in intracellular signaling, we and others hypothesized that ADAM8 mediates these functions through the regulation of microRNAs and indeed, initial evidence came from a study in MDA-MB-231 breast cancer cells showing that ADAM8 regulates expression levels of miR-720 (13).

MicroRNAs (miRNAs) are small non-coding RNA molecules that regulate protein expression on a post-transcriptional level by binding and thereby silencing their target messenger RNAs (mRNAs) (14). In most cases, miRNAs lead to translational repression or even degradation of their specific target mRNAs (15). Therefore, dysregulated miRNA expression profiles alter many critical pathways related to cancer progression (16). Consequently, in GBM, a large number of miRNAs are reported to be dysregulated (17, 18). In GBM, miR-181a-5p is downregulated and functions as a tumor suppressor miRNA that inhibits the translation of oncogenic proteins that are linked to tumor progression such as osteopontin (*SPP1*) (19–21). This type of sialoprotein is highly expressed in GBM and plays a key role in tumor-tumor microenvironment communication by attracting macrophages and mediating their immune response (22). Furthermore, miR-181a-5p regulates cell apoptosis and cell colony formation by targeting B-cell lymphoma 2 (BCL-2), so that high expression levels of miR-181a-5p can induce radiosensitivity of U87 GBM cells (23, 24). In addition, miR-181a-5p contains inhibitory binding sites to members of the MAPK family and its downstream targets, namely mitogen-activated protein kinase kinase 1 (MEK1), cAMP response element-binding protein 1 (CREB-1), and extracellular signal-regulated kinase 2 (ERK2) (25, 26). Given an important functional role in GBM, the signaling pathways regulating miR-181a-5p itself, however, remain unclear.

Matrix metalloproteinase 9 (MMP9), a zinc-dependent endopeptidase, plays a central role in the process of tumor cell migration, infiltration, and metastasis (27). Matrix metalloproteinases degrade extracellular matrix molecules and basement membrane components and thereby contribute to glioma progression (28). Consequently, MMP9 is upregulated in GBM compared to its expression in the normal brain parenchyma (29). Gliomas that display high MMP9 levels are associated with an aggressive course and are linked to reduced survival (30). Previous studies demonstrated that MMP9 expression can be elevated *via* MAPK-signaling (31, 32). ADAM8 and MMP9 levels are correlated in GBM tissue samples as well breast cancer-derived brain metastasis (8, 33). Whether MMP9 can be directly targeted by miR-181a-5p or indirectly *via* miR-181a-5p induced downregulation of the MAPK pathway has not been explored yet.

Cancer invasion is closely associated with the interaction of infiltrating tumor cells and the tumor microenvironment (TME) (34). As a means of communication, extracellular vesicles (EVs) are secreted by tumor cells as well as by cells of the TME. Their cargo contains lipids and proteins as well as nucleic acids including miRNAs (35). Because EVs modulate tumor growth, immune-escape, and tumor cell niche formation, they function as central regulators of the TME (34).

In the current work, we explored the mechanism by which ADAM8 modulates intracellular and extracellular signaling through the regulation of miR-181a-5p expression and uncovered *MMP9* as a miR-181a-5p dependent target gene in GBM.

MATERIAL AND METHODS

Patient Specimens

In accordance with the local ethics committee (Philipps University Marburg, medical faculty, file number 185/11), tumor tissue samples of GBM patients were obtained during surgical resection and serum specimens were collected one to three days prior and three to five days after surgical resection. Each patient gave written informed consent before resection. Tissue samples were shock frozen in liquid nitrogen and then stored at -80°C. Serum samples were centrifuged at 2,000 g for 10 min prior to storage at -80°C. All included tissue and serum samples were from primary, isocitrate dehydrogenase (IDH) wild-type GBM tumors, further patient information and histopathological characteristics are summarized in **Table 1**. In three cases, we analyzed the expression of miR-181a-5p in serum-derived EVs at the time of initial manifestation and tumor recurrence (Patient 9, 23, 24 in **Table 1**).

TABLE 1 | Clinical data on patient included tumor tissue samples showed isocitrate dehydrogenase (IDH) wild-type expression.

Number	Age at diagnosis (years)	Sex	Tumor localization	Type of resection	MGMT promoter methylation	EGFR vIII	Ki67-Li	Survival (days)
1	71	m	Septum pellucidum	Subtotal	Methylated	–	Up to 30%	114
2	65	m	Left parietal lobe	Subtotal	Not methylated	+	Up to 40%	119
3	77	w	Right frontal lobe	Subtotal	Methylated	–	Up to 20%	79
4	75	m	Right temporal and parietal lobe	Subtotal	Methylated	–	10%	476
5	63	w	Left frontal lobe	Subtotal	Methylated	–	Up to 30%	76
6	87	m	Right parietal and occipital lobe	Gross Total	Methylated	++	5%	135
7	78	w	Butterfly glioma, predominantly right frontal lobe	Subtotal	Not methylated	unknown	20%	63
8	66	m	Left frontal lobe	Subtotal	Methylated	–	25%	49
9*	66	m	Right occipital lobe	Gross total	Not methylated	+	20%	336
10	65	w	Left temporal lobe	Subtotal	Not methylated	–	Up to 15%	84
11	70	w	Left frontal lobe	Subtotal	Methylated	+	Up to 25%	278
12	61	m	Right temporal lobe	Gross total	Methylated	–	30%	626
13	64	w	Right frontal and temporal lobe	Gross total	Methylated	–	20%	930
14	65	m	Left temporal lobe	Subtotal	Methylated	–	30%	579
15	66	m	Right temporal lobe and right Insula	Subtotal	Methylated	–	Up to 20%	126
16	61	m	Left temporal lobe	Gross total	Not methylated	–	50%	398
17	57	w	Right frontal lobe	Gross total	Weakly methylated	+	20%	410
18	62	m	Right temporal and parietal lobe	Gross total	Not methylated	–	Up to 20%	457
19	56	m	Left temporal lobe	Gross total	Methylated	–	20%	578
20	69	m	Right parietal and occipital lobe	Gross total	Weakly methylated	–	Up to 50%	388
21	61	m	Right frontal lobe	Gross total	Weakly methylated	–	30%	94
22	76	m	Right frontal lobe	Gross total	Not methylated	–	30%	225
23*	76	f	Left parietal	Gross total	Methylated	–	20%	unknown
24*	54	m	Right frontal lobe	Gross total	Methylated	–	30%	450
25	74	f	Left parietal lobe	Gross total	Methylated	–	40%	unknown

Only initial manifested primary glioblastomas were included. Here, we show further parameters regarding the patient cohort including age at diagnosis, sex, survival in days, and type of surgical resection (gross total or subtotal). Furthermore, histopathological data such as methylation status of the O^6-methylguanine-DNA-methyltransferase (MGMT), Ki67-Labelling index (Ki67-Li), and expression of epidermal growth factor variant III (EGFRvIII) are presented here. Patients' 1 to 22 tissue samples were analyzed for miR-181a-5p, ADAM8, *and* MMP9 *mRNA expression (**Figures 5A–D**), matched samples (initial and recurrence GBM) from patients 9, 23, and 24 (*) were used for serum-EV separation and analysis (**Figures 5H–J**) and patient 25 was used for the analysis via MR-spectroscopy (**Figures 5E–G**).*

Cell Culture

Established GBM cell lines U87 and U251 were purchased from the American Type Culture Collection (ATCC) and cell lines G112 and G28 were obtained from the Westphal Lab (UKE Hamburg). All GBM cell lines were cultivated in Dulbecco's modified Eagle's medium (DMEM) high glucose (4.5 g/L) phenol red (Capricorn Scientific, Germany), supplemented with 10% fetal calf serum (FCS, S0615, Sigma, Germany), 1% penicillin/streptomycin (2321115, Gibco, US), 1% sodium pyruvate (NPY-B, Capricorn Scientific, Germany) and 1% non-essential amino acids (11140050, Gibco, US). Primary GBM cell lines and primary glioblastoma stem-like cells (GSCs) were obtained during surgical resection. The isolation and preparation process of GSCs and primary differentiated patient-derived GBM tumor cells were each described previously by our group (12, 36). GSC lines 2017/151, 2017/74, and 2016/240 were cultivated in DMEM/F12 (DMEM-12-A, Capricorn Scientific, Germany) and supplemented with 2% B27 supplement (117504044, Gibco, US), 1% amphotericin (152290026, Gibco, US), 0.5% HEPES (H0887, Sigma, Taufkirchen, Germany) and 0.1% Gentamycin (A2712, Biochrom, Germany). Moreover, a final concentration of 0.02 ng/µL EGF (100-18B, Peprotech, Germany) and bFGF (315-09, Peprotech, Germany) was added, and GSCs were cultivated in non-cell-culture-treated petri dishes. Primary differentiated GBM cell lines GBM98, GBM42, and GBM29 were cultivated in DMEM high glucose (4.5 g/L) without phenol red (Capricorn Scientific, Germany) supplemented with 10% FCS (S0615, Sigma, Germany), 1% penicillin/streptomycin (2321115, Gibco, US), 1 mM sodium pyruvate (NPY-B, Capricorn Scientific, Germany), 1% L-glutamine (200 mM) (25030-024, Gibco, US) and 1% non-essential amino acids (11140050, Gibco, US). All cell lines were cultured in a humidified atmosphere at 37°C under 5% CO_2.

Generation of Stable U87 CRISPR/Cas9 ADAM8 KO (KO) Clones

U87 cells were transfected with two different gRNAs using the CRISPR/Cas9 knockout/knockin kit from OriGene (#

KN213386) as described previously (37). Cell clones were selected by treatment with antibiotics (1 mg/ml puromycin). The ADAM8 knockout was confirmed through RT-qPCR, western blot, and ELISA analysis. U87 wild-type cells were used as control cells.

Transient Transfection to Induce an ADAM8 Rescue in U87 ADAM8 KO Cells

To rescue ADAM8 in U87 ADAM8 KO clones, cells were seeded in 6-well-plates at a density of 500,000 cells in 2 ml. After 24 h, the transfection was performed with either ADAM8 lacking the cytoplasmatic domain or the full-length ADAM8 using LTX Lipofectamine (Invitrogen) according to the manufacturer's instructions. Cells were harvested and analyzed by RT-qPCR and western blot after 48 h of transfection.

MiR-181a-5p Mimic Transfection

To transiently overexpress miR-181a-5p, U87 cells were seeded in 6-well-plates at a density of 400,000 cells in 2 ml and were transfected with 0.01 µM miR-181a-5p mimic (miScript, Qiagen) after 24 h. 0.01 µM ON-TARGET *plus* non-targeting Control Pool (Dharmacon, US) was used as control RNA. Transfection was performed utilizing Lipofectamine RNAimax (Invitrogen, UK) according to the manufacturer's instructions. After 24 h, the transfection was repeated. Transfected cells and their controls were harvested 48 h after the second transfection. To evaluate the success of transfection, miRNA expression was analyzed by RT-qPCR.

Inhibitors

Batimastat was used as a broad-spectrum MMP-inhibitor and was purchased from Tocris (Biotechne, Wiesbaden, Germany). As a specific ADAM8-inhibitor, BK-1361 (Peptide 2.0) was utilized and described by our group previously (9). WP´066 (Sigma Aldrich, US) was used as a JAK2/STAT3 inhibitor. Cells were seeded in a 6-well-format (500,000 cells in 2 ml) and harvested 16 h after treatment with inhibitors. The concentrations used are indicated in the graphs.

Separation of Extracellular Vesicles (EVs)

EVs were separated from cellular supernatants and GBM patients' serum samples *via* sequential ultracentrifugation. Cells were incubated with 30 ml DMEM supplemented with 1% L-glutamine (200 mM), 1% penicillin/streptomycin, 1 mM sodium pyruvate solution, and 1% nonessential amino acids for 48 h. Prior to EV separation, serum samples were diluted 1:3 with HBSS (Gibco™, Life Technologies, US) (500 µl serum diluted with 1 ml HBSS). The conditioned medium and the diluted serum sample were centrifuged first at 2,000 g for 10 min at RT and then at 10,000 g for 60 min at 4°C. After a subsequent filtration (0.2 µm filter), EVs were pelleted *via* high-speed centrifugation at 100,000 g for 90 min at 4°C using an Optima XPN-80 ultracentrifuge (Beckman Coulter, Germany). Next, the EV pellet was washed with HBSS at 100,000 g for 90 min at 4°C using the Optima MAX-XP (Beckman Coulter, Germany) ultracentrifuge with a TLA-55 fixed angle rotor. EVs were resuspended in 50 µl HBSS and stored at -80°C until further use. A 5 µl aliquot was sent to the FACS Core Facility, Marburg, for determining the size and concentration of the particles by usage of nano-flow cytometry (NanoFCM Co. Ltd., Nottingham, UK).

Real-Time Quantitative Polymerase Chain Reaction (qPCR)

Total RNA with an enriched fraction of miRNAs from tumor tissue samples and cellular pellets was isolated using the miRNeasy Tissue/Cells Advanced Mini Kit (217684, Qiagen, Germany) according to the manufacturer's instructions. To quantify the miRNA expression in cells, miRCURY LNA RT Kit (Cat. Number 339340, Qiagen, Germany) and miRCURY LNA SYBR® Green PCR Kit (Cat. Number 339345, Qiagen, Germany) were used according to manufacturer's instructions. YP00203_U6 snRNA miRCURY LNA PCR Assay (YP00203907, Qiagen, Germany) and miRCURY miRNA Assay hsa-181a-5p (YP00206081, Qiagen, Germany) was used for the quantification of relative miR-181a-5p expression. In the case of tissue samples (**Figure 5**), miScript II RT Kit (218161, Qiagen, Germany) and miScript SYBR Green PCR Kit (218073, Qiagen, Germany) were used according to the manufacturer's protocols. Here, Hs_RNU6-2_11 miScript Primer Assay (MS00033740, Qiagen, Germany) and Hs_miR-181a_2 miScript Primer Assay (MS00008827, Qiagen, Germany) were used. To assess gene expression on an mRNA level, RNA was reverse transcribed with RNA to cDNA EcoDry™ Premix (Takara Bio. Inc.). Quantitative real-time PCR was performed with iTaq™ Universal SYBR Green Supermix (Bio-rad Laboratories GmbH, US). QuantiTect Primer Assay (Qiagen) or forward and reverse primer were used in a total reaction volume of 20 µl. XS13 was used as a housekeeping gene. All PCR experiments were performed on the Applied Biosystems StepOnePlus Real-time PCR system (Thermo Fisher Scientific, US). Relative gene expression was calculated utilizing either the $2^{-\Delta Ct}$- or the $2^{-\Delta\Delta Ct}$ -method as indicated.

MiRNA PCR Array – Human Finder

A pathway-focused miRNA PCR Array/Human Finder (331221 miScript, MIHS-001ZC, Qiagen, Germany) was conducted according to the manufacturer's instructions. Data analysis was performed with the online miScript miRNA Data Analysis program from Qiagen using the $2^{-\Delta\Delta Ct}$-method. Results are presented in a heatmap.

Protein Extraction and Western Blot Analysis

Cells were washed with PBS (Sigma-Aldrich, US) and detached by cell scraping. Whole cell lysates were homogenized by an incubation for 30 min in RIPA buffer (50 mM HEPES pH 7.4; 150 mM NaCl; 1% (v/v) NP-40; 0.5% (w/v) Natriumdeoxycholate; 0.1% (w/v) SDS; 10 mM Phenantrolin; 10 mM EDTA; Pierce™ Protease Inhibitor Mini Tablets, EDTA-free, Thermo Fisher Scientific; Pierce™ Phosphatase Inhibitor Mini Tablets, Thermo Fisher Scientific). Protein samples or EVs in a concentration of $1.5x10^9$ particles were prepared in 5x Laemmli buffer [60 mM Tris-HCl pH

6.8; 2% (w/v) SDS; 10% (w/v) Glycerol; 5% (v/v) ß-Mercaptoethanol; 0.01% (w/v) Bromophenol-Blue] and 10x NuPAGE™ sample reducing reagent (Thermo Fisher Scientific, US) and denatured at 95°C for 5 min before SDS PAGE. For this, a 10% SDS polyacrylamide gel was used. Separated proteins were transferred on nitrocellulose membranes (A29591442, GE Healthcare Life science, Germany) followed by blocking in 5% (w/v) milk powder (MP) in TBST (50 mM Tris, pH 7.5; 150 mM NaCl; 0.1% (w/v) Tween-20) for 1 h. The detection of proteins was performed utilizing the following primary antibodies diluted as indicated in 5% MP in TBST: anti-ADAM8 (PA5-47047, Thermo Fisher Scientific, 1:1000), anti-MMP9 (IM09L, Calbiochem, 1:1,000), anti- β-Tubulin (NB600-936, Novus Biological, 1:2,000) anti-EGFR (4267, Cell Signaling, 1:1,000), anti-pEGFR (3777, Cell Signaling, 1:1,000), anti-MAPK (4696, Cell Signaling, 1:2,000), anti-pMAPK (4370, Cell Signaling, 1:2000), anti-CALNEXIN (2679, Cell Signaling, 1:1,000), anti-FLOTILLIN-1 (PA5-18053, Thermo Scientific, 1:2,000) anti-CD81 (sc166029, Santa Cruz, 1:500), anti-STAT3 (ab68153, Abcam, 1:5,000), anti-pSTAT3 (ab76315, Abcam, 1:5,000), anti-CREB-1 (H74) (sc-25785, Santa Cruz, 1:500 in 5% MP) and anti-pCREB-1(Ser133) (4276, Cell Signaling, 1:1000 in 5% BSA in TBST). Nitrocellulose membranes were incubated with primary antibodies at 4°C overnight. After washing three times with TBST, membranes were incubated with horseradish peroxidase (HRP) conjugated antibodies (Abcam, 1:5,000) for 1 h followed by a next washing step. Chemiluminescence detection was performed by adding Western Bright Sirius substrate (Advansta, US) and using the ChemiDoc MP Imaging System (Bio-rad Laboratories GmbH, US). Western blots were quantified using Image J (NIH, Maryland).

Enzyme-Linked Immunosorbent Assay (ELISA)

Soluble ADAM8 (DY1031, R&D Systems, UK) and soluble MMP9 (DY911, R&D Systems, UK) from cell culture supernatants were determined by Sandwich-ELISA method with DuoSet ELISA Kits. All ELISA experiments were performed according to the manufacturer's instructions.

Proliferation Assay

The proliferation and survival effects on U87 cells were determined using CellTiter-Glo 3D cell viability assay (G7571, Promega, Germany). Cells were seeded in triplicates on a 96-well plate. After 24 h, miR-181a-5p mimic was transfected according to section 2.5. After 48 h, 50 µl of CellTiter-Glo 3D Reagent was added to each well and mixed while shaking for 15 min. After an additional 15 min without shaking avoiding light, Luminescence was measured with a Microplate Reader luminometer (FLUOstar OPTIMA Microplate Reader, BMG Labtech, Germany).

Spectroscopy

A T2-weighted magnetic resonance (MR) tomography together with 1H-MR spectroscopy was performed on a 3T MR System (Trio, Siemens, Erlangen, Germany) for in detail analyses of tumor heterogeneity in patient 25. Thereby, a navigated extraction of tissue samples by co-registration of MR data and integration into the neuronavigation system (Curve Ceiling-Mounted, Brainlab, Munich, Germany) was enabled.

Statistical Analysis

Student's t-tests were applied for statistical analysis. For multiple comparisons, two-way ANOVA tests were used. A Wilcoxon-signed rank test and Pearson correlation were performed to determine differences or correlation in gene expression. Results were considered as not significant (ns) ($p > 0.05$), significant (*) ($p < 0.05$), highly significant (**) ($p < 0.01$), or very highly significant (***) ($p < 0.001$). Data from multiple replicates are presented as mean ± SD and statistical analyses were performed with GraphPad Prism (version 9.1.0) and Microsoft Excel.

RESULTS

ADAM8 Regulates Expression Levels of miR-181a-5p in GBM Cells

To determine potential ADAM8 correlated miRNAs, we generated stable ADAM8 knockout (KO) U87 cell clones using two guide RNAs (U87 gRNA cl. 1, U87 gRNA cl. 2) for the CRISPR/Cas9 homologous recombination method. U87 cells expressing high endogenous levels of ADAM8 were subjected to CRISPR/Cas9 induced genomic editing. After cell selection with puromycin, independent cell clones were grown and compared to U87 cells (in the following termed U87_CTRL) for morphological features and ADAM8 expression levels. From around 30 individual cell clones, two U87 gRNA clones were selected for further analyses (**Supplementary Figure 1**). Confirmation of successful ADAM8 knockout in these two U87 gRNA cell clones was provided by qPCR, Western Blot, and ELISA (**Figures 1A–C**). U87 gRNA cl. 1 and U87 gRNA cl. 2 (termed U87_KO1 and U87_KO2) showed a strong downregulation of *ADAM8* mRNA compared to U87_CTRL, $p < 0.001$ (**Figure 1A**). Western Blots confirmed successful ADAM8 knockout on the protein level (**Figure 1B**). In addition, ELISA measurements from cell supernatants revealed soluble ADAM8 levels below the detection limit in U87_KO clones compared to U87_CTRL ($p < 0.05$, **Figure 1C**). For two representative KO clones as well as a U87 control clone, a microRNA PCR Array (Human Finder) was screened. Differences in miRNA expression (given a ratio KO/CTRL) for both U87_KO clones are presented in a heatmap (**Figure 1D**) with green color representing upregulation of miRNA in U87_KO cells.

Several miRNAs were consistently upregulated in both KO clones and miR-181a-5p was selected for further investigations due to its reported regulation of osteopontin/SPP1 which also applies to ADAM8. Moreover, of all four miRNAs upregulated in U87 *ADAM8* KO cells, miR-181a-5p was the only one regulated after treatment of U87 wild-type cells with an ERK1/2 inhibitor indicating its influence in ADAM8-mediated signaling (**Supplementary Figure 2**). To further validate our miRNA screening, qPCR experiments were performed to detect miR-181a-5p expression in U87_KO and U87_CTRL cells. We

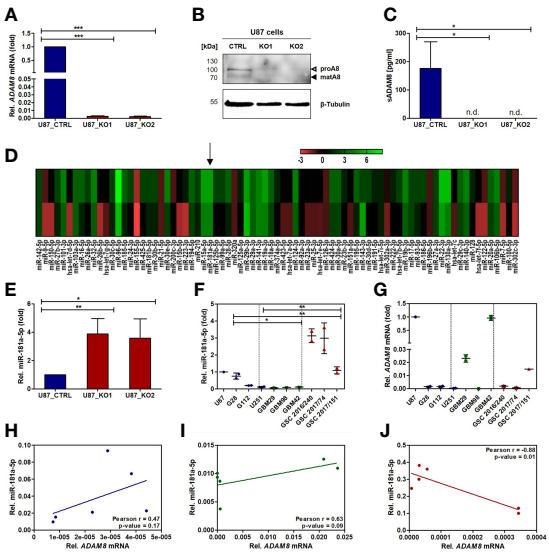

FIGURE 1 | Screening of two representative CRISPR/Cas9 ADAM8 (hA8) KO cell clones reveals an ADAM8-dependent regulation of miR-181a-5p. Confirmation of the CRISPR/Cas9 ADAM8 stable KO in U87 cells by qPCR **(A)**, Western Blot **(B)**, and ELISA **(C)**. **(D)** A RT-qPCR-based miRNA PCR Array (Human Finder, Qiagen) of U87 CRISPR/Cas9 ADAM8 KO cells enabling the analysis of a total of 84 miRNAs. The legend for the fold-changes in the heat map is given above representing the fold-change values ($2^{-\Delta\Delta CT}$) relative to U87_CTRL cells in both *ADAM8* KO clones. Note the variance in fold changes between the two KO clones **(E)** Confirmation of miR-181a-5p upregulation in U87_KO1 and U87_KO2 cells (p-value: 0.01 and 0.03). The expression of miR-181a-5p **(F)** and *ADAM8* **(G)** in GBM cell lines (G28, G112, U251), primary patient-derived cell lines (GBM29, 98, and 42), and GBM stem-like cell lines (GSCs) (GSC 2016/240, GSC 2017/74, GSC 2017/151) are shown as relative values to the expression in U87 cells. MiR-181a-5p is mostly expressed in GSCs. The patient-derived cell line GBM42 shows the highest ADAM8 expression. Pearson correlation analysis of miR-181a-5p and *ADAM8* in cell lines **(H)**, primary cell lines **(I)**, and primary GSCs **(J)** reveal a negative correlation only observed in GSCs (p-value: 0.01, Pearson r: -0.88). Results are given as mean +/- SD of two to three independent experiments. Unpaired two-tailed students *t-test* or two way ANOVA for multiple comparison **(F)** were applied to determine significance: *p < 0.05, **p < 0.01, ***p < 0.001. n.d., not detectable.

confirmed upregulation of miR-181a-5p in U87_KO1 and U87_KO2 compared to U87_CTRL cells, p < 0.05 and p < 0.01, respectively (**Figure 1E**).

Next, we analyzed the expression profiles of ADAM8 and miR-181a-5p in several GBM cell lines, including U87, U251, G112, G28, three primary patient-derived cell lines GBM42, GBM29, GBM98, and three patient-derived Glioblastoma stem-like cell lines (GSCs), 2016/240, 2017/151 and 2017/74 (**Figures 1F, G**). GSCs showed low ADAM8 mRNA and high miR-181a-5p expression levels. Primary GBM cell lines showed great variability in ADAM8 and miR-181a-5p expression with GBM42 with the highest ADAM8 levels. Interestingly, knocking ADAM8 down with siRNA showed elevated levels of miR-181a-5p in GBM42 (**Supplementary Figure 3**). Pearson correlation analyses revealed exclusively in the case of GSCs a clear negative correlation of ADAM8 and miR-181a-5p expression (**Figures 1H–J**). U87_CTRL cells as well as primary GBM42 cells showed the highest endogenous ADAM8 levels in qPCR experiments compared to all other cell lines and were selected for further experiments.

ADAM8 Regulates miR-181a-5p Expression *via* STAT3 and MAPK Signaling

To analyze the apparent ADAM8/miR-181a-5p dependence on the mechanistic level, we tested the contribution of either the metalloprotease activity or the functions of the non-proteolytic domains (DC/CD) of ADAM8 on miR-181a-5p expression. To address this, U87 cells were treated with either a broad-range metalloprotease inhibitor BB-94 (Batimastat) or with BK-1361, a selective ADAM8 inhibitor. While BB-94 did not affect miR-181a-5p expression, treatment with 10 µM and even 5 µM BK-1361 led to an increase in miR-181a-5p expression, p < 0.05 (**Figure 2A**) suggesting a contribution of the DC/CD domain on miR-181a-5p regulation by ADAM8. Moreover, we transiently re-expressed ADAM8 in U87_KO1 and analyzed the effect on miR-181a-5p expression. U87 gRNA_KO2 was transfected with either wild-type ADAM8 (hA8) or with an ADAM8 variant lacking the cytoplasmatic domain (Delta CD). Western Blots confirmed re-expression of ADAM8 variants (**Figure 2B**).

Re-expression of wild-type ADAM8 caused a downregulation of miR-181a-5p, p < 0.01 (**Figure 2B**). In contrast, cells expressing the ADAM8 delta CD variant showed no downregulation of miR-181a-5p (**Figure 2B**). These results indicate that the cytoplasmatic domain of ADAM8 triggers signaling cascades that lead to the downregulation of miR-181a-5p concomitant with a trend of increased pSTAT3 in cells transfected with wild-type ADAM8 (**Figure 2B**). Interestingly, this regulation only works in one direction, as changes in miR-181a-5p expression, i.e. by mimic transfection, do not affect expression levels of ADAM8 in U87 cells (**Figure 2C**). We explored the role of two downstream signaling pathways of ADAM8 CD, STAT3 signaling and MAPK signaling. For this purpose, U87 cells and primary GBM cells GBM42 were treated with either U0126 (MEK1/2 inhibitor) or WP1066 (STAT3 inhibitor). MEK1/2 inhibition caused an increase in miR-181a-5p expression in U87_CTRL cells (p < 0.05), and a tendency to increase in primary GBM42 cells (p-value: 0.052) (**Supplementary Figure 4**). More prominently, STAT3 inhibition by WP1066 was confirmed for both cell lines *via* western blot and resulted in increased expression levels of miR-181a-5p in both cell lines with p < 0.05 (**Figures 2D, E**).

MiR-181a-5p Regulates Cell Proliferation and MMP9 Expression

We further analyzed whether miR-181a-5p can affect the cell proliferation of GBM cells. Exemplified for U87_KO2, a decrease in cell proliferation was observed (p < 0.001, **Figure 3A**). This effect can be recapitulated when mimic miR-181a-5p was transfected into U87 cells (p < 0.01, **Figure 3B**). As an oncoprotein able to promote GBM cell proliferation, we analyzed *MMP9* expression in U87_KO2 and mimic transfected U87 cells (**Figures 3C, D**) (27). *MMP9* mRNA levels in U87_KO2 and mimic transfected cells are strongly downregulated as revealed by qPCR (p < 0.001, **Figure 3C**).

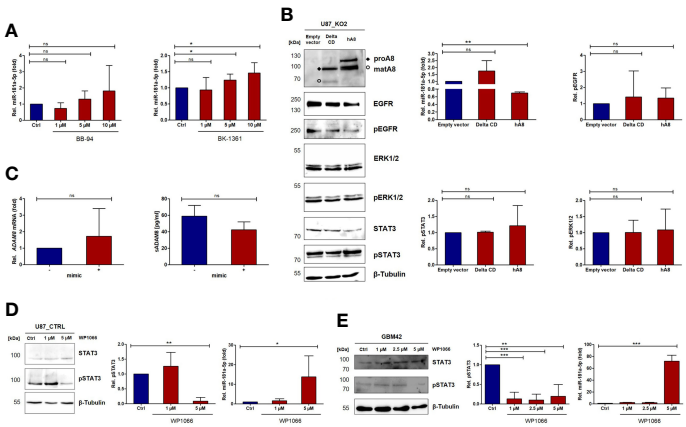

FIGURE 2 | ADAM8 regulates the expression of miR-181a-5p *via* JAK2/STAT3 signaling. **(A)** U87_CTRL cells were analyzed for miR-181a-5p expression by RT-qPCR after treatment with the broad-spectrum MMP inhibitor BB-94 (left) and the ADAM8 inhibitor BK-1361 (right). **(B)** One representative western blot of three independent experiments shows the rescue of either ADAM8 lacking the cytoplasmatic domain (Delta CD) or the full-length ADAM8 (hA8). The quantifications of pEGFR, pSTAT3, and pERK1/2 are depicted on the right side and were normalized to β-Tubulin and total-EGFR/β-Tubulin, total STAT3/β-Tubulin, or total ERK1/2/β-Tubulin. Also, RT-qPCR results show no differences in miR-181a-5p expression after the transfection of ADAM8 Delta CD but a downregulation with the full-length ADAM8 rescue (p-value: 0.002). **(C)** The expression of *ADAM8* mRNA (RT-qPCR, left) and secreted ADAM8 (ELISA, right, n=2) is not affected after miR-181a-5p mimic transfection. U87_CTRL cells **(D)** and patient-derived GBM42 cells **(E)** were treated with JAK2/STAT3 inhibitor WP1066 as indicated and analyzed *via* western blot and RT-qPCR. In **(D)**, qPCR results are shown as mean values +/- SD of four independent experiments and in **(E)**, results of miR-181a-5p are described as mean values of three technical replicates. Inhibition of JAK2/STAT3 increases miR-181a-5p expression (U87 p-value: 0.027; GBM42 p-value: 0.004). Results are shown as mean values +/- SD from three independent experiments if not otherwise stated. Unpaired two-tailed students *t-test* was applied to determine significance: ns, not significant, *p < 0.05, **p < 0.01, ***p < 0.001.

After mimic miR-181a-5p transfection of U87 cells, ELISA experiments revealed less soluble MMP9 levels in cellular supernatants ($p < 0.05$, **Figure 3D**). Comparable results were obtained for osteopontin (**Supplementary Figure 7**). Next, we explored whether miR-181a-5p dependent MMP9 downregulation is a result of direct miR-181-a/*MMP9* mRNA interaction. Three target prediction tools, miRDB, TargetScan, and TargetMiner, predicted no miR-181a-5p binding site. Also, bioinformatic analysis of the MMP9 3' UTR did not reveal a sufficiently long binding site for miR-181a-5p. Thus, we conclude that MMP9 is most likely indirectly regulated by miR-181a-5p. Indeed, literature research and the utilization of the target prediction tools miRDB and TargetScan revealed that miR-181a-5p directly targets three kinases of the MAPK pathway, CREB-1, MEK1, and ERK2 (**Supplementary Table 1**, 38, 39). To demonstrate that, transfection of U87_CTRL cells with a miR-181a-5p mimic was performed and revealed downregulation of pERK1/2 and p-CREB-1 in three independent Western Blot experiments, with $p < 0.01$ and $p < 0.001$, respectively (**Figure 3E**). Notably unphosphorylated levels of ERK1/2 and CREB-1 were not influenced by mimic transfection (**Figure 3E**). Thus, our results further support ERK2 and CREB-1 as downstream targets of miR-181a-5p.

EVs Derived From U87_KO Cells Are Associated With Higher miR-181a-5p Levels

Having demonstrated the intracellular effects of ADAM8 on miR-181a-5p and *MMP9* as a target gene, we further investigated whether EVs derived from cellular supernatants of U87_CTRL (CTRL_EVs), U87_KO1 (KO1_EVs), and U87_KO2 (KO2_EVs) are associated with miR-181a-5p expression. By Nanoflow Cytometry Measurement (NanoFCM), the size and concentration of EVs prepared from cellular supernatants were analyzed (**Figures 4A, B**). Western Blot experiments further confirmed the presence of EVs using FLOTILLIN-1 and CD81 as EV markers, CALNEXIN as a negative control, and ß-Tubulin as a predominant lysate marker (**Figure 4C**). MiR-181a-5p was detected in all three EV populations (CTRL_EVs, KO1_EVs, KO2_EVs) and consistent with our observation in U87_CTRL and U87_KO cells, KO1_EVs and KO2_EVs displayed higher miR-181a-5p levels than CTRL_EVs (**Figure 4D**). To ensure that more miR-181a-5p is packed in EVs with higher cellular expression, we separated EVs from ctrl and mimic transfected cells with a 28-fold enrichment of miR-181a-5p in EVs derived from mimic transfected cells (**Supplementary Figure 8**). Furthermore, we confirmed the uptake of KO2_EVs by U87_CTRL cells *via* immunofluorescent microscopy by incubating CFSE-stained KO2_EVs as well as CTRL_EVs with Hoechst-stained U87_CTRL cells (**Supplementary Figure 9A**). Western blot analysis showed downregulation of MMP9 in U87_CTRL cells incubated with both CTRL_EVs and KO2_EVs in comparison to the HBSS control but did not confirm a significant difference of MMP9 expression comparing cells incubated with KO2_EVs or CTRL-EVs (**Supplementary Figure 9B**). We treated U87_KO2 cells with either miR-181a-5p-mimics or a miR181a-5p inhibitor and incubated the corresponding EVs with U87_CTRL cells. An

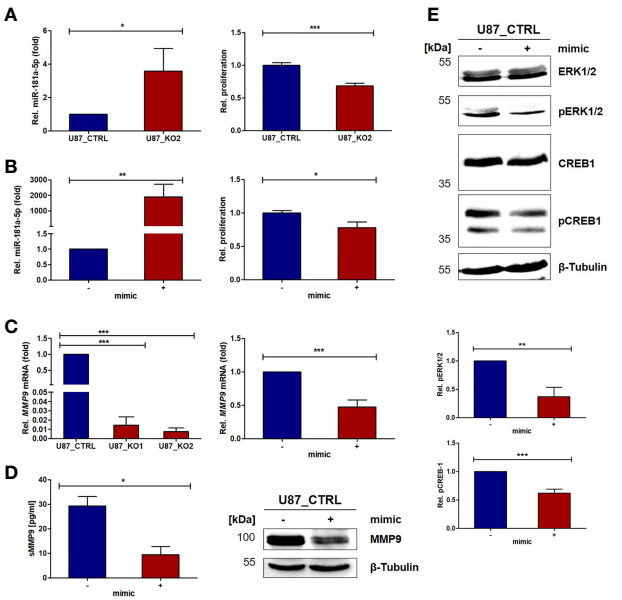

FIGURE 3 | ADAM8 affects MMP9 expression and proliferation *via* miR-181a-5p targeting ERK2 and CREB-1. **(A)** The upregulation of miR-181a-5p in U87_KO cells (RT-qPCR, n=3, left) causes inhibition of proliferation (CellTiter Glo, n=2, measurement after 48 h, right). **(B)** Overexpressing miR-181a-5p in U87_CTRL cells *via* transient transfection (RT-qPCR, n=3, left) causes inhibition of proliferation after 48 h (CellTiter Glo, n=3 technical replicates, right). **(C)** MMP9 is downregulated in U87_KO cells on mRNA (RT-qPCR, n=3, left). After miR-181a-5p mimic transfection, MMP9 is downregulated in U87 cells on the mRNA (RT-qPCR, n=3, p-value: 0.0009) **(C)** and on protein level (ELISA, n=2, p-value: 0.0004) analyzed by western blot **(D)**. **(E)** Analyses of kinase activation after miR-181a-5p mimic transfection for ERK1/2 (p-value: 0.003) and CREB-1 (p-value: 0.0007). Results are shown as mean values +/- SD of three independent experiments unless otherwise stated. Results are given in mean +/- SD. Unpaired one-tailed students *t* test was applied to determine significance: *p < 0.05, **p < 0.01, ***p < 0.001.

ELISA experiment revealed that incubation of inhibitor-treated EVs led to increased soluble MMP9 levels whilst incubation of miR-181a-5p-mimic treated EVs caused a decrease in soluble MMP9 (**Supplementary Figure 9C**).

Characterization of ADAM8, MMP9, and miR-181a-5p Expression in GBM Tumor Tissue Samples

RT-qPCR experiments were conducted on 22 tumor tissue samples from patients admitted to our clinical department to analyze the expression profiles of *ADAM8*, *MMP9*, and miR-181a-5p in GBM tissue. Further information on the patient cohort and histopathological data are listed in **Table 1**. For normalization of data (set to 1 in **Figures 5A–D**), we utilized tissue samples localized most remote from the tumor core. The majority of the examined tumor tissue samples showed downregulation of miR-181a-5p (**Figure 5C**). In contrast, mean *ADAM8* and *MMP9* expression levels were upregulated in the investigated tumor samples (**Figure 5A**). High *ADAM8* correlated with elevated *MMP9* expression levels, $p < 0.0001$ (**Figure 5D**). In the patient cohort, neither *ADAM8* mRNA levels nor *MMP9* mRNA levels correlated with miR-181a-5p expression, $p = 0.6$ and $p = 0.63$ respectively (**Figure 5D**). We then divided the patient cohort into subgroups, high *ADAM8* expression, and low *ADAM8* expression group, as well as high miR-181a-5p expression and low miR-181a-5p expression group (**Supplementary Figure 9**). *MMP9* expression was elevated in the high *ADAM8* group, $p = 0.01$ (**Figure 5B**). MiR-181a-5p expression was similar in the high *ADAM8* and low *ADAM8* groups (**Figure 5B**). *MMP9* expression was also similar in both miR-181a-5p subgroups (**Figure 5B**). To further investigate if this trend is due to the strong heterogeneity of the GBM tissue, we explored the connection between ADAM8, MMP9, and miR-181a-5p in a pilot experiment using MR-spectroscopy guided surgery at different locations in a GBM tumor tissue

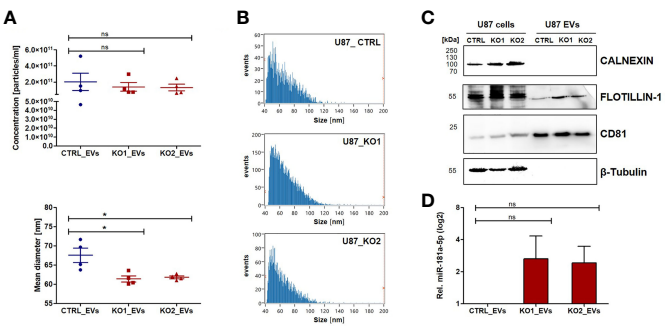

FIGURE 4 | ADAM8 affects miRNA181a-5p levels associated with EVs in U87 cells. **(A)** U87_CTRL and U87_KO derived EVs were characterized regarding their concentration (upper graph) and size (lower graph). Measurements were taken with the NanoFCM device and results are shown as mean values +/- SEM of four independent experiments. **(B)** Representative size distributions of U87_CTRL and U87_KO derived EVs (NanoFCM) are shown in bar graphs. **(C)** *Via* western blot, the presence of EVs was confirmed. CALNEXIN was used as negative control and FLOTILLIN-1 as well as CD81 as EV markers. **(D)** MiR-181a-5p is detectable in U87 derived EVs. RT-qPCR results show a non-significant tendency of miR-181a-5p upregulation in U87_ KO derived EVs. Mean values +/- SD of three independent experiments if not otherwise stated. Unpaired two-tailed students *t-test* was applied to determine significance: ns, not significant, *p < 0.05.

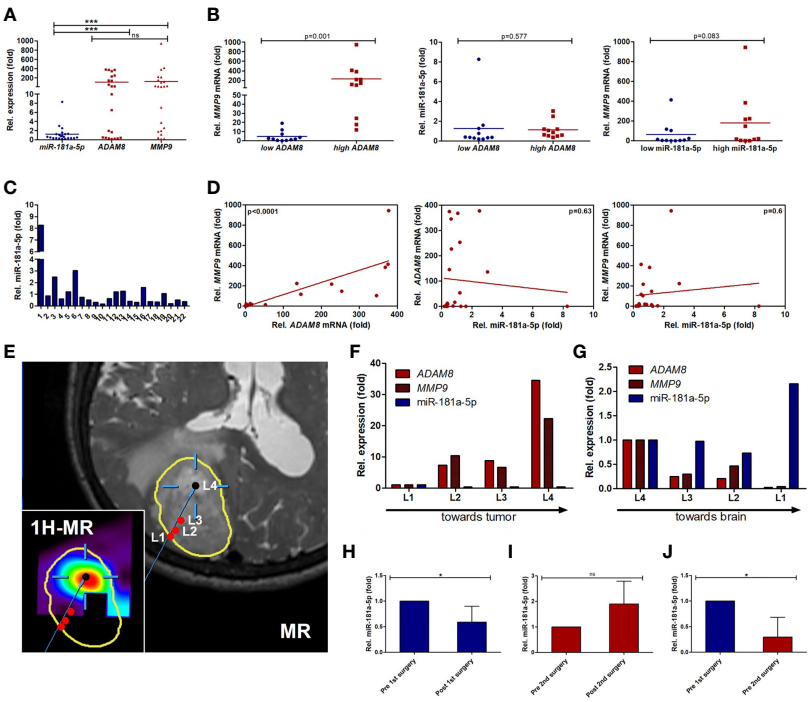

FIGURE 5 | Expression levels of *ADAM8* and *MMP9*, and miR-181a-5p in GBM tissue samples. **(A)** RT-qPCR results of GBM tissue samples (n=22, fold change normalized to 1) indicate a higher expression of *ADAM8* (p-value: 0.0009) and *MMP9* (p-value: 0.0002) than miR-181a-5p. **(B)** Dividing the RT-qPCR results and patient cohort into two groups (low/high *ADAM8* or low/high miR-181a-5p expression) reveals a correlation of *ADAM8* with *MMP9* (left graph, p-value: 0.001) but no correlation of miR-181a-5p with *ADAM8* (middle graph, p-value: 0.577) or *MMP9* (right graph, p-value: 0.083) expression. **(C)** RT-qPCR results for miR-181a-5p expression of each GBM tissue sample. **(D)** *ADAM8* and *MMP9* are correlated in GBM tissue samples ($p < 0.0001$, n=22), whereas the inverse correlations of *ADAM8* and miR-181a-5p and of miR-181a-5p and *MMP9* are non-significant (p-values: 0.63 and 0.6, respectively). **(E)** T2-weighted magnetic resonance (MR) image showing a left parietal GBM (segmented in yellow, patient 25) as well as the co-registered choline/N-acetylaspartate (NAA) maps derived from 1H-MR spectroscopy, integrated into the neuronavigation system for navigated extraction of tissue samples (L1: tumor border, L2/L3: tumor, L4: tumor, Cho/NAA hotspot) magnetic resonance (heatmap for choline metabolite). Corresponding molecular analyses are shown in **(F, G)** (patient 25). RT-qPCR results of *ADAM8* (red), *MMP9* (tiled red), and miR-181a-5p (blue) in different tissue locations normalized to either L1 **(F)** or L4 **(G)** describing the direction of surgery. **(H)** In a pilot study, three GBM patients (Patient 9, 23, 24) were analyzed for their serum-EV miR-181a-5p expression *via* RT-qPCR. The serum was collected before and after the first and second surgery. Interestingly, after first surgical resection miR-181a-5p is less expressed in serum-EVs (p-value: 0.042). **(I)** After second surgery, miR-181a-5p shows a slight increase in serum-EVs (p-value: 0.08). **(J)**, miR-181a-5p is less detectable in serum-EVs prior to the second surgery compared to pre-first surgery (p-value: 0.02; left graph). Results are shown in mean values +/- SD. Unpaired one-tailed students *t* test and Wilcoxon signed-rank test were applied to determine significance: ns, not significant, *$p < 0.05$, **$p < 0.01$, ***$p < 0.001$.

sample of one selected patient. In the non-tumorous access tissue (L1), miR-181a-5p showed the highest expression whereas *ADAM8* and *MMP9* expression is at the lowest level (**Figures 5E–G**). Analysis of tumor edge (L2 and L3) and core tumor (L4) with strongly proliferating and vascularized zones revealed reversed expression patterns for *MMP9*, *ADAM8*, and miR-181a-5p (**Figures 5E–G**). Tumor locations in L3 and L4 were also confirmed by 1H-MR spectroscopy (**Supplementary Table 2**).

MiR-181a-5p Expression in Serum-Derived EVs From GBM Patients

In a further pilot study, serum specimens from three GBM patients were obtained before and after surgical resection. All three patients suffered from tumor recurrence and underwent surgical resection for a second time. In all cases, the highest miR-181a-5p expression levels were observed in serum samples prior to the first surgical resection (**Figure 5H**). After the first surgery, a reduction in miR-181a-5p levels was observed in post-surgery serum-derived EVs, $p < 0.05$ (5H). In contrast, after the second surgery, miR-181a-5p expression was slightly upregulated (**Figure 5I**). A comparison of primary manifested GBM and recurrent GBM revealed a decrease in miR-181a-5p expression in EVs, $p < 0.05$ (5K). These results suggest that miR-181a-5p could serve as a tumor marker, but needs to be sufficiently powered in further studies.

DISCUSSION

ADAM8 as a multidomain enzyme exhibits numerous tumor-supporting characteristics by promoting invasion, angiogenesis, and chemoresistance in GBM (10, 12). Due to these multiple functions, ADAM8 affects several intracellular pathways involving several important kinases and transcription factors

such as JAK2/STAT, AKT/PI3K, ERK1/2, and CREB-1 (8–12). Mechanistically, the ADAM8 metalloprotease domain cleaves extracellular membrane components while the cytoplasmatic domain activates crucial signaling cascades in carcinogenesis (4). Thereby, ADAM8 induces the expression of several oncoproteins including MMP9 and *SPP1*/osteopontin (8, 10). Previously, we demonstrated that ADAM8-dependent MMP9 expression is mediated *via* the MAPK pathway and resulted in a strong correlation of ADAM8 and MMP9 in breast cancer-derived brain metastasis (8). By characterizing the expression profile of ADAM8 and MMP9 in GBM tissue samples, we confirmed these observations for GBM. To dissect the effects of ADAM8 on oncoproteins mechanistically, we hypothesized that ADAM8 could alter the expression levels of distinct miRNAs such as miR-720, as previously shown for breast cancer cells (13). Generation of stable ADAM8 KO clones with subsequent miRNA screening revealed that the tumor suppressor miRNA miR-181a-5p shows a significantly higher expression in GBM cells deficient in ADAM8. Since high ADAM8 levels are correlated with GBM progression, a downregulation of miRNA181a-5p would be expected. Indeed, a recent study linked the poor prognosis of GBM patients with low miRNA181a-5p expression levels (40). Together, these findings qualified miRNA181a-5p as a candidate for a detailed molecular analysis, as presented here. Transient re-expression of ADAM8 in U87_KO cells resulted in downregulation of miR-181a-5p, suggesting that ADAM8 actively suppresses the expression of miR-181a-5p. Downregulation of miR-181a-5p by ADAM8 is dependent on the presence of the cytoplasmatic domain. In GBM, miR-181a-5p acts as a tumor suppressor miRNA by reducing invasiveness and enhancing radio- and chemosensitivity (23, 41). We confirmed that overexpression of miR-181a-5p led to reduced proliferation rates in U87 cells. Moreover, a similar effect on cell proliferation was observed in ADAM8 deficient GBM cells. It was shown that miR-181a-5p suppresses cell colony formation and tumor growth, and regulates apoptosis by targeting BCL-2 (23, 41). It is interesting to note that GSCs express relatively high levels of miRNA181a-5p compared to differentiated GBM cells, which could be instrumental in regulating proliferation and cell survival of this particular cell type. We have evidence that ADAM8 and, negatively correlated, miRNA181a-5p levels change in GSCs under conditions favoring differentiation of GSCs (Schäfer, unpublished data). However, the mechanisms that lead to miR-181a-5p downregulation in GBM remained elusive until now. As ADAM8 is a membrane-anchored protein, we concluded that ADAM8 downregulates the expression of miR-181a-5p by downstream signaling and activation of transcription factors. Indeed, our results revealed that miR-181a-5p can be downregulated by the activation of STAT3 and MAPK pathways. Conversely, miRNA181a-5p can regulate either total STAT3 levels in U87 cells and, notably, affect levels of p-STAT3 in the primary GBM cell line GBM42, indicating an unknown mechanism of kinase regulation by miRNA, similar to an observation made for phospho-AKT and p-ERK in a previous study in glioma (42) Previously, the importance of STAT3 signaling in GBM has been demonstrated in numerous studies whilst our group showed that ADAM8 dependent activation of STAT3 signaling led to increased angiogenesis by upregulation of osteopontin (10, 43, 44, reviewed in 45). In agreement with these findings, the 3'UTR of *SPP1*/osteopontin contains a binding site for miR-181a-5p and can be downregulated upon miR-181a-5p overexpression (19). All these results support the existence of a possible ADAM8/STAT3/miR-181a/osteopontin axis in GBM (**Figure 6** left). In addition, increased activation of the MAPK pathway is observed in numerous malignant tumors and leads to uncontrolled cell growth and mitosis (46). One of the best-known activators of the MAPK signaling pathway is the EGFR. Frequently, primary GBM tumors display a constitutively active variant, EGFRvIII (47). Apart from EGFR dependent MAPK activation, ADAM8 can activate the MAPK pathway EGFR independently (9). Interestingly, two kinases of the MAPK pathway, ERK2, and MEK1 as well as the downstream transcription factor CREB-1 are known to contain binding sites for miR-181a-5p (25, 26). In our experiments, phosphorylated and thus activated pCREB and pERK1/2 were downregulated in U87 cells transfected with miR-181a-5p mimics. We did not observe any effects on unphosphorylated CREB-1 and ERK1/2 as well as on MEK1/2 expression. Since miRNAs are post-transcriptional regulators of protein expression, we do not fully understand these results, but a TargetScan search revealed that CRBL2, a protein regulating phosphorylation of CREB1 is directly regulated by miR181a-5p, adding one more level of complexity to the network we have described here. A study by Fu et al. showed that CREB-1 suppresses miR-181a-5p transcription by directly binding to its promoter region (48). Thus, the interaction of miR-181a-5p and the MAPK pathway may constitute a regulatory loop that requires further investigation. Furthermore, we can postulate that our results describing the regulation of miR-181a-5p by ADAM8 are not restricted to the role of ADAM8 in GBM, as all other tumor cell lines that we investigated so far such as the triple-negative breast cancer cell line MDA-MB-231 and the PDAC cell line Panc89 show elevated levels of miR-181a-5p upon ADAM8 deficiency (unpublished observations). In accordance, MDA-MB-231 were among those cell lines that showed a strong correlation between ADAM8 and MMP9 expression in our previous study on breast cancer-derived brain metastases (8).

MMP9 plays a central role in tumor progression, especially for cell proliferation and invasion (27). Moreover, MMP9 expression is a prognostic factor in GBM and negatively correlated with patient survival (30). Thus, exploring the miR-181a-5p dependent *MMP9* downregulation was particularly interesting. U87 cells overexpressing miR-181a-5p exhibited decreased MMP9 levels. This was observed in U87 ADAM8 knockout cells as well as U87_CTRL cells incubated with miR-181a-5p mimics. To further establish whether *MMP9* mRNA contains a binding site for miR-181a-5p, we utilized target prediction tools and analyzed the mRNA sequence of MMP9. However, this analysis revealed that the *MMP9* mRNA does not contain an authentic binding site for miR-181a-5p.

Consequently, we concluded that miR-181a-5p can indirectly downregulate MMP9 expression by silencing the MAPK cascade (**Figure 6** right). This conclusion is supported by data showing that ERK1/2 inhibition led to decreased MMP9 levels in U87 and GBM42 cells (**Supplementary Figure 5**).

All these results demonstrate intracellular regulatory mechanisms of ADAM8/miR-181a-5p signaling so far. Cell-cell communication in the tumor microenvironment is essential for shaping either an immunosuppressive or a tumor-supportive microenvironment (34). As one mode of cell-cell communication, tumor cells release EVs. These heterogeneous nanoparticles contain a great variety of different molecules including miRNAs (35). Clinically, EVs received increasing attention, as their function as novel diagnostic and prognostic biomarkers is discussed (49). In our study, we analyzed the miR-181a-5p expression in U87 cells and serum-derived EVs. We recapitulated the higher abundance of miR-181a-5p in EVs from ADAM8 KO cells. Concerning patient sera, miR-181-5p expression in EVs dropped after the first surgical tumor resection. Moreover, miR-181a-5p expression was downregulated in serum-derived EVs from recurrent GBM. These results suggest that miR-181a-5p is further downregulated along with tumor progression. However, additional analyses must be carried out in a larger patient cohort to support this conclusion. The uptake of EVs can alter the behavior of recipient cells (50). Therefore, EVs might also be utilized as therapeutic vehicles (51). In our experiments, miR-181a-5p enriched vesicles were taken up by naive U87 cells demonstrating a role for ADAM8 in the tumor microenvironment. It remains to be determined if GBM resident immune cells such as macrophages that constitutively express ADAM8 could release EVs that might fail to suppress MMP9 expression in target cells, in conjunction with the possible tumor-promoting role of ADAM8 in macrophages (33).

Due to limited therapeutic options as well as the absence of early diagnostic biomarkers, GBM remains challenging as an incurable disease with a grim prognosis. Therefore, the identification of potential biomarkers as well as new therapeutic targets is of high importance. In summary, we identified that ADAM8 downregulates miR-181a-5p by activation of STAT3 and MAPK signaling. Considering that miR-181a-5p is a tumor suppressor miRNA in GBM, ADAM8 dependent silencing of miR-181a-5p could further contribute to

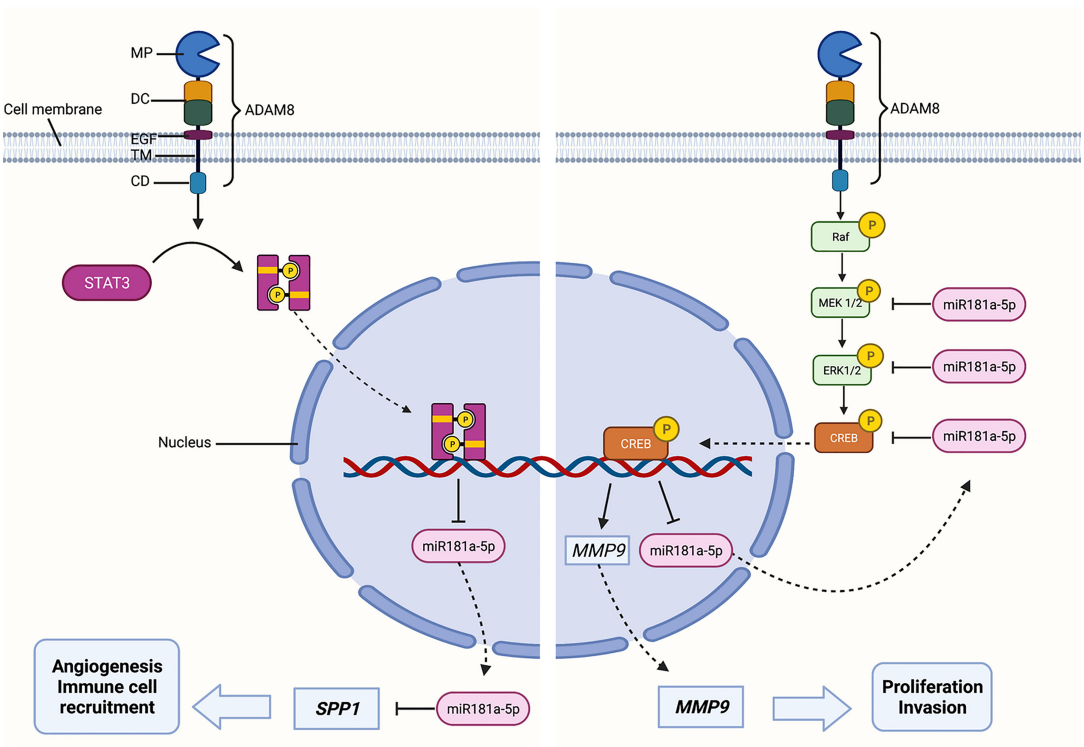

FIGURE 6 | Sketch of ADAM8-dependent effects caused by regulation of miR-181a-5p in GBM cells. ADAM8 with homologous domains including the metalloprotease domain (MP), the disintegrin/cysteine-rich domain (DC), the EGF-like domain (EGF), the transmembrane (TM), and the cytoplasmic domain (CD). ADAM8 activates intracellular signaling cascades by STAT3 and MAPK in the presence of the cytoplasmic domain. ADAM8/STAT3/miR-181a/*SPP1* axis: ADAM8 dependent STAT3 activation downregulates miR-181a-5p, as miR-181a-5p targets *SPP1*, disinhibition of *SPP1* leads to several tumor progressing effects such as induction of angiogenesis and enhanced immune cell recruitment. ADAM8/MAPK/MMP9 axis: ADAM8 activates the MAPK pathway, the transcription factor CREB-1 induces MMP9 transcription and inhibits miR-181a-5p transcription. MMP9 promotes tumor cell proliferation and invasion. By targeting CREB-1, ERK2, and MEK1, miR-181a-5p downregulates MMP9 expression most likely by an indirect mechanism. Created with BioRender.com.

tumor progression. We showed that overexpression of miR-181a-5p decreased cell proliferation and suppressed MMP9 expression by downregulation of the MAPK pathway Moreover, the presence of miR-181a-5p in clinical samples and EVs isolated from cellular supernatants as well as patient sera justifies further studies to reveal a potential role of miR-181a-5p in GBM diagnosis and progression.

DATA AVAILABILITY STATEMENT

The raw data supporting the conclusions of this article will be made available by the authors, without undue reservation.

ETHICS STATEMENT

The studies involving human participants were reviewed and approved by Local Ethics Committee (Philipps University Marburg, medical faculty, file number 185/11). The patients/participants provided their written informed consent to participate in this study.

AUTHOR CONTRIBUTIONS

JWB, ES, BC, CN, and MB conceived this study. AS, LE, LM, US, GLD, ABB, OL, and CP performed experiments and evaluated the data. ACB, MP, CN, and BC provided resources and clinical data. AS, LE, and JWB wrote the manuscript draft. MB, CN, and MP reviewed and edited the manuscript. All authors contributed to the article and approved the submitted version.

FUNDING

Work was supported in the framework of ERANET PerMed joint call 2018, project PerProGlio by the Federal Ministry for Education and Research (BMBF), grant number 01KU1915B to JWB, AS and by the Deutsche Forschungsgemeinschaft (DFG) grant BA1606/3-1 to US and JWB, and GRK 2573/1 to ES, and by a Research Grant from the University Medical Center Giessen and Marburg (UKGM). Open Access was kindly supported by the University of Marburg and the DFG.

ACKNOWLEDGMENTS

The authors thank Susanne Stei for her expert technical assistance. We also thank Dr. Miriam Frech (Clinic for Hematology and Oncology, Marburg) for her kind support with antibodies.

SUPPLEMENTARY MATERIAL

The Supplementary Material for this article can be found online at: https://www.frontiersin.org/articles/10.3389/fonc.2022.826273/full#supplementary-material

REFERENCES

1. Alifieris C, Trafalis DT. Glioblastoma Multiforme: Pathogenesis and Treatment. *Pharmacol Ther* (2015) 152:63–82. doi: 10.1016/j.pharmthera.2015.05.005
2. Vollmann-Zwerenz A, Leidgens V, Feliciello G, Klein CA, Hau P. Tumor Cell Invasion in Glioblastoma. *Int J Mol Sci* (2020) 21(6):1932. doi: 10.3390/ijms21061932
3. Murphy G. The ADAMs: Signalling Scissors in the Tumour Microenvironment. *Nat Rev Cancer* (2008) 8(12):929–41. doi: 10.1038/nrc2459
4. Conrad C, Benzel J, Dorzweiler K, Cook L, Schlomann U, Zarbock A, et al. ADAM8 in Invasive Cancers: Links to Tumor Progression, Metastasis, and Chemoresistance. *Clin Sci (Lond)* (2019) 133(1):83–99. doi: 10.1042/CS20180906
5. He S, Ding L, Cao Y, Li G, Deng J, Tu Y, et al. Overexpression of a Disintegrin and Metalloprotease 8 in Human Gliomas is Implicated in Tumor Progression and Prognosis. *Med Oncol* (2012) 29(3):2032–7. doi: 10.1007/s12032-011-0084-9
6. Romagnoli M, Mineva ND, Polmear M, Conrad C, Srinivasan S, Loussouarn D, et al. ADAM8 Expression in Invasive Breast Cancer Promotes Tumor Dissemination and Metastasis. *EMBO Mol Med* (2014) 6(2):278–94. doi: 10.1002/emmm.20130337
7. Valkovskaya N, Kayed H, Felix K, Hartmann D, Giese NA, Osinsky SP, et al. ADAM8 Expression is Associated With Increased Invasiveness and Reduced Patient Survival in Pancreatic Cancer. *J Cell Mol Med* (2007) 11(5):1162–74. doi: 10.1111/j.1582-4934.2007.00082.x
8. Conrad C, Götte M, Schlomann U, Roessler M, Pagenstecher A, Anderson P, et al. ADAM8 Expression in Breast Cancer Derived Brain Metastases: Functional Implications on MMP-9 Expression and Transendothelial Migration in Breast Cancer Cells. *Int J Cancer* (2018) 142(4):779–91. doi: 10.1002/ijc.31090
9. Schlomann U, Koller G, Conrad C, Ferdous T, Golfi P, Garcia AM, et al. ADAM8 as a Drug Target in Pancreatic Cancer. *Nat Commun* (2015) 6:6175. doi: 10.1038/ncomms7175
10. Li Y, Guo S, Zhao K, Conrad C, Driescher C, Rothbart V, et al. ADAM8 Affects Glioblastoma Progression by Regulating Osteopontin-Mediated Angiogenesis. *Biol Chem* (2021) 402(2):195–206. doi: 10.1515/hsz-2020-0184
11. Awan T, Babendreyer A, Mahmood Alvi A, Düsterhöft S, Lambertz D, Bartsch JW, et al. Expression Levels of the Metalloproteinase ADAM8 Critically Regulate Proliferation, Migration and Malignant Signalling Events in Hepatoma Cells. *J Cell Mol Med* (2021) 25(4):1982–99. doi: 10.1111/jcmm.16015
12. Dong F, Eibach M, Bartsch JW, Dolga AM, Schlomann U, Conrad C, et al. The Metalloprotease-Disintegrin ADAM8 Contributes to Temozolomide Chemoresistance and Enhanced Invasiveness of Human Glioblastoma Cells. *Neuro Oncol* (2015) 17(11):1474–85. doi: 10.1093/neuonc/nov042
13. Das SG, Romagnoli M, Mineva ND, Barillé-Nion S, Jézéquel P, Campone M, et al. miR-720 is a Downstream Target of an ADAM8-Induced ERK Signaling Cascade That Promotes the Migratory and Invasive Phenotype of Triple-Negative Breast Cancer Cells. *Breast Cancer Res* (2016) 18(1):40. doi: 10.1186/s13058-016-0699-z
14. O'Brien J, Hayder H, Zayed Y, Peng C. Overview of MicroRNA Biogenesis, Mechanisms of Actions, and Circulation. *Front Endocrinol (Lausanne)* (2018) 9:402:402. doi: 10.3389/fendo.2018.00402
15. Fabian MR, Sonenberg N, Filipowicz W. Regulation of mRNA Translation and Stability by microRNAs. *Annu Rev Biochem* (2010) 79:351–79. doi: 10.1146/annurev-biochem-060308-103103
16. Ali Syeda Z, Langden SSS, Munkhzul C, Lee M, Song SJ. Regulatory Mechanism of MicroRNA Expression in Cancer. *Int J Mol Sci* (2020) 21(5):1723. doi: 10.3390/ijms21051723

17. Møller HG, Rasmussen AP, Andersen HH, Johnsen KB, Henriksen M, Duroux M. A Systematic Review of microRNA in Glioblastoma Multiforme: Micro-Modulators in the Mesenchymal Mode of Migration and Invasion. *Mol Neurobiol* (2013) 47(1):131–44. doi: 10.1007/s12035-012-8349-7
18. Shea A, Harish V, Afzal Z, Chijioke J, Kedir H, Dusmatova S, et al. MicroRNAs in Glioblastoma Multiforme Pathogenesis and Therapeutics. *Cancer Med* (2016) 5(8):1917–46. doi: 10.1002/cam4.775
19. Marisetty A, Wei J, Kong LY, Ott M, Fang D, Sabbagh A, et al. MiR-181 Family Modulates Osteopontin in Glioblastoma Multiforme. *Cancers (Basel)* (2020) 12(12):3813. doi: 10.3390/cancers1212381
20. Ciafrè SA, Galardi S, Mangiola A, Ferracin M, Liu CG, Sabatino G, et al. Extensive Modulation of a Set of microRNAs in Primary Glioblastoma. *Biochem Biophys Res Commun* (2005) 334(4):1351–8. doi: 10.1016/j.bbrc.2005.07.030
21. Wang H, Tao T, Yan W, Feng Y, Wang Y, Cai J, et al. Upregulation of miR-181s Reverses Mesenchymal Transition by Targeting KPNA4 in Glioblastoma. *Sci Rep* (2015) 5:13072. doi: 10.1038/srep13072
22. Wei J, Marisetty A, Schrand B, Gabrusiewicz K, Hashimoto Y, Ott M, et al. Osteopontin Mediates Glioblastoma-Associated Macrophage Infiltration and is a Potential Therapeutic Target. *J Clin Invest* (2019) 129(1):137–49. doi: 10.1172/jci121266
23. Chen G, Zhu W, Shi D, Lv L, Zhang C, Liu P, et al. MicroRNA-181a Sensitizes Human Malignant Glioma U87MG Cells to Radiation by Targeting Bcl-2. *Oncol Rep* (2010) 23(4):997–1003. doi: 10.3892/or_00000725
24. Shi L, Cheng Z, Zhang J, Li R, Zhao P, Fu Z, et al. Hsa-Mir-181a and Hsa-Mir-181b Function as Tumor Suppressors in Human Glioma Cells. *Brain Res* (2008) 1236:185–93. doi: 10.1016/j.brainres.2008.07.085
25. Wang P, Chen D, Ma H, Li Y. LncRNA SNHG12 Contributes to Multidrug Resistance Through Activating the MAPK/Slug Pathway by Sponging miR-181a in non-Small Cell Lung Cancer. *Oncotarget* (2017) 8(48):84086–101. doi: 10.18632/oncotarget.20475
26. Liu Y, Zhao Z, Yang F, Gao Y, Song J, Wan Y. microRNA-181a is Involved in Insulin-Like Growth Factor-1-Mediated Regulation of the Transcription Factor CREB1. *J Neurochem* (2013) 126(6):771–80. doi: 10.1111/jnc.12370
27. Huang H. Matrix Metalloproteinase-9 (MMP-9) as a Cancer Biomarker and MMP-9 Biosensors: Recent Advances. *Sensors (Basel)* (2018) 18(10):3249. doi: 10.3390/s18103249
28. Hagemann C, Anacker J, Ernestus RI, Vince GH. A Complete Compilation of Matrix Metalloproteinase Expression in Human Malignant Gliomas. *World J Clin Oncol* (2012) 3(5):67–79. doi: 10.5306/wjco.v3.i5.67
29. Musumeci G, Magro G, Cardile V, Coco M, Marzagalli R, Castrogiovanni P, et al. Characterization of Matrix Metalloproteinase-2 and -9, ADAM-10 and N-Cadherin Expression in Human Glioblastoma Multiforme. *Cell Tissue Res* (2015) 362(1):45–60. doi: 10.1007/s00441-015-2197-5
30. Li Q, Chen B, Cai J, Sun Y, Wang G, Li Y, et al. Comparative Analysis of Matrix Metalloproteinase Family Members Reveals That MMP9 Predicts Survival and Response to Temozolomide in Patients With Primary Glioblastoma. *PloS One* (2016) 11(3):e0151815. doi: 10.1371/journal.pone.0151815
31. Das G, Shiras A, Shanmuganandam K, Shastry P. Rictor Regulates MMP-9 Activity and Invasion Through Raf-1-MEK-ERK Signaling Pathway in Glioma Cells. *Mol Carcinog* (2011) 50(6):412–23. doi: 10.1002/mc.20723
32. Lakka SS, Jasti SL, Gondi C, Boyd D, Chandrasekar N, Dinh DH, et al. Downregulation of MMP-9 in ERK-Mutated Stable Transfectants Inhibits Glioma Invasion *In Vitro*. *Oncogene* (2002) 21(36):5601–8. doi: 10.1038/sj.onc.1205646
33. Gjorgjevski M, Hannen R, Carl B, Li Y, Landmann E, Buchholz M, et al. Molecular Profiling of the Tumor Microenvironment in Glioblastoma Patients: Correlation of Microglia/Macrophage Polarization State With Metalloprotease Expression Profiles and Survival. *Biosci Rep* (2019) 39(6): BSR20182361. doi: 10.1042/bsr20182361
34. Cavallari C, Camussi G, Brizzi MF. Extracellular Vesicles in the Tumour Microenvironment: Eclectic Supervisors. *Int J Mol Sci* (2020) 21(18):6768. doi: 10.3390/ijms21186768
35. van Niel G, D'Angelo G, Raposo G. Shedding Light on the Cell Biology of Extracellular Vesicles. *Nat Rev Mol Cell Biol* (2018) 19(4):213–28. doi: 10.1038/nrm.2017.125
36. Hannen R, Selmansberger M, Hauswald M, Pagenstecher A, Nist A, Stiewe T, et al. Comparative Transcriptomic Analysis of Temozolomide Resistant Primary GBM Stem-Like Cells and Recurrent GBM Identifies Up-Regulation of the Carbonic Anhydrase CA2 Gene as Resistance Factor. *Cancers (Basel)* (2019) 11(7):921. doi: 10.3390/cancers11070921
37. Scharfenberg F, Helbig A, Sammel M, Benzel J, Schlomann U, Peters F, et al. Degradome of Soluble ADAM10 and ADAM17 Metalloproteases. *Cell Mol Life Sci* (2020) 77(2):331–50. doi: 10.1007/s00018-019-03184-4
38. McGeary SE, Lin KS, Shi CY, Pham TM, Bisaria N, Kelley GM, et al. The Biochemical Basis of microRNA Targeting Efficacy. *Science* (2019) 366(6472): eaav1741. doi: 10.1126/science.aav1741
39. Chen Y, Wang X. miRDB: An Online Database for Prediction of Functional microRNA Targets. *Nucleic Acids Res* (2020) 48(D1):D127–31. doi: 10.1093/nar/gkz757
40. Huang SX, Zhao ZY, Weng GH, He XY, Wu CJ, Fu CY, et al. The Correlation of microRNA-181a and Target Genes With Poor Prognosis of Glioblastoma Patients. *Int J Oncol* (2016) 49(1):217–24. doi: 10.3892/ijo.2016.3511
41. Wen X, Li S, Guo M, Liao H, Chen Y, Kuang X, et al. miR-181a-5p Inhibits the Proliferation and Invasion of Drug-Resistant Glioblastoma Cells by Targeting F-Box Protein 11 Expression. *Oncol Lett* (2020) 20(5):235. doi: 10.3892/ol.2020.12098
42. Wang XF, Shi ZM, Wang XR, Cao L, Wang YY, Zhang JX, et al. MiR-181d Acts as a Tumor Suppressor in Glioma by Targeting K-Ras and Bcl-2. *J Cancer Res Clin Oncol* (2012) 138(4):573–84. doi: 10.1007/s00432-011-1114-x
43. Priester M, Copanaki E, Vafaizadeh V, Hensel S, Bernreuther C, Glatzel M, et al. STAT3 Silencing Inhibits Glioma Single Cell Infiltration and Tumor Growth. *Neuro Oncol* (2013) 15(7):840–52. doi: 10.1093/neuonc/not025
44. Swiatek-Machado K, Mieczkowski J, Ellert-Miklaszewska A, Swierk P, Fokt I, Szymanski S, et al. Novel Small Molecular Inhibitors Disrupt the JAK/STAT3 and FAK Signaling Pathways and Exhibit a Potent Antitumor Activity in Glioma Cells. *Cancer Biol Ther* (2012) 13(8):657–70. doi: 10.4161/cbt.20083
45. Swiatek-Machado K, Kaminska B. STAT Signaling in Glioma Cells. *Adv Exp Med Biol* (2020) 1202:203–22. doi: 10.1007/978-3-030-30651-9_10
46. Guo YJ, Pan WW, Liu SB, Shen ZF, Xu Y, Hu LL. ERK/MAPK Signalling Pathway and Tumorigenesis. *Exp Ther Med* (2020) 19(3):1997–2007. doi: 10.3892/etm.2020.8454
47. Padfield E, Ellis HP, Kurian KM. Current Therapeutic Advances Targeting EGFR and EGFRvIII in Glioblastoma. *Front Oncol* (2015) 5:5. doi: 10.3389/fonc.2015.00005
48. Fu Y, Xin Z, Ling Z, Xie H, Xiao T, Shen X, et al. A CREB1-miR-181a-5p Loop Regulates the Pathophysiologic Features of Bone Marrow Stromal Cells in Fibrous Dysplasia of Bone. *Mol Med* (2021) 27(1):81. doi: 10.1186/s10020-021-00341-z
49. Urabe F, Kosaka N, Ito K, Kimura T, Egawa S, Ochiya T. Extracellular Vesicles as Biomarkers and Therapeutic Targets for Cancer. *Am J Physiol Cell Physiol* (2020) 318(1):C29–39. doi: 10.1152/ajpcell.00280.2019
50. Abels ER, Breakefield XO. Introduction to Extracellular Vesicles: Biogenesis, RNA Cargo Selection, Content, Release, and Uptake. *Cell Mol Neurobiol* (2016) 36(3):301–12. doi: 10.1007/s10571-016-0366-z
51. Nazimek K, Bryniarski K. Perspectives in Manipulating EVs for Therapeutic Applications: Focus on Cancer Treatment. *Int J Mol Sci* (2020) 21(13):4623. doi: 10.3390/ijms21134623

Conflict of Interest: The authors declare that the research was conducted in the absence of any commercial or financial relationships that could be construed as a potential conflict of interest.

Publisher's Note: All claims expressed in this article are solely those of the authors and do not necessarily represent those of their affiliated organizations, or those of the publisher, the editors and the reviewers. Any product that may be evaluated in this article, or claim that may be made by its manufacturer, is not guaranteed or endorsed by the publisher.

frontiers in Oncology

ORIGINAL RESEARCH
published: 23 March 2022
doi: 10.3389/fonc.2022.845009

The Long Non-Coding RNA HOXC-AS3 Promotes Glioma Progression by Sponging miR-216 to Regulate F11R Expression

Yongshuai Li[1†], *Lu Peng*[2†], *Xianwen Cao*[1†], *Kun Yang*[1], *Zhen Wang*[1], *Yong Xiao*[1], *Hong Xiao*[3], *Chunfa Qian*[1*] *and Hongyi Liu*[1*]

[1] *Department of Neurosurgery, Affiliated Nanjing Brain Hospital, Nanjing Medical University, Nanjing, China,* [2] *Department of Clinical Laboratory, Affiliated Nanjing Brain Hospital, Nanjing Medical University, Nanjing, China,* [3] *Department of Neuro-Psychiatric Institute, Affiliated Nanjing Brain Hospital, Nanjing Medical University, Nanjing, China*

OPEN ACCESS

Edited by:
Bozena Kaminska, Nencki Institute of Experimental Biology (PAS), Poland

Reviewed by:
Hernando Lopez-Bertoni, Johns Hopkins Medicine, United States
Dan Li, Hunan University, China

***Correspondence:**
Chunfa Qian
qianchunfa@126.com
Hongyi Liu
njnkyylhy@163.com

[†]*These authors have contributed equally to this work and share first authorship*

Specialty section:
This article was submitted to Neuro-Oncology and Neurosurgical Oncology, a section of the journal Frontiers in Oncology

Received: *29 December 2021*
Accepted: *01 March 2022*
Published: *23 March 2022*

Citation:
Li Y, Peng L, Cao X, Yang K, Wang Z, Xiao Y, Xiao H, Qian C and Liu H (2022) The Long Non-Coding RNA HOXC-AS3 Promotes Glioma Progression by Sponging miR-216 to Regulate F11R Expression. Front. Oncol. 12:845009. doi: 10.3389/fonc.2022.845009

HOXC cluster antisense RNA 3 (HOXC-AS3) is a long noncoding RNA (lncRNA) that plays a crucial role in various tumors; nevertheless, its role in glioma and its mechanism have not been completely elucidated. In this research, we discovered that HOXC-AS3 was over-expression in glioma cells and tissues and was associated with prognosis. Next, we determined that HOXC-AS3 targeted miR-216 as a sponge and that the F11 receptor (F11R) was the target of miR-216 by online databases analysis, qRT–PCR, and luciferase reporter assay. In addition, the rescue experiments confirmed that HOXC-AS3 regulated the expression of F11R by competitively binding miR-216 and functioning as a competing endogenous RNA (ceRNA). The intracranial glioblastoma mouse model suggested that HOXC-AS3 could promote glioma malignant progression *in vivo*. In summary, our study shows that the HOXC-AS3/miR-216/F11R axis plays an important role in the malignant progression of glioma, and may provide new ideas for the treatment of glioma.

Keywords: HOXC-AS3, miR-216, F11R, ceRNA, glioma

INTRODUCTION

Glioma, the most common primary malignant tumor, accounts for 51.4% of all primary cerebral tumors in the central nervous system (CNS) (1). Glioblastoma (GBM) is the most fatal glioma and the most common glioma in adults, with a median survival of only 14 months (2). To date, glioma is characterized by tumoral genetic heterogeneity, rapid proliferation, extensive migration, and invasion. It is difficult to achieve satisfactory outcomes with therapeutic schedules involving maximal safe surgical resection, radiotherapy, and chemotherapy (3). Thus, it is vital to identify new molecules with regulatory functions and related signaling pathways to elucidate the mechanism of glioma.

Noncoding RNAs (ncRNAs), particularly long noncoding RNAs (lncRNAs), play an important role in various types of cellular and biological functions (4). LncRNAs are defined as RNAs of more than 200 nucleotides that do not encode proteins. LncRNAs can be involved in multiple biological behaviors by regulating gene expression at the epigenetic, transcriptional, and posttranscriptional levels. An increasing number of studies have revealed that lncRNAs are connected to multiple

cellular processes, including cell differentiation, proliferation, apoptosis, migration, invasion, and immunotherapy resistance in cancer (5–9).

The lncRNA HOXC cluster antisense RNA 3 (HOXC-AS3), which is located at 12q13.13, has been observed to act as an oncogene in a variety of tumors. For instance, Yang B et al. reported that HOXC-AS3 promotes the proliferation of ovarian cancer cells by suppressing mature miR-96 (10). Yang Z et al. found that the lncRNA HOXC-AS3 accelerates pulmonary invasive mucinous adenocarcinoma progression by regulating FUS/FoxM1 and is probably considered a therapeutic marker (11). Another study showed that HOXC-AS3 modulates the tumorigenesis of gastric cancer by binding YBX1 (12). In glioma, studies have shown that HOXB13 directly binds the promoter of HOXC-AS3. In addition, HOXB13 promotes the proliferation, migration, and invasion of GBM cells through HOXC-AS3 (13). However, the specific mechanism by which HOXC-AS3 regulates GBM cell function is still unclear, and its downstream signaling pathway remains unascertained. Accordingly, it is significant to probe the potential mechanism of HOXC-AS3 in glioma.

At present, our research demonstrates that the expression level of HOXC-AS3 in glioma tissues and cell lines is elevated than that in normal tissues and cells. Furthermore, we disclosed that HOXC-AS3 modulates F11 receptor (F11R) expression by sponging miR-216 and facilitating glioma cell proliferation, migration, invasion, and tumor growth *in vivo*. Collectively, these results reveal that the HOXC-AS3/miR-216/F11R signaling pathway is involved in the biological behavior of glioma and may serve as a novel potential target for the treatment of glioma.

MATERIALS AND METHODS

Clinical Tissue Specimens

Twenty-three glioma specimens and fifteen normal brain tissues (NBTs) were obtained from the Department of Neurosurgery, the Affiliated Brain Hospital of Nanjing Medical University. The tissues were snap-frozen in liquid nitrogen and placed at -80°C for preservation after surgical resection. Ethical approval was granted by the ethics committee of the Affiliated Brain Hospital of Nanjing Medical University, and all patients signed written informed consent.

Cell Culture

The glioma cell lines (LN229, T98G, A172, U87 and U251) were purchased from the Chinese Academy of Sciences Cell Bank (Shanghai, China), while the normal human astrocytes (NHAs) were acquired from ScienCell Research Laboratories (Carlsbad, CA, USA). The glioma cells were cultured in Dulbecco's modified Eagle's medium (DMEM, Gibco, USA) supplemented with 10% fetal bovine serum (ScienCell, USA), and the NHAs were cultured in astrocyte medium (Life Technologies MA, USA). All cells were cultured in an incubator containing 5% CO_2 at 37°C.

Cell Transfection

Short hairpin RNAs (shRNAs) targeting HOXC-AS3 (sh-HOXC-AS3-1 and sh-HOXC-AS3-2) and F11R (sh-F11R), overexpression plasmids targeting HOXC-AS3 (HOXC-AS3) and F11R (F11R), and their corresponding negative control RNAs (sh-NC) were designed by GenePharma (Shanghai, China). The miR-216 mimics, inhibitors, and relative controls were obtained from Sangon Biotech (Shanghai, China). The transfection assays were conducted using Lipofectamine 3000 (Invitrogen, CA, USA). All interfering nucleotides are shown in **Table S1**.

RNA Isolation and Quantitative Real-Time PCR (qRT–PCR)

The total RNA was extracted from the specimens and cells using TRIzol (Vazyme, Nanjing, China) according to the manufacturer's protocol. qRT–PCR was carried out to test the expression levels of HOXC-AS3, miR-216, and F11R. The data was normalized to U6 and GAPDH, and the expression level was analyzed using the $2^{-\Delta\Delta Ct}$ method. Reverse transcription (RT) was conducted according to the method specified in the instructions using a C1000 Touch Thermal Cycler (Bio–Rad, California, USA). The amplification reaction under predetermined conditions was performed using Applied Biosystems QuantStudio 5 (Thermo Fisher Scientific, MA, USA). Each experiment was conducted three times. All primers are shown in **Table S2**.

Luciferase Reporter Assay

The fragment of HOXC-AS3 that contained the miR-216 binding site was inserted into GP-miRGLO vectors. The 3′-UTR fragments of F11R containing the binding sites for miR-216 were inserted into GV272 vectors. MiR-216 mimics and the relative control were transfected into the glioma cell lines with the reporter plasmids and mutated plasmids, respectively. After 48 hours, luciferase activity was observed using a Dual Luciferase Reporter Assay System (Promega, Madison, WI, USA). Sequences are shown in **Table S3**.

Western Blot Assay

The total protein was isolated from the cells with RIPA buffer (YIFEIXUE BIO TECH, Nanjing, China). A BCA Protein Assay Kit (YIFEIXUE BIO TECH, Nanjing, China) was used to detect the protein concentration. SDS-PAGE (12%) was used to resolve the protein, and after being transferred to PVDF membranes (Millipore, USA), it was blocked with skim milk (5%) for 2 h, washed three times with TBS-T, and then incubated at 4°C with primary antibodies against F11R (1:1000, Proteintech, IL, USA) overnight and HRP-conjugated secondary antibody (1:5000, Proteintech, IL, USA) for 2 hours. β-actin (1:1000, Proteintech, IL, USA) was used as a control.

Fluorescence *In Situ* Hybridization (FISH)

The HOXC-AS3 probe sequences (**Table S4**) were synthesized by GenePharma (Shanghai, China), and the fluorescent signals of the probe were tested using a FISH Kit (GenePharma, Shanghai, China). Briefly, U87 and U251 cells were fixed in 4%

paraformaldehyde for 15 min. Then were incubated at 37°C using 0.1% Triton X-100 (15 min) and 2× SSC (30 min). After that, the cells were hybridized in denatured probes (concentration of 1 μM) at 37°C overnight, washed for 5 min with 0.1% Tween 20, 5 min with 2× SSC, and 5 min with 1× SSC at 42°C. Ultimately, DAPI (Beyotime, China) was used to stain the cell nuclei. Images were captured under a Carl Zeiss microscope (Carl Zeiss, Germany).

Cell Counting Kit-8 (CCK-8) Assay

U87 and U251 were seeded into 96-well plates at 10,000 cells/well overnight, cell proliferation was measured using a CCK-8 (KeyGEN Bio TECH, Nanjing, China) assay. Ten microliters of CCK-8 solution were added to each well, incubated at 37°C, 4 hours. The absorbance of each well was read at 450nm with a microplate reader (TECAN, Switzerland). Similarly, cell proliferation was detected after 24 h, 48 h, and 72 h, and then the cell growth curve was plotted.

5-Ethynyl-20-Deoxyuridine (EdU) Assay

Cells (75,000) were plated in 24-well plates with round coverslips overnight. 200 μl of EdU (10 μM, KeyGEN Bio TECH, Nanjing, China) were added to each well, and the cells were incubated at 37°C, 2 h. The cells were fixed by adding 4% neutral paraformaldehyde to each well and removed after 30 minutes at room temperature. Then, we added 0.5% TritonX-100 (KenGEN, Nanjing, China) in PBS (200 μl) to each well for 20 min and stained the samples with 200 μl Click-iT reaction mixture (KeyGEN Bio TECH, Nanjing, China) for 30 min under lightproof conditions. Next, DAPI (Beyotime, China) was used to stain the glioma cell nuclei. Round coverslips were observed using Carl Zeiss microscope (Carl Zeiss, Germany) to analyze the proportion of EdU-positive cells.

Migration and Invasion Assays

To measure the ability of the cells to migrate and invade, Matrigel-covered (50 μl, 1:8 dilution, BD, USA) or uncovered Transwell insert chambers (Millipore, MA, USA) were utilized following the instructions. Then cells were collected and resuspended in serum-free medium and plated at 50,000 cells per upper chamber, while 500 μl medium with 10% FBS were added to the lower chambers. Forty-eight hours later, the residual cells in the upper chamber were removed. Simultaneously, penetrated cells were treated with paraformaldehyde and crystal violet (Beyotime, China). Three fields were randomly selected using the microscope (Nikon, Japan) to calculate the number of migrating and invading cells.

Immunohistochemistry

Paraffin-embedded human and nude mouse glioma samples sections were incubated with primary antibodies against F11R (1:200, Proteintech, IL, USA) or Ki-67 (1:500 dilution, Servicebio, Wuhan, China) overnight at 4°C, and then incubated with the secondary antibody (1:200 dilution, Servicebio, Wuhan, China) at room temperature for 1 h. Next, the sections were stained with diaminobenzidine until brown precipitation appeared and counterstained with hematoxylin for 5 minutes. Positive areas of the captured image were analyzed by ImageJ.

Terminal Deoxynucleotidyl Transfer-Mediated dUTP Nick End Labeling Staining (TUNEL)

After deparaffinization and rehydration, proteinase K was dropped onto the tissue sections for antigen retrieval. Following the instructions to block endogenous peroxidase, equilibrium was reached at room temperature, and the TUNEL reaction mixture was added (Servicebio, Wuhan, China). DAB development was then performed, and the nuclei were counterstained, followed by dehydration and mounting.

Intracranial GBM Mouse Model

Male BALB/c nude mice were obtained from the Vital River (Beijing, China), 1×10^6 U87 cells stably expressing EGFP-luciferase and transfected with sh-HOXC-AS3 or negative control were injected into the frontal lobes of nude mice for GBM orthotopic xenograft tumorigenesis (6 per group). The tumor volumes were measured 7, 14, and 21 days after the implantation using a bioluminescence imaging system (Caliper IVIS Spectrum, PerkinElmer, USA). D-Luciferin potassium salt (Beyotime, China) was injected intraperitoneally before the measurement. After the mice died, their brain tissue was removed and fixed with paraformaldehyde for further experiments.

Statistical Analysis

The data was analyzed using SPSS 20.0 software (IBM, New York, USA) and is expressed as the mean ± standard error. The statistical significance was evaluated by using t-tests between two groups, one/two-way ANOVA and *post hoc* test (Bonferroni) among multiple groups. Log-rank test was used for survival analysis, and the relation between HOXC-AS3 and miR-216 as well as miR-216 and F11R was assessed by Pearson's correlation analysis. $P < 0.05$ was considered statistical significance. All experiments were performed at least three times independently.

RESULTS

HOXC-AS3 Expression Is Upregulated in Both Glioma Tissues and Cell Lines

First, we evaluated the expression level of HOXC-AS3 using RNA sequencing data of 169 glioma tissues and 5 normal tissues in The Cancer Genome Atlas (TCGA) (https://portal.gdc.cancer.gov/) and found that HOXC-AS3 expression was markedly increased in GBM tissues compared to that in normal tissues ($P < 0.05$) (**Figure 1A**). Then, by conducting a GSEA (gene set enrichment analysis) (http://www.broadinstitute.org/gsea/index.jsp), we found that HOXC-AS3 may be related to some pathways involved in tumor metabolism (**Figure 1B**). Furthermore, we searched the TCGA dataset from GEPIA (http://gepia.cancer-pku.cn/index.html) (14), and the survival analysis indicated that the HOXC-AS3 expression level was inversely correlated with the overall survival of GBM patients (**Figure 1C**).

We also collected clinical samples during surgery, tested the expression of HOXC-AS3 in glioma and normal brain tissues (15) by qRT–PCR and found that the expression level of HOXC-

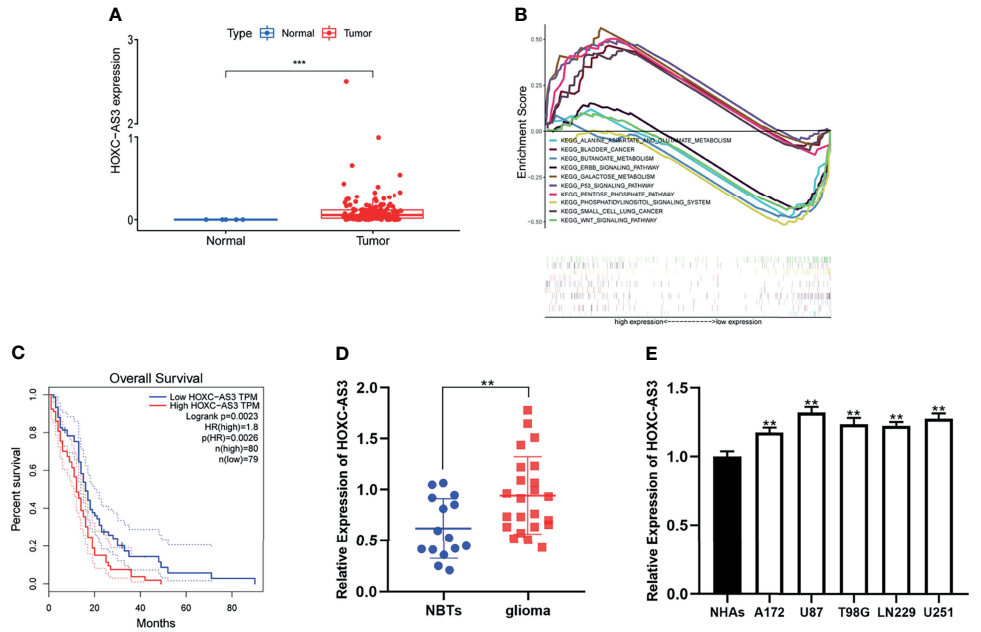

FIGURE 1 | HOXC-AS3 was upregulated in glioma and associated with poor prognosis. **(A)** The expression level of HOXC-AS3 in TCGA. **(B)** HOXC-AS3 associated pathways were investigated using gene set enrichment analysis (GSEA) by TCGA genes data. **(C)** The Survival Plots of HOXC-AS3 in GEPIA. **(D)** Expression of HOXC-AS3 in 15 normal brain tissues and 23 glioma tissues. **(E)** Expression of HOXC-AS3 in normal human astrocytes and glioma cell lines. Mann-Whitney test for **(A)**; Log-rank test for **(C)**; t-test for **(D)**; one-way ANOVA and *post hoc* test for **(E)**. ***P < 0.001, **P < 0.01.

AS3 was similar to that predicted by online databases (**Figure 1D**). Then, we examined the expression of HOXC-AS3 in normal human astrocytes (NHAs) and glioma cell lines (LN229, T98G, A172, U87, and U251). The results demonstrated that the expression level of HOXC-AS3 in the glioma cell lines was elevated than that in the NHAs (**Figure 1E**).

HOXC-AS3 Promotes Glioma Cell Proliferation, Migration, and Invasion *In Vitro*

To analyze the effect of HOXC-AS3 in glioma, U87 and U251 cells were transfected with a shRNA targeting HOXC-AS3 (sh-HOXC-AS3-1 and sh-HOXC-AS3-2). The transfection efficiency was determined by qRT–PCR, and sh-HOXC-AS3-1 had better knockdown efficiency and was used for subsequent research (**Figures S1A, B**). Cell proliferation was identified by EdU and CCK-8 assays, and the migration and invasion abilities were assessed by Transwell assays. The results indicate that the functions of sh-HOXC-AS3 include inhibiting glioma cell proliferation, migration, and invasion *in vitro* (**Figures S1C–L**). In contrast, the upregulation of HOXC-AS3 showed the opposite results (**Figures S2A–L**). These results show that HOXC-AS3 acts as an oncogene that affects the biological processes of glioma cells *in vitro*.

HOXC-AS3 Directly Targeted miR-216 as a Sponge

Recently, numerous studies have confirmed that lncRNAs can serve as molecular sponges of miRNAs, thereby playing a role in regulating cell functions (16–18). We speculate that HOXC-AS3 may function through a competing endogenous RNA (ceRNA) pathway, i.e., HOXC-AS3 binds miRNAs to modulate the cell progression of glioma. Through a FISH analysis, we found that HOXC-AS3 was predominantly expressed in the cytoplasm of glioma cells (**Figure 2A**). This result further confirms our hypothesis that HOXC-AS3 functions through a ceRNA mechanism. Accordingly, we used the online databases starBase (http://starbase.sysu.edu.cn/) and miRcode (http://www.mircode.org/) to identify miRNAs that might interact with HOXC-AS3. We identified seven possible biological target miRNAs of HOXC-AS3 (**Figure 2B**). The expression of the target miRNAs in the U87 and U251 cells transfected with sh-HOXC-AS3 and NC was analyzed by qRT–PCR. The results showed that miR-216 expression was the most notably upregulated (**Figures 2C, D**). Potential miR-216 binding sites in HOXC-AS3 transcripts were identified by using starBase (**Figure 2E**). Furthermore, miR-216 was downregulated in glioma as revealed by qRT–PCR (**Figure 2F**). We tested the expression of miR-216 in five glioma cell lines and NHAs, and the results showed that miR-216 was underexpressed in glioma cells compared to NHAs (**Figure 2G**). Moreover, Pearson correlation analysis indicated that HOXC-AS3 was inversely correlated with miR-216 (**Figure 2H**). Finally, luciferase reporter plasmids were constructed including HOXC-AS3-WT and HOXC-AS3-MUT. The results indicated that miR-216 overexpression markedly reduced the luciferase activity of HOXC-AS3-WT without affecting the luciferase activity of HOXC-AS3-MUT (**Figure 2I**). These findings suggest that HOXC-AS3 directly targets miR-216 as a sponge.

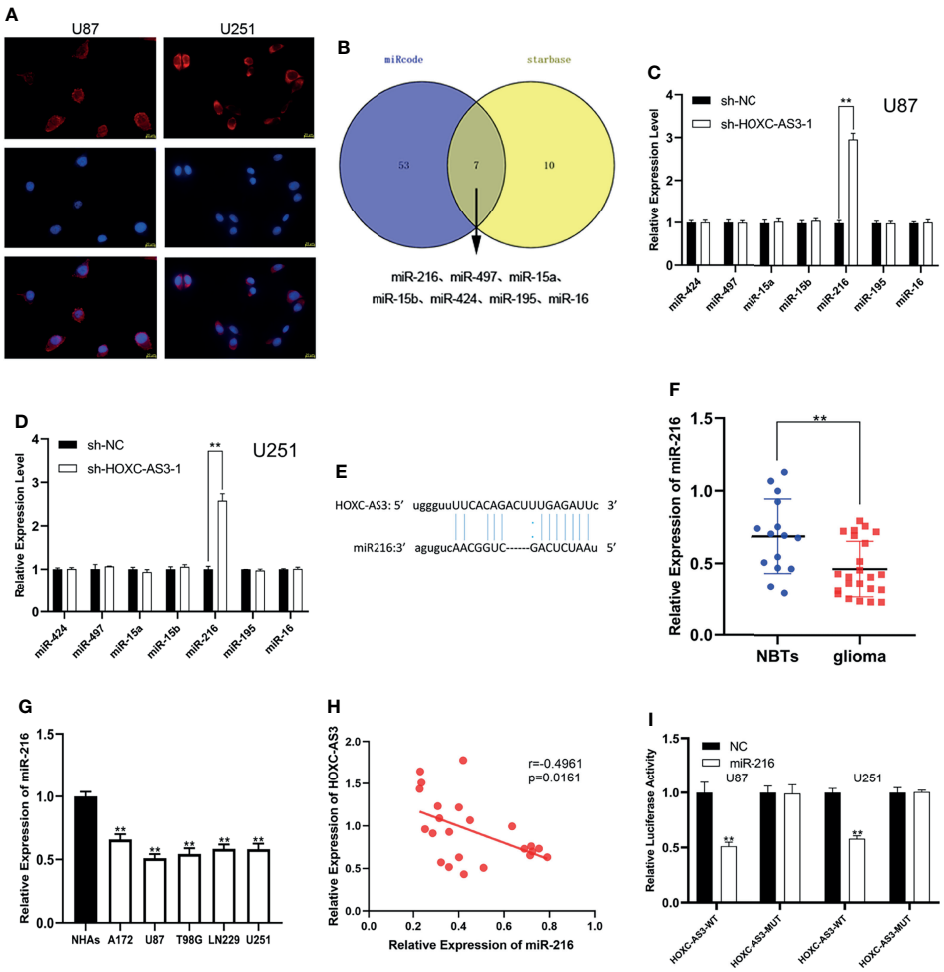

FIGURE 2 | HOXC-AS3 acts as a sponge for miR-216. **(A)** The distribution of HOXC-AS3 in U87 and U251 cells was evaluated by FISH assays. **(B)** Targets of HOXC-AS3 were predicted by online databases. **(C, D)** The expression of seven miRNAs was detected in glioma cells transfected with sh-HOXC-AS3-1 or shNC. **(E)** Binding sites of miR-216 on HOXC-AS3. **(F)** Expression of miR-216 in normal brain tissues and glioma tissues. **(G)** Expression of miR-216 in glioma cell lines. **(H)** Pearson correlation analysis showed that HOXC-AS3 was inversely correlated with miR-216 in glioma tissues. **(I)** The association between miR-216 and HOXC-AS3 was verified by luciferase reporter assay. Pearson's correlation analysis for **(H)**; t-test for **(C, D, I)**; Mann-Whitney test for **(F)**; one-way ANOVA and *post hoc* test for **(G)**. **P < 0.01.

MiR-216 Inhibits Glioma Progression by Regulating F11R Expression

To explore the mechanism of miR-216, we predicted 24 possible downstream mRNAs using four bioinformatics tools: RNA22 (https://cm.jefferson.edu/rna22/Precomputed/), starBase, miRDB (http://mirdb.org/), and TargetScan (http://www.targetscan.org/vert_72/). (**Figure 3A**). We searched the expression level of candidate genes by GEPIA and found that only five genes (F11R, YBX1, BCAT1, IMPAD1, and RP2) were significantly upregulated in gliomas (**Figure S3** and **Table S5**). Subsequently, the changes in the mRNA expression levels after the miR-216 mimic/inhibitor transfection were examined by qRT–PCR, and we discovered that F11R expression was the most substantially downregulated/upregulated (**Figures 3B, C**). Additionally, we predicted the potential binding sites between miR-216 and F11R through a bioinformatic analysis using TargetScan (**Figure 3D**). The inverse correlation between miR-216 and F11R expression was also observed in Pearson correlation analysis (**Figure 3E**). The interaction between miR-216 and F11R was verified through a luciferase reporter assay, and results indicate that the overexpression of miR-216 significantly reduced the luciferase activity of the F11R-WT plasmid. However, no substantial change was detected in the F11R-MUT plasmid (**Figure 3F**). We collected clinical samples and detected the expression of F11R by qRT–PCR and immunohistochemistry. F11R is overexpressed in glioma and positively related to the grade of glioma, and similar results were obtained in the NHAs and glioma cell lines (**Figures 3G–I**). The western blot analysis further verified the above results (**Figure 3J**). These findings indicate that F11R is the target of miR-216.

To further explore the relationship between miR-216 and F11R, a shRNA against F11R (sh-F11R), miR-216 mimics, and miR-216 mimics along with the F11R plasmid were transfected into glioma cells. As shown by qRT–PCR and a western blot analysis, the

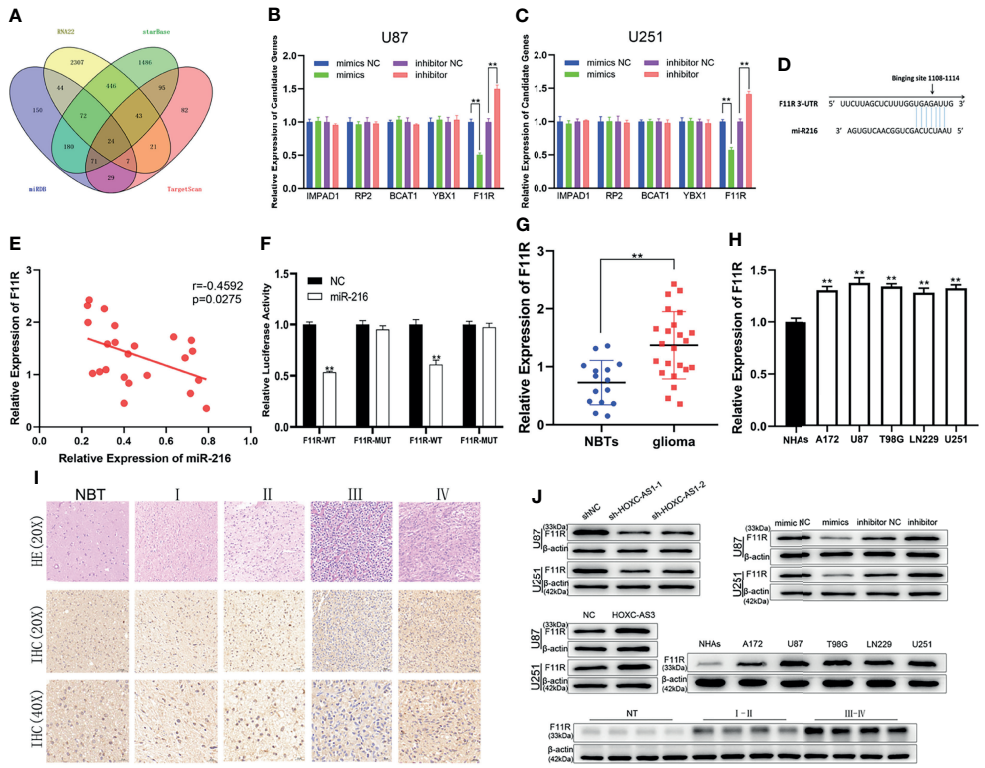

FIGURE 3 | | MiR-216 directly binds F11R to regulate the level of F11R. **(A)** 24 potential downstream genes of miR-216 were predicted using online databases. **(B, C)** The effect of miR-216 on the expression of candidate mRNAs in U87 and U251 cells was detected by qRT-PCR. **(D)** Binding sites of miR-216 on F11R. **(E)** Pearson correlation analysis showed that F11R was inversely correlated with miR-216 in glioma tissues. **(F)** The association between miR-216 and F11R was verified by luciferase reporter assay. **(G)** Expression of F11R in normal brain tissues and glioma tissues. **(H)** Expression of F11R in normal human astrocytes and glioma cell lines. **(I)** Expression of F11R in different grades of glioma identified using immunohistochemistry. **(J)** The expression levels of F11R in different tissues and cell lines were tested by western blot analysis. At the same time, it was verified that F11R was regulated by HOXC-AS3 and miR-216. Pearson's correlation analysis for **(E)**; t-test for **(B, C, F, G)**; one-way ANOVA and *post hoc* test for **(H)**. **P < 0.01.

expression of F11R was decreased by the sh-F11R and miR-216 mimics, and this inhibitory effect was partially recovered by the F11R plasmid (**Figures 4A–C**). We also obtained some interesting results. According to the EdU and CCK-8 assay results, the reduced proliferation caused by the miR-216 mimics was ameliorated by the transfection with the F11R plasmid (**Figures 4D–I**). The inhibitory effect of the miR-216 mimics on migration and invasion was reversed by the F11R plasmid (**Figures 4J–M**). Hence, we deduce that miR-216 inhibits glioma progression by regulating F11R expression.

HOXC-AS3, as a ceRNA, Regulates F11R by Competitively Binding miR-216

Current research suggests that HOXC-AS3 targets miR-216 as a sponge and that miR-216 regulates glioma progression by acting on F11R. To elucidate the HOXC-AS3-mediated ceRNA mechanism in glioma, the following rescue assays were conducted to analyze whether HOXC-AS3 modulates the expression of F11R in a miR-216-dependent manner. An shRNA against HOXC-AS3 (sh-HOXC-AS3), and sh-HOXC-AS3 along with miR-216 inhibitors were transfected into glioma cells. As shown by qRT–PCR and a western blot analysis, sh-HOXC-AS3 downregulated the expression of F11R, and the suppressive effect was partially counteracted by the miR-216 inhibitors (**Figures 5A–C**). Moreover, the effect of sh-HOXC-AS3 on glioma cell proliferation, migration, and invasion was also largely abrogated by the miR-216 inhibitor (**Figures 5D–M**). Overall, these results demonstrate that HOXC-AS3, as a ceRNA, regulates F11R by competitively binding miR-216.

HOXC-AS3 Promotes Tumor Growth By Regulating miR-216 And F11R *In Vivo*

To assess the oncogenic function of HOXC-AS3 *in vivo*, an orthotopic xenograft tumorigenicity assay was performed by stereotactic intracerebral injection of luciferase-expressing U87 cells (lacking HOXC-AS3 expression and negative control). The *in vivo* imaging conducted on the 7th, 14th, and 21st days after implantation showed that tumor growth in the sh-HOXC-AS3 group was significantly inhibited (**Figures 6A, B**). The survival rate of the mice injected with sh-HOXC-AS3-expressing cells was also elevated than that of the control mice (**Figure 6C**). The immunohistochemical results of the tumor sections showed that the expression level of Ki-67 in the sh-HOXC-AS3 group was substantially decreased; however, TUNEL staining was upregulated (**Figures 6D, E**). We further analyzed the expression of miR-216 and F11R in the brain sections, and the results indicated that silencing HOXC-AS3 raised the expression of miR-216

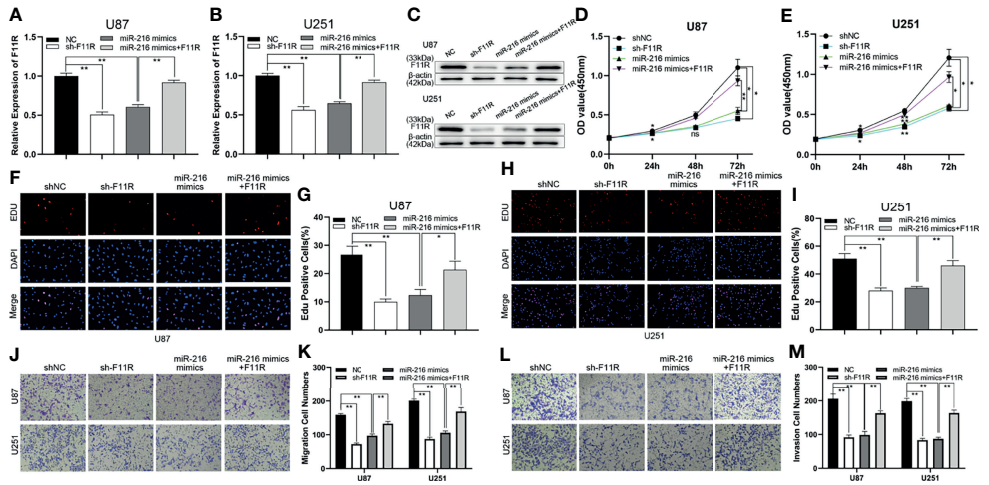

FIGURE 4 | MiR-216 could inhibit glioma proliferation, migration, and invasion by targeting F11R. **(A–C)** qRT-PCR and western blot were used to test the expression of F11R in U87 and U251 cells transfected with NC, sh-F11R, miR-216 mimics, or miR-216 mimics together with F11R plasmids. **(D, E)** CCK-8 assay was used to test the proliferation of U87 and U251 cells transfected with NC, sh-F11R, miR-216 mimics, or miR-216 mimics together with F11R plasmids. **(F–I)** EdU assay was used to test the proliferation of U87 and U251 cells transfected with NC, sh-F11R, miR-216 mimics, or miR-216 mimics together with F11R plasmids. **(J, K)** Transwell assay was used to test the migration of U87 and U251 cells transfected with NC, sh-F11R, miR-216 mimics, or miR-216 mimics together with F11R plasmids. **(L, M)** Transwell assay was used to test the invasion of U87 and U251 cells transfected with NC, sh-F11R, miR-216 mimics, or miR-216 mimics together with F11R plasmids.One-way ANOVA and *post hoc* test for **(A, B, G, I, K, M)**. Two-way ANOVA and *post hoc* test for **(D, E)**. *P < 0.05, **P < 0.01.

and suppressed F11R expression (**Figures 6F–I**). In conclusion, HOXC-AS3 facilitates glioma growth through regulating miR-216 and F11R expression *in vivo*.

DISCUSSION

Temozolomide (TMZ) is the most commonly used chemotherapy protocol for glioma treatment. Resistance to TMZ is the leading cause of inefficient chemotherapy (19). LncRNA CASC2 increased the sensitivity of glioma cells to TMZ by upregulating the expression of tumor suppressor PTEN through sponging miR-181a (20). LncRNA TALC was overexpressed in drug-resistant GBM cells, and TALC/miR-20b-3p/c-Met axis induced GBM chemotherapy resistance by promoting O6-methylguanine DNA methyltransferase (MGMT) function (21). Moreover, LncRNA SNHG12 was upregulated in TMZ-resistant tissues and cells. SNHG12 served as a sponge for miR-129-5p and raised E2F7 and MAPK1 expression. Silencing SNHG12 improved glioma cell sensitivity to TMZ (17). Therefore, LncRNA can directly affect sensitivity to TMZ, thus guiding the development of chemotherapeutic agents.

Exosomes are small vesicles secreted by cells, ranging in diameter from 40nm to 140nm, that play a vital role in intercellular signaling. Exosomes involved in various cellular and biological functions are the current research focus (22). Drug-resistant GBM cells could deliver SBF2-AS1 to drug-sensitive GBM cells through exosomes, leading to wide-spread chemotherapy resistance (23). Exosomes are small in size and can act as lncRNA carriers across the blood-brain barrier (BBB). Targeting exosome may be a promising treatment strategy (24). MiR-146b-overexpressing exosomes released by MSCs could significantly inhibit glioma growth in a primary glioma rat model (25). MSCs could also deliver anti-miR-9 exosomes to promote GBM sensitivity to TMZ (26). Marleau et al. proposed to use plasmapheresis technology combined with renal dialysis to selectively capture or retain exosomes in the circulatory system for subsequent treatment (27). However, the specificity of exosome packaging molecules and the mechanisms by which exosomes target cells or tissues need to be further researched, thus their clinical use is still challenging.

Recently, research has shown that lncRNAs play an indispensable role in the biological progression of various tumors. For instance, Li SY et al. reported that Lnc-APUE is restrained by HNF4α and facilitates hepatocellular carcinoma growth through the HNF4α/lnc-APUE/miR-20b/E2F1 axis (28). Chen C et al. showed that exosomal LNMAT2 facilitated lymphangiogenesis, lymphatic metastasis, HLEC tube formation, and migration by upregulating PROX1 expression in bladder cancer (29). Liu et al. demonstrated that lncRNA-HOTAIR sponges miR-126 as a ceRNA to facilitate glioma progression (30). In this research, we elucidated the mechanism of HOXC-AS3 in glioma progression.

By analyzing the differentially expressed lncRNA data in the TCGA database, we discovered that the expression of HOXC-AS3 in tumor tissues was significantly higher than that in normal tissues. HOXC-AS3 is a lncRNA that acts in many human tumors. For instance, Su J et al. reported that HOXC-AS3 can combine with YBX1 to directly transcriptionally activate TK1 and then regulate breast cancer progression (31). Fu T et al. found that HOXC-AS3 might regulate a series of HOX genes and has great value in the diagnosis of gastric adenocarcinoma (32). Li B et al. showed that HOXC-AS3 can interact with HOXC10, which increases the stability of HOXC10 and then promotes its expression, thereby reducing the osteogenic potential of

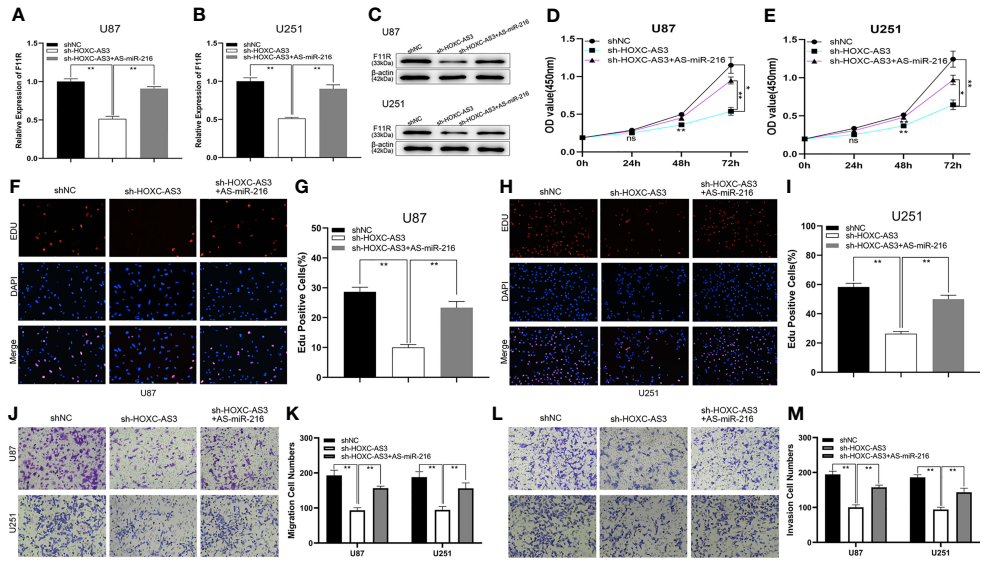

FIGURE 5 | HOXC-AS3 promoted the glioma malignancy phenotype by targeting the miR-216/F11R axis. **(A–C)** qRT-PCR and western blot were used to test the expression of F11R in U87 and U251 cells transfected with NC, sh-HOXC-AS3, or sh-HOXC-AS3 together with miR-216 inhibitors. **(D, E)** CCK-8 assay was used to test the proliferation of U87 and U251 cells transfected with NC, sh-HOXC-AS3, or sh-HOXC-AS3 together with miR-216 inhibitors. **(F–I)** EdU assay was used to test the proliferation of U87 and U251 cells transfected with NC, sh-HOXC-AS3, or sh-HOXC-AS3 together with miR-216 inhibitors. **(J, K)** Transwell assay was used to test the migration of U87 and U251 cells transfected with NC, sh-HOXC-AS3, or sh-HOXC-AS3 together with miR-216 inhibitors. **(L, M)** Transwell assay was used to test the invasion of U87 and U251 cells transfected with NC, sh-HOXC-AS3, or sh-HOXC-AS3 together with miR-216 inhibitors. *P < 0.05, **P < 0.01. One-way ANOVA and *post hoc* test for **(A, B, G, I, K, M)**. Two-way ANOVA and *post hoc* test for **(D, E)**. *P < 0.05, **P < 0.01.

Mesenchymal stem cells (MSCs) (33). These studies suggest that HOXC-AS3 may play a role as an oncogene in various tumors; however, the potential mechanism requires further investigation. In this study, we first confirmed the overexpression of HOXC-AS3 in both glioma tissues and cells. A high expression of HOXC-AS3 predicted a detrimental prognosis in glioma patients. The function of HOXC-AS3 on glioma cell proliferation, migration, invasion, and tumor growth *in vivo* was also examined.

Ample evidence has indicated that lncRNAs sponge miRNAs as ceRNAs and suppress the target binding of miRNAs to mRNAs, therefore modulating the expression of target mRNAs. Previous studies have shown that HOXC-AS3 can promote breast cancer metastasis by acting as a miR-3922-5p sponge (34). Our FISH assay identified that HOXC-AS3 is principally expressed in the cytoplasm of glioma cells. Based on these studies, HOXC-AS3 may function *via* a ceRNA mechanism in glioma. We subsequently probed the bound miRNA of HOXC-AS3 by a biological analysis, and seven miRNAs were predicted as targets of HOXC-AS3. MiR-216 was determined to be a target of HOXC-AS3 through qRT–PCR and a luciferase reporter analysis. It also has been shown to have an antitumor effect in various human tumors. For instance, Roscigno G et al. reported that miR-216a acts as a suppressor to reduce stem-like properties and influence the interaction between cells and the microenvironment in breast cancer (35). Qu XH et al. showed that miR-216 affects the growth, metastasis, and cell apoptosis of OSCC cells (36). Sun T et al. demonstrated that miR-216 inhibits the cell progression of ESCC through the miR-216/KIAA0101 axis (37). Wang W et al. found that miR-216a suppressed glioma cell progression and promoted apoptosis through the miR-216a/LGR5 axis (38). In this research, we demonstrate that miR-216 could interact with HOXC-AS3 and that the expression of miR-216 was negatively correlated with HOXC-AS3 expression in glioma cells and clinical samples.

Subsequently, the target mRNA of miR-216 was examined. F11R is a functional target of miR-216. In previous studies, F11R was originally identified as a monoclonal antibody receptor (39) that acts as a tight junction protein and is expressed in several leukocyte populations and platelets (40, 41). A series of studies revealed that the expression of F11R is inversely correlated with prognosis in many tumors, such as multiple myeloma (42), oral squamous cell carcinoma (43), and epithelial ovarian cancer (44). F11R is overexpressed in tumor tissues and promotes biological processes in HNSCC (45). However, in some tumors, a low expression of F11R may lead to a poor prognosis; for example, Communal L et al. showed that expression of F11R is a reliable prognostic biomarker of HGSC that may be used to distinguish tumors that respond to EMT therapy. The decreased F11R gene indicates a poor outcome (46). F11R can also act as a tumor suppressor gene in anaplastic thyroid carcinoma (47) and nasopharyngeal carcinoma (48). In glioma cancer stem cells (CSCs), F11R functions to promote tumor initiation, cell proliferation, and self-renewal *in vitro*, and F11R is suppressed by miR-145 (49). Rosager AM et al. reported that F11R is colocalized with stem cell markers and that the expression of F11R is positively correlated with the grade of glioma. In GBMs, F11R is an independent prognostic factor (50, 51). In the female

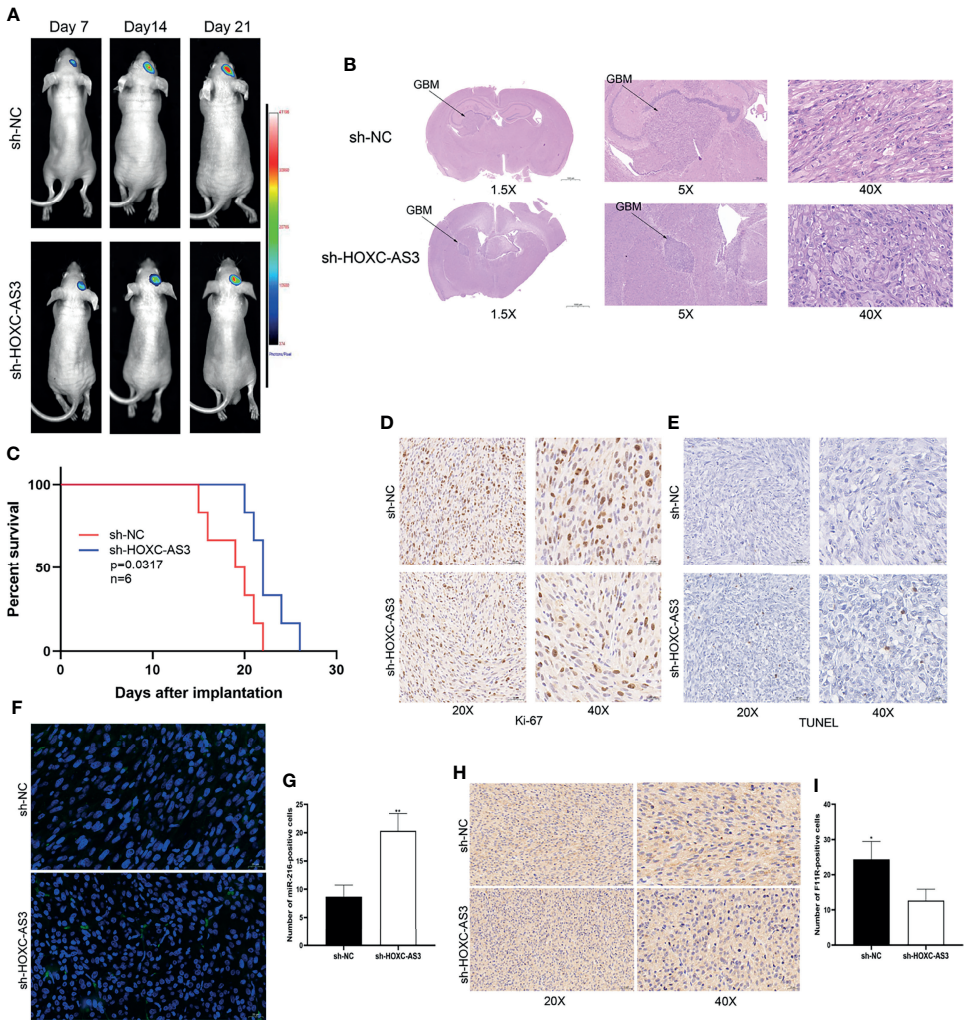

FIGURE 6 | HOXC-AS3 promotes glioma growth *in vivo*. **(A)** Luciferase signals were assessed at 7,14 and 21 days after implantation of glioma cells (6 mice per group). **(B)** Tumor maximum diameter was determined using H&E staining. **(C)** Overall survival of the sh-HOXC-AS3 and control groups was compared by Kaplan-Meier survival curves. **(D)** Ki-67 expression in the sh-HOXC-AS3 and sh-NC groups was measured by immunohistochemistry. **(E)** TUNEL staining was used to detect cell apoptosis in the sh-HOXC-AS3 and sh-NC groups. **(F, G)** Expression and quantification of miR-216 in the brain sections. **(H, I)** Expression and quantification of F11R in the brain sections. Log-rank test for **(C)** and t-test for **(G, I)**. *P < 0.05, **P < 0.01.

tumor microenvironment, F11R inhibits pathogenic microglial activation and indicates sex differences in glioma initiation (52). However, its biological function has not been described in detail. In this study, we discovered that the expression of F11R increased with the grade of glioma and that F11R promoted malignant progression downstream of miR-216. We also performed rescue experiments, and the results showed that the effect of miR-216 mimics was abolished by F11R plasmids and that the function of sh-HOXC-AS3 could be reversed by miR-216 inhibitors in glioma cells.

In conclusion, HOXC-AS3 facilitates glioma progression *via* miR-216 to regulate F11R. Hence, the HOXC-AS3/miR-216/F11R signaling pathway may provide a potential target for the treatment of glioma. HOXC-AS3 may become a target to improve TMZ sensitivity, or regulate glioma tumorigenesis through exosome packaging, which requires further research.

DATA AVAILABILITY STATEMENT

The datasets presented in this study can be found in online repositories. The names of the repository/repositories and accession number(s) can be found in the article/**Supplementary Material**.

ETHICS STATEMENT

The studies involving human participants were reviewed and approved by the institute ethical committee of the Affiliated Brain Hospital of Nanjing Medical University. The patients/participants provided their written informed consent to participate in this study. The animal study was reviewed and

approved by the Institutional Animal Care and Use Committee of Nanjing Medical University.

AUTHOR CONTRIBUTIONS

CQ and HL designed and funded the study. YL, LP, and XC performed experiments and wrote the paper. KY collected clinical specimens. ZW directed and participated in animal experiments. HX contributed suitable reagents or analytic tools. YX conducted bioinformatics analysis to guide the experiment. All authors read and approved the final manuscript.

FUNDING

National Natural Science Foundation of China (81972350). This research was funded by the National Natural Science Foundation of China (81972350).

ACKNOWLEDGMENTS

Experimental operation skills were instructed by Huaqing Chen and Zhen Jia.

SUPPLEMENTARY MATERIAL

The Supplementary Material for this article can be found online at: https://www.frontiersin.org/articles/10.3389/fonc.2022.845009/full#supplementary-material

Supplementary Figure 1 | Downregulation of HOXC-AS3 inhibits proliferation, migration, and invasion of glioma *in vitro*. **(A, B)** qRT-PCR was used to test the expression of HOXC-AS3 in U87 and U251 cells transfected with shNC, sh-HOXC-AS3-1, or sh-HOXC-AS3-2. **(C, D)** CCK-8 assay was used to test the proliferation of U87 and U251 cells transfected with shNC, sh-HOXC-AS3-1, or sh-HOXC-AS3-2. **(E–H)** EdU assay was used to test the proliferation of U87 and U251 cells transfected with shNC, sh-HOXC-AS3-1, or sh-HOXC-AS3-2. **(I, J)** Transwell assay was used to test the migration of U87 and U251 cells transfected with shNC, sh-HOXC-AS3-1, or sh-HOXC-AS3-2. **(K, L)** Transwell assay was used to test the invasion of U87 and U251 cells transfected with shNC, sh-HOXC-AS3-1, or sh-HOXC-AS3-2. One-way ANOVA and *post hoc* test for **(A, B, F, H, J, L)**. Two-way ANOVA and *post hoc* test for **(C, D)**. *P < 0.05, **P < 0.01.

Supplementary Figure 2 | Upregulation of HOXC-AS3 promotes proliferation, migration, and invasion of glioma *in vitro*. **(A, B)** qRT-PCR was used to detect the expression of HOXC-AS3 in U87 and U251 cells transfected with NC or HOXC-AS3 plasmid. **(C, D)** CCK-8 assay was used to detect the proliferation of U87 and U251 cells transfected with NC or HOXC-AS3 plasmid. **(E–H)** EdU assay was used to detect the proliferation of U87 and U251 cells transfected with NC or HOXC-AS3 plasmid. **(I, J)** Transwell assay was used to detect the migration of U87 and U251 cells transfected with NC or HOXC-AS3 plasmid. **(K, L)** Transwell assay was used to detect the invasion of U87 and U251 cells transfected with NC or HOXC-AS3 plasmid. T-test for **(A, B, F, H, J, L)**. Two-way ANOVA and *post hoc* test for **(C, D)**. *P < 0.05, **P < 0.01.

Supplementary Figure 3 | The expression of 24 genes downstream of miR-216 was predicted by GEPIA.

Supplementary Figure 4 | Quantification and statistical analysis of the tumors in xenograft mouse model. T-test was used. *P < 0.05, **P < 0.01.

Supplementary Figure 5 | Median survival analysis of xenograft mouse model. Log-rank test was used. *P < 0.05, **P < 0.01.

Supplementary Figure 6 | Statistical analysis of the three random fields of the expression level of Ki-67 and TUNEL staining. T-test was used. *P < 0.05, **P < 0.01.

REFERENCES

1. Zhou X, Liu J, Zhang J, Wei Y, Li H. Flubendazole Inhibits Glioma Proliferation by G2/M Cell Cycle Arrest and Pro-Apoptosis. *Cell Death Discov* (2018) 4:18. doi: 10.1038/s41420-017-0017-2
2. Liu SJ, Malatesta M, Lien BV, Saha P, Thombare SS, Hong SJ, et al. CRISPRi-Based Radiation Modifier Screen Identifies Long Non-Coding RNA Therapeutic Targets in Glioma. *Genome Biol* (2020) 21(1):83. doi: 10.1186/s13059-020-01995-4
3. Cheng J, Meng J, Zhu L, Peng Y. Exosomal Noncoding RNAs in Glioma: Biological Functions and Potential Clinical Applications. *Mol Cancer* (2020) 19(1):66. doi: 10.1186/s12943-020-01189-3
4. Han M, Wang S, Fritah S, Wang X, Zhou W, Yang N, et al. Interfering With Long Non-Coding RNA MIR22HG Processing Inhibits Glioblastoma Progression Through Suppression of Wnt/beta-Catenin Signalling. *Brain* (2020) 143(2):512–30. doi: 10.1093/brain/awz406
5. Tang G, Luo L, Zhang J, Zhai D, Huang D, Yin J, et al. lncRNA LINC01057 Promotes Mesenchymal Differentiation by Activating NF-kappaB Signaling in Glioblastoma. *Cancer Lett* (2021) 498:152–64. doi: 10.1016/j.canlet.2020.10.047
6. Statello L, Guo CJ, Chen LL, Huarte M. Gene Regulation by Long Non-Coding RNAs and Its Biological Functions. *Nat Rev Mol Cell Biol* (2021) 22(2):96–118. doi: 10.1038/s41580-020-00315-9
7. Liu L, Shi Y, Shi J, Wang H, Sheng Y, Jiang Q, et al. The Long non-Coding RNA SNHG1 Promotes Glioma Progression by Competitively Binding to miR-194 to Regulate PHLDA1 Expression. *Cell Death Dis* (2019) 10(6):463. doi: 10.1038/s41419-019-1698-7
8. Chai Y, Wu HT, Liang CD, You CY, Xie MX, Xiao SW. Exosomal lncRNA ROR1-AS1 Derived From Tumor Cells Promotes Glioma Progression *via* Regulating miR-4686. *Int J Nanomedicine* (2020) 15:8863–72. doi: 10.2147/IJN.S271795
9. Cai H, Yu Y, Ni X, Li C, Hu Y, Wang J, et al. LncRNA LINC00998 Inhibits the Malignant Glioma Phenotype *via* the CBX3-Mediated C-Met/Akt/mTOR Axis. *Cell Death Dis* (2020) 11(12):1032. doi: 10.1038/s41419-020-03247-6
10. Yang B, Sun L, Liang L. LncRNA HOXC-AS3 Suppresses the Formation of Mature miR-96 in Ovarian Cancer Cells to Promote Cell Proliferation. *Reprod Sci* (2021) 28(8):2342–9. doi: 10.1007/s43032-021-00500-x
11. Yang Z, Hu T. Long Noncoding RNA HOXC-AS3 Facilitates the Progression of Invasive Mucinous Adenocarcinomas of the Lung *via* Modulating FUS/Foxm1. *In Vitro Cell Dev Biol Anim* (2020) 56(1):15–23. doi: 10.1007/s11626-019-00414-8
12. Zhang E, He X, Zhang C, Su J, Lu X, Si X, et al. A Novel Long Noncoding RNA HOXC-AS3 Mediates Tumorigenesis of Gastric Cancer by Binding to YBX1. *Genome Biol* (2018) 19(1):154. doi: 10.1186/s13059-018-1523-0
13. Wang X, Sun Y, Xu T, Qian K, Huang B, Zhang K, et al. HOXB13 Promotes Proliferation, Migration, and Invasion of Glioblastoma Through Transcriptional Upregulation of lncRNA HOXC-As3. *J Cell Biochem* (2019) 120(9):15527–37. doi: 10.1002/jcb.28819
14. Tang Z, Li C, Kang B, Gao G, Li C, Zhang Z. GEPIA: A Web Server for Cancer and Normal Gene Expression Profiling and Interactive Analyses. *Nucleic Acids Res* (2017) 45(W1):W98–W102. doi: 10.1093/nar/gkx247
15. DeWitt JC, Mock A, Louis DN. The 2016 WHO Classification of Central Nervous System Tumors: What Neurologists Need to Know. *Curr Opin Neurol* (2017) 30(6):643–9. doi: 10.1097/WCO.0000000000000490
16. Wang F, Wang Q, Liu B, Mei L, Ma S, Wang S, et al. The Long Noncoding RNA Synage Regulates Synapse Stability and Neuronal Function in the Cerebellum. *Cell Death Differ* (2021) 28(9):2634–50. doi: 10.1038/s41418-021-00774-3

17. Lu C, Wei Y, Wang X, Zhang Z, Yin J, Li W, et al. DNA-Methylation-Mediated Activating of lncRNA SNHG12 Promotes Temozolomide Resistance in Glioblastoma. *Mol Cancer* (2020) 19(1):28. doi: 10.1186/s12943-020-1137-5
18. Zeng Z, Xia L, Fan S, Zheng J, Qin J, Fan X, et al. Circular RNA CircMAP3K5 Acts as a MicroRNA-22-3p Sponge to Promote Resolution of Intimal Hyperplasia *Via* TET2-Mediated Smooth Muscle Cell Differentiation. *Circulation* (2021) 143 (4):354–71. doi: 10.1161/CIRCULATIONAHA.120.049715
19. Messaoudi K, Clavreul A, Lagarce F. Toward an Effective Strategy in Glioblastoma Treatment. Part I: Resistance Mechanisms and Strategies to Overcome Resistance of Glioblastoma to Temozolomide. *Drug Discov Today* (2015) 20(7):899–905. doi: 10.1016/j.drudis.2015.02.011
20. Liao Y, Shen L, Zhao H, Liu Q, Fu J, Guo Y, et al. LncRNA CASC2 Interacts With miR-181a to Modulate Glioma Growth and Resistance to TMZ Through PTEN Pathway. *J Cell Biochem* (2017) 118(7):1889–99. doi: 10.1002/jcb.25910
21. Wu P, Cai J, Chen Q, Han B, Meng X, Li Y, et al. Lnc-TALC Promotes O(6)-Methylguanine-DNA Methyltransferase Expression *via* Regulating the C-Met Pathway by Competitively Binding With miR-20b-3p. *Nat Commun* (2019) 10(1):2045. doi: 10.1038/s41467-019-10025-2
22. Koritzinsky EH, Street JM, Star RA, Yuen PS. Quantification of Exosomes. *J Cell Physiol* (2017) 232(7):1587–90. doi: 10.1002/jcp.25387
23. Zhang Z, Yin J, Lu C, Wei Y, Zeng A, You Y. Exosomal Transfer of Long non-Coding RNA SBF2-AS1 Enhances Chemoresistance to Temozolomide in Glioblastoma. *J Exp Clin Cancer Res* (2019) 38(1):166. doi: 10.1186/s13046-019-1139-6
24. Lai CP, Mardini O, Ericsson M, Prabhakar S, Maguire C, Chen JW, et al. Dynamic Biodistribution of Extracellular Vesicles *In Vivo* Using a Multimodal Imaging Reporter. *ACS Nano* (2014) 8(1):483–94. doi: 10.1021/nn404945r
25. Katakowski M, Buller B, Zheng X, Lu Y, Rogers T, Osobamiro O, et al. Exosomes From Marrow Stromal Cells Expressing miR-146b Inhibit Glioma Growth. *Cancer Lett* (2013) 335(1):201–4. doi: 10.1016/j.canlet.2013.02.019
26. Munoz JL, Bliss SA, Greco SJ, Ramkissoon SH, Ligon KL, Rameshwar P. Delivery of Functional Anti-miR-9 by Mesenchymal Stem Cell-Derived Exosomes to Glioblastoma Multiforme Cells Conferred Chemosensitivity. *Mol Ther Nucleic Acids* (2013) 2:e126. doi: 10.1038/mtna.2013.60
27. Marleau AM, Chen CS, Joyce JA, Tullis RH. Exosome Removal as a Therapeutic Adjuvant in Cancer. *J Transl Med* (2012) 10:134. doi: 10.1186/1479-5876-10-134
28. Li SY, Zhu Y, Li RN, Huang JH, You K, Yuan YF, et al. LncRNA Lnc-APUE Is Repressed by HNF4alpha and Promotes G1/S Phase Transition and Tumor Growth by Regulating MiR-20b/E2F1 Axis. *Adv Sci (Weinh)* (2021) 8 (7):2003094. doi: 10.1002/advs.202003094
29. Chen C, Luo Y, He W, Zhao Y, Kong Y, Liu H, et al. Exosomal Long Noncoding RNA LNMAT2 Promotes Lymphatic Metastasis in Bladder Cancer. *J Clin Invest* (2020) 130(1):404–21. doi: 10.1172/JCI130892
30. Liu L, Cui S, Wan T, Li X, Tian W, Zhang R, et al. Long non-Coding RNA HOTAIR Acts as a Competing Endogenous RNA to Promote Glioma Progression by Sponging miR-126-5p. *J Cell Physiol* (2018) 233(9):6822–31. doi: 10.1002/jcp.26432
31. Su J, Yu B, Zhang C, Yi P, Li H, Xu C, et al. Long Noncoding RNA HOXC-AS3 Indicates a Poor Prognosis and Regulates Tumorigenesis by Binding to YBX1 in Breast Cancer. *Am J Transl Res* (2020) 12(10):6335–50.
32. Fu T, Ji X, Bu Z, Zhang J, Wu X, Zong X, et al. Identification of Key Long Non-Coding RNAs in Gastric Adenocarcinoma. *Cancer Biomark* (2020) 27(4):541–53. doi: 10.3233/CBM-192389
33. Li B, Han H, Song S, Fan G, Xu H, Zhou W, et al. HOXC10 Regulates Osteogenesis of Mesenchymal Stromal Cells Through Interaction With Its Natural Antisense Transcript lncHOXC-As3. *Stem Cells* (2019) 37(2):247–56. doi: 10.1002/stem.2925
34. Shi SH, Jiang J, Zhang W, Sun L, Li XJ, Li C, et al. A Novel lncRNA HOXC-AS3 Acts as a miR-3922-5p Sponge to Promote Breast Cancer Metastasis. *Cancer Invest* (2020) 38(1):1–12. doi: 10.1080/07357907.2019.1695816
35. Roscigno G, Cirella A, Affinito A, Quintavalle C, Scognamiglio I, Palma F, et al. miR-216a Acts as a Negative Regulator of Breast Cancer by Modulating Stemness Properties and Tumor Microenvironment. *Int J Mol Sci* (2020) 21 (7):2313. doi: 10.3390/ijms21072313
36. Qu XH, Shi YL, Ma Y, Bao WW, Yang L, Li JC, et al. LncRNA DANCR Regulates the Growth and Metastasis of Oral Squamous Cell Carcinoma Cells *via* Altering miR-216a-5p Expression. *Hum Cell* (2020) 33(4):1281–93. doi: 10.1007/s13577-020-00411-0
37. Sun T, An Q, Yan R, Li K, Zhu K, Dang C, et al. MicroRNA216a5p Suppresses Esophageal Squamous Cell Carcinoma Progression by Targeting KIAA0101. *Oncol Rep* (2020) 44(5):1971–84. doi: 10.3892/or.2020.7751
38. Wang W, Li Y, Ma Q, Yan H, Su W. Differentiation Antagonizing non-Protein Coding RNA Modulates the Proliferation, Migration, and Angiogenesis of Glioma Cells by Targeting the miR-216a/LGR5 Axis and the PI3K/AKT Signaling Pathway. *Oncol Targets Ther* (2019) 12:2439–49. doi: 10.2147/OTT.S196851
39. Kornecki E, Walkowiak B, Naik UP, Ehrlich YH. Activation of Human Platelets by a Stimulatory Monoclonal Antibody. *J Biol Chem* (1990) 265 (17):10042–8. doi: 10.1016/S0021-9258(19)38776-9
40. Naik UP, Eckfeld K. Junctional Adhesion Molecule 1 (JAM-1). *J Biol Regul Homeost Agents* (2003) 17(4):341–7.
41. Ebnet K, Suzuki A, Ohno S, Vestweber D. Junctional Adhesion Molecules (JAMs): More Molecules With Dual Functions? *J Cell Sci* (2004) 117(Pt 1):19–29. doi: 10.1242/jcs.00930
42. Solimando AG, Brandl A, Mattenheimer K, Graf C, Ritz M, Ruckdeschel A, et al. JAM-A as a Prognostic Factor and New Therapeutic Target in Multiple Myeloma. *Leukemia* (2018) 32(3):736–43. doi: 10.1038/leu.2017.287
43. Upadhaya P, Barhoi D, Giri A, Bhattacharjee A, Giri S. Joint Detection of Claudin-1 and Junctional Adhesion Molecule-A as a Therapeutic Target in Oral Epithelial Dysplasia and Oral Squamous Cell Carcinoma. *J Cell Biochem* (2019) 120(10):18117–27. doi: 10.1002/jcb.29115
44. Ivana B, Emina M, Marijana MK, Irena J, Zoran B, Radmila J. High Expression of Junctional Adhesion Molecule-A Is Associated With Poor Survival in Patients With Epithelial Ovarian Cancer. *Int J Biol Markers* (2019) 34(3):262–8. doi: 10.1177/1724600819850178
45. Kakiuchi A, Kakuki T, Ohwada K, Kurose M, Kondoh A, Obata K, et al. HDAC Inhibitors Suppress the Proliferation, Migration and Invasiveness of Human Head and Neck Squamous Cell Carcinoma Cells *via* P63mediated Tight Junction Molecules and P21mediated Growth Arrest. *Oncol Rep* (2021) 45(4):46. doi: 10.3892/or.2021.7997
46. Communal L, Medrano M, Sircoulomb F, Paterson J, Kobel M, Rahimi K, et al. Low Junctional Adhesion Molecule-A Expression Is Associated With an Epithelial to Mesenchymal Transition and Poorer Outcomes in High-Grade Serous Carcinoma of Uterine Adnexa. *Mod Pathol* (2020) 33(11):2361–77. doi: 10.1038/s41379-020-0586-0
47. Orlandella FM, Mariniello RM, Iervolino PLC, Auletta L, De Stefano AE, Ugolini C, et al. Junctional Adhesion Molecule-A Is Down-Regulated in Anaplastic Thyroid Carcinomas and Reduces Cancer Cell Aggressiveness by Modulating P53 and GSK3 Alpha/Beta Pathways. *Mol Carcinog* (2019) 58 (7):1181–93. doi: 10.1002/mc.23001
48. Jiang X, Dai B, Feng L. miR-543 Promoted the Cell Proliferation and Invasion of Nasopharyngeal Carcinoma by Targeting the JAM-A. *Hum Cell* (2019) 32 (4):477–86. doi: 10.1007/s13577-019-00274-0
49. Alvarado AG, Turaga SM, Sathyan P, Mulkearns-Hubert EE, Otvos B, Silver DJ, et al. Coordination of Self-Renewal in Glioblastoma by Integration of Adhesion and microRNA Signaling. *Neuro Oncol* (2016) 18(5):656–66. doi: 10.1093/neuonc/nov196
50. Rosager AM, Sorensen MD, Dahlrot RH, Boldt HB, Hansen S, Lathia JD, et al. Expression and Prognostic Value of JAM-A in Gliomas. *J Neurooncol* (2017) 135(1):107–17. doi: 10.1007/s11060-017-2555-0
51. Pong WW, Walker J, Wylie T, Magrini V, Luo J, Emnett RJ, et al. F11R is a Novel Monocyte Prognostic Biomarker for Malignant Glioma. *PloS One* (2013) 8(10):e77571. doi: 10.1371/journal.pone.0077571
52. Turaga SM, Silver DJ, Bayik D, Paouri E, Peng S, Lauko A, et al. JAM-A Functions as a Female Microglial Tumor Suppressor in Glioblastoma. *Neuro Oncol* (2020) 22(11):1591–601. doi: 10.1093/neuonc/noaa148

Conflict of Interest: The authors declare that the research was conducted in the absence of any commercial or financial relationships that could be construed as a potential conflict of interest.

this article, or claim that may be made by its manufacturer, is not guaranteed or endorsed by the publisher.

frontiers | Frontiers in Oncology

ORIGINAL RESEARCH
published: 17 June 2022
doi: 10.3389/fonc.2022.898614

Impact of Neoadjuvant Bevacizumab on Neuroradiographic Response and Histological Findings Related to Tumor Stemness and the Hypoxic Tumor Microenvironment in Glioblastoma: Paired Comparison Between Newly Diagnosed and Recurrent Glioblastomas

Jun Takei[1], Nei Fukasawa[2], Toshihide Tanaka[1,3], Yohei Yamamoto[4], Ryota Tamura[5], Hikaru Sasaki[5], Yasuharu Akasaki[1], Yuko Kamata[6], Mutsunori Murahashi[6], Masayuki Shimoda[2] and Yuichi Murayama[1]*

[1] Department of Neurosurgery, Jikei University School of Medicine, Tokyo, Japan, [2] Department of Pathology, Jikei University School of Medicine, Tokyo, Japan, [3] Department of Neurosurgery, Jikei University School of Medicine Kashiwa Hospital, Kashiwa, Japan, [4] Department of Neurosurgery, Jikei University School of Medicine Daisan Hospital, Tokyo, Japan, [5] Department of Neurosurgery, Keio University School of Medicine, Tokyo, Japan, [6] Division of Oncology, Research Center for Medical Sciences, Jikei University School of Medicine, Tokyo, Japan

Background: Previously, we reported that bevacizumab (Bev) produces histological and neuroradiographic alterations including changes in tumor oxygenation, induction of an immunosupportive tumor microenvironment, and inhibition of stemness. To confirm how those effects vary during Bev therapy, paired samples from the same patients with newly diagnosed glioblastoma (GBM) who received preoperative neoadjuvant Bev (neoBev) were investigated with immunohistochemistry before and after recurrence.

Methods: Eighteen samples from nine patients with newly diagnosed GBM who received preoperative neoBev followed by surgery and chemoradiotherapy and then autopsy or salvage surgery after recurrence were investigated. The expression of carbonic anhydrase 9 (CA9), hypoxia-inducible factor-1 alpha (HIF-1α), nestin, and Forkhead box M1 (FOXM1) was evaluated with immunohistochemistry.For comparison between neoBev and recurrent tumors, we divided the present cohort into two groups based on neuroradiographic response: good and poor responders (GR and PR, respectively) to Bev were defined by the tumor regression rate on T1-weighted images with gadolinium enhancement (T1Gd) and fluid-attenuated inversion recovery images. Patterns of recurrence after Bev therapy were classified as cT1 flare-up and T2-diffuse/T2-circumscribed. Furthermore, we explored the possibility of utilizing FOXM1 as a biomarker of survival in this cohort.

OPEN ACCESS

Edited by:
Bozena Kaminska, Nencki Institute of Experimental Biology (PAS), Poland

Reviewed by:
Hiroaki Wakimoto, Massachusetts General Hospital and Harvard Medical School, United States
Katayoun Ayasoufi, Mayo Clinic, United States
Serena Pellegatta, IRCCS Carlo Besta Neurological Institute Foundation, Italy

***Correspondence:**
Toshihide Tanaka
ttanaka@jikei.ac.jp

Specialty section:
This article was submitted to Neuro-Oncology and Neurosurgical Oncology, a section of the journal Frontiers in Oncology

Received: *17 March 2022*
Accepted: *17 May 2022*
Published: *17 June 2022*

Citation:
Takei J, Fukasawa N, Tanaka T, Yamamoto Y, Tamura R, Sasaki H, Akasaki Y, Kamata Y, Murahashi M, Shimoda M and Murayama Y (2022) Impact of Neoadjuvant Bevacizumab on Neuroradiographic Response and Histological Findings Related to Tumor Stemness and the Hypoxic Tumor Microenvironment in Glioblastoma: Paired Comparison Between Newly Diagnosed and Recurrent Glioblastomas. Front. Oncol. 12:898614. doi: 10.3389/fonc.2022.898614

Results: A characteristic "pseudo-papillary"-like structure containing round-shaped tumor cells clustered adjacent to blood vessels surrounded by spindle-shaped tumor cells was seen only in recurrent tumors. Tumor cells at the outer part of the "pseudo-papillary" structure were CA9-positive (CA9+)/HIF-1α+, whereas cells at the inner part of this structure were CA9–/HIF-1α+ and nestin+/FOXM1+. CA9 and HIF-1α expression was lower in T1Gd-GR and decreased in the "T2-circumscribed/T2-diffuse" pattern compared with the "T1 flare-up" pattern, suggesting that tumor oxygenation was frequently observed in T1Gd-GR in initial tumors and in the "T2-circumscribed/T2-diffuse" pattern in recurrent tumors. FOXM1 low-expression tumors tended to have a better prognosis than that of FOXM1 high-expression tumors.

Conclusion: A "pseudo-papillary" structure was seen in recurrent GBM after anti-vascular endothelial growth factor therapy. Bev may contribute to tumor oxygenation, leading to inhibition of stemness and correlation with a neuroimaging response during Bev therapy. FOXM1 may play a role as a biomarker of survival during Bev therapy.

Keywords: bevacizumab, glioblastoma, FOXM1, magnetic resonance imaging (MRI), tumor microenvironment, pseudo-papillary structure

INTRODUCTION

Bevacizumab (Bev) is a monoclonal antibody against vascular endothelial growth factor (VEGF)/vascular permeability factor and blocks endothelial proliferation and vascular permeability, thus reducing enhancement and perifocal edema in glioblastoma (GBM). The effect of Bev on GBM depends on not only inhibition of tumor angiogenesis but also alteration of the tumor microenvironment (TME) from immunosuppressive to immunosupportive (1).

The alteration in the TME induces tumor oxygenation from a hypoxic TME, leading to inhibition of stemness in the perivascular niche (2–4) and infiltration of immunosuppressive cells including regulatory T cells and M2 tumor-associated macrophages (5, 6). Although these effects including an immunosupportive TME are sustained for a long time, improvement in tumor oxygenation is transient (3), indicating that the therapeutic efficacy of Bev is difficult to maintain over a long period of time. Bev induces oxygenation of the TME, leading to tumor dormancy. A hypoxic TME restimulates stemness, which may be a reason for the dismal clinical outcome of GBM in a short period of time (7). The duration of maintenance of the TME in a dormant state may impact the clinical outcome, regardless of the initial response to Bev on gadolinium-enhanced neuroimages and perifocal edema.

In recent years, glioma stem cells (GSCs) have become a cell type of increasing interest. GSCs survive in hypoxic and starvation conditions (8, 9). A number of molecular markers are generally used to isolate and characterize GSCs (10, 11). The TME, including vascularity and tumor oxygenation, is very important for the survival of GSCs. More importantly, GSCs are resistant to radiation (RT) and temozolomide (TMZ) compared with differentiated tumor cells (12). In addition, a hypoxic TME induces VEGF expression, resulting in resistance to RT and TMZ and difficulty in controlling GSCs in recurrent tumors (13, 14).

CD133-positive (CD133+) cells include vascular endothelial cells and other cells in the perivascular niche that maintain GSC characteristics *via* VEGF and NOTCH signaling in the microenvironment (2). Bev is considered to be a reasonable treatment to control GSCs and maintain an oxygenated and immunosupportive TME. However, its efficacy is transient, and the biomarkers that predict survival remain unknown.

Among these molecular markers, nestin is an intermediate filament protein expressed in neural progenitor stem cells (15). Nestin is expressed in many GBMs, and the differentiation of GBM cells leads to the downregulation of nestin, a potential marker for GSCs (16). Whether the level of nestin expression is correlated with the histological grade of malignancy in gliomas and the clinical outcome is still controversial (17–19). Therefore, whether nestin expression is a biomarker for survival is uncertain.

We also focused on the possibility that Forkhead box M1 (FOXM1) may be a biomarker of survival during Bev therapy. FOXM1 is a key transcription factor, plays a critical role in tumorigenesis and transformation of normal astrocytes, and is overexpressed in GBM (20). FOXM1 also binds to the *VEGF* promoter and contributes to angiogenesis and growth of GSCs in GBM by upregulation of VEGF (21). Furthermore, FOXM1 is upregulated in recurrent GBM, both at the mRNA and protein levels, and a high level of FOXM1 expression is associated with poor prognosis in recurrent GBM (22). However, no previous studies have investigated alterations in FOXM1 expression or its reliability as a predictive biomarker of survival in GBM during anti-VEGF therapy.

Previously, we reported that Bev induces tumor oxygenation in accordance with a decrease in microvessel density (MVD) and inhibition of immunosuppressive cell and stem cell infiltration

by comparative analyses among initial GBM (naive-Bev), GBM with radiological effectiveness of Bev at the time of treatment with preoperative neoadjuvant Bev (neoBev, effective-Bev), and recurrent GBM after Bev failure (refractory-Bev) (3, 5). However, in our previous studies, all samples of refractory-Bev were derived from patients who did not receive neoBev.

As far as we know, the present study is the first report to investigate the neuroradiographic response before and after recurrence with a comparison of paired samples from the same patients who received preoperative neoBev followed by surgery combined with RT, TMZ, and Bev, and then autopsy or salvage surgery after Bev failure. The purpose of this study was to investigate the following: 1) the difference between neoBev and refractory-Bev according to histological and immunohistochemical findings, 2) changes in FOXM1 expression during anti-VEGF therapy and its potential as a biomarker of survival, and 3) TME change in accordance with the neuroradiographic response during Bev therapy.

METHODS

Patient Characteristics and Treatment Protocol

The present study used 18 paired surgical samples from nine patients with newly diagnosed GBM obtained from surgery at the time of initial and recurrent tumors, including nine tumor samples obtained from surgery following neoBev, eight tumor samples obtained from autopsy, and one recurrent tumor. Four of these nine patients were included in the Japan Registry of Clinical Trials (jRCT1031180233).

All patients were treated with preoperative neoBev at a dose of 10 mg/kg on day 0. Surgical resection was performed 3–4 weeks after neoBev. Concomitant RT and TMZ were commenced more than 2 weeks after surgery. Maintenance treatment with TMZ began more than 4 weeks after completion of RT at a starting dose of 150 mg/m^2 for 5 consecutive days of a 28-day cycle. Bev (at a dose of 10 mg/kg) concomitant with TMZ (every 4 weeks at a dose of 150 mg/m^2) was readministered every 2 weeks at the time of recurrence and continued until reprogression or beyond reprogression in tolerant patients. The mean number of cycles of Bev was 16.1 (range, 7~38 cycles).

Neuroradiological Assessment

The tumor volumes of T1-weighted images with gadolinium enhancement (T1Gd) or fluid-attenuated inversion recovery (FLAIR) were estimated by the sum of each slice on neuroimages and multiplication of longitudinal and transverse slices. Tumor volume was assessed by the sum of perpendicular diameters as previously described (23). The tumor regression rate with neoBev was evaluated by the change in tumor volume before and after treatment. Patterns of recurrence after Bev therapy were classified as cT1 flare-up, T2-diffuse, or T2-circumscribed as previously described (3, 24).

Briefly, the cT1 flare-up is characterized by an initial decrease in contrast enhancement (CE) on T1-weighted images after treatment initiation and an increase (flare-up) of CE again at tumor progression. T2 signal stays stable or increased. T2-diffuse is characterized by a signal increase on T2-weighted images with a poorly defined border despite the fact that CE on T1-weighted images remains decreased. Hypointensity on T1-weighted images is faint and disproportionally smaller than T2 hyperintensity. T2-circumscribed is characterized by a signal increase on T2-weighted images with a bulky structure and sharp borders that correspond to a T1 hypointense signal. CE on T1-weighted images remains decreased, or only a few faintly speckled CE lesions are visible.

Immunohistochemical Analyses

Immunohistochemical analyses were performed on 4-μm sections of formalin-fixed, paraffin-embedded tissue from 18 tumors. Sections were stained with anti-FOXM1 antibody (1:250, #ab207298, abcam), anti-hypoxia-inducible factor-1 alpha (HIF-1α) antibody (1:100, #ab82832, Dako), anti-nestin antibody (1:1,000, MAB5326, Chemical), anti-carbonic anhydrase 9 (CA9) antibody (1:1,000, #ab15086, abcam), and anti-CD34 antibody (1:100, M7165, abcam). Antigen retrieval was performed in 10 mM citrate buffer (pH 6.0) using an autoclave for FOXM1, HIF-1α, and CD34 staining. Immunohistochemical staining was assessed by three authors (JT, NF, and TT) who were blinded to the clinical information, and the results of consensus among these authors were reported.

Immunohistochemical findings were assessed as previously described (5, 25, 26). For FOXM1 quantitative evaluation, the percentage of tumor nuclei reactive to FOXM1 antibody was estimated following examination of a middle-power field (×200) using the software Gunma labeling index (27). The expression of nestin was assessed as a positive cell ratio analyzed in five high-power fields (×400) and calculated as the mean value of [(positive cells/positive cell + negative cell) × 100] from five areas. The expression of HIF-1α was predominantly detected in the nuclei of tumor cells around sites of necrosis and was also found in tumor cells not directly adjacent to necrotic areas. The degree of expression was assessed as follows: ++, expression in >10% of tumor cells; +, expression in ≤10% of tumor cells; −, negative staining. The membranous expression of CA9 was predominantly found in perinecrotic tumor cells as previously reported (28). The degree of expression was assessed as follows: ++, universal strong expression around necrotic regions; +, occasional expression (typically around necrotic regions); −, negative staining. For quantitative evaluation of CD34+ vessels, the stained sections were screened in a low-power field (×40), and five middle-power fields (×200) with the most dense spots were assessed. The mean MVD in these areas was determined using Fiji software (version 2.0.0-re-69/1.52p) (29).

Statistical Analyses

Continuous data are described as the mean ± standard deviation, median, and interquartile range, and categorical data as numbers

and percentages. The Mann–Whitney U test and Wilcoxon signed rank test were used for comparison of continuous data between two groups. Fisher's exact test was used to determine if non-random associations were present between two categorical variables. All p-values were two-sided with the significance level set to ≤0.05. Statistical analyses were performed with STATA 14 (Stata Corp. LP, College Station, TX, USA).

RESULTS

Description of the Present Cohort

The characteristics of the patients in the present study are summarized in **Table 1**. Patients who were enrolled in the present study consisted of eight men and one woman with a mean age of 65.6 years (range, 50–78 years). Histological findings revealed that all tumors were diagnosed as GBM, isocitrate dehydrogenase (IDH)-wild type. Median tumor regression rates after neoBev were 38% and 54% on T1Gd and FLAIR magnetic resonance imaging (MRI), respectively. Median progression-free survival (PFS) (the interval from initial Bev administration to recurrence) was 9.8 months. Median overall survival (OS) (the interval from initial Bev to death) was 16.6 months.

Illustrative Neuroimages After NeoBev

Patients receiving neoBev were selected according to MRI findings that represented "typical" GBM including a ring-enhanced tumor (**Figures 1A, B**) with perifocal edema (**Figures 1C, D**). After a single dose of Bev (10 mg/kg), the tumor and the perifocal edema regressed as shown by a representative maximal (**Figures 1E, F**) and minimal response (**Figures 1G, H**) 2 weeks after treatment.

Typical Histological Findings of "Pseudo-Papillary Structures" at the Time of Recurrence After NeoBev Demonstrating Colocalization of FOXM1, Nestin, CA9, and HIF-1α Expression

Histological findings of initial tumors after neoBev demonstrated that typical glomeruloid microvasculature was seldom observed. Tumor cells predominantly accumulated around the vessels (the so-called vascular co-option), and CD34+ cells were observed along the vessel walls (**Figures 2A, B**). The expression of CA9 was predominantly found in perinecrotic tumor cells (**Figure 2C**), but the positive expression of HIF-1α, nestin, and FOXM1 was widely distributed (**Figures 2F**).

Round-shaped tumor cells clustered adjacent to the blood vessels were further surrounded by spindle-shaped tumor cells (**Figures 2G, H**). We defined these characteristic histological findings as "pseudo-papillary" structures that were seen only in recurrent tumors but not in initial tumors. On the whole sections, these structures were observed in three out of nine recurrent tumors (33%).

Spindle-shaped cells were CA9+, and HIF-1α was strongly positive away from the blood vessels (**Figures 2I, J**). The distance from the blood vessel to the CA9+ cells was approximately 150 μm (data not shown). Interestingly, we noted a discrepancy in which the cells in the outer part of "pseudo-papillary" structures were CA9+/HIF-1α+, whereas the cells in the inner part of the structures were CA9−/HIF-1α+ (**Figures 2I, J**).

In the inner part of "pseudo-papillary" structures, nestin+ and FOXM1+ cells were clustered in round-shaped tumor cells adjacent to the blood vessels (**Figures 2K, L**), suggesting that proliferating GSCs adjacent to the microvasculature were surrounded by hypoxic tumor cells in recurrent tumors at the time of Bev failure.

TABLE 1 | Patient characteristics.

		Total (n = 9)	
		No. of Patients	(%)
Age (years)	Mean	65.6	
	SD	10.8	
Sex	Women	1	11.1
	Men	8	88.9
Neuroradiographic response after neoBev			
T1Gd	Median	38%	
	IQR	15-56	
FLAIR	Median	54%	
	IQR	27-63	
Recurrence pattern	Nonresponder	0	0
	T2-circumscribed	2	22.2
	T2-diffuse	2	22.2
	cT1 flare-up	5	55.6
PFS (months)	Mean	9.8	
	SD	4.6	
OS (months)	Mean	16.6	
	SD	5.1	

FLAIR, fluid-attenuated inversion recovery; neoBev, neoadjuvant bevacizumab; OS, overall survival; PFS, progression-free survival; SD, standard deviation; T1Gd, T1-weighted image with gadolinium enhancement.

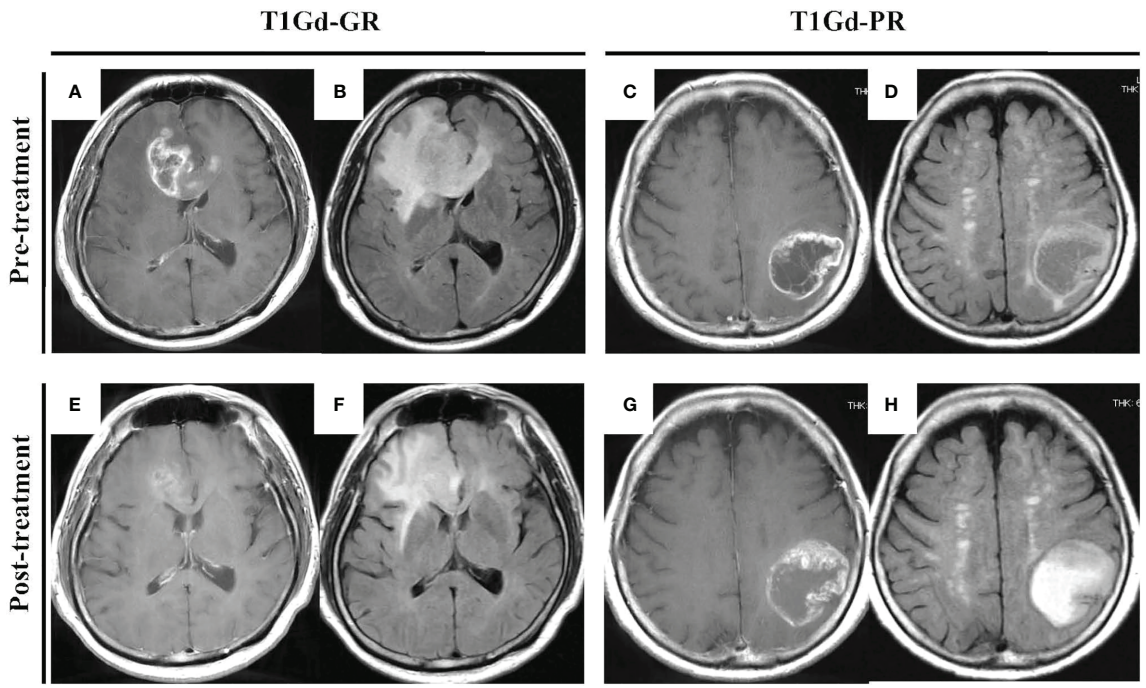

FIGURE 1 | "Typical" GBM demonstrating a huge enhanced tumor with perifocal edema before **(A–D)** and after **(E–H)** neoBev. Regression rates of T1Gd-GR **(A, E)**, T1Gd-PR **(C, G)**, FLAIR-GR **(B, F)**, and FLAIR-PR **(D, H)** after neoBev were –61%, –14%, –71%, and –26%, respectively. FLAIR, fluid-attenuated inversion recovery; GBM, glioblastoma; GR, good rensponder; PR, poor responder; T1Gd, T1-weighted images with gadolinium enhancement.

MVD was not different between tumors with and without "pseudo-papillary" structures. However, the expression of FOXM1, nestin, and hypoxic markers including CA9 and HIF-1α tended to be higher in recurrent tumors with "pseudo-papillary" structures (**Figures 2M–Q**).

Patient characteristics, neuroradiological response rate after neoBev, recurrent pattern after Bev failure, and extent of resection were compared between the presence and absence of "pseudo-papillary" structures. The clinical outcome and clinical parameters were not significantly different (**Table 2**).

Comparison of Tumor Vascularity and Tumor Oxygenation Between Initial Tumors After NeoBev and Recurrent Tumors After NeoBev

To assess vascular density and stemness in accordance with tumor oxygenation, the expression levels of FOXM1, nestin, CD34, CA9, and HIF-1α were analyzed with immunohistochemistry using paired samples from the same patients treated with neoBev followed by surgery, RT, TMZ, and TMZ/Bev combined therapy, and then salvage surgery or autopsy at the time of recurrence after Bev (**Figure 3**).

FOXM1 tended to decrease at the time of recurrence (**Figure 3A**), and nestin was found to be significantly decreased at the time of recurrence (**Figure 3B**). MVD diminished during Bev therapy, but the difference was not statistically significant (**Figure 3C**). The expression of CA9 (++) was slightly higher in recurrent tumors compared with initial tumors, but HIF-1α expression decreased in recurrent tumors (**Figures 3D, E**). To determine whether or not these parameters have prognostic significance, we investigated CD34, CA9, HIF-1a, nestin, and FOXM1. We divided the current cohort into two groups according to the median index score of those parameters in initial specimens. FOXM1 low-expression tumors tended to occur in patients with a better prognosis than FOXM1 high-expression tumors ($p = 0.053$, log-rank test) (**Figure 3F**). Whereas other parameters including expression levels of nestin ($p = 0.89$, log-rank test) (**Figure 3G**), microvascular density as quantified by CD34 positivity ($p = 0.43$, log-rank test) (**Figure 3H**), qualitative reaction of CA9 ($p = 0.72$, log-rank test) (**Figure 3I**), and qualitative reaction of HIF-1α ($p = 0.83$, log-rank test) (**Figure 3J**) were not associated with OS in the current cohort.

T1Gd-GR vs. T1Gd-PR in the Tumor Microenvironment Including Tumor Oxygenation, Stemness, and Tumor Vascularity

To analyze the correlation between the TME assessed with immunohistochemistry and responsiveness to neoBev assessed with T1Gd and FLAIR, the expression of FOXM1, nestin, CD34, CA9, and HIF-1α was compared between GR and PR after neoBev.

We divided this cohort into two groups according to the imaging neoadjuvant therapy response rate. Thus, T1Gd good

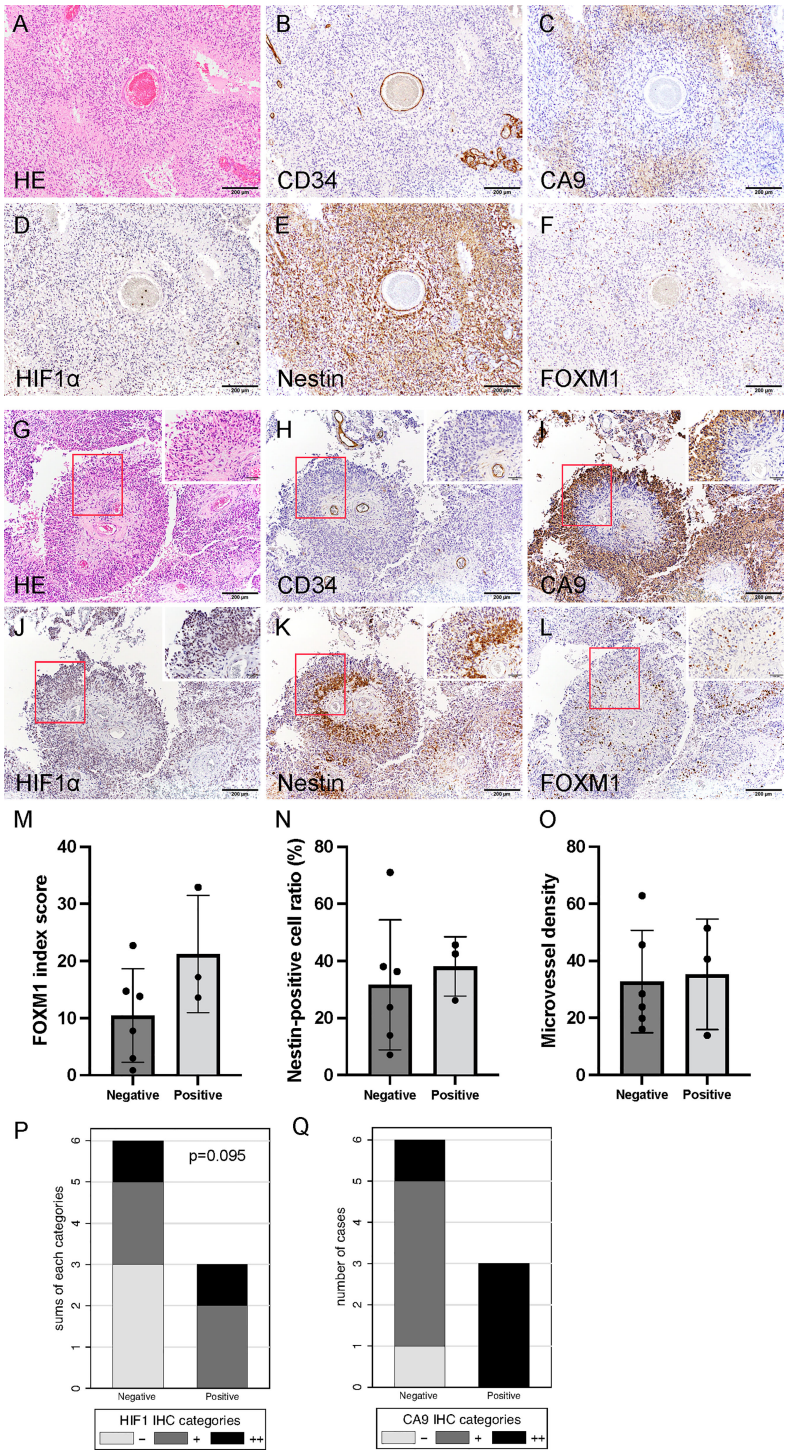

FIGURE 2 | Histological finding of initial tumors revealing that tumor cells predominantly accumulated around the vessels (so-called vascular co-option). Hematoxylin and eosin staining **(A)** and CD34 **(B)**, CA9 **(C)**, HIF-1α **(D)**, nestin **(E)**, and FOXM1 expression **(F)**. Photomicrograph of immunohistochemistry (×200) (bar = 100 μm). Note that CA9 expression was found in the perinecrotic tumor cells, and the expression of HIF-1α, nestin, and FOXM1 was widely distributed. Typical histological findings of "pseudo-papillary" structures resembling "vascular co-option" in recurrent tumors. Hematoxylin and eosin staining **(G)** and CD34 **(H)**, CA9 **(I)**, HIF-1α **(J)**, nestin **(K)**, and FOXM1 expression **(L)**. Photomicrograph of immunohistochemistry (×200; bar = 100 μm); (×400; bar = 100 μm). Note that colocalization of FOXM1- and HIF-1α-positive cells was prominent in the perivascular area. Comparison of expression of FOXM1, MVD, and tumor oxygenation between the presence and absence of "pseudo-papillary" structures. FOXM1 **(M)**, nestin **(N)**, MVD **(O)**, CA9 **(P)**, and HIF-1α expression **(Q)**. Error bar; standard deviation. CA9, carbonic anhydrase 9; FOXM1, Forkhead box M1; HIF-1α, hypoxia inducible factor-1 alpha; MVD, microvessel density.

TABLE 2 | Comparison of clinical characteristics between positive and negative "pseudo-papillary" structures.

		Pseudo-papillary structures				
		Positive (n = 3) No. of Patients	(%)	Negative (n = 6) No. of Patients	(%)	p value
Age (years)	Mean	57.7		69.5		0.121*
	SD	10.8		9.2		
Sex	Women	0.0	0.0	1	16.7	1.000†
	Men	3.0	100.0	5	83.3	
Neuroradiographic response after neoBev						
T1Gd	Mean	12.7%		41.7%		0.302*
	SD	37.8		23.1		
FLAIR	Mean	47.3%		46.7%		0.796*
	SD	20.8		20.2		
Surgical removal	Total	2	66.7	4	66.7	1.000†
	Not total	1	33.3	2	33.3	
Recurrence pattern	Not described	0	0	0	0.0	0.762†
	T2-circumscribed	0	0	2	33.3	
	T2-diffuse	0	0	2	33.3	
	cT1 flare-up	3	100	2	33.3	
PFS (months)	Mean	8.7		10.4		0.663‡
	SD	1.5		5.6		
OS (months)	Mean	15.7		17.1		0.927‡
	SD	5.1		5.8		
FOXM1 index score at the time of recurrence						
	Mean	21.2		10.3		0.197*
	SD	10.3		8.4		

**Mann–Whitney U test.*
†Fisher's exact test.
‡Log-rank test.

responders (T1Gd-GRs) and T1Gd poor responders (T1Gd-PRs) were defined as having a response rate of ≥35% and <35%, respectively.

Regarding stemness, FOXM1 in recurrent tumors was significantly decreased in T1Gd-GRs, whereas no significant difference was found in T1Gd-PRs (**Figure 4A**). Nestin expression in recurrent tumors tended to be decreased in both T1Gd-GRs and PRs (**Figure 4B**). MVD showed no significant difference between T1Gd-GRs and T1Gd-PRs (**Figure 4C**).

Regarding the hypoxic TME, comparing initial tumors, the expression of CA9 and HIF-1α was higher in T1Gd-PRs, and tumor oxygenation was frequently observed in T1Gd-GRs, although no significant difference was found between the two groups (**Figures 4D, E**). Thus, these results suggested that the responsiveness to neoBev determined on T1Gd may reflect tumor oxygenation.

FLAIR-GR vs. FLAIR-PR in the Tumor Microenvironment Including Tumor Oxygenation, Stemness, and Tumor Vascularity

FLAIR good responders (FLAIR-GRs) and FLAIR poor responders (FLAIR-PRs) were defined as having a response rate of ≥50% and <50%, respectively. No significant difference in FOXM1 or nestin expression was found between FLAIR-GRs and FLAIR-PRs in the initial tumors. However, the expression of both FOXM1 and nestin significantly decreased in FLAIR-GRs at the time of recurrence (**Figures 5A, B**). MVD showed no significant difference between FLAIR-GR and FLAIR-PR (**Figure 5C**).

Regarding the hypoxic TME, CA9 and HIF-1α expression tended to decrease in FLAIR-PRs compared with that in FLAIR-GRs in both initial and recurrent tumors (**Figures 5D, E**). No significant difference was found between groups. Thus, neuroradiographic response on T1Gd and FLAIR to neoBev may illustrate opposite changes in both CA9 and HIF-1α expressions.

Recurrence Pattern in Tumor Oxygenation, Stemness, and Immunological Tumor Microenvironment

To analyze the correlation between the TME assessed with immunohistochemistry and the recurrence pattern after Bev therapy as previously described (24), the expression of FOXM1, nestin, CD34, CA9, and HIF-1α was compared between "T1 flare-up" and "T2-circumscribed/T2-diffuse" patterns. FOXM1 expression tended to decrease in the "T2-circumscribed/T2-diffuse" pattern at the time of recurrence (**Figure 6A**). Nestin expression was reduced at recurrence in both patterns, but this reduction was not statistically significant (**Figure 6B**).

MVD was not significantly different between the two groups (**Figure 6C**).

Regarding the hypoxic TME, CA9 and HIF-1α expression decreased in the "T2-circumscribed/T2-diffuse" pattern compared with that in the "T1 flare-up" pattern in recurrent

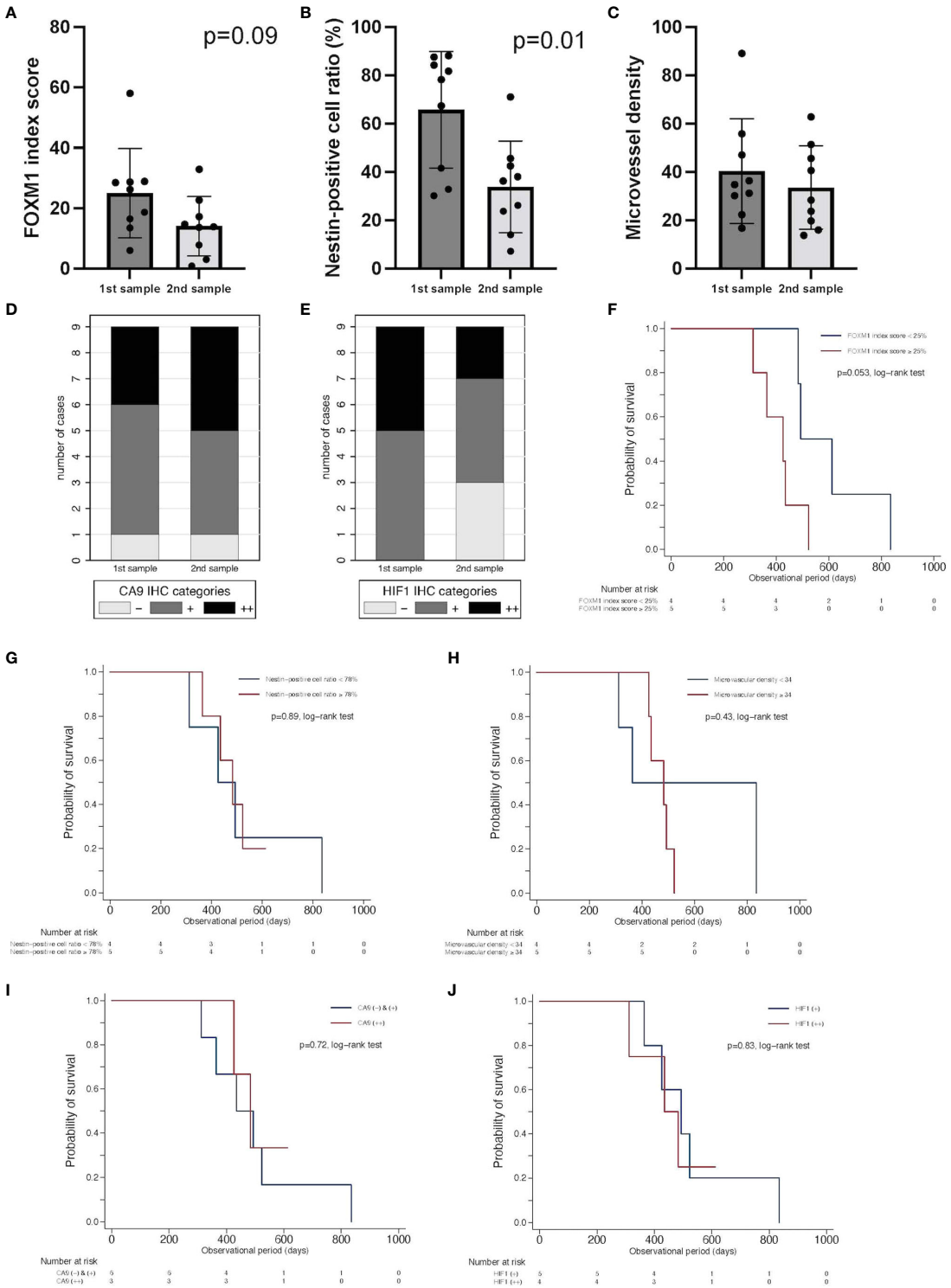

FIGURE 3 | Comparison of expression of FOXM1, tumor vascularity, and tumor oxygenation between initial tumors after neoBev and recurrent tumors after neoBev. FOXM1 **(A)**, nestin **(B)**, MVD **(C)**, CA9 **(D)**, and HIF-1α expression **(E)**. Error bar; standard deviation. Kaplan–Meier survival curves showing overall survival stratified by labeling index of FOXM1 expression (p = 0.053, log-rank test) **(F)**, labeling index of nestin expression (p = 0.89, log-rank test) **(G)**, microvascular density (p = 0.43, log-rank test) **(H)**, qualitative reaction of CA9 expression (p = 0.72, log-rank test) **(I)**, and qualitative reaction of HIF-1α expression (p = 0.83, log-rank test) **(J)**. CA9, carbonic anhydrase 9; FOXM1, Forkhead box M1; HIF-1α, hypoxia inducible factor-1 alpha; MVD, microvessel density; neoBev, neoadjuvant bevacizumab.

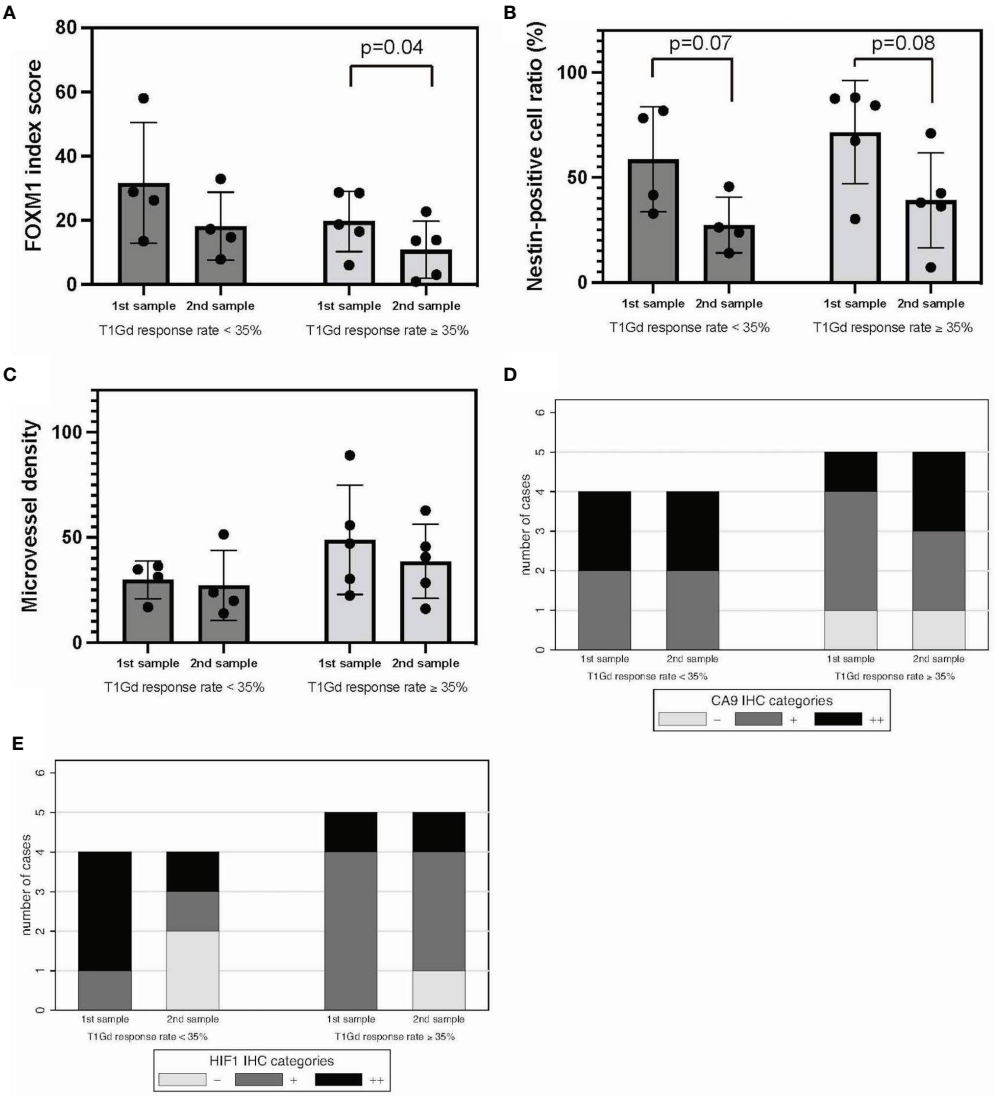

FIGURE 4 | T1Gd-GRs vs. T1Gd-PRs in tumor oxygenation, stemness, and immunological TME. FOXM1 **(A)**, nestin **(B)**, MVD **(C)**, CA9 **(D)**, and HIF-1α expression **(E)**. Error bar; standard deviation. CA9, carbonic anhydrase 9; FOXM1, Forkhead box M1; GR, good rensponder; HIF-1α, hypoxia inducible factor-1 alpha; MVD, microvessel density; PR, poor responder; TME, tumor microenvironment; T1Gd, T1-weighted images with gadolinium enhancement.

tumors (**Figures 6D, E**). HIF-1α expression in particular significantly indicated oxygenation (p = 0.024, Fisher's exact test). Thus, the recurrence pattern after Bev therapy may be correlated with tumor oxygenation after multidisciplinary treatment of GBM including Bev.

DISCUSSION

Histological Assessment and Bevacizumab Responsiveness

Our previous reports described histological findings of GBM with resistance to Bev (refractory-Bev) because Bev is usually administered to patients with recurrent GBM (3, 26). Over the past decade, the measurement of tumor vascularity with MVD has been suggested to provide histological assessment, be correlated with the invasiveness of cancer, and provide prognostic information (30). In addition, histological assessment of both tumor oxygenation and angiogenesis may be useful for the assessment of the effectiveness of antiangiogenic therapy such as Bev. However, in the present study, no relationship between hypoxia and MVD was found, as previously described (31). More reliable histological parameters are required.

Vascular co-option has received particular attention as a major mechanism of resistance to antiangiogenic treatment (32–34). Vascular co-option is a mechanism by which tumors incorporate the existing vessels of the host organs, preserving the

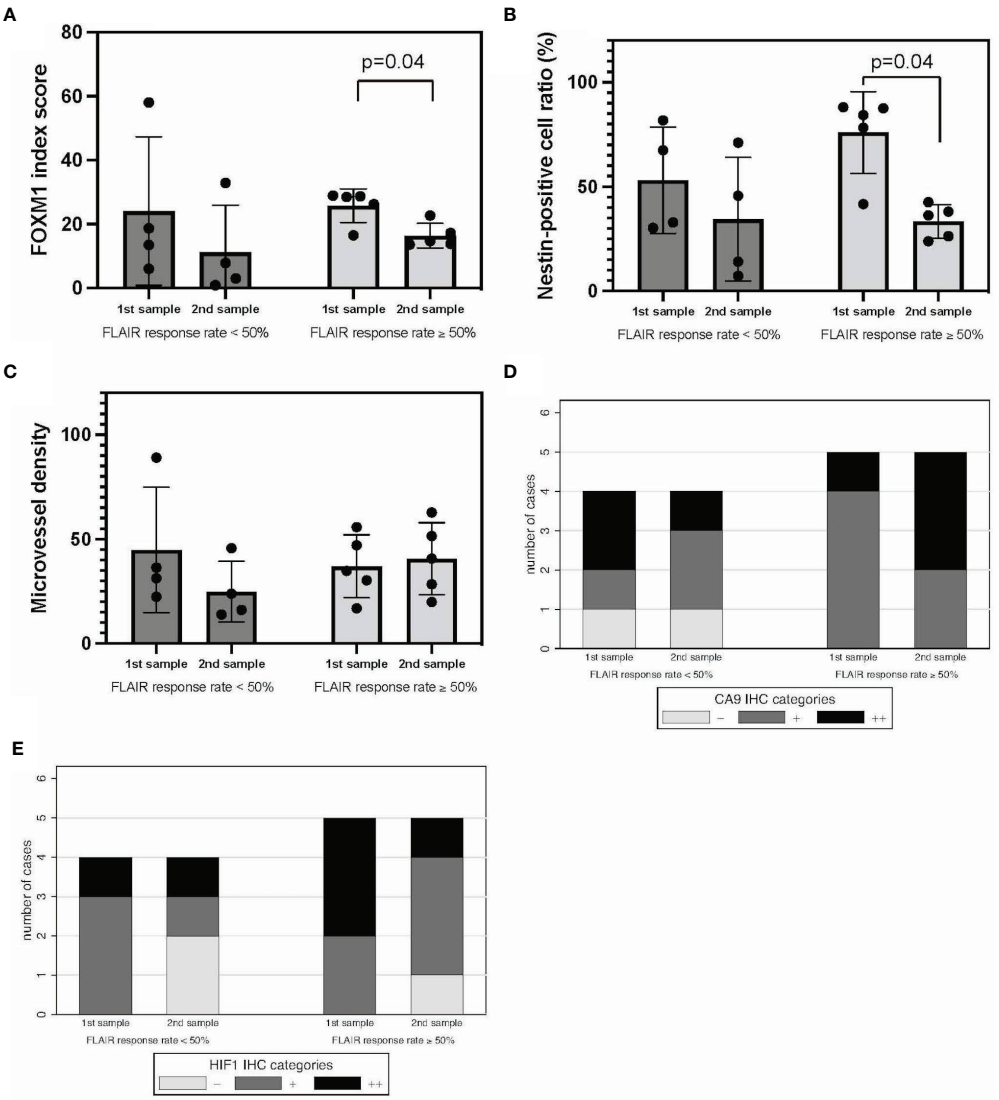

FIGURE 5 | FLAIR-GRs vs. FLAIR-PRs in tumor oxygenation, stemness, and immunological TME. FOXM1 **(A)**, nestin **(B)**, MVD **(C)**, CA9 **(D)**, and HIF-1α expression **(E)**. Error bar; standard deviation. CA9, carbonic anhydrase 9; FLAIR, fluid-attenuated inversion recovery; FOXM1, Forkhead box M1; GR, good rensponder; HIF-1α, hypoxia inducible factor-1 alpha; MVD, microvessel density; PR, poor responder; TME, tumor microenvironment.

vascular scaffold of the surrounding tissue. Vascular co-option may be an adaptive mechanism that enables tumors to survive and progress when angiogenesis is inhibited. In the present study, "pseudo-papillary" structures containing nestin +/FOXM1+ cells in the perivascular niche and CA9/HIF-1α positivity in the area surrounding stem cell accumulation resembled co-opted tumor vessels and were observed in refractory-Bev (**Figure 2**). Recurrent GBM may exploit vascular co-option as a strategy to escape anti-VEGF treatment. Optimization of anticancer therapy should consider the importance of hypoxia as a master driver of tumor angiogenesis and immunoregulatory response.

In the present study, we found that "pseudo-papillary" structures were only present in recurrent tumors. Because they are not found in initial tumors after neoBev, this phenomenon may be the result of long-term anti-VEGF therapy. A peculiar point regarding "pseudo-papillary" structures is the discrepancy in the expression pattern between CA9 and HIF-1α and nestin +/FOXM1+ cells revealed by immunohistochemical staining. The outer cells were CA9+/HIF-1α+/nestin−/FOXM1−, and the inner cells were CA9−/HIF-1α+/nestin+/FOXM1+. The discrepancy between CA9 and HIF-1α expression has been reported by Kaluz et al. (35) and reproduced *in vivo*. HIF-1α expression is induced not only in hypoxic conditions but also for various reasons, especially in RAS and phosphoinositol-3 kinase (PI3K) hyperactivation (35). Furthermore, nestin+ GSCs located in the perivascular niche adjacent to the blood vessels may survive *via* PI3K pathway hyperactivation after RT (36).

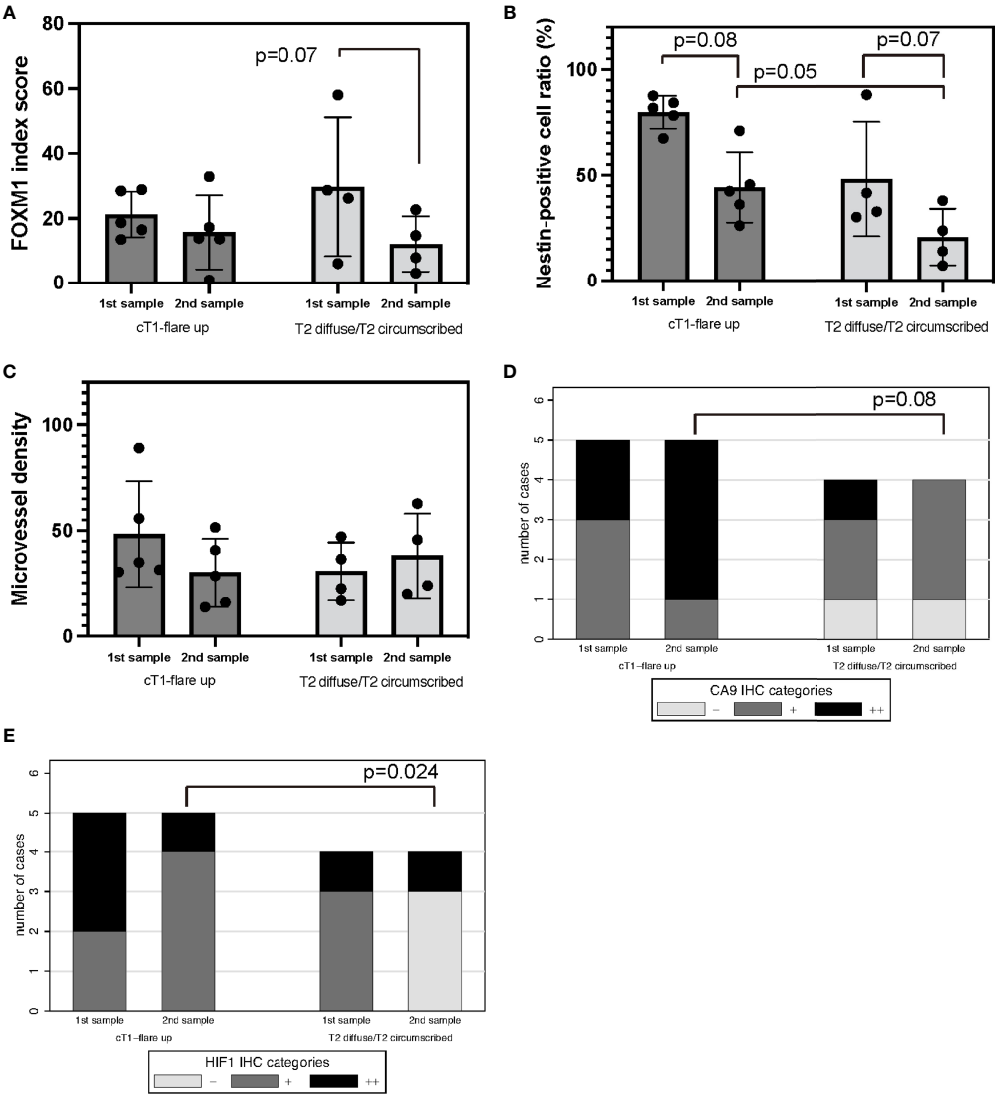

FIGURE 6 | Recurrence pattern on MRI after Bev therapy; "cT1 flare-up" vs. "T2-diffuse/T2-circumscribed" in tumor oxygenation, stemness, and immunological TME. Recurrent GBM after Bev therapy in cT1 flare-up and T2-diffuse GBM. FOXM1 **(A)**, nestin **(B)**, MVD **(C)**, CA9 **(D)**, and HIF-1α expression **(E)**. Error bar; standard deviation. Bev, bevacizumab; CA9, carbonic anhydrase 9; FOXM1, Forkhead box M1; GBM, glioblastoma; HIF-1α, hypoxia inducible factor-1 alpha; MRI, magnetic resonance imaging; MVD, microvessel density; TME, tumor microenvironment.

In addition, the distance of more than 150 μm of cells from the blood vessels indicates that the cells are in a hypoxic TME (37–39). The present study demonstrated that CA9+ cells were present at 150 μm from the blood vessels in the "pseudo-papillary" structures, which is in agreement with a previous theory. CA9 is also induced by downregulation of tumor suppressor genes such as *p53* and *PTEN*, induction of oncogenic pathways including PI3K, and other environmental conditions including acidosis and glucose deprivation (35). These findings suggest that the inner cells of "pseudo-papillary" structures may consist of nestin+ GSCs with enhanced PI3K activity in a hypoxic environment as evidenced by high expression of HIF-1α. In other words, "pseudo-papillary" structures may reflect a mechanism of resistance of tumor cells to anti-VEGF therapy by producing a favorable TME for GSCs.

FOXM1 as a Potential Biomarker for Survival

In the present study, we investigated FOXM1 and nestin expression and found that changes in the expression of both were similar during Bev therapy. FOXM1 is involved in tumorigenesis and transformation of normal astrocytes, reflects the histological malignancy of glioma, and is proposed to be a surrogate marker for OS (20, 22). Interestingly, FOXM1 also binds the *VEGF* promoter and contributes to the angiogenesis and growth of GSCs in GBM by upregulation of VEGF (21). Thus, FOXM1 may be a marker for GSCs with growth potential

and a prediction biomarker for survival and may thus be useful for optimizing VEGF-targeted antiangiogenic therapy including neoBev in newly diagnosed GBM.

To verify this hypothesis, the present cohort was restricted to preoperative and recurrent GBM after neoBev in the same patients. The cohort was divided into high and low levels of FOXM1 in initial samples to compare OS. Patients in the group with lower expression of FOXM1 after neoBev tended to show better OS than those with higher expression of FOXM1, suggesting that FOXM1 as a marker of proliferating GSCs may be a predictive factor for long-term survival during Bev therapy for newly diagnosed GBM. No previous studies have investigated this point.

An additional interesting finding about FOXM1 in the present study was that FOXM1 expression tended to decrease in recurrent samples and was significantly decreased in T1Gd-GRs and FLAIR-GRs. This finding is contrary to that of Zhang et al. (22) who found that FOXM1 expression is upregulated in recurrent GBM samples. This inconsistency may be due to the presence or absence of anti-VEGF therapy. The previous study by Zhang et al. (22) included 38 pairs of primary and recurrent GBM tumor samples, and all 38 patients received concomitant RT and TMZ after surgery. The present study included nine patients who received neoBev, followed by TMZ plus RT after surgery, and then subsequent Bev. Hence, anti-VEGF therapy for GBM may inhibit FOXM1 expression for a long period of time up to the point of recurrence, or recurrent GBM may be able to proliferate without FOXM1 upregulation during anti-VEGF therapy. Further investigation is needed to address this question.

Neuroimaging and Bevacizumab Responsiveness

With regard to the therapeutic response to Bev assessed with neuroimaging, the type of radiological progression after Bev therapy and its relationship to PFS and OS were investigated. Newly diagnosed GBM responded to Bev therapy, but the therapeutic effects are usually transient. GBM progression during Bev therapy can exhibit non-enhancing T2-weighted image/FLAIR-bright growth with invasion or restricted enhancement with contrast medium. The difference between non-enhancing and enhancing lesions after Bev therapy in terms of PFS and OS is controversial (40, 41). Whether favorable and poor responsiveness during Bev therapy determines the clinical outcome is still controversial. Previous studies in the cohort of newly diagnosed and recurrent GBM concluded that complete resolution of CE during treatment is a favorable factor for the clinical outcome (40, 42).

In contrast, Ellingson et al. (43) insisted that objective response rates are not clinically meaningful in newly diagnosed GBM and suggested that a measure of early PFS or treatment failure rates during the maintenance phase may be extremely useful for predicting the long-term outcome. Despite this observation, a survival difference in patients with growing vs. shrinking tumors was not maintained, suggesting that this may not be the most sensitive method for evaluating efficacy and predicting OS in newly diagnosed GBM (43). The mechanism of sustaining tumor dormancy is probably related to the TME and is an important issue to be investigated. Understanding the mechanism of sustaining tumor dormancy by comparing histological or molecular features between the effective and refractory phase during Bev therapy may be useful. Volumetric analyses as described above investigated newly diagnosed and recurrent GBM in different therapeutic situations of Bev combined with surgical resection followed by RT and TMZ. To the best of our knowledge, the present study is the first report to include an exploratory volumetric analysis during Bev treatment alone in newly diagnosed GBM.

One of the most important issues for comprehending the mechanism of Bev effectiveness and resistance is the variable TME from hypoxic and normoxic conditions with reversible alterations. Tumor oxygenation in relation to Bev effectiveness was demonstrated by neuroimaging using a representative hypoxia positron emission tomography (PET) tracer, ^{18}F-fluoromisonidazole (FMISO) PET. According to a previous investigation regarding the association between FMISO PET findings and Bev treatment for high-grade glioma, recurrent gliomas with decreasing FMISO accumulation after short-term Bev application derive a survival benefit from Bev therapy (44). In addition, a correlation was found between FMISO uptake and HIF-1α/VEGF expression detected with immunohistochemistry in newly diagnosed GBM (45). These results suggested that tumor oxygenation was maintained during Bev effectiveness as evidenced by histological findings with support of neuroimaging.

In the present study, the difference in stemness and oxygenation during effectiveness and refractoriness was demonstrated with immunohistochemistry. In addition, responsiveness to neoBev was also represented by neuroradiological findings including T1Gd. A comparison of stemness/oxygenation of the TME assessed with FMISO PET and immunohistochemistry between the Bev-effective and Bev-refractory periods is of great interest.

A hypoxic TME causes resistance to Bev due to stem cell accumulation (46). We previously reported that Bev-effective GBM exhibits reduced hypoxia along with reduced infiltration of GSCs compared with naive-Bev GBM (3). Very few reports have demonstrated that tumor oxygenation is maintained during Bev effectiveness in GBM by histological analysis with molecular profiling.

We investigated the expression levels of hypoxic markers (CA9 and HIF-1α) and a GSC marker (nestin) using GBM samples obtained from three different settings including tumors before Bev therapy (naive-Bev), tumors resected following neoBev (effective-Bev), and recurrent tumors following Bev therapy (refractory-Bev) (3). Recurrent tumors after neoBev were not included in those studies. The clinical outcome following neoBev and the impact of a change in response on OS assessed with neuroradiological findings and the TME, including oxygenation and stemness with immunohistochemical analysis, has not been previously investigated. Thus, to confirm whether a change in the TME determines disease control during Bev therapy, paired samples between effective-Bev and refractory-Bev were compared using neuroradiological and histological analyses.

Recurrent Pattern and Change in the Tumor Microenvironment After Bevacizumab Failure

Regarding molecular features when the tumor recurred during Bev therapy, DeLay et al. (41) showed that non-enhancing Bev-resistant GBM and enhancing Bev-resistant GBM have different molecular features and that the TME including vessel density and hypoxia is also different. Compared with paired samples before Bev therapy, non-enhancing Bev-resistant GBM exhibited reduced vessel density and increased hypoxia as evidenced by increased CA9 and HIF-1α staining. In contrast, enhancing Bev-resistant and naive-Bev GBM exhibited unchanged vessel density and hypoxia. Interestingly, VEGF/VEGF receptor expression was not altered in pre-Bev compared to post-Bev therapy tumors in their series. However, invasion molecules including integrin β1 were elevated in non-enhancing Bev-resistant GBM, indicating that neuroimaging reflects molecular profiling (41). In the present study, CA9 and HIF-1α expression decreased in the "T2-circumscribed/T2-diffuse" pattern compared with the "T1 flare-up" pattern in recurrent tumors (**Figure 6**). This result seemed to be inconsistent with the previous study by DeLay et al. (41), but the background was different in two ways. First, the present study focused on paired comparisons of GBM during effectiveness (effective-Bev) and refractoriness of Bev (refractory-Bev), whereas DeLay et al. (41) described naive-Bev and refractory-Bev. Second, the current study followed the definition of the recurrence pattern as described by Nowosielski et al. (24), whereas DeLay et al. (41) used the percentage of FLAIR-bright volume exhibiting T1Gd enhancement. Therefore, our results suggested that the growth potential was preserved in recurrent GBM with the "T2-circumscribed/T2-diffuse" pattern in the absence of severe hypoxia at the time of recurrence.

Mechanism of Duration of Bevacizumab Effectiveness in Light of Metabolic Adaptation

According to a previous report (47), mutant epidermal growth factor receptor variant III (EGFR vIII) mutation and EGFR overexpression glioma cells impaired physiological adaptation to starvation and rendered cells sensitive to hypoxia-induced cell death. Theoretically, the activation of EGFR enhances vulnerability to hypoxia-inducing therapies *via* a decrease in Nicotinamide adenine dinucleotide phosphate (NAPDH) levels. Therefore, we should consider the possibility of the biological behavior of tumor cells related to their metabolism adaptation during Bev therapy.

As we indicated in the current and previous papers, Bev could change from normoxic during its effectiveness to hypoxic TME after its failure (3). The duration of Bev effectiveness might be associated with the status of EGFR overexpression or EGFR vIII mutation in GBM probably due to the impact of Bev on metabolism adaptation (48). To address these issues, further investigation is needed.

Limitations

The present study using infrequently available clinical specimens has some limitations. The first limitation is the paucity of the number of paired samples from the same patients due to the extreme rarity of salvage surgery or autopsy for recurrent GBM after the failure of RT and TMZ with Bev. The second limitation is that the influence of RT and TMZ combined with Bev was not considered. The third limitation is that the present study evaluated surgically resectable large enhanced tumors with expanding perifocal edema as seen with neuroimaging, which adds bias.

The fourth limitation is that an initial favorable neuroradiographic response to neoBev on a FLAIR image does not always reflect prolonged PFS and OS, thus initial neuroradiological responsiveness after Bev therapy could not reflect a clinical benefit of Bev, especially for newly diagnosed GBM. Based on the present study, FOXM1 seemed to be a predictive prognostic biomarker, but it was not verified whether the expression level of this biomarker should determine the duration of Bev effectiveness and advantage of neoBev. Further investigation would be needed to solve this clinical question.

In summary, whether a visible favorable response on neuroimaging following Bev therapy predicts the clinical outcome is uncertain. However, this is the first report regarding an investigation of neuroradiographic response to neoBev associated with hypoxic and stem cell markers as evidenced by immunohistochemistry. Based on results in the present study demonstrating that Bev produced an oxygenated TME in addition to stemness inhibition, combination therapy with Bev and immunotherapy may contribute to improvements in the currently dismal clinical outcome of GBM.

CONCLUSION

"Pseudo-papillary" structures were seen in recurrent GBM after anti-VEGF therapy. An interesting discrepancy in CA9 and HIF-1α expression in these "pseudo-papillary" structures was observed. A neuroradiographic response after neoBev may reflect the status of the TME including stemness and oxygenation. Bev may produce tumor oxygenation, leading to suppression of proliferation of GSCs. Results in the present study suggested that FOXM1 plays a potential role as a biomarker of survival during anti-VEGF therapy.

DATA AVAILABILITY STATEMENT

The raw data supporting the conclusions of this article will be made available by the authors without undue reservation.

ETHICS STATEMENT

The studies involving human participants were reviewed and approved by the Ethical Committee of Jikei University School of

Medicine. The patients/participants provided their written informed consent to participate in this study. Written informed consent was obtained from the individual(s) for the publication of any potentially identifiable images or data included in this article.

AUTHOR CONTRIBUTIONS

TT: design of the present study. JT, NF, and YY: data collection and analysis. RT, HS, and YA: article survey. KY, MM, MS, and YM: suggestions for the article. All authors contributed to the article and approved the submitted version.

FUNDING

The study was supported by the Ministry of Education, Culture, Sports, Science and Technology and the Japan Society for Promotion of Science (KAKENHI) (Grant Number 21K09161).

ACKNOWLEDGMENTS

The authors greatly thank Ms. Eri Honzawa at the Division of Diagnostic Pathology, Jikei University School of Medicine Kashiwa Hospital, for technical assistance with laboratory work and sample preparation.

REFERENCES

1. Huang Y, Goel S, Duda DG, Fukumura D, Jain RK. Vascular Normalization as an Emerging Strategy to Enhance Cancer Immunotherapy. *Cancer Res* (2013) 73:2943–8. doi: 10.1158/0008-5472.CAN-12-4354
2. Calabrese C, Poppleton H, Kocak M, Hogg TL, Fuller C, Hamner B, et al. A Perivascular Niche for Brain Tumor Stem Cells. *Cancer Cell* (2007) 11:69–82. doi: 10.1016/j.ccr.2006.11.020
3. Yamamoto Y, Tamura R, Tanaka T, Ohara K, Tokuda Y, Miyake K, et al. "Paradoxical" Findings of Tumor Vascularity and Oxygenation in Recurrent Glioblastomas Refractory to Bevacizumab. *Oncotarget* (2017) 8:103890–9. doi: 10.18632/oncotarget.21978
4. Tamura R, Tanaka T, Sasaki H. *Development and Perspectives of Histopathological Findings of Glioblastoma Treated by Bevacizumab*. VB Leon, editor. New York: Nova Publishers (2019) p. 1–37.
5. Tamura R, Tanaka T, Ohara K, Miyake K, Morimoto Y, Yamamoto Y, et al. Persistent Restoration to the Immunosupportive Tumor Microenvironment in Glioblastoma by Bevacizumab. *Cancer Sci* (2019) 110:499–508. doi: 10.1111/cas.13889
6. Lu-Emerson C, Snuderl M, Kirkpatrick ND, Goveia J, Davidson C, Huang Y, et al. Increase in Tumor-Associated Macrophages After Antiangiogenic Therapy is Associated With Poor Survival Among Patients With Recurrent Glioblastoma. *Neuro-oncology* (2013) 15:1079–87. doi: 10.1093/neuonc/not082
7. Mahase S, Rattenni RN, Wesseling P, Leenders W, Baldotto C, Jain R, et al. Hypoxia-Mediated Mechanisms Associated With Antiangiogenic Treatment Resistance in Glioblastomas. *Am J Pathol* (2017) 187:940–53. doi: 10.1016/j.ajpath.2017.01.010
8. Shibao S, Minami N, Koike N, Fukui N, Yoshida K, Saya H, et al. Metabolic Heterogeneity and Plasticity of Glioma Stem Cells in a Mouse Glioblastoma Model. *Neuro-oncology* (2018) 20:343–54. doi: 10.1093/neuonc/nox170
9. Soeda A, Park M, Lee D, Mintz A, Androutsellis-Theotokis A, McKay R, et al. Hypoxia Promotes Expansion of the CD133-Positive Glioma Stem Cells Through Activation of HIF-1α. *Oncogene* (2009) 28:3949–59. doi: 10.1038/onc.2009.252
10. Bradshaw A, Wickremsekera A, Tan ST, Peng L, Davis PF, Itinteang T. Cancer Stem Cell Hierarchy in Glioblastoma Multiforme. *Front Surg* (2016) 3:21. doi: 10.3389/fsurg.2016.00021
11. Ludwig K, Kornblum HI. Molecular Markers in Glioma. *J Neurooncol* (2017) 134:505–12. doi: 10.1007/s11060-017-2379-y
12. Beier D, Schulz JB, Beier CP. Chemoresistance of Glioblastoma Cancer Stem Cells-Much More Complex Than Expected. *Mol Cancer* (2011) 10:1–11. doi: 10.1186/1476-4598-10-128
13. Bao S, Wu Q, McLendon RE, Hao Y, Shi Q, Hjelmeland AB, et al. Glioma Stem Cells Promote Radioresistance by Preferential Activation of the DNA Damage Response. *Nature* (2006) 444:756–60. doi: 10.1038/nature05236
14. Eramo A, Ricci-Vitiani L, Zeuner A, Pallini R, Lotti F, Sette G, et al. Chemotherapy Resistance of Glioblastoma Stem Cells. *Cell Death Differ* (2006) 13:1238–41. doi: 10.1038/sj.cdd.4401872
15. Lendahl U, Zimmerman LB, McKay RD. CNS Stem Cells Express a New Class of Intermediate Filament Protein. *Cell* (1990) 60:585–95. doi: 10.1016/0092-8674(90)90662-X
16. Jin X, Jin X, Jung J, Beck S, Kim H. Cell Surface Nestin is a Biomarker for Glioma Stem Cells. *Biochem Biophys Res Commun* (2013) 433:496–501. doi: 10.1016/j.bbrc.2013.03.021
17. Zhang M, Song T, Yang L, Chen R, Wu L, Yang Z, et al. Nestin and CD133: Valuable Stem Cell-Specific Markers for Determining Clinical Outcome of Glioma Patients. *J Exp Clin Cancer Res* (2008) 27:1–7. doi: 10.1186/1756-9966-27-85
18. Dahlrot RH, Hermansen SK, Hansen S, Kristensen BW. What is the Clinical Value of Cancer Stem Cell Markers in Gliomas? *Int J Clin Exp Pathol* (2013) 6:334–48.
19. Behling F, Barrantes-Freer A, Behnes CL, Stockhammer F, Rohde V, Adel-Horowski A, et al. Expression of Olig2, Nestin, NogoA and AQP4 Have No Impact on Overall Survival in IDH-Wildtype Glioblastoma. *PloS One* (2020) 15:e0229274. doi: 10.1371/journal.pone.0229274
20. Liu M, Dai B, Kang S, Ban K, Huang F, Lang FF, et al. FoxM1B is Overexpressed in Human Glioblastomas and Critically Regulates the Tumorigenicity of Glioma Cells. *Cancer Res* (2006) 66:3593–602. doi: 10.1158/0008-5472.CAN-05-2912
21. Zhang Y, Zhang N, Dai B, Liu M, Sawaya R, Xie K, et al. FoxM1B Transcriptionally Regulates Vascular Endothelial Growth Factor Expression and Promotes the Angiogenesis and Growth of Glioma Cells. *Cancer Res* (2008) 68:8733–42. doi: 10.1158/0008-5472.CAN-08-1968
22. Zhang N, Wu X, Yang L, Xiao F, Zhang H, Zhou A, et al. FoxM1 Inhibition Sensitizes Resistant Glioblastoma Cells to Temozolomide by Downregulating the Expression of DNA-Repair Gene Rad51. *Clin Cancer Res* (2012) 18:5961–71. doi: 10.1158/1078-0432.CCR-12-0039
23. Wen PY, Macdonald DR, Reardon DA, Cloughesy TF, Sorensen AG, Galanis E, et al. Updated Response Assessment Criteria for High-Grade Gliomas: Response Assessment in Neuro-Oncology Working Group. *J Clin Oncol* (2010) 28:1963–72. doi: 10.1200/JCO.2009.26.3541
24. Nowosielski M, Wiestler B, Goebel G, Hutterer M, Schlemmer HP, Stockhammer G, et al. Progression Types After Antiangiogenic Therapy are Related to Outcome in Recurrent Glioblastoma. *Neurology* (2014) 82:1684–92. doi: 10.1212/WNL.0000000000000402
25. Takei J, Tanaka T, Teshigawara A, Tochigi S, Hasegawa Y, Murayama Y. Alteration of FOXM1 Expression and Macrophage Polarization in Refractory Meningiomas During Long-Term Follow-Up. *Transl Cancer Res* (2021) 10:553–66. doi: 10.21037/tcr-20-1896
26. Tamura R, Tanaka T, Miyake K, Tabei Y, Ohara K, Sampetrean O, et al. Histopathological Investigation of Glioblastomas Resected Under Bevacizumab Treatment. *Oncotarget* (2016) 7:52423–35. doi: 10.18632/oncotarget.9387
27. Tanaka G, Nakazato Y. Automatic Quantification of the MIB-1 Immunoreactivity in Brain Tumors. *Int Congr Ser* (2004) 1259:15–9. doi: 10.1016/S0531-5131(03)01668-6
28. Beasley NJ, Wykoff CC, Watson PH, Leek R, Turley H, Gatter K, et al. Carbonic anhydrase IX, an Endogenous Hypoxia Marker, Expression in Head and Neck Squamous Cell Carcinoma and its Relationship to Hypoxia, Necrosis, and Microvessel Density. *Cancer Res* (2001) 61:5262–7.
29. Schindelin J, Arganda-Carreras I, Frise E, Kaynig V, Longair M, Pietzsch T, et al. Fiji: An Open-Source Platform for Biological-Image Analysis. *Nat Methods* (2012) 9:676–82. doi: 10.1038/nmeth.2019

30. Weidner N, Semple JP, Welch WR, Folkman J. Tumor Angiogenesis and Metastasis—Correlation in Invasive Breast Carcinoma. *N Engl J Med* (1991) 324:1–8. doi: 10.1056/NEJM199101033240101
31. West CM, Cooper RA, Loncaster JA, Wilks DP, Bromley M. Tumor Vascularity: A Histological Measure of Angiogenesis and Hypoxia. *Cancer Res* (2001) 61:2907–10.
32. Belotti D, Pinessi D, Taraboletti G. Alternative Vascularization Mechanisms in Tumor Resistance to Therapy. *Cancers* (2021) 13:1912. doi: 10.3390/cancers13081912
33. Bergers G, Hanahan D. Modes of Resistance to Anti-Angiogenic Therapy. *Nat Rev Cancer* (2008) 8:592–603. doi: 10.1038/nrc2442
34. di Tomaso E, Snuderl M, Kamoun WS, Duda DG, Auluck PK, Fazlollahi L, et al. Glioblastoma Recurrence After Cediranib Therapy in Patients: Lack of "Rebound" Revascularization as Mode of Escape. *Cancer Res* (2011) 71:19–28. doi: 10.1158/0008-5472.CAN-10-2602
35. Kaluz S, Kaluzová M, Liao S, Lerman M, Stanbridge EJ. Transcriptional Control of the Tumor-and Hypoxia-Marker Carbonic Anhydrase 9: A One Transcription Factor (HIF-1) Show? *Biochim Biophys Acta (BBA)-Reviews Cancer* (2009) 1795:162–72. doi: 10.1016/j.bbcan.2009.01.001
36. Hambardzumyan D, Becher OJ, Rosenblum MK, Pandolfi PP, Manova-Todorova K, Holland EC. PI3K Pathway Regulates Survival of Cancer Stem Cells Residing in the Perivascular Niche Following Radiation in Medulloblastoma. *Vivo Genes Dev* (2008) 22:436–48. doi: 10.1101/gad.1627008
37. Brown JM, Giaccia AJ. The Unique Physiology of Solid Tumors: Opportunities (and Problems) for Cancer Therapy. *Cancer Res* (1998) 58:1408–16.
38. Cairns RA, Kalliomaki T, Hill RP. Acute (Cyclic) Hypoxia Enhances Spontaneous Metastasis of KHT Murine Tumors. *Cancer Res* (2001) 61:8903–8. doi: 10.1158/0008-5472.CAN-03-3196
39. Cairns RA, Hill RP. Acute Hypoxia Enhances Spontaneous Lymph Node Metastasis in an Orthotopic Murine Model of Human Cervical Carcinoma. *Cancer Res* (2004) 64:2054–61. doi: 10.1158/0008-5472.CAN-03-3196
40. Nowosielski M, Ellingson BM, Chinot OL, Garcia J, Revil C, Radbruch A, et al. Radiologic Progression of Glioblastoma Under Therapy—an Exploratory Analysis of AVAglio. *Neuro-oncology* (2018) 20:557–66. doi: 10.1093/neuonc/nox162
41. DeLay M, Jahangiri A, Carbonell WS, Hu YL, Tsao S, Tom MW, et al. Microarray Analysis Verifies Two Distinct Phenotypes of Glioblastomas Resistant to Antiangiogenic Therapy. *Clin Cancer Res* (2012) 18:2930–42. doi: 10.1158/1078-0432.CCR-11-2390
42. Takigawa K, Hata N, Michiwaki Y, Hiwatashi A, Yonezawa H, Kuga D, et al. Volumetric Study Reveals the Relationship Between Outcome and Early Radiographic Response During Bevacizumab-Containing Chemoradiotherapy for Unresectable Glioblastoma. *J Neurooncol* (2021) 154:187–96. doi: 10.1007/s11060-021-03812-9
43. Ellingson BM, Abrey LE, Garcia J, Chinot O, Wick W, Saran F, et al. Post-Chemoradiation Volumetric Response Predicts Survival in Newly Diagnosed Glioblastoma Treated With Radiation, Temozolomide, and Bevacizumab or Placebo. *Neuro-oncology* (2018) 20:1525–35. doi: 10.1093/neuonc/noy064
44. Yamaguchi S, Hirata K, Toyonaga T, Kobayashi K, Ishi Y, Motegi H, et al. Change in 18F-Fluoromisonidazole PET is an Early Predictor of the Prognosis in the Patients With Recurrent High-Grade Glioma Receiving Bevacizumab Treatment. *PloS One* (2016) 11:e0167917. doi: 10.1371/journal.pone.0167917
45. Kawai N, Lin W, Cao W, Ogawa D, Miyake K, Haba R, et al. Correlation Between 18 F-Fluoromisonidazole PET and Expression of HIF-1α and VEGF in Newly Diagnosed and Recurrent Malignant Gliomas. *Eur J Nucl Med Mol Imaging* (2014) 41:1870–8. doi: 10.1007/s00259-014-2776-9
46. Piao Y, Liang J, Holmes L, Zurita AJ, Henry V, Heymach JV, et al. Glioblastoma Resistance to Anti-VEGF Therapy is Associated With Myeloid Cell Infiltration, Stem Cell Accumulation, and a Mesenchymal Phenotype. *Neuro-oncology* (2012) 14:1379–92. doi: 10.1093/neuonc/nos158
47. Luger AL, Lorenz NI, Urban H, Dive I, Engel AL, Strassheimer F, et al. Activation of Epidermal Growth Factor Receptor Sensitizes Glioblastoma Cells to Hypoxia-Induced Cell Death. *Cancers* (2020) 12:2144. doi: 10.3390/cancers12082144
48. Fack F, Espedal H, Keunen O, Golebiewska A, Obad N, Harter PN, et al. Bevacizumab Treatment Induces Metabolic Adaptation Toward Anaerobic Metabolism in Glioblastomas. *Acta Neuropathol* (2015) 129:115–31. doi: 10.1007/s00401-014-1352-5

Conflict of Interest: The authors declare that the research was conducted in the absence of any commercial or financial relationships that could be construed as a potential conflict of interest.

frontiers | Frontiers in Oncology

REVIEW
published: 07 July 2022
doi: 10.3389/fonc.2022.891543

Tumor-Associated Microenvironment of Adult Gliomas: A Review

Vincenzo Di Nunno[1], Enrico Franceschi[2], Alicia Tosoni[2], Lidia Gatto[1], Stefania Bartolini[2] and Alba Ariela Brandes[2]*

[1] Department of Oncology, Azienda Unità Sanitaria Locale (AUSL) Bologna, Bologna, Italy, [2] Nervous System Medical Oncology Department, Istituto di Ricovero e Cura a Carattere Scientifico (IRCCS) Istituto delle Scienze Neurologiche di Bologna, Bologna, Italy

The glioma-associated tumor microenvironment involves a multitude of different cells ranging from immune cells to endothelial, glial, and neuronal cells surrounding the primary tumor. The interactions between these cells and glioblastoma (GBM) have been deeply investigated while very little data are available on patients with lower-grade gliomas. In these tumors, it has been demonstrated that the composition of the microenvironment differs according to the isocitrate dehydrogenase status (mutated/wild type), the presence/absence of codeletion, and the expression of specific alterations including H3K27 and/or other gene mutations. In addition, mechanisms by which the tumor microenvironment sustains the growth and proliferation of glioma cells are still partially unknown. Nonetheless, a better knowledge of the tumor-associated microenvironment can be a key issue in the optic of novel therapeutic drug development.

Keywords: microenvironment, glioma, oligodendroglioma, astrocytoma, H3K27 altered glioma, midline glioma, IDH wild type glioma

OPEN ACCESS

Edited by:
Aleksi Sedo, Charles University, Czechia

Reviewed by:
Pravesh Gupta, University of Texas MD Anderson Cancer Center, United States
Tomas Kazda, Masaryk Memorial Cancer Institute (MMCI), Czechia

***Correspondence:**
Enrico Franceschi
enricofra@yahoo.it

Specialty section:
This article was submitted to Neuro-Oncology and Neurosurgical Oncology, a section of the journal Frontiers in Oncology

Received: *07 March 2022*
Accepted: *06 June 2022*
Published: *07 July 2022*

Citation:
Di Nunno V, Franceschi E, Tosoni A, Gatto L, Bartolini S and Brandes AA (2022) Tumor-Associated Microenvironment of Adult Gliomas: A Review. Front. Oncol. 12:891543. doi: 10.3389/fonc.2022.891543

INTRODUCTION

Gliomas are the most frequent primary tumors of the central nervous system (CNS) with an estimated incidence of 7.1/100,000 cases in the United States (1). Glioblastoma (GBM) encounters 55% of all glioma diagnoses while the remaining 45% of cases are represented by other glioma subtypes (1). Overall, gliomas are mainly divided into isocitrate dehydrogenase (IDH) mutant and IDH wild-type (wt) tumors (1–3). In the primary group, composed of IDH-mutated tumors, the World Health Organization (WHO) 2021 classification recognizes oligodendroglioma (presenting 1p19q codeletion) and astrocytoma (without 1p19q codeletion) (4). These tumors can be further divided into WHO grade 2 (oligodendroglioma and diffuse astrocytoma) and 3 (anaplastic oligodendroglioma and anaplastic astrocytoma) gliomas.

Gliomas without IDH mutations are defined as IDH-wt gliomas. According to the WHO 2021 classification, the presence of IDH-wt and other molecular alterations such as TERT (Telomerase Reverse Transcriptase), EGFR (Epidermal Growth Factor Receptor), or gain of chromosome 7/loss of chromosome 10 allows defining these tumors as a molecular GBM (4). Gliomas with H3K27 alterations (27th amino acid of Histone 3) is a new entity of IDH-wt gliomas diagnosed in pediatric patients but occasionally also in adults (4).

The prognosis of patients with gliomas (5) is extremely variable, ranging from decades in low-grade IDH-mutated gliomas to a few months in IDH-wt tumors (6). The standard clinical

therapeutic approach is represented by maximal safe surgical resection followed by radiation therapy and chemotherapy (2, 3, 6).

In the last few years, important improvements toward a better understanding of genetic and epigenetic pathways regulating glioma development and growth have been done. These mechanisms could explain the different clinical courses and evolution of these malignancies. Indeed, genomic and epigenomic alterations differ in each glioma subtype explaining the different histology, clinical course, and biological behavior. The tumor-associated microenvironment appears to be another key element influencing the development, progression, and clinical evolution of gliomas.

Indeed, the tumor microenvironment (TME) composition is manipulated directly by cancer cells; therefore, TME composition changes according to the different alterations expressed by tumors. On the other hand, TME can sustain tumor growth and development in different ways (7).

Interactions between TME and GBM have been largely evaluated (7), while few data are available on patients with IDH-mutated/wt low-grade gliomas.

In this review, we examine current knowledge toward TME surrounding IDH-mutated and IDH-wt glioma (excluding GBM). To better understand TME composition, we analyzed the genomic landscape of each tumor subtype. Finally, we investigated possible therapeutic strategies aimed to target TME. Our focus is mainly oriented on adult gliomas; thus, we exclude pediatric malignancies and GBM from this review.

IDH-MUTATED GLIOMAS

Microscopically IDH-mutated, 1p19q codeleted oligodendrogliomas appear as tumor cells with rounded nuclei, clear perinuclear halons, frail capillaries, and focal microcalcification (3, 4, 6). An increased number of mitoses, vascular proliferation, and necrosis is observed in CNS WHO grade 3 oligodendrogliomas (3, 4, 6).

IDH-mutated 1p19q non-codeleted astrocytomas spread with perineuronal, perivascular, or subpial patterns and present nuclear atypia and pleomorphism (**Table 1**). The higher tumor grade is associated with increased mitotic activity, angiogenesis, and necrosis (3, 4, 6).

Oligodendrogliomas and astrocytomas represent 40%–45% and 50%–55% of all glioma diagnoses with an estimated survival ranging from 6.5 to over 15 years (6, 11–13).

Maximal safe surgical resection is the standard of care for these tumors (2, 3). In WHO grade 2 astrocytomas and oligodendrogliomas, follow-up after surgery is considered in low-risk patients while adjuvant radiation therapy (RT) followed by chemotherapy [temozolomide/TMZ (9) or procarbazine plus lomustine plus vincristine/PCV (10, 15)] is commonly used in high-risk patients (8, 9).

Genomic Landscape of IDH-Mutated Gliomas

Oligodendroglioma and astrocytoma significantly differ in their genomic alterations (16).

In addition to IDH1 or IDH2 mutations and 1p19q codeletion, oligodendrogliomas frequently present mutations of TERT (96%), CIC (Capicua Transcriptional Repressor, 62%), FUBP1 (Far Upstream Element Binding Protein 1, 29%), and/or PI3K (phosphoinositide 3-kinase, 20%) with overexpression of NOTCH1 (Notch homolog 1, translocation-associated, 31%) genes (16). Notably, ATRX (X-linked nuclear protein) mutations are rare in oligodendrogliomas and are mutually exclusive with TERT since both these two genes target the lengthening telomeres (16).

TABLE 1 | Summary of adult glioma clinical behaviors.

Name	Percentage of all non-GBM gliomas	IDH	1p19q	Grade	H3K27	TERTEGFR7 gain/10 loss	Median age at diagnosis	Prognosis	Treatment after surgery
Oligodendroglioma (3, 4, 6, 8–12)	19%–26%	Mutated	Codeleted	2	No	No	42–44	17.5 years	Follow-up or RT→CT (PCV preferred to TMZ)
Anaplastic oligodendroglioma (3, 4, 6, 8–12)	14%–20%	Mutated	Codeleted	3	No	No	48–48.5	11.2 years	RT→CT (PCV preferred to TMZ)
Diffuse astrocytoma (3, 4, 6, 8–12)	24%–26%	Mutated	Non-codeleted	2	No	No	36–37	8.5–11	RT→CT (PCV preferred to TMZ)
Anaplastic astrocytoma (3, 4, 6, 8–12)	10%–23%	Mutated	Non-codeleted	3	No	No	35–40	6.5-9.3	RT→CT (TMZ preferred to PCV)
IDH-wt glioma (3, 4, 6, 11–14)	6%–12%	Wild-type	Non-codeleted	2–3	No	No	44–46	Unknown	RT→CT (TMZ) could be considered
Molecular GBM (3, 4, 6, 11–14)		Wild-type	No-codeleted	2–3	No	Yes	44–46	9–24 months	RT→CT (TMZ) *OR* RT/CT→ (TMZ)
Midline Glioma (4, 14)	<5%	Wild-type	No-codeleted	2	Yes	No	Young adult	6–20 months	RT→CT (TMZ) could be considered

RT, radiation therapy; CT, chemotherapy; PCV, procarbazine, CCNU, vincristine; TMZ, temozolomide; GBM, glioblastoma; IDH, isocitrate dehydrogenase.

Almost all astrocytomas present p53 (94%) alterations, ATRX (86%) loss, or CDKN2A/CDKN2B (cyclin-dependent kinase inhibitor 2A/2B, 10%) homozygous deletion (16, 17). Curiously, astrocytomas present often non-canonical IDH1 mutations that are associated with improved survival (18–20). Recently, a next-generation sequencing (NGS) analysis carried out on 432 patients with anaplastic astrocytomas enrolled in the CATNON trial revealed a prognostic role of some selected genes. In particular, amplification of PDGFR (platelet-derived growth factor receptor) genes, CDKN2A/CDKN2B homozygous deletion, and PI3K mutations were independently associated with worse prognosis in patients with anaplastic (WHO grade 3) astrocytomas (17).

Another improvement toward a better knowledge of glioma genomic assessment was carried out in a large study adopting single-cell RNA sequencing (21). Researchers were able to evaluate with high precision the single-cell expression silencing confounding factors related to intratumoral genetic heterogeneity and genomic analysis of TME that can pollute large NGS studies (16).

In this study, researchers were able to identify, within tumor specimens assessed, three specific cellular populations: two differentiated tumoral cells belonging to oligodendrogliomas or astrocytomas and an undifferentiated phenotype (21). Through this precise gene expression analysis, the authors highlighted a shared expression between undifferentiated cells from oligodendrogliomas and astrocytomas, suggesting a shared progenitor of these two entities. These progenitor cancer cells presented alterations of key transcription factors such as SOX4 (SRY-Box Transcription Factor 4), SOX11 (SRY-Box Transcription Factor 11), and TCF4 (Transcription Factor 4). The percentage of these alterations increased according to CNS grade and the number of recurrences (21).

IDH-mutated gliomas seem to originate from a shared progenitor stem cell. Early acquired alterations are IDH with or without 1p19q codeletion. These events drive subsequent genomic alterations and explain the differences in terms of gene expression and TME (see below) within these two subtypes (21).

The progenitor cell of oligodendrogliomas and astrocytomas has a transcriptional phenotype similar to progenitor neural cells. These neural lineages can differentiate toward astrocytic or oligodendrocyte-like tumoral cancer cells (21, 22). These findings overturned the previous belief that there were two distinct progenitor cells for oligodendrogliomas and astrocytomas (23).

Differently, the progenitor cells of IDH-wt gliomas assume high levels of cellular state plasticity. Indeed, these ancestral cells can differentiate toward different transcriptional subtypes named mesenchymal, classic, and/or proneural (24). Subsequent studies differentiated the transcriptional subtypes into four main groups named astrocyte (EGFR amplified), oligodendrocyte (PDGFRA amplified), neural progenitor (CDK mutated), and mesenchymal (NF1 mutated)-like lineages (25).

Another important issue is the absence of a defined hierarchy between tumoral subtypes within IDH-wt gliomas (25). Thus, cancer cells can proliferate and switch from one subtype to another with high plasticity and heterogeneity (25). This finding diverges from what was observed in IDH-mutated and IDH-wt H3K27 gliomas. Indeed, IDH-wt H3K27 altered gliomas present a specific progenitor cell that has an oligodendrocyte-like transcription lineage (26). During the evolution, these progenitor cells lose (due to the alterations of histone 3) oligodendrocyte lineage differentiating toward an astrocyte-like cancer cell phenotype (26).

Microenvironment of IDH-Mutated Gliomas

Interactions between tumor cells and surrounding cells are complex and depend on the genetic expression of a specific tumor subtype (**Figure 1**). In general, tumor cells interact with immune cells, endothelial cells, and neurons (**Table 2**).

Important insights into connections between IDH mutant gliomas and immune cells have been provided by the study carried out by Venteicher et al. investigating single-cell RNA expression (21).

The authors identified an inflammatory expression derived from two specific and different signatures (21). The first was a microglia signature characterized by specific markers such as CX3CR1 (C-X-C motif chemokine receptor 1), P2RY12 (purigenic receptor P2Y12), and P2RY13 (purigenic receptor P2Y13). The second signature was a macrophage signature identified by the expression of CD163, TGFβ1 (transforming growth factor β1), and F13A1 (coagulation factor XIII A chain) (21). Notably, the distribution of the signature markers of both microglia and macrophages followed a continuum more than a bimodal scheme. Therefore, a macrophage that has reached the TME can acquire a microglia-like expression according to the phenotype expressed by cancer cells (21). On the other hand, microglia cannot differentiate to a macrophage immune profile (21). Finally, a subtle but reported difference between resident and tissue-derived macrophages has been reported (21).

Other important findings of this study revealed that macrophage signature and expression were more frequently associated with astrocytoma as compared to oligodendroglioma (21). Moreover, the macrophage signature was significantly associated with angiogenesis and endothelial activities. The same association was not true in cells expressing microglia signature.

According to these results, the presence of macrophages seems to enhance angiogenesis, progression, and glioma development. However, the mechanisms behind these interactions are unknown (21).

In this optic, it is essential to observe that the role of macrophages on glioma proliferation and development has only been investigated with a single-cell approach; thus, no definitive conclusions can be deduced. This is mainly because mechanisms beyond macrophage and glioma proliferation stimulation are largely unknown.

A subsequent study investigated TME composition in patients with IDH-mutated gliomas. These studies adopted

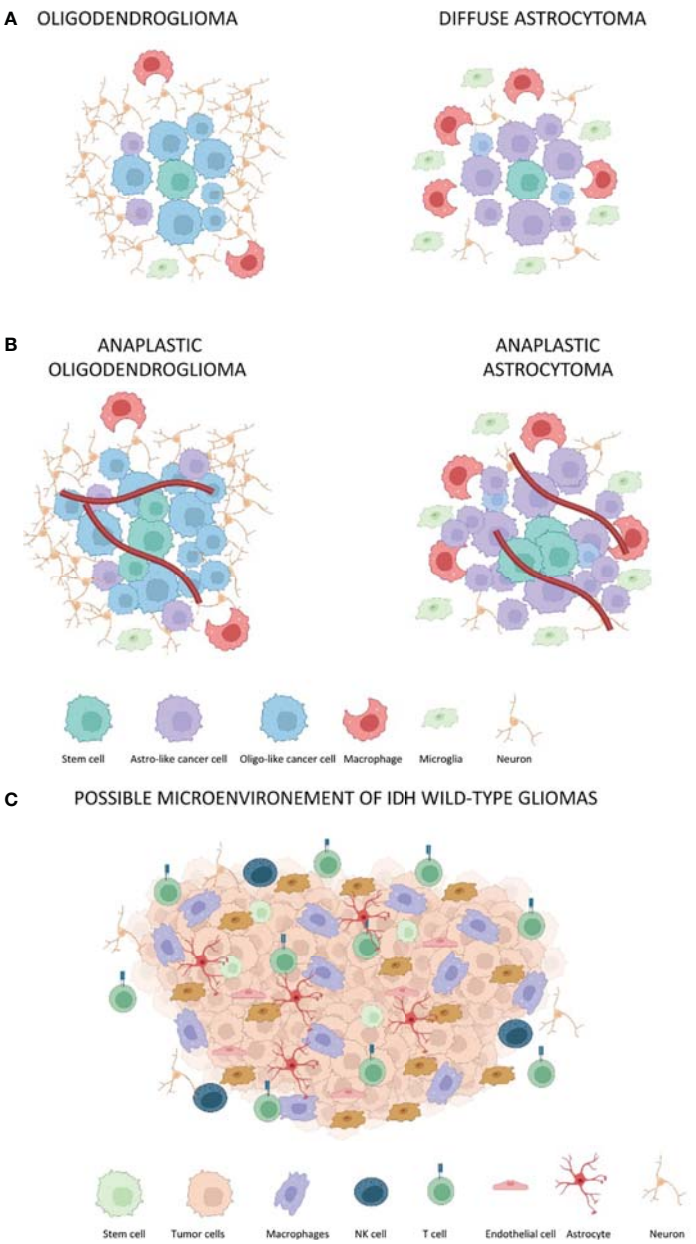

FIGURE 1 | The tumor-associated microenvironment of IDH-mutated and IDH-wt gliomas. Red lines represent blood vessels. **(A)** Oligodendroglioma and diffuse astrocytoma without a significant blood vessel proliferation. The oligodendroglioma microenvironment presents a reduced percentage of macrophages, microglia, and astro-like cells as compared to diffuse astrocytoma. **(B)** The same composition of microenvironment associated with oligodendroglioma and astrocytoma is maintained in anaplastic gliomas. However, there is an increased tumor cell proliferation as well as increased angiogenesis. **(C)** Composition of microenvironment associated to GBM with CD4 immune regulatory and CD8 T-lymphocyte. Notably, CD8 lymphocytes assume the classical exhaustion phenotype expressing several inhibitory receptors including the PD-1, T-cell membrane protein 3 (TIM3), lymphocyte activation gene 3 protein (LAG3), and T-cell immunoreceptor with immunoglobulin and ITIM domains (TIGIT) (27).

different approaches involving flow cytometry, RNA sequencing, protein arrays, culture assays, and spatial tissue characterization (42) or also high-dimensional single-cell profiling (43). These assessments revealed a disease-specific enrichment of immune cells with a significant difference in proportional abundance of microglia, macrophages, neutrophils, and T cells (42). In particular, macrophages showed a distinctive signature trajectory that differs according to the primary tumor subtype (43).

A similar interaction has also been observed in GBM. This confirms that the macrophage signature is associated with angiogenesis and tumor progression (28–32). GBM cancer cells can attract monocyte, microglia, and macrophage by the production of several factors including CCL2 (C-C motif

TABLE 2 | The microenvironment of low-grade glioma.

Oligodendroglioma	Astrocytoma	H3K27 glioma	IDH-wt gliomas**
The microenvironment expression reflects a microglia signature (CX3CR1, P2RY12/13) * more than the macrophage one (21, 28–32).	Inflammatory expression following macrophage signature (CD163, TGFβ1, and F13A1) (21, 28–32).	Microglia assumes a specific morphology with enlarged cell bodies and shorter processes (33–35).	The environment is mainly composed of microglia and tumor-associated macrophages (7, 36).
Microglia signature is not associated with angiogenesis (21).	Macrophage signature is associated with angiogenesis (21).	Microenvironment enriched in microglia and macrophage concentration (33–35) with low lymphocytes	Recruitment of monocytes by secretion of CCL2-7, GDNF, TNF, CSF-1, and GM-CSF (7, 36).
Lower percentage of CD8+PD1 +, CD4+ TIM3+, and regulatory T cells is associated with a less immune-suppressive stroma (37).	Increased percentage of CD8 +PD1+, CD4+ TIM3+, and regulatory T cells is associated with an increased immune-suppressive stroma (37).	Macrophages associated with H3K27 gliomas present a lower expression of IL6, IL1A, IL1B, CCL3, and CCL4 (33–35). Increased percentage of CCL2, CCL5, CSF1, CXCL12, and PDGFA (14).	Macrophages are associated with immune-suppressive stroma mainly due to the secretion of TGFβ (7, 36).
Unknown interactions with neurons. Possible release of glutamate by SLC7A11, which interacts with NMDA receptor inducing calcium intake (38–40).		Unknown interactions with neurons.	Astrocytes switch from a physiological phenotype to tumor-initiating cells. Neurons can stimulate tumor growth by secretion of glutamate, PI3K, FAK, HSPA5, and neuroglin 3 (7, 36).

** CX3CR1 and P2RY12/13 could be associated with specific functions carried out by microglia regulating trophic functions and interactions with neurons (41).*
*** The majority of data about microenvironment composition in patients with IDH-wt gliomas are provided by studies investigating glioblastoma cancer cells.*
CCL3-4, C-C motif chemokine ligand 3-4; CX3CR1, C-X-C motif chemokine receptor 1; CSF-1, colony-stimulating factor 1; FAK, focal adhesion kinase; F13A1, coagulation factor XIII A chain; GDNF, glial cell-derived neurotrophic factor; GM-CSF, granulocyte-macrophage colony-stimulating factor; HSPA5, health shock protein family A; IL6/1A/1B, interleukin 6; interleukin 1A; interleukin 1B; PD1, programmed death receptor 1; PI3K, phosphoinositide 3-kinase; P2RY12/13, purigenic receptor P2Y12/13; SLC7A11, solute carrier family 7 member 11; TGFβ1, transforming growth factor β1; TIM3, T-cell immunoglobulin and mucin-domaining containing-3; TNF, tumor necrosis factor.

chemokine ligand 2), CCL7 (C-C motif chemokine ligand 7), GDNF (glial cell-derived neurotrophic factor), SDF1 (stromal cell-derived factor 1), TNF (tumor necrosis factor), VEGF (vascular endothelial growth factor), ATP (adenosine triphosphate), CSF-1 (colony-stimulating factor 1), GM-CSF (granulocyte-macrophage colony-stimulating factor), and expression of OLIG2 (oligodendrocyte transcription factor 2). Once attracted into the TME, macrophages can attract monocytes by the production of CCL2 and CCR2. Monocytes can be further oriented toward a macrophage signature by factors secreted by GBM (7, 28–32).

Macrophages contribute to the development of an immune-suppressive environment by the production of TGFβ1, ARG1 (arginase 1), and/or IL-10 (interleukin 10) (44). Macrophages can further stimulate angiogenesis through the production of VEGF (vascular endothelial growth factor) and metalloproteases (44).

It is important to remark that all these interactions have been demonstrated in GBM while no data are available on low-grade IDH-mutated gliomas.

A recent study investigating transcriptomic data of low-grade gliomas associated with TME identified three specific immune signatures (45). The first signature (Im1) identified a high number of T cells, Th17, and mast cells. The second signature (Im2) was composed of macrophages and exhausted CD8+ T cells. Tumors harboring the Im2 signature were associated with worst prognosis. Finally, the third signature (Im3) was composed of T-helper, antigen-presenting cells, and macrophages; 23.7% of tumor samples analyzed in this study were IDH-wt tumors; therefore, it is unknown which patterns are present in IDH mutant low-grade gliomas (45).

Another trial (37) assessed the single-cell expression of TME associated with 10 WHO grade 2 astrocytomas and 4 WHO grade 2 oligodendrogliomas. This study identified the presence of several immune cells like CD8+, CD4+, regulatory T cells, and natural killer cells (37). This is one of the first studies characterizing tumor-associated lymphocytes in low-grade gliomas. Notably, the authors identified that TME associated with astrocytoma presented a more inhibitory feature as compared with those observed in oligodendrogliomas. Finally, the increased percentage of CD8+ PD-1 (programmed death receptor 1) expressing T cell and CD4+ TIM3 (T-cell immunoglobulin and mucin-domaining containing-3) expressing T cell in association with regulatory T cells and macrophages was mainly responsible for an immune-suppressive contexture (37).

Interactions between IDH-mutated glioma cells and neurons and normal glial cells are largely unknown. It is well known that glioma is clinically associated with several neurological symptoms including cognitive or motility deficits, verbal fluency, headaches, and seizures (46–48). Notably, before diagnosis, low-grade gliomas often have a pre-symptomatic period. At this time, tumors may occupy a significant volume of the brain without manifesting significant symptoms. It has been proposed that neurons and glial cells can adapt to the tumor presence by activating a reactive response resulting in plasticity (49–51). There are several remarkable examples of this plasticity (50).

Brain tissue could adapt to the presence of tumors even if the mechanisms of this plasticity remain largely hidden. Furthermore, we ignore if low-grade IDH-mutated tumor cells can directly interact with neurons and altered glial cells. Tumor cells produce glutamate, which is released through the SLC7A11 (solute carrier family 7 member 11) glutamate–cysteine exchanger (38–40). The glutamate excess interacts with NMDA

(N-methyl-D-aspartate receptor) receptors, inducing an influx of calcium on neurons and resulting in seizure onset and neuron death (38–40). Astrocytes activated after an injury can promote the secretion of cytokines and growth factors (52). Furthermore, astrocytes can also alter the permeability of the blood–brain barrier (BBB) (52). It has been demonstrated that GBM cells use astrocyte activation to sustain tumor growth and development while this has not been demonstrated in low-grade IDH-mutated tumors. Curiously, a recent study recognizes the importance of the glucose transporter GLUT1, which seems to mediate glioma cells' perineuronal satellitosis in mice (53).

The study of the interactions between low-grade IDH-mutated tumor cells and surrounding neurons/glial cells is one of the most attractive and emerging issues. Future studies will probably offer novel insights into these important connections. Notably, it has been demonstrated that GBM interacting with neurons in a specific niche can differentiate toward an oligodendrocyte subtype (54), losing their infiltrative behaviors. Neuron stimulation could therefore modify tumor cell proliferation and development, making these interactions of particular interest.

IDH-WT GLIOMAS

The IDH-wt gliomas represent a heterogeneous family of tumors. In general, IDH-wt astrocytoma represent 5%–12% of all low-grade gliomas (6, 11–13). These tumors are diagnosed in older age (45–55 years) compared to IDH-mutated gliomas and are associated with shorter survival (from 15 to 36 months) (6, 11–13).

No randomized trials have been designed to assess the role of systemic treatments in IDH-wt WHO grade 2 or 3 tumors (2, 3). A second interim analysis of the CATNON trial showed in a subgroup analysis that neither concurrent nor adjuvant TMZ was associated with a survival improvement in this population (8). To date, the most appropriate clinical management after surgical resection of IDH-wt gliomas (excluding GBM) is unclear.

The diffuse midline H3K27M glioma is a novel entity recognized by the WHO 2021 classification (4). This tumor involves 80% of brain stem tumors in children and adolescents with an estimated median survival of 9–11 months. Occasionally, these tumors can also be diagnosed in adult patients and are associated with the same dismal prognosis observed in children (1). To date, no standard therapeutic approaches for midline gliomas have been approved, and inclusion in clinical trials should be encouraged (3).

Genomic Landscape of IDH-wt Gliomas

The TCGA assessed 282 low-grade gliomas, of which 56 (19.8%) were low-grade IDH-wt subtypes. In this study, the most frequent mutated genes were as follows: TERT (64%), EGFR (27%), PTEN (23%, phosphatase and tensin homolog), NF1 (20%, neurofibromin 1), TP53 (14%), and PIK3CA (9%) (16). Focal deletions of CDKN2A and RB1 (retinoblastoma-associated protein 1) occurred in 63% and 25% of cases, respectively. Gain of chromosome 7/loss of chromosome 10 was evident in 56% of cases (16).

As previously reported, IDH-mutated tumors could share a common progenitor that can differentiate into an astrocytic or oligodendroglioma phenotype (21). IDH-wt tumors are composed of cancer cells with the ability to modify their transcriptional profile assuming cellular plasticity (24, 25, 55, 56) and assuming all transcriptional subtypes (57) exchange within the same tumors (24, 25, 56). In other words, IDH-wt cancer cells can modify their phenotype ranging from the following subtypes:

1) Astrocytic-like cells characterized mainly by EGFR amplification,
2) Oligodendrocyte/neural progenitor phenotype frequently associated with PDGFRA/CDK4 amplification, and
3) Mesenchymal transcriptome associated with NF1 mutation.

The complexity of this scheme makes it clear how IDH-wt can be heterogeneous and therefore extremely similar to GBM (25).

It is important to remark that all these data have been provided by patients harboring an IDH-wt GBM while no studies focused on precursor cells within low-grade IDH-wt gliomas.

Genomic Landscape of IDH-wt H3K27 Midline Gliomas

In midline gliomas, the pathognomonic alterations are represented by the lysine-to-methionine substitution at position 27 of histones 3.1 and 3.3 (58–61).

These alterations lead to the inactivation of the PRC2 (polycomb repressive complex-2 methyltransferases complex) hiding gene expression (58–61). This alteration is diagnosed in about 80% of cases of midline glioma. Nonetheless, other mechanisms converge to PRC2 altered function (4). Indeed, the EZH inhibitory protein (EZHIP, CXorf7) is overexpressed in some midline gliomas and posterior fossa type A ependymomas (62). The hyperexpression of EZHIP leads to an inhibitory activity on PCR2 similar to H3 mutations (62). These tumors often present p53 (42%), ACVR1 (activin A receptor type 1), PPM1D (9%–23%, phosphatase Mg2+/Mn2+-dependent 1D), and PI3K mutations (58–61, 63, 64). Notably, PPM1D mutations are mutually exclusive with p53 (activation of PPM1D leads to p53 inactivation) (65). Other amplified genes are PDGFB (platelet-derived growth factor B), CCND1 (cyclin D1), CCND2 (cyclin D2), CCND3 (cyclin D3), CDK4 (cyclin-dependent kinase 4), and CDK6 (cyclin-dependent kinase 6) (58–61, 63, 64).

Precursor cells of diffuse midline gliomas display an oligodendrocyte phenotype (26). Nonetheless, the alteration occurring in PRC2 blocks the differentiation toward oligodendrocyte subtype; thus, the cancer cells assume an astrocyte-like phenotype instead of an oligodendrocyte one (26).

Microenvironment of IDH-wt Gliomas

Before the 2021 WHO classification, which recognized the diagnosis of "molecular glioblastoma", IDH-wt gliomas were

considered distinct tumor subtypes (66). In a study published in 2015 by Reuss et al. evaluating the molecular assessment of 160 IDH-wt glioma specimens, almost all tumors were finally classified as GBM or midline glioma (66). Not surprisingly, studies assessing TME on IDH-wt gliomas present the same results observed in similar analyses carried out on GBM patients (7, 67). In 2020, a study assessed and validated a specific immune signature in cohorts of patients with low-grade IDH wild-type gliomas (68). The authors identified an immune signature associated with a worse prognosis and characterized by high expression of immune-exhaustion markers and immune-depressive cytokines released by macrophages (68). On the other hand, researchers also identified a second phenotype associated with an elevated expression of lymphocyte and plasma cell-related genes (68).

In conclusion, most studies assessing TME on IDH-wt gliomas assessed the TME composition of GBM (7, 67). The complex interactions between tumor cells and TME (42, 43, 69, 70) required a specific and detailed discussion and are outside the scope of the current paper.

There are few studies investigating the TME of patients with midline gliomas. Nonetheless, there are particular issues concerning the tumor immune-associated stroma of these malignancies. These are immunologically cold tumors with a low percentage of T/NK cells (14). The main factors expressed are CCL2, CCL5, CSF1, CXCL12, and PDGFA with mainly enhanced microglia surrounding tumor cells (14).

It has been demonstrated that microglia associated with midline glioma assume their morphology with enlarged cell bodies and shorter processes (33–35). Similar to IDH-mutated astrocytomas and GBM, the microenvironment of midline gliomas is also enriched with macrophages. The PDGFB seems to be mainly responsible for macrophage recruitment (33–35). Compared to other CNS primary tumors, macrophages associated with midline gliomas have a lower expression of IL6, IL1A, IL1B, CCL3, and CCL4. Of interest, a gene-expression study demonstrated a significant difference between macrophages associated with GBM and midline gliomas (35). In particular, GBM-associated macrophages express mainly genes related to monocyte/neutrophil chemotaxis and chemokine while midline glioma-associated macrophages express genes related to angiogenesis, extracellular matrix organization, and angiogenesis (33–35). Furthermore, these tumors present a non-inflammatory environment as demonstrated by a low concentration of natural killer cells and infiltrating lymphocytes. This inflammation-desert microenvironment can be partially attributed to the reduced presence of key cytokines including the IL2 resulting from high levels of TGFβ and IL8 (14, 34). The other two key factors commonly observed in midline gliomas are a high concentration of the chemokines CCL2, CCL5, and the receptor PDGFRA, which directly support proliferation and cell survival (71).

While the midline glioma-associated immune contexture has just begun to be investigated, there is no data regarding interactions of these cells with other elements such as neurons, white matter, and glial cells.

In brief, GBM TME has a large infiltration of immune cells; however, their immune activity is mainly shifted toward an immune-suppressive phenotype. Midline glioma TME presents unique macrophages and microglia with its characteristics and morphology. Midline glioma shows a reduced presence of inflammation cells rather than a high number of immune cells with an inhibited response as observed in GBM TME.

THERAPEUTIC IMPLICATIONS AND FUTURE DEVELOPMENTS

The TME offers novel targets for the treatment of malignant gliomas (72–74). The clinical importance of TME has been largely investigated in GBM (7), while only recently has it been assessed in patients with low-grade gliomas. Furthermore, the majority of studies concentrate their investigation on the immune cells' composition of TME excluding other important elements such as neurons, stromal cells (such as fibroblasts), and other glial cells (75).

Among patients with IDH-mutated gliomas, the importance of tumor-associated cells is gaining increasing interest; however, no therapeutic drugs are acting directly on TME.

There are several systemic agents shown to modify the TME (76).

Immune checkpoint inhibitors (ICIs) are agents able to restore a suppressed immune response against tumors by targeting specific receptors named immune checkpoints. The programmed death receptor 1 (PD1) is the target of the monoclonal antibodies nivolumab and pembrolizumab, which have been tested in patients with GBM. In GBM, pembrolizumab has been investigated as a neoadjuvant treatment shown to induce a significant modification of the TME. These modifications consisted of an increased number of T cells, reduced monocytic population, activation of interferon γ-related gene expression, and downregulation of cell-cycle-related genes (77). Similarly, also the PD-1 inhibitor nivolumab can modulate the TME composition of GBM patients (78). Despite these positive results, no trials demonstrated that ICIs improved the clinical outcome of patients with GBM (79). To date, nivolumab is under evaluation in combination with the IDH inhibitor ivosidenib in patients with IDH-mutated tumors (NCT04056910).

Vaccines are other treatment strategies employed for the treatment of patients with gliomas (80). The NOA16 trial was a phase I study testing an IDH1-specific peptide vaccine among patients with IDH1-mutated gliomas. Notably, of the 33 patients receiving the vaccine, 93.3% presented an immune response (81). Patients responding to the vaccine more frequently had a pseudo-progression suggesting inflammation on the tumor site. Moreover, these same patients showed an increased T-cell response switching from an immune-inhibited to an immune-active environment (81). IDH vaccines are under evaluation in patients with gliomas (NCT03893903).

IDH inhibitors are a promising treatment approach (82), and a phase III trial (INDIGO, NCT04164901) is currently assessing

the IDH pan-inhibitor vorasidenib. Modifications of TME during IDH inhibition are unknown and could be an interesting issue to investigate in case of a successful approval of these drugs.

Differently, manipulation of the TME is an emerging treatment strategy in patients with IDH-wt gliomas and especially H3K27 altered diffuse midline gliomas.

Peptide vaccines targeting the H3K27 mutation as well as dendritic cell vaccines have been investigated in the pre-clinical model (83, 84). In particular, peptide vaccine was shown to improve immune response against tumors shifting from an immune-suppressive microenvironment to an active one.

Phase I studies (NCT03396575 and NCT02960230) are currently investigating vaccines in this setting.

Other strategies that aimed to switch the immune microenvironment of midline gliomas consist of oncolytic virus (NCT02960230) and ICIs (NCT03330197 and NCT02359565). Engineered T lymphocytes (CAR T cells) are a new class of compounds consisting of lymphocytes obtained from patients, amplified and activated against tumor cells artificially, and then reinjected into the patients (85). This approach has been successfully tested on hematological malignancies and will also be evaluated in solid tumors. A phase I study employing HER 2 oriented CAR T cells showed promising activity in midline gliomas and a safety profile (86). There are some phase I trials evaluating this approach on patients with newly diagnosed (NCT04099797, NCT04196413, and NCT04185038) and recurrent (NCT04099797) midline glioma.

IDH-wt diffuse gliomas represent a heterogeneous class of tumors. It is reasonable to suppose that these tumors display a similar TME of GBM and thus could benefit from strategies aimed to target angiogenesis as well as an immune response against tumors (7). To date, there are no trials investigating agents modifying TME tailored for patients with IDH-wt diffuse gliomas.

The study of microenvironment composition is an emerging issue in patients with low-grade gliomas. In the majority of cases, we have only limited data about its composition according to tumor subtype. On the other hand, improved knowledge of this key element would improve the clinical management of these tumors in different possible ways. For example, microenvironment composition could be an element associated with prognosis and/or different responses to treatment provided. In this optic, the microenvironment could be assessed as a prognostic or predictive factor independently associated with clinical outcomes. A deeper knowledge of microenvironment composition would also improve the selection of patients to enroll in clinical trials (which is essential considering the rarity of the diseases and the long follow-up required for final data). Targeting microenvironment composition could also be a promising therapeutic option. Due to the approval of ICIs, the composition of immune cells surrounding tumors is the most assessed issue. Nonetheless, interactions between neurons, glial cells, endothelial cells, and stromal cells could hide important potential targets for therapy.

CONCLUSION

Few studies investigated the TME of patients with glioma (excluding GBM). The composition of TME differs according to the genomic expression and mutations exhibited by cancer cells and can be modified by systemic treatments. Vaccines built with IDH1 and H3K27 peptides could be an interesting approach as these agents showed to modify microenvironment composition and improve immune response against tumors. A combination of different agents can further amplify the effect on TME resulting in improved anti-tumor activity.

AUTHOR CONTRIBUTIONS

VN and LG: writing and draft. EF, AB, AT, and SB: project conception and reviewing. All authors contributed to the article and approved the submitted version.

REFERENCES

1. Miller KD, Ostrom QT, Kruchko C, Patil N, Tihan T, Cioffi G, et al. Brain, and Other Central Nervous System Tumor Statistics, 2021. *CA Cancer J Clin* (2021) 71(5):381–406. doi: 10.3322/caac.21693
2. Weller M, van den Bent M, Preusser M, Le Rhun E, Tonn JC, Minniti G, et al. EANO Guidelines on the Diagnosis and Treatment of Diffuse Gliomas of Adulthood. *Nat Rev Clin Oncol* (2021) 18(3):170–86. doi: 10.1038/s41571-020-00447-z
3. Mohile NA, Messersmith H, Gatson NT, Hottinger AF, Lassman A, Morton J, et al. Therapy for Diffuse Astrocytic and Oligodendroglial Tumors in Adults: ASCO-SNO Guideline. *J Clin Oncol* (2022) 40(4):403–26. doi: 10.1200/JCO.21.02036
4. Louis DN, Perry A, Wesseling P, Cree IA, Figarella-Branger D, Hawkins C, et al. The 2021 WHO Classification of Tumors of the Central Nervous System: A Summary. *Neuro Oncol* (2021) 23(8):1231–51. doi: 10.1093/neuonc/noab106
5. Compostella A, Tosoni A, Blatt V, Franceschi E, Brandes AA. Prognostic Factors for Anaplastic Astrocytomas. *J Neurooncol* (2007) 81(3):295–303. doi: 10.1007/s11060-006-9232-z
6. Mair MJ, Geurts M, van den Bent MJ, Berghoff AS. A Basic Review on Systemic Treatment Options in WHO Grade II-III Gliomas. *Cancer Treat Rev* (2021) 92:102124. doi: 10.1016/j.ctrv.2020.102124
7. Broekman ML, Maas SLN, Abels ER, Mempel TR, Krichevsky AM, Breakefield XO. Multidimensional Communication in the Microenvirons of Glioblastoma. *Nat Rev Neurol* (2018) 14(8):482–95. doi: 10.1038/s41582-018-0025-8
8. van den Bent MJ, Tesileanu CMS, Wick W, Sanson M, Brandes AA, Clement PM, et al. Adjuvant and Concurrent Temozolomide for 1p/19q non-Co-Deleted Anaplastic Glioma (CATNON; EORTC Study 26053-22054): Second Interim Analysis of a Randomised, Open-Label, Phase 3 Study. *Lancet Oncol* (2021) 22(6):813–23. doi: 10.1016/S1470-2045(21)00090-5
9. van den Bent MJ, Baumert B, Erridge SC, Vogelbaum MA, Nowak AK, Sanson M, et al. Interim Results From the CATNON Trial (EORTC Study 26053-22054) of Treatment With Concurrent and Adjuvant Temozolomide for 1p/19q Non-Co-Deleted Anaplastic Glioma: A Phase 3, Randomised, Open-Label Intergroup Study. *Lancet* (2017) 390(10103):1645–53. doi: 10.1016/S0140-6736(17)31442-3
10. Shaw EG, Wang M, Coons SW, Brachman DG, Buckner JC, Stelzer KJ, et al. Randomized Trial of Radiation Therapy Plus Procarbazine, Lomustine, and

Vincristine Chemotherapy for Supratentorial Adult Low-Grade Glioma: Initial Results of RTOG 9802. *J Clin Oncol* (2012) 30(25):3065–70. doi: 10.1200/JCO.2011.35.8598
11. Reuss DE, Mamatjan Y, Schrimpf D, Capper D, Hovestadt V, Kratz A, et al. IDH Mutant Diffuse and Anaplastic Astrocytomas Have Similar Age at Presentation and Little Difference in Survival: A Grading Problem for WHO. *Acta Neuropathol* (2015) 129(6):867–73. doi: 10.1007/s00401-015-1438-8
12. Aoki K, Nakamura H, Suzuki H, Matsuo K, Kataoka K, Shimamura T, et al. Prognostic Relevance of Genetic Alterations in Diffuse Lower-Grade Gliomas. *Neuro Oncol* (2018) 20(1):66–77. doi: 10.1093/neuonc/nox132
13. Pekmezci M, Rice T, Molinaro AM, Walsh KM, Decker PA, Hansen H, et al. Adult Infiltrating Gliomas With WHO 2016 Integrated Diagnosis: Additional Prognostic Roles of ATRX and TERT. *Acta Neuropathol* (2017) 133(6):1001–16. doi: 10.1007/s00401-017-1690-1
14. Price G, Bouras A, Hambardzumyan D, Hadjipanayis CG. Current Knowledge on the Immune Microenvironment and Emerging Immunotherapies in Diffuse Midline Glioma. *EBioMedicine* (2021) 69:103453. doi: 10.1016/j.ebiom.2021.103453
15. van den Bent MJ, Carpentier AF, Brandes AA, Sanson M, Taphoorn MJ, Bernsen HJ, et al. Adjuvant Procarbazine, Lomustine, and Vincristine Improves Progression-Free Survival But Not Overall Survival in Newly Diagnosed Anaplastic Oligodendrogliomas and Oligoastrocytomas: A Randomized European Organisation for Research and Treatment of Cancer Phase III Trial. *J Clin Oncol* (2006) 24(18):2715–22. doi: 10.1200/JCO.2005.04.6078
16. Brat DJ, Verhaak RG, Aldape KD, Yung WK, Salama SR, Cooper LA, et al. Comprehensive, Integrative Genomic Analysis of Diffuse Lower-Grade Gliomas. *N Engl J Med* (2015) 372(26):2481–98.doi: 10.1056/NEJMoa1402121
17. Tesileanu CMS, van den Bent MJ, Sanson M, Wick W, Brandes AA, Clement PM, et al. Prognostic Significance of Genome-Wide DNA Methylation Profiles Within the Randomized, Phase 3, EORTC CATNON Trial on non-1p/19q Deleted Anaplastic Glioma. *Neuro Oncol* (2021) 23(9):1547–59. doi: 10.1093/neuonc/noab088
18. Di Nunno V, Franceschi E, Tosoni A, Gatto L, Maggio I, Lodi R, et al. Clinical and Molecular Features of Patients With Gliomas Harboring IDH1 Non-Canonical Mutations: A Systematic Review and Meta-Analysis. *Adv Ther* (2022) 39(1):165–77. doi: 10.1007/s12325-021-01977-3
19. Franceschi E, Biase D, Di Nunno V, Pession A, Tosoni A, Gatto L, et al. IDH1 (105GGT) Single Nucleotide Polymorphism Improves Progression Free Survival in Patients With IDH Mutated Grade II and III Gliomas. *Pathol Res Pract* (2021) 221:153445. doi: 10.1016/j.prp.2021.153445
20. Franceschi E, De Biase D, Di Nunno V, Pession A, Tosoni A, Gatto L, et al. IDH1 Non-Canonical Mutations and Survival in Patients With Glioma. *Diagnostics (Basel)* (2021) 11(2):342. doi: 10.3390/diagnostics11020342
21. Venteicher AS, Tirosh I, Hebert C, Yizhak K, Neftel C, Filbin MG, et al. Decoupling Genetics, Lineages, and Microenvironment in IDH-Mutant Gliomas by Single-Cell RNA-Seq. *Science* (2017) 355(6332):eaai8478. doi: 10.1126/science.aai8478
22. Tirosh I, Venteicher AS, Hebert C, Escalante LE, Patel AP, Yizhak K, et al. Single-Cell RNA-Seq Supports a Developmental Hierarchy in Human Oligodendroglioma. *Nature* (2016) 539(7628):309–13. doi: 10.1038/nature20123
23. Pei Y, Wechsler-Reya RJ. A Malignant Oligarchy: Progenitors Govern the Behavior of Oligodendrogliomas. *Cancer Cell* (2010) 18(6):546–7. doi: 10.1016/j.ccr.2010.11.031
24. Patel AP, Tirosh I, Trombetta JJ, Shalek AK, Gillespie SM, Wakimoto H, et al. Single-Cell RNA-Seq Highlights Intratumoral Heterogeneity in Primary Glioblastoma. *Science* (2014) 344(6190):1396–401. doi: 10.1126/science.1254257
25. Neftel C, Laffy J, Filbin MG, Hara T, Shore ME, Rahme GJ, et al. An Integrative Model of Cellular States, Plasticity, and Genetics for Glioblastoma. *Cell* (2019) 178(4):835–849.e21. doi: 10.1016/j.cell.2019.06.024
26. Filbin MG, Tirosh I, Hovestadt V, Shaw ML, Escalante LE, Mathewson ND, et al. Developmental and Oncogenic Programs in H3K27M Gliomas Dissected by Single-Cell RNA-Seq. *Science* (2018) 360(6386):331–5. doi: 10.1126/science.aao4750
27. Wherry EJ, Kurachi M. Molecular and Cellular Insights Into T Cell Exhaustion. *Nat Rev Immunol* (2015) 15(8):486–99. doi: 10.1038/nri3862
28. Li W, Graeber MB. The Molecular Profile of Microglia Under the Influence of Glioma. *Neuro Oncol* (2012) 14(8):958–78. doi: 10.1093/neuonc/nos116
29. Hambardzumyan D, Gutmann DH, Kettenmann H. The Role of Microglia and Macrophages in Glioma Maintenance and Progression. *Nat Neurosci* (2016) 19(1):20–7. doi: 10.1038/nn.4185
30. Chang AL, Miska J, Wainwright DA, Dey M, Rivetta CV, Yu D, et al. CCL2 Produced by the Glioma Microenvironment Is Essential for the Recruitment of Regulatory T Cells and Myeloid-Derived Suppressor Cells. *Cancer Res* (2016) 76(19):5671–82. doi: 10.1158/0008-5472.CAN-16-0144
31. Brandenburg S, Müller A, Turkowski K, Radev YT, Rot S, Schmidt C, et al. Resident Microglia Rather Than Peripheral Macrophages Promote Vascularization in Brain Tumors and are Source of Alternative Pro-Angiogenic Factors. *Acta Neuropathol* (2016) 131(3):365–78. doi: 10.1007/s00401-015-1529-6
32. Bayik D, Zhou Y, Park C, Hong C, Vail D, Silver DJ, et al. Myeloid-Derived Suppressor Cell Subsets Drive Glioblastoma Growth in a Sex-Specific Manner. *Cancer Discov* (2020) 10(8):1210–25. doi: 10.1158/2159-8290.CD-19-1355
33. Ross JL, Chen Z, Herting CJ, Grabovska Y, Szulzewsky F, Puigdelloses M, et al. Platelet-Derived Growth Factor Beta Is a Potent Inflammatory Driver in Paediatric High-Grade Glioma. *Brain* (2021) 144(1):53–69. doi: 10.1093/brain/awaa382
34. Lin GL, Nagaraja S, Filbin MG, Suvà ML, Vogel H, Monje M, et al. Non-Inflammatory Tumor Microenvironment of Diffuse Intrinsic Pontine Glioma. *Acta Neuropathol Commun* (2018) 6(1):51. doi: 10.1186/s40478-018-0553-x
35. Gieryng A, Pszczolkowska D, Walentynowicz KA, Rajan WD, Kaminska B. Immune Microenvironment of Gliomas. *Lab Invest* (2017) 97(5):498–518. doi: 10.1038/labinvest.2017.19
36. Di Nunno V, Franceschi E, Tosoni A, atto L, Bartolini S, Brandes AA. Glioblastoma Microenvironment: From an Inviolable Defense to a Therapeutic Chance. *Front Oncol* (2022) 12:852950. doi: 10.3389/fonc.2022.852950
37. Fu W, Wang W, Li H, Jiao Y, Weng J, Huo R, et al. High Dimensional Mass Cytometry Analysis Reveals Characteristics of the Immunosuppressive Microenvironment in Diffuse Astrocytomas. *Front Oncol* (2020) 10:78. doi: 10.3389/fonc.2020.00078
38. Buckingham SC, Campbell SL, Haas BR, Montana V, Robel S, Ogunrinu T, et al. Glutamate Release by Primary Brain Tumors Induces Epileptic Activity. *Nat Med* (2011) 17(10):1269–74. doi: 10.1038/nm.2453
39. Campbell SL, Buckingham SC, Sontheimer H. Human Glioma Cells Induce Hyperexcitability in Cortical Networks. *Epilepsia* (2012) 53(8):1360–70. doi: 10.1111/j.1528-1167.2012.03557.x
40. Sontheimer H. A Role for Glutamate in Growth and Invasion of Primary Brain Tumors. *J Neurochem* (2008) 105(2):287–95. doi: 10.1111/j.1471-4159.2008.05301.x
41. Nakanishi H, Ni J, Nonaka S, Hayashi Y. Microglial Circadian Clock Regulation of Microglial Structural Complexity, Dendritic Spine Density and Inflammatory Response. *Neurochem Int* (2021) 142:104905. doi: 10.1016/j.neuint.2020.104905
42. Klemm F, Maas RR, Bowman RL, Kornete M, Soukup K, Nassiri S, et al. Interrogation of the Microenvironmental Landscape in Brain Tumors Reveals Disease-Specific Alterations of Immune Cells. *Cell* (2020) 181(7):1643–1660.e17. doi: 10.1016/j.cell.2020.05.007
43. Friebel E, Kapolou K, Unger S, Núñez NG, Utz S, Rushing EJ, et al. Single-Cell Mapping of Human Brain Cancer Reveals Tumor-Specific Instruction of Tissue-Invading Leukocytes. *Cell* (2020) 181(7):1626–1642.e20. doi: 10.1016/j.cell.2020.04.055
44. Ma T, Hu C, Lal B, Zhou W, Ma Y, Ying M, et al. Reprogramming Transcription Factors Oct4 and Sox2 Induce a BRD-Dependent Immunosuppressive Transcriptome in GBM-Propagating Cells. *Cancer Res* (2021) 81(9):2457–69. doi: 10.1158/0008-5472.CAN-20-2489
45. Wu F, Wang ZL, Wang KY, Li GZ, Chai RC, Liu YQ, et al. Classification of Diffuse Lower-Grade Glioma Based on Immunological Profiling. *Mol Oncol* (2020) 14(9):2081–95. doi: 10.1002/1878-0261.12707
46. Bosma I, Vos MJ, Heimans JJ, Taphoorn MJ, Aaronson NK, Postma TJ, et al. The Course of Neurocognitive Functioning in High-Grade Glioma Patients. *Neuro Oncol* (2007) 9(1):53–62. doi: 10.1215/15228517-2006-012
47. Miotto EC, Junior AS, Silva CC, Cabrera HN, Machado MA, Benute GR, et al. Cognitive Impairments in Patients With Low Grade Gliomas and High Grade

Gliomas. *Arq Neuropsiquiatr* (2011) 69(4):596–601. doi: 10.1590/S0004-282X2011000500005
48. Taphoorn MJ, Klein M. Cognitive Deficits in Adult Patients With Brain Tumours. *Lancet Neurol* (2004) 3(3):159–68. doi: 10.1016/S1474-4422(04)00680-5
49. Duffau H. Diffuse Low-Grade Gliomas and Neuroplasticity. *Diagn Interv Imaging* (2014) 95(10):945–55. doi: 10.1016/j.diii.2014.08.001
50. Kong NW, Gibb WR, Tate MC. Neuroplasticity: Insights From Patients Harboring Gliomas. *Neural Plast* (2016) 2016:2365063. doi: 10.1155/2016/2365063
51. Torres D, Canoll P. Alterations in the Brain Microenvironment in Diffusely Infiltrating Low-Grade Glioma. *Neurosurg Clin N Am* (2019) 30(1):27–34. doi: 10.1016/j.nec.2018.08.001
52. Liddelow SA, Barres BA. Reactive Astrocytes: Production, Function, and Therapeutic Potential. *Immunity* (2017) 46(6):957–67. doi: 10.1016/j.immuni.2017.06.006
53. Miyai M, Kanayama T, Hyodo F, Kinoshita T, Ishihara T, Okada H, et al. Glucose Transporter Glut1 Controls Diffuse Invasion Phenotype With Perineuronal Satellitosis in Diffuse Glioma Microenvironment. *Neurooncol Adv* (2021) 3(1):vdaa150. doi: 10.1093/noajnl/vdaa150
54. Brooks LJ, Clements MP, Burden JJ, Kocher D, Richards L, Devesa SC, et al. The White Matter Is a Pro-Differentiative Niche for Glioblastoma. *Nat Commun* (2021) 12(1):2184. doi: 10.1038/s41467-021-22225-w
55. Bhaduri A, Di Lullo E, Jung D, Müller S, Crouch EE, Espinosa CS, et al. Outer Radial Glia-Like Cancer Stem Cells Contribute to Heterogeneity of Glioblastoma. *Cell Stem Cell* (2020) 26(1):48–63.e6. doi: 10.1016/j.stem.2019.11.015
56. Weng Q, Wang J, Wang J, He D, Cheng Z, Zhang F, et al. Single-Cell Transcriptomics Uncovers Glial Progenitor Diversity and Cell Fate Determinants During Development and Gliomagenesis. *Cell Stem Cell* (2019) 24(5):707–723.e8. doi: 10.1016/j.stem.2019.03.006
57. Nicholson JG, Fine HA. Diffuse Glioma Heterogeneity and Its Therapeutic Implications. *Cancer Discov* (2021) 11(3):575–90. doi: 10.1158/2159-8290.CD-20-1474
58. Khuong-Quang DA, Buczkowicz P, Rakopoulos P, Liu XY, Fontebasso AM, Bouffet E, et al. K27M Mutation in Histone H3.3 Defines Clinically and Biologically Distinct Subgroups of Pediatric Diffuse Intrinsic Pontine Gliomas. *Acta Neuropathol* (2012) 124(3):439–47. doi: 10.1007/s00401-012-0998-0
59. Lewis PW, Müller MM, Koletsky MS, Cordero F, Lin S, Banaszynski LA, et al. Inhibition of PRC2 Activity by a Gain-of-Function H3 Mutation Found in Pediatric Glioblastoma. *Science* (2013) 340(6134):857–61. doi: 10.1126/science.1232245
60. Schwartzentruber J, Korshunov A, Liu XY, Jones DT, Pfaff E, Jacob K, et al. Driver Mutations in Histone H3.3 and Chromatin Remodelling Genes in Paediatric Glioblastoma. *Nature* (2012) 482(7384):226–31. doi: 10.1038/nature10833
61. Wu G, Broniscer A, McEachron TA, Lu C, Paugh BS, Becksfort J, et al. Somatic Histone H3 Alterations in Pediatric Diffuse Intrinsic Pontine Gliomas and non-Brainstem Glioblastomas. *Nat Genet* (2012) 44(3):251–3. doi: 10.1038/ng.1102
62. Jain SU, Rashoff AQ, Krabbenhoft SD, Hoelper D, Do TJ, Gibson TJ, et al. H3 K27M and EZHIP Impede H3K27-Methylation Spreading by Inhibiting Allosterically Stimulated Prc2. *Mol Cell* (2020) 80(4):726–735.e7. doi: 10.1016/j.molcel.2020.09.028
63. Wu G, Diaz AK, Paugh BS, Rankin SL, Ju B, Li Y, et al. The Genomic Landscape of Diffuse Intrinsic Pontine Glioma and Pediatric Non-Brainstem High-Grade Glioma. *Nat Genet* (2014) 46(5):444–50. doi: 10.1038/ng.2938
64. Zarghooni M, Bartels U, Lee E, Buczkowicz P, Morrison A, Huang A, et al. Whole-Genome Profiling of Pediatric Diffuse Intrinsic Pontine Gliomas Highlights Platelet-Derived Growth Factor Receptor Alpha and Poly (ADP-Ribose) Polymerase as Potential Therapeutic Targets. *J Clin Oncol* (2010) 28(8):1337–44. doi: 10.1200/JCO.2009.25.5463
65. Zhang L, Chen LH, Wan H, Yang R, Wang Z, Feng J, et al. Exome Sequencing Identifies Somatic Gain-of-Function PPM1D Mutations in Brainstem Gliomas. *Nat Genet* (2014) 46(7):726–30. doi: 10.1038/ng.2995
66. Reuss DE, Kratz A, Sahm F, Capper Schrimpf D, Koelsche D, C, et al. Adult IDH Wild Type Astrocytomas Biologically and Clinically Resolve Into Other Tumor Entities. *Acta Neuropathol* (2015) 130(3):407–17. doi: 10.1007/s00401-015-1454-8
67. Chen Z, Hambardzumyan D. Immune Microenvironment in Glioblastoma Subtypes. *Front Immunol* (2018) 9. doi: 10.3389/fimmu.2018.01004
68. Wu F, Li GZ, Liu HJ, Zhao Z, Chai RC, Liu YQ, et al. Molecular Subtyping Reveals Immune Alterations in IDH Wild-Type Lower-Grade Diffuse Glioma. *J Pathol* (2020) 251(3):272–83. doi: 10.1002/path.5468
69. Abdelfattah N, Kumar P, Wang C, Leu JS, Flynn WF, Gao R, et al. Single-Cell Analysis of Human Glioma and Immune Cells Identifies S100A4 as an Immunotherapy Target. *Nat Commun* (2022) 13(1):767. doi: 10.1038/s41467-022-28372-y
70. Liu F, Peng B, Li M, Ma J, Deng G, Zhang S, et al. Targeted Disruption of Tumor Vasculature *via* Polyphenol Nanoparticles to Improve Brain Cancer Treatment. *Cell Rep Phys Sci* (2022) 3(1):100691. doi: 10.1016/j.xcrp.2021.100691
71. Paugh BS, Zhu X, Qu C, Endersby R, Diaz AK, Zhang J, et al. Novel Oncogenic PDGFRA Mutations in Pediatric High-Grade Gliomas. *Cancer Res* (2013) 73(20):6219–29. doi: 10.1158/0008-5472.CAN-13-1491
72. Di Nunno V, Franceschi E, Tosoni A, Di Battista M, Gatto L, Lamperini C, et al. Treatment of Recurrent Glioblastoma: State-of-the-Art and Future Perspectives. *Expert Rev Anticancer Ther* (2020) 20(9):785–95. doi: 10.1080/14737140.2020.1807949
73. Di Nunno V, Franceschi E, Tosoni A, Gatto L, Lodi R, Bartolini S, et al. Glioblastoma: Emerging Treatments and Novel Trial Designs. *Cancers (Basel)* (2021) 13(15):3750. doi: 10.3390/cancers13153750
74. Gatto L, Di Nunno V, Franceschi E, Tosoni A, Bartolini S, Brandes AA. Pharmacotherapeutic Treatment of Glioblastoma: Where Are We to Date? *Drugs* (2022) 82(5):491–510. doi: 10.1007/s40265-022-01702-6
75. Busek P, Mateu R, Zubal M, Kotackova L, Sedo A. Targeting Fibroblast Activation Protein in Cancer - Prospects and Caveats. *Front Biosci (Landmark Ed)* (2018) 23(10):1933–68. doi: 10.2741/4682
76. Tosoni A, Franceschi E, Poggi R, Brandes AA. Relapsed Glioblastoma: Treatment Strategies for Initial and Subsequent Recurrences. *Curr Treat Options Oncol* (2016) 17(9):49. doi: 10.1007/s11864-016-0422-4
77. Cloughesy TF, Mochizuki AY, Orpilla JR, Hugo W, Lee AH, Davidson TB, et al. Neoadjuvant Anti-PD-1 Immunotherapy Promotes a Survival Benefit With Intratumoral and Systemic Immune Responses in Recurrent Glioblastoma. *Nat Med* (2019) 25(3):477–86. doi: 10.1038/s41591-018-0337-7
78. Schalper KA, Rodriguez-Ruiz ME, Diez-Valle R, López-Janeiro A, Porciuncula A, Idoate MA, et al. Neoadjuvant Nivolumab Modifies the Tumor Immune Microenvironment in Resectable Glioblastoma. *Nat Med* (2019) 25(3):470–6. doi: 10.1038/s41591-018-0339-5
79. Reardon DA, Brandes AA, Omuro A, Mulholland P, Lim M, Wick A, et al. Effect of Nivolumab vs Bevacizumab in Patients With Recurrent Glioblastoma: The CheckMate 143 Phase 3 Randomized Clinical Trial. *JAMA Oncol* (2020) 6(7):1003–10. doi: 10.1001/jamaoncol.2020.1024
80. Crunkhorn S. Vaccine for IDH Mutant Glioma. *Nat Rev Drug Discov* (2021) 20(5):344. doi: 10.1038/d41573-021-00058-y
81. Platten M, Bunse L, Wick A, Bunse T, Le Cornet L, Harting I, et al. A Vaccine Targeting Mutant IDH1 in Newly Diagnosed Glioma. *Nature* (2021) 592(7854):463–8. doi: 10.1038/s41586-021-03363-z
82. Gatto L, Franceschi E, Tosoni A, Di Nunno V, Maggio I, Lodi R, et al. IDH Inhibitors and Beyond: The Cornerstone of Targeted Glioma Treatment. *Mol Diagn Ther* (2021) 25(4):457–73. doi: 10.1007/s40291-021-00537-3
83. Benitez-Ribas D, Cabezón R, Flórez-Grau G, Molero MC, Puerta P, Guillen A, et al. Immune Response Generated With the Administration of Autologous Dendritic Cells Pulsed With an Allogenic Tumoral Cell-Lines Lysate in Patients With Newly Diagnosed Diffuse Intrinsic Pontine Glioma. *Front Oncol* (2018) 8:127. doi: 10.3389/fonc.2018.00127
84. Ochs K, Ott M, Bunse T, Sahm F, Bunse L, Deumelandt K, et al. K27M-Mutant Histone-3 as a Novel Target for Glioma Immunotherapy. *Oncoimmunology* (2017) 6(7):e1328340. doi: 10.1080/2162402X.2017.1328340
85. Gatto L, Nunno VD, Franceschi E, Brandes AA. Chimeric Antigen Receptor Macrophage for Glioblastoma Immunotherapy: The Way Forward. *Immunotherapy* (2021) 13(11):879–83. doi: 10.2217/imt-2021-0054
86. Vitanza NA, Johnson AJ, Wilson AL, Brown C, Yokoyama JK, Künkele A, et al. Locoregional Infusion of HER2-Specific CAR T Cells in Children and

Young Adults With Recurrent or Refractory CNS Tumors: An Interim Analysis. *Nat Med* (2021) 27(9):1544–52. doi: 10.1038/s41591-021-01404-8

Conflict of Interest: The authors declare that the research was conducted in the absence of any commercial or financial relationships that could be construed as a potential conflict of interest.

Publisher's Note: All claims expressed in this article are solely those of the authors and do not necessarily represent those of their affiliated organizations, or those of the publisher, the editors and the reviewers. Any product that may be evaluated in this article, or claim that may be made by its manufacturer, is not guaranteed or endorsed by the publisher.

Frontiers in Oncology

Advances knowledge of carcinogenesis and tumor progression for better treatment and management

The third most-cited oncology journal, which highlights research in carcinogenesis and tumor progression, bridging the gap between basic research and applications to imrpove diagnosis, therapeutics and management strategies.

Discover the latest Research Topics

See more →

Frontiers

Avenue du Tribunal-Fédéral 34
1005 Lausanne, Switzerland
frontiersin.org

Contact us

+41 (0)21 510 17 00
frontiersin.org/about/contact